Utrecht University

Hydrodynamics of charged Dirac electrons

Kitinan Pongsangangan

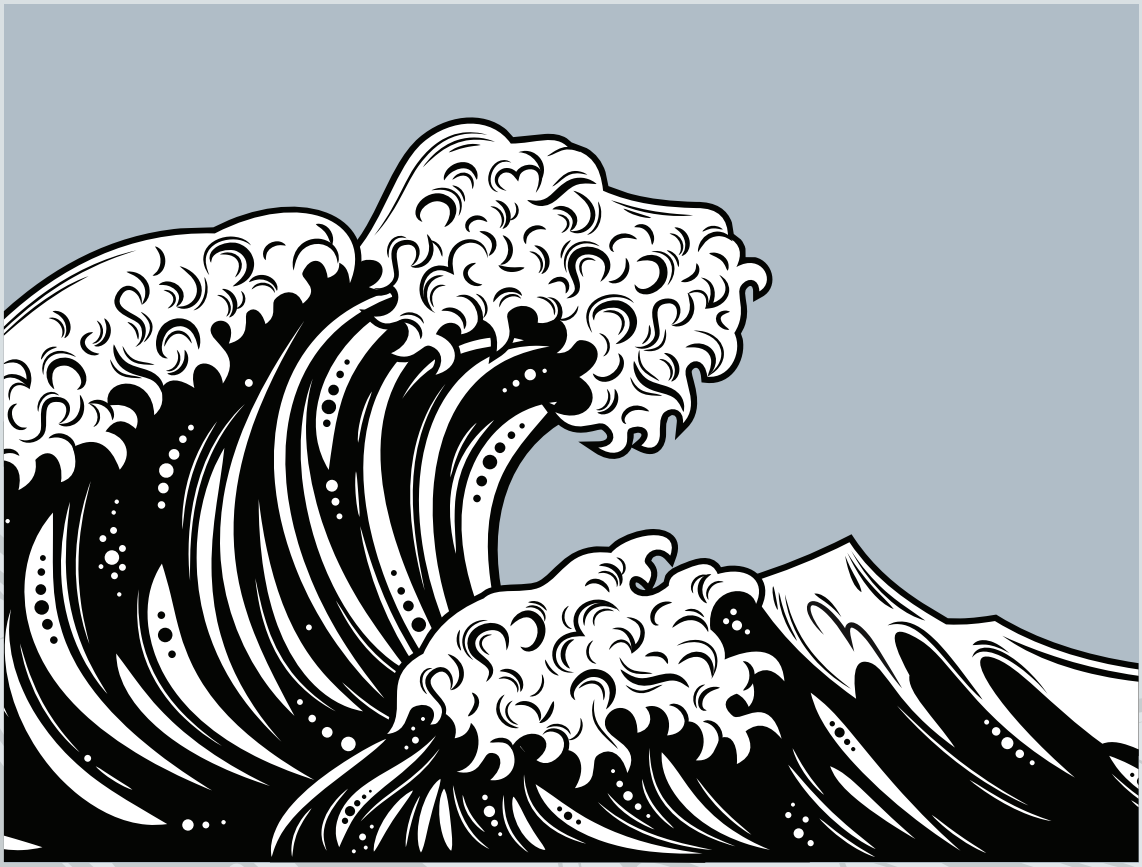

Institute for Theoretical Physics

2022

Hydrodynamics of charged Dirac electrons

Kitinan Pongsangangan

PhD thesis, Utrecht University, the Netherlands (2022)
Printing: ProefschriftMaken — www.proefschriftmaken.nl
ISBN 978-94-6469-142-9

Hydrodynamics of charged Dirac electrons

Hydrodynamica van geladen Dirac-elektronen

(met een samenvatting in het Nederlands)

Proefschrift

ter verkrijging van de graad van doctor aan de
Universiteit Utrecht
op gezag van de
rector magnificus, prof.dr. H.R.B.M. Kummeling,
ingevolge het besluit van het college voor promoties
in het openbaar te verdedigen op

donderdag 24 november 2022 des middags te 4.15 uur

door

Kitinan Pongsangangan

geboren op 10 december 1993
te Chaiyaphum, Thailand

Promotor:
Prof. dr. H.T.C. Stoof

Copromotor:
Dr. L. Fritz

Beoordelingscommissie:
Prof. A. Kamenev PhD
Prof. T. Scaffidi PhD
Prof. dr. R.A. Duine
Prof. dr. R.H.H.G. van Roij
Prof. dr. C. de Morais Smith

Dit proefschrift werd mogelijk gemaakt met financiële steun van The Institute for the Promotion of Teaching Science and Technology (IPST) of Thailand

Contents

List of publications

This thesis is based on the following publications:

- K. Pongsangangan, T. Ludwig, H.T.C. Stoof, and L. Fritz, *Hydrodynamics of charged Dirac electrons in two dimensions. I. Thermoelectric transport.* (accepted at PRB) (2022).

- K. Pongsangangan, T. Ludwig, H.T.C. Stoof, and L. Fritz, *Hydrodynamics of charged Dirac electrons in two dimensions. II. Role of collective modes.* (accepted at PRB) (2022).

- K. Pongsangangan, S. Grubinska, and L.Fritz, *Thermo-electric response in two-dimensional Dirac systems: the role of particle-hole pairs.* (accepted at PRResearch) (2022).

Other publications to which the author has contributed:

- R. Ciola, K. Pongsangangan, R. Thomale, and L. Fritz. *Chiral symmetry breaking through spontaneous dimerization in kagomé metals.* physical Review B **104**, 245138 (2021).

Chapter 1
Introduction

This thesis is about transport phenomena in a system of interacting electrons. This subject has a long history dated back to 1900 when Drude proposed a model, later named after him, of electrical conduction in metals. It was assumed that electrons are classical particles; The electron's acceleration due to an external electric field is relaxed by its collision with a lattice leading to a finite conductivities [1]. It turned out, however, that several properties of electrons in metal, for example, the specific heat and thermal conductivity at low temperature could not be understood until early 1928 when Sommerfeld modified Drude's model by treating the electrons as independent quantum particles that obey Fermi-Dirac statistics and are subjected to the Pauli exclusion principle [2, 3]. Since then, a picture of non-interacting electrons scattering from lattice impurities and/or lattice oscillations or phonons have provided a successful description of transport properties of normal metals [4]. Its validity, however, is far from obvious and has been a subject of investigations already 70 years ago [5, 6]. The main question is: Why and how do long-range Coulomb interactions between charged electrons become ineffective? Bohm and Pines addressed this question in their series of seminal papers in the 1960s. They argued that there are two components associated with the Coulomb interaction: short- and long-range. The short range part leads to a quasiparticle renormalization in the spirit of Landau's Fermi liquid theory [7, 8, 9, 10]. On the other hand, the primary manifestation of the long-range part is plasma oscillations or plasmons [5, 6]. They further argued, however,

that, in the standard theory of metallic transport, these plasmons play essentially no role. The reason goes as follows: in a 3d metal, the energy of plasmons is so large, much larger than the Fermi energy of the electronic system, that it can not be excited at accessible energy scales [11][1]. Consequently, only electrons are relevant at the low-energy limit and they interact with each other by the residue short-range component of the interaction [5, 12, 13].

Although the subject has a long and successful history, this thesis revisits the problem of transport phenomena in interacting charged electrons. The main reason is that, in recent years, another variant of conducting and interacting electronic systems called Dirac or Weyl systems [14] have been discovered. Their defining feature is a linear band crossing in isolated points in the Brillouin zone of which the excitations resemble relativistic electrons. These systems are semimetals because they are gapless, like a metal, but have a strong suppression of the density of states, like an insulator. The most famous example is graphene, a two-dimensional honeycomb lattice of carbon atoms, which has been at the forefront of research for almost two decades [15, 16, 17]. In this thesis, we study the role of the Coulomb interaction in transport phenomena of electrons in graphene.

1.1 Graphene

One of the motivation of this thesis is the measurements of thermoelectric transport coefficients of graphene in the hydrodynamic regime [18, 19]. This is the regime where the electron-electron scattering due to the Coulomb interaction becomes the dominant relaxation process in limiting the transports.

Graphene consists of carbon atoms arranged in a honeycomb lat-

[1] A comparison of the plasmon energy to the Fermi energy of some elemental metals

Element	Be	Mg	Al
ω_p(eV)[a]	19	11	16
ϵ_F (eV)[b]	14.3	7.08	11.07

[a] David Pines (1960). Plasma oscillations of electron gases.
[b] Ashcroft, N.W. ,and Mermin, N.D. (1978). Solid state Physics.

tice. The unit cell of graphene contains two inequivalent sites called A and B as depicted in Fig.(1.1). It is a truly two-dimensional material that was first discovered by Konstantin Novoselov and André Geim, together with their group in Manchester in 2004 by using the Scotch tape to peel off a one-atomic thick layer of carbon from graphite [15]. Since then, graphene has received a lot of attentions from physicists in a broad range of fields. One of the reasons is that it has a very high quality. Besides being superclean with very little disorder scattering, the concentration of phonons is also suppressed in those devices. Consequently, the usual momentum relaxation of electrons by means of collisions with impurities and phonons becomes less frequent. In the pioneering work by Novoselov and Geim, graphene was found to exhibit very good electronic transport properties. Graphene with mobilities up to $10,000$ cm^2/V·s were obtained at room temperature promising several technological applications. Novoselov and Geim were awarded the Nobel prize in physics for their discovery in 2010. Due to the recent advancement in synthesizing graphene encapsulated in hexagonal boron nitride (h-BN), it is now possible to reach the mobility up to $300,000$ cm^2/V·s [18, 20, 21, 22, 23]. This beats InSb, the semiconductor that is known to reach the highest mobility of $77,000$ cm^2/V·s.

In graphene, three of the valence electrons of the carbon atoms hybridize into three sp^2 orbitals. They form sigma bonds with sp^2-electrons on neighboring atoms and create the honeycomb lattice structure. On the other hand, the remaining valance electrons of the carbons atoms in p_z orbitals form a much weaker π-bonds. The electrons in the π-bonds becomes delocalized by hoping from one atom to the nearest neighboring atoms. This process can be described by a tight-binding model [24] reading as

$$H_0 = -t \sum_{\vec{x}} \sum_{n=1}^{3} a^\dagger_{\vec{x}} b_{\vec{x}+\vec{\delta}_n} + b^\dagger_{\vec{x}+\vec{\delta}_n} a_{\vec{x}} \ , \tag{1.1}$$

where the hopping parameter $t \approx 2.8$ eV measures the hoping energy between nearest-neighbor sites. We define creation and annihilation operators, $a^\dagger_{\vec{x}}$ and $a_{\vec{x}}$, for electrons on the carbon atoms locating at position $\vec{x}$ in the A sublattice. The creation and annihilation operators for electrons on the atoms of B sublattice are $b^\dagger_{\vec{x}}$, and $b_{\vec{x}}$,

respectively. Each carbon atom has $n = 3$ nearest neighbors with the nearest-neighboring vectors as

$$\vec{\delta}_1 = \frac{a}{2}(\sqrt{3}, 1), \quad \vec{\delta}_2 = \frac{a}{2}(-\sqrt{3}, 1), \quad \text{and} \quad \vec{\delta}_3 = a(0, -1). \tag{1.2}$$

The carbon atoms are separated by a distance $a = 1.42$ Å. To determine the energy-momentum relation, a Fourier transformation is performed by the relation

$$a_{\vec{x}} = \frac{1}{\sqrt{N_c}} \sum_{\vec{k}} a_k e^{i\vec{k}\cdot\vec{x}}, \tag{1.3}$$

where N_c is the number of unit cells. After the transformation, the Hamiltonian in the reciprocal space has the form of

$$H_0 = \sum_k \psi^\dagger_{\vec{k}} \mathcal{H} \psi_{\vec{k}}, \tag{1.4}$$

with $\psi^\dagger_{\vec{k}} = \begin{pmatrix} a^\dagger_{\vec{k}} & b^\dagger_{\vec{k}} \end{pmatrix}$. The Hamiltonian density is defined according to

$$\mathcal{H} = -t \begin{pmatrix} 0 & \gamma_{\vec{k}} \\ \gamma^*_{\vec{k}} & 0 \end{pmatrix}, \tag{1.5}$$

where

$$\gamma_{\vec{k}} = \sum_{n=1}^{3} e^{i\vec{k}\cdot\vec{\delta}_n}. \tag{1.6}$$

The energy-momentum relation $E_{\vec{k}}$ of electrons in graphene is given by the eigenvalues of the Hamiltonian H_0, hence

$$E_{\vec{k}} = \pm t\left|\gamma_{\vec{k}}\right| = \pm\sqrt{1 + 4\cos^2\left(\sqrt{3}ak_y/2\right) + 4\cos\left(\sqrt{3}ak_x/2\right)}. \tag{1.7}$$

The two energy bands are shown in Figure. (1.2). For the charge neutral system, the lower band which is the valence band is completely filled while the upper band which is the conduction band is completely empty. The conduction and valence bands touch each other at isolated points in the Brillouin zone. These points are

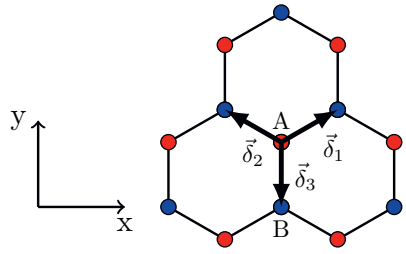

Figure 1.1: The honeycomb lattice of graphene with the inequivalent sublattices A (red) and B (blue) and the nearest-neighbor vectors $\vec{\delta}_1$, $\vec{\delta}_2$, and $\vec{\delta}_3$.

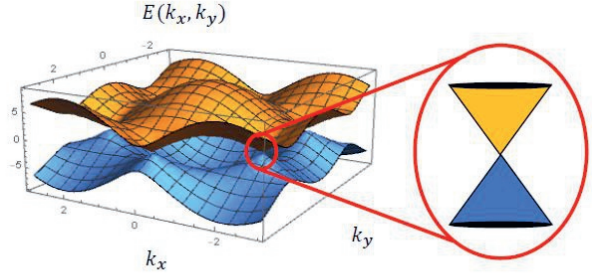

Figure 1.2: The full energy dispersion of graphene and zoom-in on the K point around which the dispersion is linear.

called the Dirac or charge neutrality point. There are two in equivalent Dirac point at $K' = \left(-\frac{4\pi}{3\sqrt{3}a}, 0\right)$ and $K = \left(\frac{4\pi}{3\sqrt{3}a}, 0\right)$. The low-energy effective Hamiltonian can be obtained by expanding the Hamiltonian around these points. After the expansion, the Hamiltonian is brought into the simple form. It reads as

$$H_0^{\xi} = \sum_{\vec{k}} \psi^{\dagger} \mathcal{H}_{\xi} \psi_{\vec{k}} \tag{1.8}$$

where

$$\mathcal{H}_0^{\xi} = v_F \begin{pmatrix} 0 & \xi k_x - i k_y \\ \xi k_x + i k_y & 0 \end{pmatrix}. \tag{1.9}$$

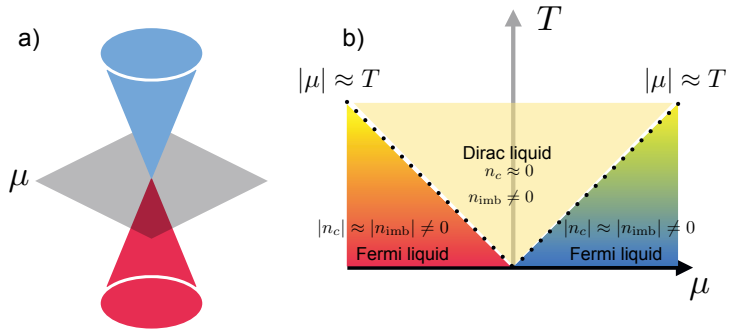

Figure 1.3: a) Schematic of the dispersion relation of graphene near its Dirac point. b) 'Phase diagram' of clean graphene at finite temperature. The region above $\mu = 0$ is referred to as Dirac liquid. At $\mu \approx T$ it crosses over to a Fermi liquid.

Here $\xi = 1$ ($\xi = -1$) for the expansion around the K point (K' point) and the Fermi velocity $v_F = 3at/2\hbar \approx 10^6$ m/s. It is straightforward to see that the energy-momentum dispersion becomes linear $E = \pm v_F k$. It should be noted that, although we expanded the Hamiltonian around both the K and K' point, usually, the two valleys are decoupled. In this situation, it is sufficient to focus on the expansion around the K point and keep the valley degeneracy as a multiplicative factor for all physical observables. Around the K point, the low-energy Hamiltonian has a form of the Dirac Hamiltonian

$$H_0 = \sum_{\vec{k}} \psi^\dagger_{\vec{k}} \left(v_F \vec{k} \cdot \vec{\sigma} \right) \psi_{\vec{k}}. \tag{1.10}$$

Hence electrons in graphene has similarities with relativistic massless fermions with the effective velocity v_F that is 300 times smaller than the speed of light. In its undoped state, it is neither a metal nor an insulator, but a semimetal [17, 25]. As such, it has a vanishing density of states at zero energy, but it is linear in energy everywhere else [17, 25].

Graphene near the charge-neutral point has the plasma character [26]. The essence is summarized in Fig. 1.3 b) which shows the 'phase diagram' of graphene as a function of the chemical potential μ (x-axis) and temperature T (y-axis). The chemical potential

controls the filling of the Dirac cones: the charge density $n_c \propto \mu^2$. Consequently, at the charge neutrality ($\mu = 0$), we have $n_c = 0$. However, there are still excitations at finite temperature T. This is captured by the imbalance density $n_{\rm imb} \propto T^2$. The physics behind this density is that there is a thermal cloud of electrons and one of holes, both of equal density, which ensures $n_c = 0$. The finite temperature region above μ has been dubbed the 'Dirac liquid' and it has thermodynamic properties that are very different from Fermi liquids. The crossover region is defined by the condition $|\mu| \approx T$ (up to renormalizations due to interactions). For $|\mu| \gg T$, the system behaves like a Fermi liquid of electron or hole type.

1.2 Coulomb interactions in graphene

Although the non-interacting Dirac and Wely semimetals are already interesting for the exotic electronic properties, the interaction effects are more interesting [27, 28, 29, 30]. In particular, inelastic electron-electron scattering by the Coulomb forces is expected to be crucial for determining the conductivity of clean sample at low temperatures [31, 32, 33, 34, 35].

In recent years, graphene has been a prime candidate to observe a hydrodynamical transport behavior of Dirac electrons. This is mainly determined by electron-electron collisions due to Coulomb interactions [16, 17, 36, 37, 38, 39]. It made possible due to recent advances in the preparation of ultrapure samples of graphene encapsulated in h-BN [21, 40, 22, 23, 20]. The prerequisite for experimental observation of the electron hydrodynamics is that microscopic momentum-conserving electron-electron collisions due to the Coulomb interaction must be fast compared to momentum-relaxing scatterings of electrons against, for example, impurities and/or phonons. Hence, the electron-electron interactions provide the dominant scattering mechanism [12, 32, 33, 34, 41, 36]. One can therefore speak of conservation laws and open the door for the observation of electron hydrodynamics [42, 43, 44, 45, 46].

The role of the Coulomb interactions in thermo-electric transport properties of monolayer graphene has been investigated theoretically for more than a decade [33, 34, 32, 47]. It received a lot more atten-

tion, recently, in the context of electron hydrodynamics mainly due to the increasing number of experimental observations in ultrapure sample [48, 49]; For instance, Figures (2.4b), (2.4d), (2.5c), and (2.6c) show the experimental measurements of the thermo-electric transport coefficients in graphene in the hydrodynamic regime taken from Refs. [18, 19].

However, as we will show in the subsequent chapters, electron hydrodynamics should be expected to behave differently in many respects from the archetypal example of the flow of a neutral fluid like water. The reason is that for an electronic system, in addition to said inelastic scatterings, the Coulomb interaction enters as a classical internal long-range force between electrons themselves. This internal force results theoretically from the so-called Hartree potential and has been known for its important role in facilitating emergence of collective excitations associated with plasma oscillations or plasmons. Hence, in addition to electrons and holes, there exist plasmons constituting an independent type of quasi-particle that is sensitive to, for example, a temperature gradient. Plasmons do not only collide with electrons and holes and relax heat current but also carry heat current themselves. This has been discussed to some extent in the Fermi liquid literature where the effect was usually found to be negligible [50, 51]. With the new ultrapure samples, it is possible to ask questions regarding the Coulomb interaction that could not be addressed before. It is well known that decreasing dimensionality increases the effect of long-range interactions in electronic systems. Plasmons in a one-dimensional conductor, for instance, contribute significantly to thermal transport [52]. This begs the question about two dimensions. In two dimensions, the plasmon is a massless mode following a square-root energy dispersion relation [53, 54, 55]. It should be possible to excite it easily in a sample at ordinary conditions and can therefore be relevant to the transport phenomena, especially thermal transport. This thesis attempts to investigate the contribution of plasmons to thermal conductivity and other thermoelectric responses of a nearly clean graphene sheet at the Dirac point as well as away from it. Furthermore, we are also interested in seeing whether we can describe the crossover to the Fermi liquid [50, 51].

The main idea of this thesis is schematically illustrated in Figure.

1.4. In the presence of an external temperature gradient, electrons and holes, as expected, transport heat from a hot bath to a cold bath. In addition, they drag plasmons along with them which results in increasing the energy current being transported. On the other hand, when the system is exposed to an electric field, electrons and holes travel in opposite directions. Their drag forces on the plasmons compensate each other. Therefore, the plasmons remain in equilibrium. Away from the Dirac point, however, the concentration of electrons and holes are different. The plasmons distribution will also be 'dragged' out of equilibrium along with the majority carriers. They will not contribute to charge transport though, because they are electrically neutral. However, they can relax electrons.

1.3 Outline

This thesis centers around interaction effects in transport properties of two-dimensional Dirac electrons. The analysis is mainly based on a non-equilibrium quantum-field theory, known as Keldysh formalism. The organization of this thesis is as follows.

We start in Chapter 2 by studying thermo-electric transport in interacting two-dimensional Dirac-type systems using a phenomenological Boltzmann approach with a relaxation-time approximation. We consider the electron-hole hydrodynamics, a model that is popular in the context of graphene, and its transport properties. Furthermore, we propose a novel type of hydrodynamics. In that setup, the 'fluid' consists of electrons, holes, and plasmons. We introduce a simple relaxation time approximation for two-fluid hydrodynamic model of electrons and holes interacting via Coulomb drag and for three-fluid model of interacting system of electrons, holes, and plasmons. We study its transport properties, especially the thermoelectric behavior.

Next, We provide a technical justification of the Boltzmann equations analyzed in Chapter 2. We derived the Coupled Boltzmann equations from the non-equilibrium quantum-field theory. To this end, we start in Chapter 3 by setting up the Keldysh quantum field theory for Coulomb-interacting Dirac electrons in two dimensions. We keep the discussion as general as possible such that with minor

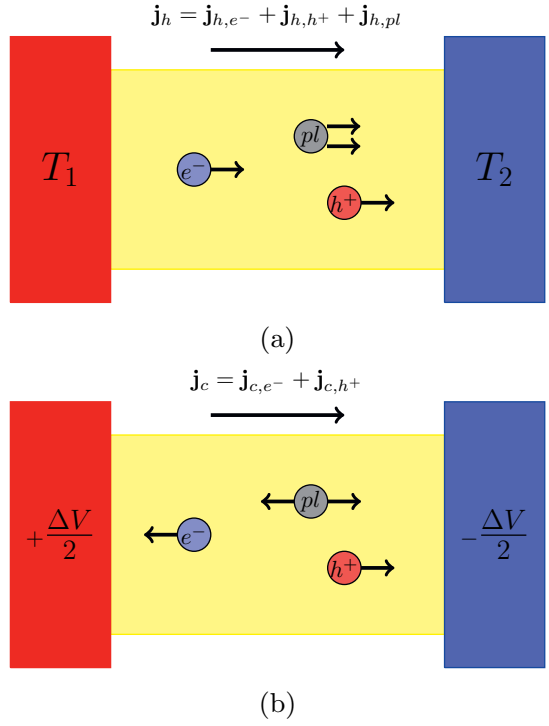

Figure 1.4: The difference between heat and charge current in the system of interacting charged Dirac electrons.(a) Electrons, holes, and plasmons react to a temperature gradient in the same manner. Plasmons make a direct contribution to the heat current. (b) Electrons and holes react oppositely to an applied voltage drop. Plasmons do not couple directly to the voltage difference, however, they experience drag and serve as a source of inelastic scattering.

modifications, this chapter can also apply to other systems, for example, a system of itinerant electrons or localized spins interacting via long-range dipole-dipole interactions, and a system of interacting Dirac electrons in a strong and uniform magnetic field. The research in the remainder of this thesis builds upon this formalism.

Next, we investigate the role of the Coulomb interaction in the Dirac system. Using a series of approximations, we derive semiclassical Boltzmann equations from a fully quantum mechanical treat-

ment based on Keldysh quantum-field theory. The weak coupling analysis is studied in Chapter 4. We show that two-component hydrodynamics as currently used for the description of graphene emerges within a weak-coupling approach to second order in Coulomb interaction. Within weak coupling, Coulomb interaction plays two different roles: (i) It is seen by an electron as an internal mean-field, known as the Hartree potential. This is the result of perturbation theory to first order, called the Hartree-Fock scheme [56]. The Fock term leads to a renormalization of the Fermi velocity [57, 58]; (ii) The Coulomb interaction manifests itself as an inelastic and momentum conserving scattering mechanism [33, 34, 32, 59, 12].

It has been known that low-order perturbation theory is unable to describe many important physical phenomena, for instance, collective modes, such as plasmons. We thus proceed by a strong-coupling analysis within the random phase approximation (RPA) or large-N approximation in Chapter 5. To this end, we introduce a new quantum field associated with a plasmon excitation by means of a Hubbard-Stratonovich transformation [60, 61]. This transformation maps our original model to an equivalent model describing an interacting system of electrons, holes, and plasmons. We show that our results respect the conservation laws of charge, momentum, and energy.

Finally, in Chapter 6, we numerically solve the coupled system of Boltzmann equations for the combined system of Dirac electrons, holes, and plasmons. We calculate, within linear response regime, the deviation of the distribution functions for the system that is exposed to an external electric field and a temperature gradient. From this solution, we calculate the thermo-electric conductivities. We find that plasmons give an extra contribution to the heat transport leading to an enhancement of the Wiedemann-Franz ratio at high dopings. We show that the simple models that we introduced in Chapter 2 provided qualitative results for conductivity, Seebeck coefficient, and thermal conductivity as same as the numerical solution.

Chapter 2

Thermo-electric response in two-dimensional Dirac systems: phenomenological approach

This chapter summarizes the main findings of the thesis. We discuss thermo-electric transport properties in Coulomb-interacting Dirac electrons. There are several different methods of studying transport theory. In this chapter, we employ a phenomenological approach based on the standard Boltzmann transport theory with a relaxation-time approximation. The justification and more detailed calculations, from a microscopic theory, will be discussed in subsequent chapters. The Coulomb interaction enters in two different ways that have different natures; (i) It enters as a collision integral explaining the charge current relaxation due to electron-electron scattering; (ii) It enters as a classical internal force term between electrons themselves, known as Hartree potential. This will be discussed in Sec. 2.2. The internal force is responsible for the emergence of the plasmon. We show in Sec. 2.3 the existence of the plasmons mode as a result of the Hartree potential and derive the energy-momentum relation. We find that the plasmon is gapless and follows a square-root energy dispersion, hence, we recover the plasmon dispersion that can be obtained from a more formal approach, the random-phase approximation (RPA). Next, we consider the transport phenomena of interacting Dirac electrons in two different scenarios. We consider the electron-hole plasma and study its

thermo-electric response in Sec. 2.4.1. We then proceed to study the thermo-electric response of the coupled system of electrons, holes, and plasmons in Sec. 2.4.2. This part can furthermore easily be adapted to the transport responses of a strongly coupled electron-boson liquid, for example, electron-phonon and itinerant electron-magnon systems. We finish the chapter with a conclusion and an outlook in Sec. 2.5[1].

2.1 Introduction

Hydrodynamic behavior of interacting electrons in solid-state systems has received a renewal of interest in recent years. This came from theorists and experimentalists alike, but was mostly driven by an increasing number of experimental observations in a broad range of materials [39, 62, 63]. The prime representative in terms of materials has been graphene and to a lesser extent bilayer graphene [64]. Although the physical condition required for observing hydrodynamic behavior of electrons is demanding, the advancement in synthesizing nearly clean graphene sheets encapsulated in boron nitride [21] allowed the community to explore several electron hydrodynamic phenomena over the past few years [18, 19, 37, 36, 65, 38]. Besides being superclean with very little disorder scattering, the concentration of phonons is also suppressed in these devices. Consequently, the usual momentum relaxation of electrons by means of collisions with impurities and phonons becomes less frequent. As a result, electron-electron collisions which conserve total charge density, total momentum density, and total energy density can become the dominant relaxational process [12, 59, 33, 34, 32]. If that is the case, the dynamics of the electrons can be described by the hydrodynamic transport theory of a typical fluid [45, 44, 48, 66, 49].

There is a different set of systems, that has been discussed recently. It uses phonons to its advantage: instead of destroying the hydrodynamic behavior, it is proposed that, when the electron-phonon collision is the dominant scattering process and phonons

[1]This chapter is based on part of K. Pongsangangan, T. Ludwig, H.T.C. Stoof, and L. Fritz, *Hydrodynamics of charged Dirac electrons in two dimensions. I. Thermoelectric transport.* (accepted at PRB) (2022).

cannot relax momentum in the lattice or from higher-order scattering, electrons and phonons transfer their momentum between each other and form a single strongly coupled fluid that can again be described by a hydrodynamic theory. This electron-phonon hydrodynamics reveals unique transport properties which are different from the electron hydrodynamics; for example, in the temperature dependence of thermo-electric conductivities [67, 68, 69].

Collective oscillations of particles about their equilibrium position, like phonons, are ubiquitous phenomena in solid-state systems [70]. In addition to phonons that arise from lattice oscillations, there are also emergent collective excitations in interacting-electron systems; for example, plasmons and/or magnons. This naturally leads to a question: can exotic hydrodynamics arise also from a combined system of electrons and their collective modes? These excitations are bosonic in nature. So, in thermal equilibrium, they obey the Bose-Einstein distribution. Furthermore, they have no obvious innate relaxation mechanism; unlike phonons, which have the lattice. The interplay between the collective modes and the electrons may give rise to rich effects in transport phenomena. One such example is the interplay between magnons and itinerant electrons in metallic magnetic heterostructures that has been studied in the context of spintronics [71]. Here, we focus on plasmons.

The problem of interactions between electrons and plasmons was put forth by a series of seminal works by Bohm and Pines in the 1960s [5, 6, 51, 72, 11]. We revisit this problem; we present and solve the kinetic theory for a coupled system of electrons and plasmons in two-dimensional interacting Dirac electrons. In particular, we will show that—in heat-transport experiments—plasmons make a direct contribution that can potentially be of the same order of magnitude as the electronic contributions [73].

In this chapter, we theoretically investigate the full thermo-electric transport properties of an interacting system of electrons and a collective mode that are coupled via perfect drag in the hydrodynamic limit. We use an approach based on a Boltzmann transport equation with a relaxation-time approximation. We treat electrons and bosons on an equal footing and discuss the hydrodynamic behavior of the combined system. While being particularly interested in the

hydrodynamics of the coupled system of electrons and plasmons, we develop a theory that can be applied straighforwardly to any hybrid system of electrons, holes, and bosons.

2.2 Boltzmann equations for Coulomb-interacting Dirac electrons

We start with a brief review of the Boltzmann transport theory. The basic assumption is that the system can be regarded as a collection of well-defined excitations, the so-called quasi-particles. It is quite remarkable that several strongly correlated many-particle systems can be regarded as a collection of weakly interacting quasi-particles [70]. The most prominent example is the Landau Fermi liquids [7, 8, 9]. This requires that the excitation with momentum $\vec{p}$ possesses a definite complex energy spectrum, says $\hbar\omega(\vec{p}) = \epsilon(\vec{p}) - i\gamma(\vec{p})$, where the real part $\epsilon(\vec{p})$ is the energy band dispersion and the imaginary part $\gamma(\vec{p})$ describes a decay rate which is inversely proportional to the lifetime of the excitation. Moreover, the excitation must be long-lived which means that the decay rate must be at least underdamped $\gamma(\vec{p}) \ll \epsilon(\vec{p})$ [70].

One assumes the existence of the distribution function $f_\lambda(\vec{x}, \vec{p}, t)$ and uses it to describe the behaviors of the quasi-particles. It gives the probability that the particle of momentum $\vec{p}$ in a state λ is found in a neighborhood of a spatial position $\vec{x}$ at time t. The knowledge of the distribution function is used to determined any physical observables in a straightforward fashion, for example, the electric current and heat current in Eq.(2.23) are given by

$$\vec{j} = -Ne \sum_\lambda \int \frac{d\vec{p}}{(2\pi)^2}\, \vec{v}_\lambda f_\lambda, \tag{2.1}$$

and

$$\vec{j}^Q = N \sum_\lambda \int \frac{d\vec{p}}{(2\pi)^2}\, \vec{v}_\lambda \epsilon_\lambda(\vec{p}) f_\lambda, \tag{2.2}$$

respectively, where $\epsilon_\lambda(\vec{p})$ is the energy of the particle in the state $\vec{p}$ and λ which is measured with respect to a chemical potential.

Here $v_\lambda(\vec{p}) = \vec{\nabla}_{\vec{p}}\epsilon_\lambda(\vec{p})$ is the corresponding group velocity and N is the number of degeneracy. Hereafter we set $\hbar = e = v_F = 1$ unless stated otherwise. The Boltzmann transport equation is an integro-differential equation governing the evolution of $f_\lambda(\vec{x}, \vec{p}, t)$ in time through phase space. A set of Boltzmann transport equations for Coulomb-interacting charged Dirac electrons in two dimensions reads as

$$\left(\partial_t + \vec{v}_\lambda(\vec{p}) \cdot \vec{\nabla} - \vec{\nabla} V^H(\vec{x}) \cdot \vec{\nabla}_{\vec{p}}\right) f_\lambda(\vec{x}, \vec{p}, t) = \mathcal{C}_\lambda^{\text{e-e}}[f_+, f_-](\vec{p}) + C_\lambda^{\text{dis}}[f_\lambda](\vec{p}). \quad (2.3)$$

The subscript λ here takes on the value $+$ and $-$ denoting the conduction-band and valence-band electrons, respectively. $f_\lambda(\vec{x}, \vec{p}, t)$ represents the distribution functions for electrons in the conduction band, when $\lambda = +$ and valence band, when $\lambda = -$. The Dirac electron follows a linear energy-momentum dispersion relation $\epsilon_\pm(\vec{p}) = \pm\hbar v_F p - \mu$, where v_F is Fermi velocity and μ is chemical potential. Here p denote the magnitude of the two-dimensional momentum $\vec{p}$. The group velocity $\vec{v}_\pm(\vec{p})$ is determined from the corresponding energy band by means of $\vec{v}_\pm(\vec{p}) = \vec{\nabla}_{\vec{p}}\epsilon_\pm(\vec{p}) = \pm\hbar v_F \hat{p}$, where $\hat{p}$ denotes a unit vector in the direction of $\vec{p}$. Since electrons are charged, they are correlated with each other via the internal long-range forces $-\vec{\nabla} V^H(\vec{x})$, where

$$V^H(\vec{x}) = \int d\vec{x}' V(\vec{x} - \vec{x}') \left(n(\vec{x}') - n_0\right). \quad (2.4)$$

This potential energy is typically known as the Hartree potential resulting from the Coulomb interaction compensated by an interaction between electrons and a positively charged background of ions. This potential is responsible for non-local transport responses where the conductivities are spacetime dependent and has been studied elsewhere [74, 75]. We are interested in another important manifestation of the Hartree potential which is the collective mode associated with the plasma oscillations or plasmons. In the subsequent section, starting from Eq. (2.3), the dispersion relation for the plasmon will be derived

The right-hand side is the central part of the Boltzmann equation. It is collision integrals which describes the relaxation pro-

cesses for the transport phenomena. It can be derived, for example, using Fermi's Golden Rule or from a microscopic non-equilibrium quantum-field theory. We consider effects from two scattering processes here: the electron-electron scattering denoted by $C^{\text{e-e}}[f_+, f_-](\vec{p})$, and the electron-disorder scattering denoted by $C_\lambda^{\text{dis}}[f_\lambda](\vec{p})$.

While the explicit expression of the collision integrals is not important for our discussion here, some of their properties are assumed.

The electron-electron scattering possesses three collisional invariants which are charge, momentum, and energy. This implies that multiplying the collision integral by the collisional invariants followed by summing over all states results in an answer of zero:

$$\sum_{\lambda=\pm} \int \frac{d\vec{p}}{(2\pi)^2}\, C_\lambda^{\text{e-e}}[f_+, f_-](\vec{p}) = 0, \tag{2.5}$$

$$\sum_{\lambda=\pm} \int \frac{d\vec{p}}{(2\pi)^2}\, \vec{p}\, C_\lambda^{\text{e-e}}[f_+, f_-](\vec{p}) = 0, \tag{2.6}$$

$$\sum_{\lambda=\pm} \int \frac{d\vec{p}}{(2\pi)^2}\, \left(\epsilon_\pm(\vec{p}) + V^H(\vec{x})\right) C_\lambda^{\text{e-e}}[f_+, f_-](\vec{p}) = 0. \tag{2.7}$$

In contrast, the group velocity is not a collisional invariant. Therefore, the current density is not conserved by electron-electron interactions especially at charge neutrality. This implies that

$$\sum_{\lambda=\pm} \int \frac{d\vec{p}}{(2\pi)^2}\, \lambda v_F p C_\lambda[f](\vec{p}) \approx -\frac{\vec{j}}{\tau_c}. \tag{2.8}$$

For the purpose of this chapter, we resort to a relaxation time approximation and introduce a mean free-time τ_c for charge transport due to electron-electron collisions.

The electron-disorder scattering conserves energy and charge but relax momentum and elctric current. This implies that

$$\sum_{\lambda=\pm} \int \frac{d\vec{p}}{(2\pi)^2}\, C_\lambda^{\text{dis}}[f_\lambda](\vec{p}) = 0, \tag{2.9}$$

$$\sum_{\lambda=\pm} \int \frac{d\vec{p}}{(2\pi)^2}\, \vec{p}\, C_\lambda^{\text{dis}}[f_\lambda](\vec{p}) \approx -\frac{\delta \vec{n}^{\vec{p}}}{\tau^{\text{dis}}}, \tag{2.10}$$

$$\sum_{\lambda=\pm}\int\frac{d\vec{p}}{(2\pi)^2}\,\left(\epsilon_{\pm}(\vec{p})+V^H(\vec{x})\right)C_\lambda^{\rm dis}[f_\lambda](\vec{p})=0, \tag{2.11}$$

$$\sum_{\lambda=\pm}\int\frac{d\vec{p}}{(2\pi)^2}\,\lambda v_F p C_\lambda[f](\vec{p})\approx-\frac{\vec{j}}{\tau^{\rm dis}}. \tag{2.12}$$

Here $\delta n^{\vec{p}}$ defines the deviation of the momentum density from its equilibrium value and $\tau^{\rm dis}$ is the relaxation time due to electron-disorder collisions.

It is interesting to note that, due to the linear dispersion relation of the Dirac system, the energy current is proportional to the momentum density by means of $\vec{j}^{\epsilon}=v_F^2 n^{\vec{p}}$. The charge current and the momentum density are distinct.

2.3 Plasmons

In this section, we show the existence of plasmon in the two-dimensional interacting Dirac electrons and derive its energy dispersion relation[2]. To this end, we consider equations of motion for charge density

$$\partial_t n(\vec{x},t)+\vec{\nabla}\cdot\vec{j}(\vec{x},t)=0, \tag{2.13}$$

and charge current

$$\partial_t\vec{j}+\vec{\nabla}\cdot\vec{\vec{\Xi}}(\vec{x},t)+\vec{\nabla}V^H(\vec{x})\cdot\vec{\vec{\Lambda}}(\vec{x},t)=-\frac{\vec{j}(\vec{x},t)}{\tau_c}-\frac{\vec{j}(\vec{x},t)}{\tau^{\rm dis}}, \tag{2.14}$$

as the plasmon is a collective mode associated with oscillations of charge density fluctuations. The equation for charge currents are obtained by integrating each Boltzmann equation over the corresponding group velocity $v_\pm(\vec{p})$ and subsequently multiplying the resulting equations with $-e$. We defined above two second-rank tensors ac-

[2]This discussion is based on part of K. Pongsangangan, T. Ludwig, H.T.C. Stoof, and L. Fritz, *Hydrodynamics of charged Dirac electrons in two dimensions. II. Role of collective modes.* (accepted at PRB) (2022).

cording to

$$\vec{\vec{\Xi}}(\vec{x},t) = N\sum_{\lambda=\pm}\int\frac{d\vec{p}}{(2\pi)^2}\Big[\vec{v}_+(\vec{p})\vec{v}_+(\vec{p})f_+(\vec{x},t,\vec{p}) - \vec{v}_-(\vec{p})\vec{v}_-(\vec{p})(1-f_-(\vec{x},t,\vec{p}))\Big], \tag{2.15}$$

and

$$\vec{\vec{\Lambda}}(\vec{x},t) = N\int\frac{d\vec{p}}{(2\pi)^2}\Big[\vec{\nabla}_{\vec{p}}\vec{v}_+(\vec{p})f_+(\vec{x},t,\vec{p}) -\vec{\nabla}_{\vec{p}}\vec{v}_-(\vec{p})(1-f_-(\vec{x},t,\vec{p}))\Big]. \tag{2.16}$$

Consider small density fluctuations around the constant and homogeneous solution, says $n = n_0 + \delta n$, and a small current $\vec{j}$. We insert this solution into Eqs.(2.13), and (2.14) and keep terms up to linear order in the fluctuations. This yields

$$\begin{aligned}\partial_t\delta n(\vec{x},t) + \vec{\nabla}\cdot\vec{j}(\vec{x},t) &= 0,\\ \partial_t\vec{j} + \vec{\nabla}\cdot\vec{\vec{\Xi}}(\vec{x},t) + \vec{\nabla}V^H(\vec{x})\cdot\vec{\vec{\Lambda}}(\vec{x},t) &= -\frac{\vec{j}(\vec{x},t)}{\tau_c} - \frac{\vec{j}(\vec{x},t)}{\tau^{\rm dis}}.\end{aligned} \tag{2.17}$$

Here

$$\vec{\vec{\Xi}}_{ij} = \delta n v_F^2/2\delta_{ij}, \tag{2.18}$$

and

$$\vec{\vec{\Lambda}}_{ij} = \Lambda^{(0)}\delta_{ij} = \frac{N}{4\pi}T\log(2+2\cosh\mu/T)\delta_{ij}. \tag{2.19}$$

The solution to this equation are propagating waves of the form

$$\begin{pmatrix}\delta n(\vec{x},t)\\ \vec{j}(\vec{x},t)\end{pmatrix} = \begin{pmatrix}\delta n(\vec{p},\omega)\\ \vec{j}(\vec{p},\omega)\end{pmatrix}e^{i\vec{p}\cdot\vec{x}-i\omega t}. \tag{2.20}$$

We insert this solution into the linearized equations above followed by a projection of the current equation onto $\hat{p}$. We obtain

$$\begin{pmatrix}-i\omega & ip\\ i2\pi\alpha v_F\Lambda^{(0)} + ipv_F^2/2 & -i\omega + \frac{1}{\tau_c} + \frac{1}{\tau^{\rm dis}}\end{pmatrix}\begin{pmatrix}\delta n\\ j_\parallel\end{pmatrix} = \begin{pmatrix}0\\0\end{pmatrix} \tag{2.21}$$

For this equation to be valid, the frequency of the density fluctuations has to satisfy the dispersion relation

$$\omega_{\pm}(\vec{p}) = \pm\sqrt{\frac{N}{2}\alpha v_F T p \log(2 + 2\cosh \mu/T) + \frac{v_F^2 p^2}{2} - \frac{1}{4\tau^2}} - \frac{i}{2\tau}. \tag{2.22}$$

Here $1/\tau = 1/\tau_c + 1/\tau^{\text{dis}}$. In Fig. (2.1), real and imaginary parts of the plasmon frequency in Eq.(2.22) is plotted at the charge neutrality point. The real part gives the energy of plasmon which follows a square-root energy dispersion relation. The imaginary part gives the decay rate. We find that due to electron-electron and electron-disorder collisions, plasmon frequency at low momentum becomes purely imaginary which gives an over-damped mode. We will see in the subsequent chapter that, when we neglect this effect by setting $1/\tau = 0$, this result agrees with the RPA calculation.

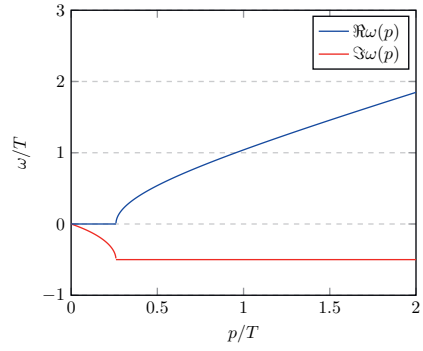

Figure 2.1: The figure shows the real and imaginary parts of the frequency of the density fluctuations as a function of momentum at the charge neutrality point $\mu/T = 0$. In the plot, the momentum and frequency are in the unit of T. The values for the parameters are chosen for illustrative purpose and given by $\alpha = 0.3$, $1/\tau = 1$, and $N = 4$.

2.4 Thermo-electric transport coefficients for Coulomb-interacting Dirac electrons

In this section, we derive thermo-electric transport coefficients of a system of two-dimensional Dirac electrons interacting via Coulomb interactions. We consider a setup that can accommodate electrons, holes, and collective modes. First, we consider the electron-hole hydrodynamics, a model that is popular in the context of graphene, and its transport properties. Next, we propose a novel type of hydrodynamics. In that setup, the 'fluid' consists of electrons, holes, and plasmons. We study its transport properties, especially the thermo-electric behavior. The results of this part can also be adapted to the study of a fluid consisting of electrons and phonons.

When an external electric field $\vec{E}$ and a temperature gradient $-\vec{\nabla}T$ are applied to a conductor, in linear response regime, electric current $\vec{j}$ and heat current $\vec{j}^Q$ are given by constitutive relations of the form

$$\begin{pmatrix} \vec{j} \\ \vec{j}^Q \end{pmatrix} = \begin{pmatrix} \sigma & \alpha \\ T\bar{\alpha} & \bar{\kappa} \end{pmatrix} \begin{pmatrix} \vec{E} \\ -\vec{\nabla}T \end{pmatrix}, \tag{2.23}$$

where σ is the electrical conductivity and $\bar{\kappa}$ is the thermal conductivity. The heat current $\vec{j}^Q$ is a combination of energy current $\vec{j}^\epsilon$ and charge current $\vec{j}$ according to

$$\vec{j}^Q = \vec{j}^\epsilon - \frac{\mu}{e}\vec{j}. \tag{2.24}$$

In a typical thermal transport experiment, the heat current is measured with the condition that $\vec{j} = 0$. With a straightforward algebra, the thermal conductivity in this case is given $\kappa = \bar{\kappa} - T\alpha\bar{\alpha}/\sigma$.

Furthermore, we assume that the system respects time reversal symmetry and, consequently, the Onsager reciprocal relation [76] requires that

$$\alpha = \bar{\alpha}. \tag{2.25}$$

Later, we use this relation to establish the relationship between the relaxation times associated with the drag effect.

2.4.1 Thermo-electric responses of an electron-hole plasma

In this section, we determine the thermo-electric transport coefficients of the Coulomb interacting charged Dirac electron by solving the coupled Boltzmann equations in the presence of an external electric field $\vec{E}$ and a temperature gradient $-\vec{\nabla}T$ within linear response theory. The Boltzmamm equation is a non-linear integro-differential equation, so, in general, it is very complicated to solve it exactly. However, within linear response theory, the system of interest is assumed to be near-equilibrium and, thus, the distribution function f takes the form $f \approx f^0 + \delta f$, where f^0 is the equilibrium solution and the deviation of the distribution function δf is linear order in external fields. The solution of the linearized coupled Boltzmann equations can be obtained by converting the Bolzmann equation to a linear algebra problem and solve it numerically [77]. This will be discussed in details in the subsequently chapter. In this chapter, we resort to the relaxation-time approximation to discuss the qualitative feature of thermo-electric responses [78]. In this approximation, all the collisional processes are summarized in one quantity, the relaxation time τ. Within this approximation, the collision integral on the right-hand side of Eq.(2.3) is given by

$$C_{\lambda}^{\text{e-e}}[f_+, f_-](\vec{p}) = -\frac{\delta f_\lambda}{\tau_\lambda} + \frac{\delta f_{-\lambda}}{\tau_{-\lambda}}, \tag{2.26}$$

and

$$C_{\lambda}^{\text{dis}}[f_\lambda](\vec{p}) = -\frac{\delta f_\lambda}{\tau^{\text{dis}}}. \tag{2.27}$$

In the presence of an external electric field $\vec{E}$ and a temperature gradient $-\vec{\nabla}T$, after the linearization, the driving term on the left-hand side of Eq.(2.3) becomes

$$D_\lambda[f_\lambda] = \partial_t \delta f_\lambda - \left(\epsilon_\lambda(\vec{p})\frac{\vec{\nabla}T}{T} + e\vec{E}\right)\cdot\vec{\nabla}_{\vec{p}} f^0_\lambda, \tag{2.28}$$

where $\epsilon_\lambda(\vec{p})$ defines the energy of Dirac electrons measured with respect to the chemical potential μ. Here we neglect the internal

electric field, its contribution to thermo-electric transport phenomena by means of plasmons will be discussed in subsequent section. We are interested in the steady state, *i.e.*, $\partial_t f_\lambda = 0$. The linearized Boltzmann equations may be cast into the matrix form according to

$$\begin{pmatrix} \frac{1}{\tau_+} + \frac{1}{\tau^{\rm dis}} & -\frac{1}{\tau_-} \\ -\frac{1}{\tau_+} & \frac{1}{\tau_-} + \frac{1}{\tau^{\rm dis}} \end{pmatrix} \begin{pmatrix} \delta f_+ \\ \delta f_- \end{pmatrix} = \frac{\vec{\nabla} T}{T} \cdot \begin{pmatrix} \epsilon_+(\vec{p}) \vec{\nabla}_{\vec{p}} f_+^0 \\ \epsilon_-(\vec{p}) \vec{\nabla}_{\vec{p}} f_-^0 \end{pmatrix} + e\vec{E} \cdot \begin{pmatrix} \vec{\nabla}_{\vec{p}} f_+^0 \\ \vec{\nabla}_{\vec{p}} f_-^0 \end{pmatrix} . \tag{2.29}$$

It is straightforward to solve this matrix equation for $\delta f_\pm$ in terms of the external disturbances $\vec{E}$ and $-\vec{\nabla} T$. Subsequently, by substituting the result into the charge and heat currents defined in Eqs.(2.1), and (2.2), we find the longitudinal response functions that are defined in Eq.(2.23). They are given by

$$\sigma = -\frac{e^2 \left(\mathcal{E}_+ \left(\frac{1}{\tau^{\rm dis}} + \frac{1}{\tau_-} - \frac{1}{\tau_+} \right) + \mathcal{E}_- \left(\frac{1}{\tau^{\rm dis}} + \frac{1}{\tau_+} - \frac{1}{\tau_-} \right) \right)}{\frac{1}{\tau^{\rm dis}} \left(\frac{1}{\tau^{\rm dis}} + \frac{1}{\tau_+} + \frac{1}{\tau_-} \right)} , \tag{2.30}$$

$$\bar{\kappa} = -\frac{1}{T} \frac{\left(\mathcal{S}_+ + \mathcal{S}_- \right) \left(\frac{1}{\tau^{\rm dis}} + \frac{1}{\tau_-} + \frac{1}{\tau_+} \right) + 2\mu \left(\frac{\mathcal{T}_+}{\tau_+} + \frac{\mathcal{T}_-}{\tau_-} \right)}{\frac{1}{\tau^{\rm dis}} \left(\frac{1}{\tau^{\rm dis}} + \frac{1}{\tau_+} + \frac{1}{\tau_-} \right)} , \tag{2.31}$$

$$\alpha = \frac{e}{T} \frac{\mathcal{T}_+ \left(\frac{1}{\tau^{\rm dis}} + \frac{1}{\tau_-} - \frac{1}{\tau_+} \right) + \mathcal{T}_- \left(\frac{1}{\tau^{\rm dis}} + \frac{1}{\tau_+} - \frac{1}{\tau_-} \right)}{\frac{1}{\tau^{\rm dis}} \left(\frac{1}{\tau^{\rm dis}} + \frac{1}{\tau_+} + \frac{1}{\tau_-} \right)} , \tag{2.32}$$

Here $\mathcal{E}_\pm$, $\mathcal{T}_\pm$, and $\mathcal{S}_\pm$ are main diagonal elements of second-rank tensors

$$\begin{aligned} \vec{\vec{\mathcal{E}}}_\pm &= \int_{\vec{k}} \vec{v}_\pm(\vec{k}) \partial_{\vec{k}} f_\pm^0(\vec{k}) , \\ \vec{\vec{\mathcal{T}}}_\pm &= \int_{\vec{k}} \vec{v}_\pm(\vec{k}) \epsilon_\pm(\vec{k}) \partial_{\vec{k}} f_\pm^0(\vec{k}) , \\ \vec{\vec{\mathcal{S}}}_\pm &= \int_{\vec{k}} \vec{v}_\pm(\vec{k}) \left(\epsilon_\pm(\vec{k}) \right)^2 \partial_{\vec{k}} f_\pm^0(\vec{k}) . \end{aligned} \tag{2.33}$$

Hence, $\vec{\vec{\mathcal{E}}}_\pm = \mathcal{E}_\pm \vec{\vec{\mathbb{1}}}$, $\vec{\vec{\mathcal{T}}}_\pm = \mathcal{T}_\pm \vec{\vec{\mathbb{1}}}$, and $\vec{\vec{\mathcal{S}}}_\pm = \mathcal{S}_\pm \vec{\vec{\mathbb{1}}}$. For Dirac fermions with a linear energy dispersion, we find that

$$\begin{aligned}
\mathcal{E}_\pm &= \frac{T}{4\pi}\mathrm{Li}_1\left(-e^{\pm\mu/T}\right) \\
\mathcal{T}_\pm &= \pm\frac{T^2}{2\pi}\mathrm{Li}_2\left(-e^{\pm\mu/T}\right) - \frac{T\mu}{4\pi}\mathrm{Li}_1\left(-e^{\pm\mu/T}\right) , \\
\mathcal{S}_\pm &= -\frac{T}{4\pi}\Big[-3T^2\mathrm{Li}_3\left(-e^{\pm\mu/T}\right) \pm 4T\mu\mathrm{Li}_2\left(-e^{\pm\mu/T}\right) \\
&\quad -\mu^2\mathrm{Li}_1\left(-e^{\pm\mu/T}\right)\Big]. \qquad (2.34)
\end{aligned}$$

Furthermore, for the Onsager reciprocal relation in Eq.(2.25) to hold, the relaxation time for the electron-hole drag must satisfy the relation

$$\frac{1}{\tau_-}\left(\mathcal{T}_{-,xx} + \mu\mathcal{E}_{-,xx}\right) = -\frac{1}{\tau_+}\left(\mathcal{T}_{+,xx} + \mu\mathcal{E}_{+,xx}\right). \qquad (2.35)$$

Therefore, we can choose

$$\begin{aligned}
\frac{1}{\tau_+} &= \frac{1}{\tau_0}\frac{\mathcal{T}_- + \mu\mathcal{E}_-}{\left(\mathcal{T}_- + \mu\mathcal{E}_-\right) - \left(\mathcal{T}_+ + \mu\mathcal{E}_+\right)} , \\
\frac{1}{\tau_-} &= -\frac{1}{\tau_0}\frac{\mathcal{T}_+ + \mu\mathcal{E}_+}{\left(\mathcal{T}_- + \mu\mathcal{E}_-\right) - \left(\mathcal{T}_+ + \mu\mathcal{E}_+\right)} . \qquad (2.36)
\end{aligned}$$

where τ_0 is a relaxation time that has to be determined from a Boltzmann equation. All the quantities in Eq. (2.35) and Eq. (2.36) depend strongly on μ/T; including τ_0. Since the system at charge neutrality is a quantum critical system, the relaxation time there is of order $1/T$, saturating at the Planckian limit. This fixes $1/\tau_0 \propto T$. Upon moving away from charge neutrality, all drag effects are strongly suppressed. In Appendix 2.6.1, we demonstrate this explicitly. For practical calculations using the relaxation time approximation, we used the interpolation function $1/\tau_0 = 0.6T\exp(-|\mu|/T)$. This function shows good qualitative agreement with the actual functions calculated in Appendix 2.6.1. An important consequence of this is that at large $|\mu|/T$, everything is disorder dominated.

In Fig. 2.2, we show the relaxation time for the electron-hole drag.

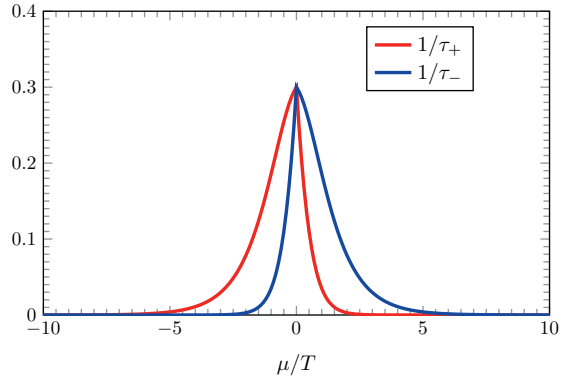

Figure 2.2: The relaxation time for the electron-hole drag near the charge neutrality point $\mu = 0$ calculated from Eq. (2.36). The chemical potential and the relaxation time are scaled in the units of T. We use $1/\tau_0 = 0.6T \exp(-|\mu|/T)$ here for illustrative purposes.

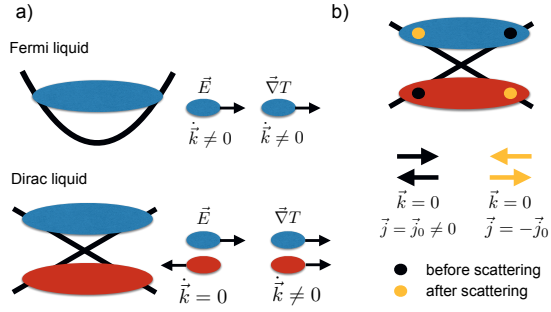

Figure 2.3: a) In a Fermi liquid, an applied electric field as well as a temperature gradient excite nonzero momentum. In the Dirac liquid, a temperature gradient excites a nonzero momentum, whereas an electric field does not. b) In the Dirac liquid, momentum and current decouple. One can relax current without relaxing momentum.

In Figures.(2.4), (2.5), (2.6), and (2.7), we show that the transport coefficients calculated from our theory have the qualitative feature as the experimental resuls taken from Refs.[18] and [19].

The electrical conductivity

In Fig.(2.4), we plot the electrical conductivity at various values of chemical potential near the neutrality point. A key signature of the electron-hole plasmas sits in their electrical conductivity and becomes most apparent at charge neutrality $\mu = 0$. It revolves around a somewhat paradoxically looking situation. The system has a total charge zero, $n_c = 0$. Nevertheless, the d.c. conductivity in the clean limit is finite. From Eq. (2.30), we find that the electrical conductivity at charge neutrality is given by

$$\sigma(\mu = 0) = -e^2 \frac{\mathcal{E}_+ + \mathcal{E}_-}{\frac{1}{\tau^{\rm dis}} + \frac{1}{\tau_+} + \frac{1}{\tau_-}} \tag{2.37}$$

where, as depicted in Fig.(2.2), the inverse drag scattering times for electron and hole are identical at charge neutrality , *i.e.*, $1/\tau_- = 1/\tau_+$, and, according to Eq. (2.34), $\mathcal{E}_+ + \mathcal{E}_- \neq 0$. This implies that the electrical conductivity is finite, even in the absence of disorder, *i.e.*, for $1/\tau^{\rm dis} = 0$. The key to understanding it is that while the charge density $n_c = 0$, the imbalance density $n_{\rm imb} \neq 0$. This is in stark contrast to a conventional Fermi liquid in which there is essentially no distinction between the two densities. Importantly, at finite temperature, there are two thermal clouds of equal density, one of electrons and one of holes. An applied electric field will pull the different types of charge carriers into opposite directions. One consequence of this is that while electrons and holes are pulled apart, the total momentum of the system remains zero. This is different in a Fermi liquid, in which an applied field automatically excites momentum. Since there is no net momentum induced, it is also no issue that there are no impurities to relax the momentum. However, there is still a mechanism which 'glues' the electrons and holes, which is drag. This is sufficient to establish a finite electric current, even in the absence of disorder. A graphical illustration of this situation in shown in Fig. (2.3).

With a bit of algebra, one can show that Eq. (2.30) takes the form

$$\sigma = \sigma(\mu = 0) + \frac{e^2 \left(\mathcal{E}_- - \mathcal{E}_+\right) \left(\frac{1}{\tau_-} - \frac{1}{\tau_+}\right)}{\frac{1}{\tau^{\rm dis}} \left(\frac{1}{\tau^{\rm dis}} + \frac{1}{\tau_+} + \frac{1}{\tau_-}\right)} \,. \tag{2.38}$$

The second part becomes singular in the limit of zero disorder: upon tuning away from charge neutrality, $\mu \neq 0$, both $\mathcal{E}_- - \mathcal{E}_+$ and $1/\tau_- - 1/\tau_+$ are non-zero. This implies that the electrical conductivity is not finite in the absence of disorder ($1/\tau^{\rm dis} \to 0$), but diverges, as one would expect. This situation is qualitatively discussed in Fig. (2.3).

The thermoelectric coefficient

In Fig.(2.5), we plot the Seebeck coeeficient which is the ratio of the thermoelectric cofficient α to the electrical conductivity σ at various values of chemical potential near the neutrality point. A main signature of electron-hole plasmas is that at the charge neutrality, the Seebeck coefficient vanishes as

$$\alpha(\mu = 0) = \frac{e}{T} \frac{\mathcal{T}_+ + \mathcal{T}_-}{\frac{1}{\tau^{\rm dis}} + \frac{2}{\tau_+}} = 0. \tag{2.39}$$

The key to understanding it is that when the Dirac plasma is exposed to a temperature gradient, both thermal clouds of electrons and holes of equal concentration move in the same direction. As a result, $\vec{j}_c = 0$, this implies that $\alpha = 0$.

The heat conductivity

Here, we consider the response $\vec{j}^Q = -\kappa \vec{\nabla} T$, which is the heat conductivity in the absence of current flow, where the longitudinal thermal conductivity $\kappa = \bar{\kappa} - T\alpha^2/\sigma$. In Fig.(2.6), we plot the thermal conductivity of two-dimensional Dirac electrons doping close to the neutrality point. At the charge neutrality point, we find that

$$\kappa(\mu = 0) = -\frac{1}{T} \frac{\mathcal{S}_+ + \mathcal{S}_-}{\frac{1}{\tau^{\rm dis}}}. \tag{2.40}$$

Contrary to the electrical conductivity, the thermal conductivity decays from disorder and cannot be relaxed due to drag at the charge neutrality point. The reason is simple: the two thermal clouds, electrons and holes, are both dragged into the same direction. Consequently, a net momentum is induced. This implies that momentum has to be relaxed to establish a stationary state with a finite conductivity. This can only be achieved by scattering from impurities,

meaning in the clean system it diverges. This is again explained in Fig. (2.3).

The Wiedemann-Franz ratio

An important quantity in the study of metals is the Wiedemann-Franz ratio. This was already established in 1853 [79], based upon the observation that for a variety of metals, the ratio $\kappa/(T\sigma)$ tends to a constant, universal value at low temperatures, called the Lorenz number [56]. It was experimentally found that the Lorenz number is given by

$$L = \frac{\kappa}{T\sigma} = L_0 = \frac{\pi^2}{3}\left(\frac{k_B}{e}\right)^2 . \tag{2.41}$$

Whether a system tends to this value or not is still often taken as an empirical evidence of whether the system is a Fermi liquid or not. The standard understanding is that both heat and electrical currents are transported by the same type of (quasi-)particle. Additionally, both heat and electrical current undergo the same relaxational mechanism. In the case of a standard metal, this means that both heat and electrical current are limited by the same scattering time, $1/\tau^{\mathrm{dis}}$. We find

$$L/L_0 = \frac{\mathcal{S}_+ + \mathcal{S}_-}{\mathcal{E}_+ + \mathcal{E}_-}\left(1 + \frac{\tau_{\mathrm{dis}}\left(\tau_+ + \tau_-\right)}{\tau_+\tau_-}\right) \tag{2.42}$$

at the charge neutrality point. Not only does this ratio diverge for a clean system, it is also, in general, not a universal quantity: one should expect a possibly strong violation of the Wiedemann-Franz law close to charge neutrality as well as a strong variation across different samples. However, it is an excellent measure to determine the relative strength of elastic and inelastic scattering in the system. In Fig. 2.7, we plot the Lorenz number for the two-dimensional Dirac fluid around the charge neutrality point.

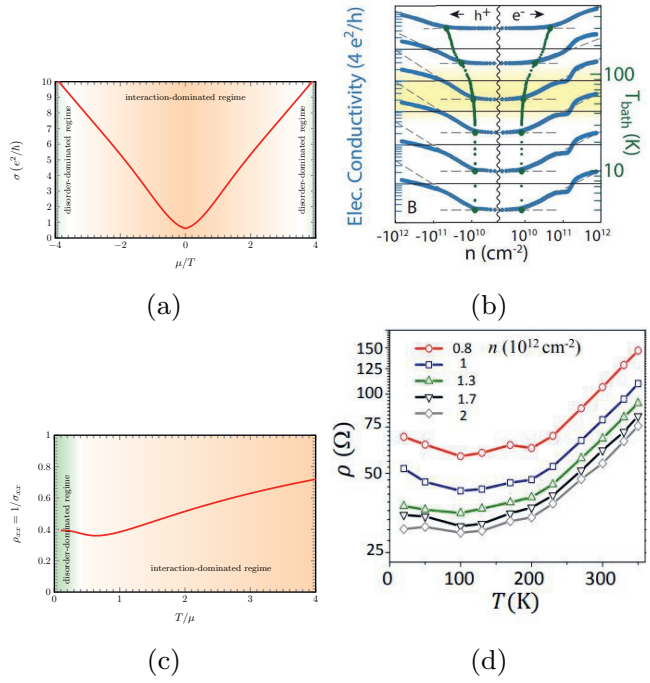

Figure 2.4: Comparison of the electrical conductivity of the Dirac electron-hole plasma evaluated from our kinetic theory within the relaxation time approximation with the experimental results. (a) The electrical conductivity evaluated from Eq. (2.30) as a function of the chemical potential μ, where $1/\tau_\pm$ satisfies the relation in Eq.(2.35) with $1/\tau_0 = 0.6Te^{-|\mu|/T}$ and $\tau^{\rm dis} = 8$. (b) The experimental measurement of the electrical conductivity of clean graphene as a function of doping. The figures is taken from Ref.[18] and reprinted with permission from . (c) The electrical resistivity $\rho = 1/\sigma$ evaluated from Eq.(2.30) as a function of the temperature. (d) The experimental result of the electrical resistivity of clean graphene as a function of the temperature. The figure is taken from Ref.[19] and reprinted with permission from APS.

2.4.2 Thermo-electric responses of a hybrid system of electrons, holes, and plasmons

In the previous section, we consider the thermo-electric transport in a electron-hole fluid. In this section, we discuss the role of the

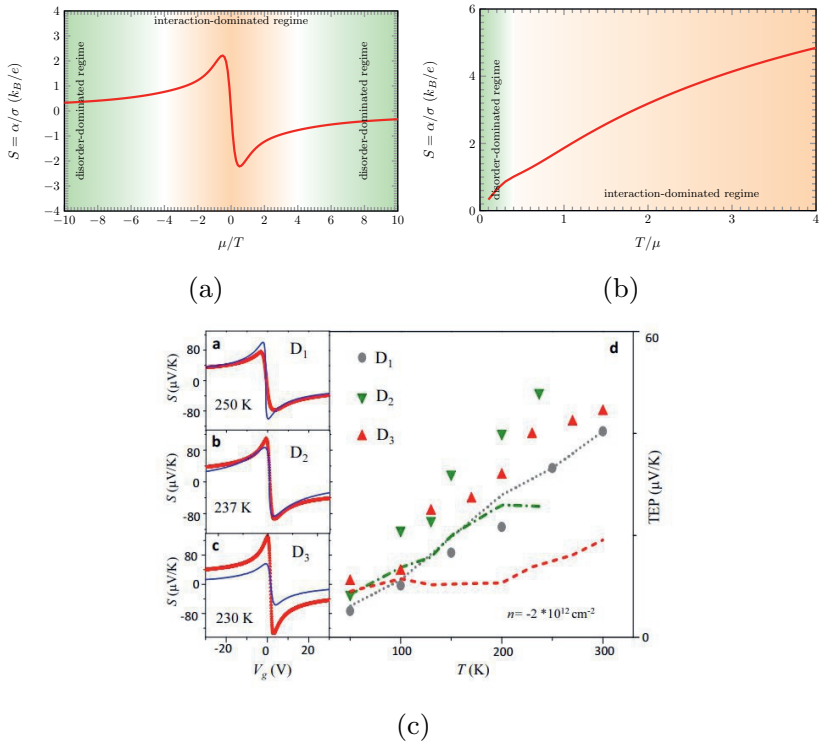

Figure 2.5: Comparison of the Seebeck coefficient of the Dirac electron-hole plasma evaluated from our kinetic theory within the relaxation time approximation with the experimental results. (a) The Seebeck coefficient evaluated from our theory as a function of chemical potential μ. (b) The Seebeck coefficient evaluated from our theory as a function of temperature T. Here we use the same values of parameters as we use in Fig.(2.4). (d) The experimental result of the Seebeck coefficient of clean graphene as a function of temperature as well as chemical potential. The figure is taken from Ref.[19] and reprinted with permission from APS.

internal electric potential in thermo-electric transport phenomena. One interesting effect of this force is the non-local transport response which has been investigated, for example, in Refs.[75, 74]. In this thesis, we focus on local thermo-electric transport. In this case, the Hartree potential has a direct contribution to thermo-electric

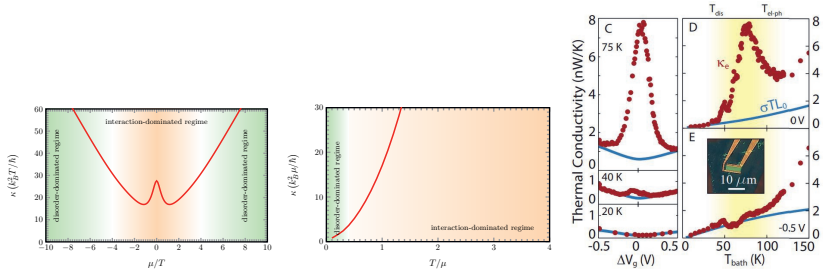

(a) (b) (c)

Figure 2.6: Comparison of the thermal conductivity of the Dirac electron-hole plasma evaluated from our kinetic theory within the relaxation time approximation with the experimental results. (a) The thermal conductivity evaluated from our theory as a function of the chemical potential μ. (b) The thermal conductivity evaluated from our theory as a function of the temperature T. Here we use the same values of parameters as we use in Fig.(2.4). (c) The experimental result of the thermal conductivity of clean graphene as a function of temperature as well as the charge density. The figure is taken from Ref.[18] and reprinted with permission from AAAS.

transport phenomena via the collective charge density oscillations or plasmons.

We theoretically investigate the full thermo-electric transport properties of an interacting system of electrons and a collective mode that are coupled via perfect drag in the hydrodynamic limit. In this section, to summarize the main feature of our findings, we use an approach based on a Boltzmann transport equation with a relaxation-time approximation. We treat electrons and bosons on an equal footing and discuss the hydrodynamic behavior of the combined system. While being particularly interested in the hydrodynamics of the coupled system of electrons and plasmons, we develop a theory that can be applied straighforwardly to any hybrid system of electrons, holes, and bosons.

Plasmons do not contribute directly to charge transport, because they are electrically neutral. However, they give an extra contribu-

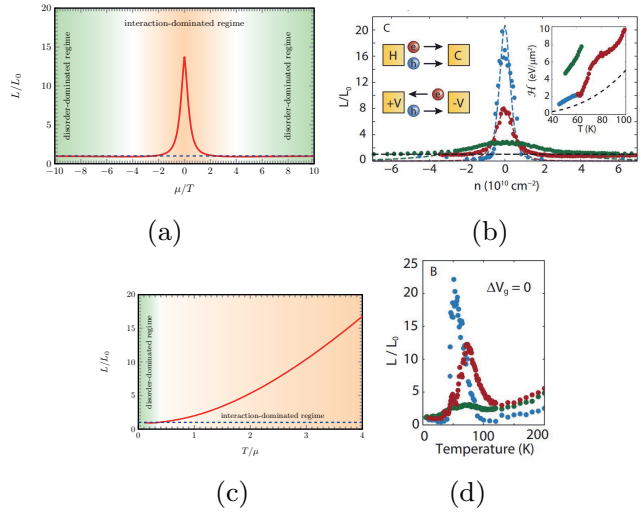

Figure 2.7: Comparison of the Lorenz number $L = \frac{\kappa}{\sigma T}$ of the Dirac electron-hole plasma evaluated from our kinetic theory within the relaxation time approximation with the experimental results. The Lorenz number evaluated from our theory as a function of (a) the chemical potential μ and (c) the temperature T. Here we use the same values of parameters as we use in Fig.(2.4). The experimental result of the thermal conductivity of clean graphene as a function of (b) the electron charge density and (d) the temperature. The figure is taken from Ref.[18] and reprinted with permission from AAAS.

tion to the heat current which is given by

$$\vec{J}_b^Q = \int \frac{d\vec{p}}{(2\pi)^2} \vec{v}_b(\vec{p})\omega(\vec{p})\delta b \,, \tag{2.43}$$

where δb is deviation of the distribution function for plasmons from the equilibrium solution. The deviation δb is a solution of the linearized coupled Boltzmann equations. Here $\omega(\vec{p})$ is the energy dispersion of the plasmon given by Eq.(2.22). However, we neglect the plasmon decay due to electron-electron and electron-disorder scatterings. This gives the collisionless plasmon energy dispersion that

agrees with the microscopic RPA result [54, 55]. It reads

$$\omega(\vec{p}) = \sqrt{\frac{N}{2}\alpha v_F T p \log\left(2 + 2\cosh(\mu/T)\right)}\,. \tag{2.44}$$

We obtain the coupled system of Boltzmann equations for a hybrid system of the electrons, holes, and plasmons and it takes the form

$$\begin{aligned}\left(\partial_t + \vec{v}_\lambda(\vec{p})\cdot\vec{\nabla}\right) f_\lambda(\vec{x},\vec{p},t) &= \mathcal{C}_\lambda[f_+,f_-,b](\vec{p}) \\ \left(\partial_t + \vec{v}_b(\vec{p})\cdot\vec{\nabla}\right) b(\vec{x},\vec{p},t) &= \mathcal{C}_b[f_+,f_-,b](\vec{p}),\end{aligned} \tag{2.45}$$

where $b(\vec{x},\vec{p},t)$ is the distribution function for the plasmon which the velocity $\vec{v}_b(\vec{p})$. To obtain the qualitative feature of the thermoelectric responses, we resort to the relaxation-time approximation.

$$C_\lambda[f_+,f_-,b](\vec{p}) = -\frac{\delta f_\lambda}{\tau_\lambda} + \frac{\delta f_{-\lambda}}{\tau_{-\lambda}} - \frac{\delta f_\lambda}{\tau^{\rm dis}} + \frac{\delta b}{\tau_b}, \tag{2.46}$$

and

$$C_b[f_+,f_-,b](\vec{p}) = -\frac{\delta b}{\tau_b/2}, \tag{2.47}$$

where τ_b is the Landau damping of a plasmon into an electron-hole pair. Within linear response theory, in the presence of an external electric field $\vec{E}$ and a temperature gradient $-\vec{\nabla}T$, we linearize the Boltzmann equations to linear order in external fields. The driving term on the left-hand side of the Boltzmann equation for fermion remains the same as Eq.(2.28). The driving term for the plasmon reads

$$D_b[b](\vec{p}) = \partial_t \delta b - \omega(\vec{p})\frac{\vec{\nabla}T}{T}\vec{\nabla}_{\vec{p}} b^0\,. \tag{2.48}$$

The deviation of the distribution functions to linear order in the external disturbances can be solved from The Boltzmann equations. This solution is used to determined charge and heat currents and, consequently, thermo-electric coefficients. We find that the expression for the electric conductivity remains the same as Eq.(2.30), since plasmons do not have a direct contribution to the charge current.

However, they can relax electrons, and thus modify the relaxation time for electron-hole drag according to

$$\begin{aligned}\frac{1}{\tau_+} &= \frac{\frac{1}{\tau_0'}\left(\mathcal{K}_- + 2\left(\mathcal{T}_- + \mu\mathcal{E}_-\right)\right)}{\left(\mathcal{K}_- + 2\left(\mathcal{T}_- + \mu\mathcal{E}_-\right)\right) - \left(\mathcal{K}_+ + 2\left(\mathcal{T}_+ + \mu\mathcal{E}_+\right)\right)}, \\ \frac{1}{\tau_-} &= \frac{-\frac{1}{\tau_0'}\left(\mathcal{K}_+ + 2\left(\mathcal{T}_+ + \mu\mathcal{E}_+\right)\right)}{\left(\mathcal{K}_- + 2\left(\mathcal{T}_- + \mu\mathcal{E}_-\right)\right) - \left(\mathcal{K}_+ + 2\left(\mathcal{T}_+ + \mu\mathcal{E}_+\right)\right)}.\end{aligned} \tag{2.49}$$

where

$$\begin{aligned}\mathcal{K}_+ &= \int_{\vec{k}} \vec{\nabla}_{\vec{k}} b^0 \vec{v}_+ \omega(k)\ , \\ \mathcal{K}_- &= \int_{\vec{k}} \vec{\nabla}_{\vec{k}} b^0 \vec{v}_- \omega(\vec{k})\ .\end{aligned} \tag{2.50}$$

Note that in calculating $\mathcal{K}_\pm$ above, the integrations have the momentum cutoff given by $k_c = \frac{N}{2}\alpha T \log(2 + 2\cosh(\mu/T))$. Beyond this value, the plasmons become over-damped and thus its corresponding distribution function is not well-defined. We assume that $\tau_0' = \tau_b$ since the electron-hole drag results effectively from the Landau damping.

In contrast, the themoelectric coefficient has an additional contribution from drag. It is given by

$$\alpha = \alpha_e + \alpha_{\text{drag}}\ , \tag{2.51}$$

where

$$\alpha_{\text{drag}} = \frac{e}{T}\frac{\left(\frac{1}{\tau^{\text{dis}}} + \frac{2}{\tau_-}\right)\mathcal{K}_+ + \left(\frac{1}{\tau^{\text{dis}}} + \frac{2}{\tau_+}\right)\mathcal{K}_-}{\frac{2}{\tau^{\text{dis}}}\left(\frac{1}{\tau^{\text{dis}}} + \frac{1}{\tau_+} + \frac{1}{\tau_-}\right)} \tag{2.52}$$

and α_e is given by Eq.(2.32). We observe that $\alpha_{\text{drag}} = 0$ at the charge neutrality. Similarly, there are three contributions the thermal conductivity according to

$$\kappa = \kappa_e + \kappa_b + \kappa_{\text{drag}}. \tag{2.53}$$

Here κ_e is from electrons and holes which is given by Eq.(2.31); κ_b is a direct contribution form plasmons which is given by

$$\kappa_b = -\frac{\tau_b/2}{T}\int_{\vec{k}} \vec{v}_b \left(\omega(\vec{k})\right)^2 \vec{\nabla}_{\vec{k}} b^0. \tag{2.54}$$

In addition, there is a contribution due to plasmon drag according to

$$\begin{aligned}\kappa_{\text{drag}} \quad = \quad & -\frac{1}{T}\frac{1}{\frac{2}{\tau^{\text{dis}}}\left(\frac{1}{\tau^{\text{dis}}}+\frac{1}{\tau_-}+\frac{1}{\tau_+}\right)} \times \\ & \int_{\vec{k}} \omega(\vec{k}) \left(\frac{\vec{v}_-(\epsilon_- - \mu)}{\frac{1}{\tau^{\text{dis}}}+\frac{2}{\tau_+}} + \frac{\vec{v}_+(\epsilon_+ - \mu)}{\frac{1}{\tau^{\text{dis}}}+\frac{2}{\tau_-}}\right) \vec{\nabla}_{\vec{k}} b^0.\end{aligned} \tag{2.55}$$

Figure 2.8 shows the thermo-electric coefficients of the hybrid system of electrons, holes, and plasmons. We observe the enhancement of the Weidemann-Franz ratio not only at the charge neutrality point but also at high doping due to the extra contribution from plasmon to the heat transport. This seems to be a feature that is also encountered in experiments in recent years [80].

2.5 Conclusion and Outlook

In this chapter, we investigated the full thermo-electric transport properties of an interacting fluid of electrons, holes, and a collective mode from a theoretical point of view. In the hydrodynamic limit we used an approach based on a Boltzmann transport equation within a relaxation-time approximation that mimics a full numerical solution of the set of equations. We treated electrons, holes and plasmons on equal footing and discussed the hydrodynamic behavior of the combined system. We discussed the thermo-electric behavior in the very clean system. One of our findings is that in that situation the plasmons make a sizeable contribution to transport properties and, therefore, cannot be neglected. We hypothesize that this also applies to other quantities sensitive to the energy-momentum tensor, such as the viscosity. The approach we develop can also be applied in a

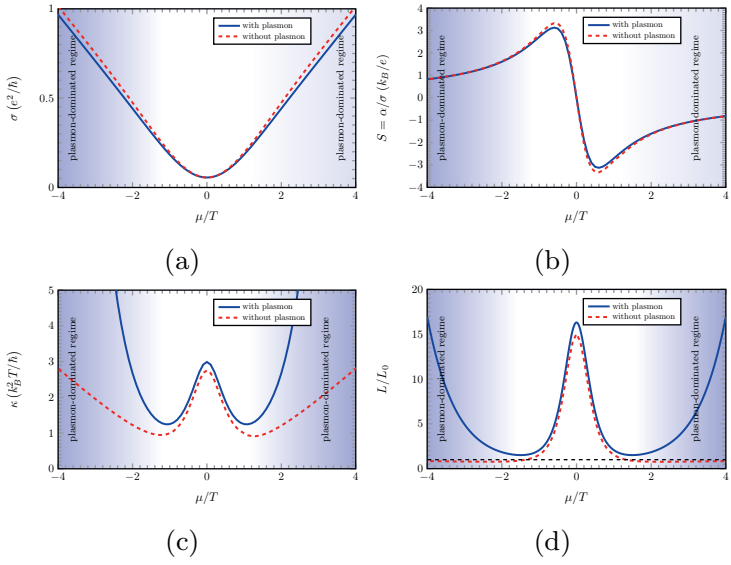

Figure 2.8: Thermo-electric transport coefficients of the hybrid system of electrons, holes, and plasmons as a function of chemical potential, (a) electrical conductivity, (b) Seebeck coefficient, (d) thermal conductivity (d) Wiedemann-Franz ratio. We use $\tau_0' = \tau_b$ and $\tau^{\text{dis}} = 8$.

straightforward manner to any hybrid system of electrons, holes, and bosons. In subsequent chapters we show the technical underpinnings of our theory based on the Schwinger-Keldysh approach. Not only do we derive the set of coupled Boltzmann equations there, we also establish explicitly all the conservation laws that we use here.

2.6 Appendices

2.6.1 Numerical evaluation of the scattering time for electron-hole drag

In this appendix, we evaluate the relaxation time for electron-hole drag. To this end, we consider a set of coupled Boltzmann equations for a two-dimensional Dirac electron-hole plasma. In the subsequent

chapter, we derive these equations from a Keldysh quantum-field theory within a perturbation theory up to second order. The equations read

$$\begin{aligned}
&\partial_t f_\lambda(\vec{x},t,\vec{k}) + \lambda v_F \hat{k}\cdot\partial_{\vec{x}} f_\lambda(\vec{x},t,\vec{k}) - \ e\vec{E}\cdot\partial_{\vec{k}} f_\lambda(\vec{x},t,\vec{k}) \\
&\quad = -\int \frac{d\vec{k}_1}{(2\pi)^2}\frac{d\vec{q}}{(2\pi)^2} R_{\lambda\lambda_1\lambda_3\lambda_2}(\vec{k},\vec{k}_1,\vec{q}) \\
&\quad 2\pi\delta(\epsilon_\lambda(\vec{k}) - \epsilon_{\lambda_1}(\vec{k}-\vec{q}) - \epsilon_{\lambda_2}(\vec{k}_1+\vec{q}) + \epsilon_{\lambda_3}(\vec{k}_1)) \\
&\quad \Big[f_\lambda(\vec{k}) f_{\lambda_3}(\vec{k}_1)(1-f_{\lambda_1}(\vec{k}-\vec{q}))(1-f_{\lambda_2}(\vec{k}_1+\vec{q})) \\
&\quad -(1-f_\lambda(\vec{k}))(1-f_{\lambda_3}(\vec{k}_1)) f_{\lambda_1}(\vec{k}-\vec{q}) f_{\lambda_2}(\vec{k}_1+\vec{q}) \Big].
\end{aligned} \tag{2.56}$$

We introduce the shorthand notation for the transition probability that is

$$\begin{aligned}
&R_{\lambda\lambda_1\lambda_3\lambda_2}(\vec{k},\vec{k}_1,\vec{q}) = \\
&2\Big[|T_{\lambda\lambda_1\lambda_3\lambda_2} - T_{\lambda\lambda_2\lambda_1\lambda_3}|^2 + (N-1)\left(|T_{\lambda\lambda_1\lambda_3\lambda_2}|^2 + |T_{\lambda\lambda_2\lambda_1\lambda_3}|^2 \right) \Big],
\end{aligned} \tag{2.57}$$

where

$$T_{\lambda\lambda_1\lambda_2\lambda_3}(\vec{k},\vec{k}_1,\vec{q}) = \frac{V(\vec{q})}{2} M^{\lambda\lambda_1}_{\vec{k},\vec{k}-\vec{q}} M^{\lambda_2\lambda_3}_{\vec{k}_1,\vec{k}_1+\vec{q}}\,. \tag{2.58}$$

The Coulomb interaction in the Fourier space $V(\vec{q}) = 2\pi\alpha/q$ where $\alpha = \frac{e^2}{4\pi\epsilon v_F}$ is the fine-structure constant characterizing the strength of the interaction. The coherent factor coming from the overlap of the wavefunction is defined according to

$$M^{\lambda\lambda_1}_{\vec{k},\vec{k}_1} = \left(\mathcal{U}^\dagger_{\vec{k}} \mathcal{U}_{\vec{k}_1} \right)_{\lambda\lambda_1}\,, \tag{2.59}$$

where

$$\mathcal{U}_{\vec{k}} = \frac{1}{\sqrt{2}} \begin{pmatrix} -\exp\left(-i\theta_{\vec{k}}\right) & \exp\left(-i\theta_{\vec{k}}\right) \\ 1 & 1 \end{pmatrix}. \tag{2.60}$$

Here $\tan\left(\theta_{\vec{k}}\right) = k_y/k_x$ and k denotes the magnitude of the momentum $\vec{k}$. Here λ, λ_1, λ_2, $\lambda_3 = \pm$ are energy-band indices, $+$ for the

conduction band and $-$ for the valence band. The collision integral on the right-hand side describes a process that an electron in the energy band λ and the momentum state $\vec{k}$ is scattered into the energy band λ_1 and momentum state $\vec{k}+\vec{q}$ by a collision with another electron in band λ_3 and state $\vec{k}_1$, which is itself scattered into the energy band λ_2 and state $\vec{k}_1-\vec{q}$. The initial states $\vec{k}$ and $\vec{k}_1$ have to be filled and the final states $\vec{k}-\vec{q}$ and $\vec{k}_1+\vec{q}$ must be empty for this event to take place. The factors $f_\lambda(\vec{k})$ and $f_{\lambda_3}(\vec{k}_1)$ are the occupation number of these state, while $1-f_{\lambda_1}(\vec{k}-\vec{q})$ and $1-f_{\lambda_2}(\vec{k}_1+\vec{q})$ describe the probability that the final states are unoccupied. The conservation of energy is taking into account by the delta function. The transition probability of this event is $R_{\lambda\lambda_1\lambda_3\lambda_2}$.

Next, we consider the electron-hole drag part of the collision integral that is when $\lambda=\lambda_1$ and $\lambda_2=\lambda_3=-\lambda$. Moreover, we are interested in a steady state and homogeneous solution, so the time-derivative and space-derivative term on the left-hand side of the Boltzmann equations are zero. Within linear response regime, one may solve the Boltzmann equations to linear order using the ansatz $f_\lambda(\vec{k})=f^0_\lambda(\vec{k})+\delta f_\lambda(\vec{k})$, where

$$\delta f_\lambda(\vec{k})=g_\lambda(\vec{k})e\vec{E}\cdot\partial_{\vec{k}}f^0_\lambda(\vec{k})=g_\lambda(\vec{k})e\vec{E}\cdot\lambda v_F\frac{\vec{k}}{k}f^0_\lambda(\vec{k})(1-f^0_\lambda(\vec{k})) \tag{2.61}$$

The unknown function $g_\lambda(k)$ is determined by solving the Boltzmann equations. It is usually expand in term of an appropriate set of basis $g_\lambda(\vec{k})=\sum\tau^{(n,p)}_\lambda\phi^{(n,p)}_\lambda(k)$, where $\tau^{(m,p)}_\lambda$ can be interpreted as a relaxation time for the corresponding mode. Here we use $\phi^{(n,p)}_\lambda(k)=$

$\lambda^p k^n$. After linearizing the Boltzmann equations, we obtain

$$\begin{aligned}\vec{\nabla}_{\vec{k}} f^0_\lambda(\vec{k}) &= -\int \frac{d\vec{k}_1}{(2\pi)^2}\frac{d\vec{q}}{(2\pi)^2}\mathcal{P}(\vec{k},\vec{k}_1,\vec{q}) \\ &\Big[f^0_\lambda(\vec{k}) f^0_{-\lambda}(\vec{k}_1)(1-f^0_\lambda(\vec{k}-\vec{q}))(1-f^0_{-\lambda}(\vec{k}_1+\vec{q}))\Big] \\ &\Big[\lambda v_F \frac{\vec{k}}{k} g_\lambda(k) - \lambda v_F \frac{\vec{k}_1}{k_1} g_{-\lambda}(k_1) \\ &-\lambda v_F \frac{\vec{k}-\vec{q}}{|\vec{k}-\vec{q}|} g_\lambda(|\vec{k}-\vec{q}|) + \lambda v_F \frac{\vec{k}_1+\vec{q}}{|\vec{k}_1+\vec{q}|} g_{-\lambda}(|\vec{k}_1+\vec{q}|)\Big].\end{aligned} \tag{2.62}$$

Here we introduce a shorthand

$$\begin{aligned}&\mathcal{P}(\vec{k},\vec{k}_1,\vec{q}) = \\ &2\pi\delta(\epsilon_\lambda(\vec{k}) - \epsilon_{\lambda_1}(\vec{k}-\vec{q}) - \epsilon_{\lambda_2}(\vec{k}_1+\vec{q}) + \epsilon_{\lambda_3}(\vec{k}_1)) R_{\lambda\lambda_1\lambda_3\lambda_2}(\vec{k},\vec{k}_1,\vec{q}).\end{aligned} \tag{2.63}$$

We are particularly interested in current relaxation, so we look at the current mode $\phi^{(0,1)}_\lambda(k) = \lambda$ and assume that the other modes are not excited. By projecting the Boltzmann equation into this mode, we find

$$\begin{aligned}\int \frac{d\vec{k}}{(2\pi)^2}\phi^{(0,1)}_\lambda(k)\frac{\vec{k}}{k}\cdot\vec{\nabla}_{\vec{k}} f^0_\lambda(\vec{k}) &= -\int \frac{d\vec{k}}{(2\pi)^2}\frac{d\vec{k}_1}{(2\pi)^2}\frac{d\vec{q}}{(2\pi)^2}\mathcal{P}(\vec{k},\vec{k}_1,\vec{q}) \\ &\Big[f^0_\lambda(\vec{k}) f^0_{-\lambda}(\vec{k}_1)(1-f^0_\lambda(\vec{k}-\vec{q}))(1-f^0_{-\lambda}(\vec{k}_1+\vec{q}))\Big] \\ &\phi^{(0,1)}_\lambda(k)\frac{\vec{k}}{k}\cdot\Big[\lambda v_F \frac{\vec{k}}{k}\tau^{(0,1)}_\lambda \phi^{(0,1)}_\lambda(k) - \lambda v_F \frac{\vec{k}_1}{k_1}\tau^{(0,1)}_{-\lambda}\phi^{(0,1)}_{-\lambda}(k_1) \\ -\lambda v_F \frac{\vec{k}-\vec{q}}{|\vec{k}-\vec{q}|}\tau^{(0,1)}_\lambda \phi^{(0,1)}_\lambda(|\vec{k}-\vec{q}|) &+ \lambda v_F \frac{\vec{k}_1+\vec{q}}{|\vec{k}_1+\vec{q}|}\tau^{(0,1)}_{-\lambda}\phi^{(0,1)}_{-\lambda}(|\vec{k}_1+\vec{q}|)\Big].\end{aligned} \tag{2.64}$$

To evaluate the current relaxation time $\tau^{(0,1)}_\lambda$, we again assume that

the mode corresponding to $\phi^{(0,1)}_{-\lambda}$ is not excited, this gives

$$\begin{aligned}
&\frac{1}{\tau^{(0,1)}_{\lambda}} \times \left(\int \frac{d\vec{k}}{(2\pi)^2} \phi^{(0,1)}_{\lambda}(k) \frac{\vec{k}}{k} \cdot \vec{\nabla}_{\vec{k}} f^0_{\lambda}(\vec{k}) \right) = \\
&\quad - \int \frac{d\vec{k}}{(2\pi)^2} \frac{d\vec{k}_1}{(2\pi)^2} \frac{d\vec{q}}{(2\pi)^2} \mathcal{P}(\vec{k}, \vec{k}_1, \vec{q}) \\
&\quad \Big[f^0_{\lambda}(\vec{k}) f^0_{-\lambda}(\vec{k}_1)(1 - f^0_{\lambda}(\vec{k} - \vec{q}))(1 - f^0_{-\lambda}(\vec{k}_1 + \vec{q})) \Big] \\
&\quad \phi^{(0,1)}_{\lambda}(k) \frac{\vec{k}}{k} \cdot \Big[\lambda v_F \frac{\vec{k}}{k} \phi^{(0,1)}_{\lambda}(k) - \lambda v_F \frac{\vec{k} - \vec{q}}{|\vec{k} - \vec{q}|} \phi^{(0,1)}_{\lambda}(|\vec{k} - \vec{q}|) \Big],
\end{aligned} \tag{2.65}$$

and similarly $\tau^{(0,1)}_{-\lambda}$ is determined from

$$\begin{aligned}
&\frac{1}{\tau^{(0,1)}_{-\lambda}} \times \left(\int \frac{d\vec{k}}{(2\pi)^2} \phi^{(0,1)}_{\lambda}(k) \frac{\vec{k}}{k} \cdot \vec{\nabla}_{\vec{k}} f^0_{\lambda}(\vec{k}) \right) = \\
&- \int \frac{d\vec{k}}{(2\pi)^2} \frac{d\vec{k}_1}{(2\pi)^2} \frac{d\vec{q}}{(2\pi)^2} \mathcal{P}(\vec{k}, \vec{k}_1, \vec{q}) \\
&\Big[f^0_{\lambda}(\vec{k}) f^0_{-\lambda}(\vec{k}_1)(1 - f^0_{\lambda}(\vec{k} - \vec{q}))(1 - f^0_{-\lambda}(\vec{k}_1 + \vec{q})) \Big] \\
&\phi^{(0,1)}_{\lambda}(k) \frac{\vec{k}}{k} \cdot \Big[- \lambda v_F \frac{\vec{k}_1}{k_1} \phi^{(0,1)}_{-\lambda}(k_1) + \lambda v_F \frac{\vec{k}_1 + \vec{q}}{|\vec{k}_1 + \vec{q}|} \phi^{(0,1)}_{-\lambda}(|\vec{k}_1 + \vec{q}|) \Big].
\end{aligned} \tag{2.66}$$

These integrals can be evaluate numerically. In Fig.(2.9), we plot the relaxation time for electron-hole drag $1/\tau_{\pm}$ which we defined from the discussion above according to

$$\begin{aligned}
\frac{1}{\tau_+} \quad = \quad & - \int \frac{d\vec{k}}{(2\pi)^2} \frac{d\vec{k}_1}{(2\pi)^2} \frac{d\vec{q}}{(2\pi)^2} \mathcal{P}(\vec{k}, \vec{k}_1, \vec{q}) \\
& \Big[f^0_{+}(\vec{k}) f^0_{-}(\vec{k}_1)(1 - f^0_{+}(\vec{k} - \vec{q}))(1 - f^0_{-}(\vec{k}_1 + \vec{q})) \Big] \\
& \phi^{(0,1)}_{+}(k) \frac{\vec{k}}{k} \cdot \Big[v_F \frac{\vec{k}}{k} \phi^{(0,1)}_{+}(k) - v_F \frac{\vec{k} - \vec{q}}{|\vec{k} - \vec{q}|} \phi^{(0,1)}_{+}(|\vec{k} - \vec{q}|) \Big] ,
\end{aligned}$$

$$\begin{aligned}\frac{1}{\tau_-} &= -\int \frac{d\vec{k}}{(2\pi)^2}\frac{d\vec{k}_1}{(2\pi)^2}\frac{d\vec{q}}{(2\pi)^2}\mathcal{P}(\vec{k},\vec{k}_1,\vec{q}) \\ &\quad \Big[f_+^0(\vec{k})f_-^0(\vec{k}_1)(1-f_+^0(\vec{k}-\vec{q}))(1-f_-^0(\vec{k}_1+\vec{q}))\Big] \\ &\quad \phi_+^{(0,1)}(k)\frac{\vec{k}}{k}\cdot\Big[-v_F\frac{\vec{k}_1}{k_1}\phi_-^{(0,1)}(k_1)+v_F\frac{\vec{k}_1+\vec{q}}{|\vec{k}_1+\vec{q}|}\phi_-^{(0,1)}(|\vec{k}_1+\vec{q}|)\Big]\,.\end{aligned} \tag{2.67}$$

We find the the relaxation time decays exponentially in the large-μ limit which is the Fermi liquid regime. One may understand this by observing that the relaxation time takes the form

$$\begin{aligned}\frac{1}{\tau_\pm} &= \int f_+^0(\vec{k})f_-^0(\vec{k}_1)(1-f_+^0(\vec{k}-\vec{q}))(1-f_-^0(\vec{k}_1+\vec{q}))\Big[\dots\Big], \\ &= \int \frac{1}{e^{\frac{k-\mu}{T}}+1}\frac{1}{e^{\frac{-k_1-\mu}{T}}+1}\frac{1}{e^{\frac{-|\vec{k}-\vec{q}|+\mu}{T}}+1}\frac{1}{e^{\frac{|\vec{k}_1+\vec{q}|+\mu}{T}}+1}\Big[\dots\Big].\end{aligned}$$

In the large-μ limit, these becomes

$$\frac{1}{\tau_\pm} \approx \int \Theta(\mu-k)\Theta(|\vec{k}-\vec{q}|-\mu)\exp(-\mu/T)\Big[\dots\Big]. \tag{2.68}$$

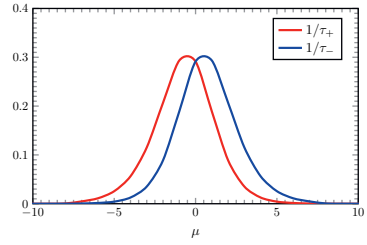

Figure 2.9: Numerical solution of the relaxation time for electron-hole drag as a function of chemical potential μ.

2.6.2 Plasmon mode within the RPA approximation

In this appendix, we derive the energy dispersion relation as well as the Landau damping for the plasmon in a two-dimensional Dirac

system within the RPA approximation. To this end, let us consider the RPA dielectric function

$$\epsilon_{\mathrm{RPA}}(\vec{q},\omega) = 1 - V(\vec{q})\Pi(\vec{q},\omega), \tag{2.69}$$

The polarization function $\Pi(\vec{k},\omega)$ is given by the Lindhard formula

$$\Pi(\vec{q},\omega) = N \sum_{\lambda\lambda'=\pm 1} \int \frac{d\vec{p}}{(2\pi)^2} \mathcal{F}_{\lambda\lambda'}(\vec{p},\vec{q}) \frac{f^0_\lambda(\vec{p}) - f^0_{\lambda'}(\vec{q}+\vec{p})}{\omega + i0^+ + \epsilon_\lambda(\vec{p}) - \epsilon_{\lambda'}(\vec{q}+\vec{p})}, \tag{2.70}$$

where $\lambda, \lambda' = \pm$ denote the energy band; $+$ denotes the conduction band and $-$ denotes the valence band. The coherence factor defined as

$$\mathcal{F}_{\lambda\lambda'}(\vec{p},\vec{q}) = \frac{1}{2}(1 + \lambda\lambda' \cos(\theta_{\vec{p}+\vec{q}} - \theta_{\vec{q}})). \tag{2.71}$$

The Fermi-Dirac distribution function

$$f^0_\pm(\vec{p}) = \frac{1}{e^{\frac{\epsilon_\pm(\vec{p})-\mu}{T}} + 1}. \tag{2.72}$$

Note that here we use the different notation from the main text. The plasmon frequency ($\omega = \omega_p - i\gamma_p$) is obtained from zero of the RPA dielectric function. Let us note that by defining it in this way the decay rate γ_p is positive. If the damping is sufficiently weak ($\gamma_p \ll \omega_p$), one can expand the polarization function to leading order in γ_p. This gives

$$\Pi(\vec{q},\omega_p - i\gamma_p) \approx \mathrm{Re}\,\Pi(\vec{q},\omega_p) - i\gamma_p \partial_\omega \,\mathrm{Re}\,\Pi(\vec{q},\omega)\Big|_{\omega=\omega_p} + i\,\mathrm{Im}\,\Pi(\vec{q},\omega_p). \tag{2.73}$$

By substituting this expansion into Eq.(2.69), one finds that the energy of the plasmon is determined from the real part according to

$$1 - V(\vec{q})\,\mathrm{Re}\,\Pi(\vec{q},\omega_p) = 0, \tag{2.74}$$

whereas the decay rate is a solution of the imaginary part which is given by

$$\gamma_p = \frac{\mathrm{Im}\,\Pi(\vec{q},\omega)}{\partial_\omega \,\mathrm{Re}\,\Pi(\vec{q},\omega)}\bigg|_{\omega=\omega_p}. \tag{2.75}$$

Solutions to (2.74) exist only when $\mathrm{Re}\,\Pi > 0$. In the upper panel of Fig.(2.10), we show the real part of the polarization in the momentum-frequency plane. We observe that $\mathrm{Re}\,\Pi$ is positive when $\omega > q$. Furthermore, by considering Eq.(2.75), we find that a stable plasmon solution requires $\mathrm{Im}\,\Pi = 0$. In lower panel of Fig.(2.10), we plot the imaginary part of the polarization function. We observe that although it is not identically zero, it is still negligibly small in the low-momentum limit and $\omega > q$. Consequently, one may expect a long-wavelength underdamped plasmon mode with almost infinitely long lifetime. Having this observation, we expand the polarization

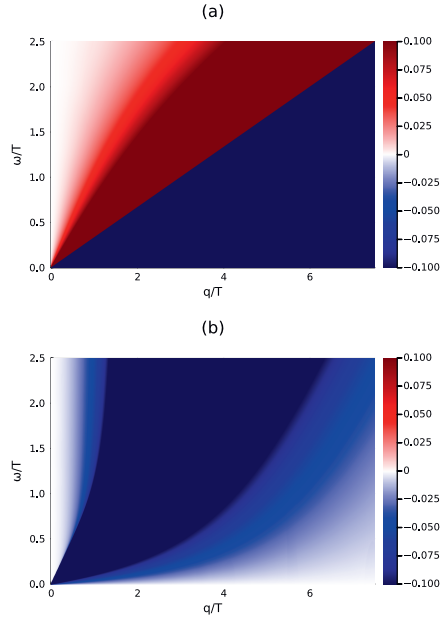

Figure 2.10: Polarization function, in the unit of temperature $T = 1$, at a non-zero temperture and a chemical potential $\mu/T = 1$ in the momentum-frequency plane. The above plot shows the real part and the lower plot shows the imaginary part.

function up to first order in q/ω by making use of the following

expressions:

$$\begin{aligned}
\mathcal{F}_{\pm\pm}(\vec{p},\vec{q}) &= \frac{1}{2}\left(1+\cos\left(\theta_{\vec{p}+\vec{q}}-\theta_{\vec{q}}\right)\right)\approx 1,\\
\mathcal{F}_{\pm\mp}(\vec{p},\vec{q}) &= \frac{1}{2}\left(1-\cos\left(\theta_{\vec{p}+\vec{q}}-\theta_{\vec{q}}\right)\right)\approx \frac{1}{4}\left(\vec{p}\cdot\vec{\nabla}_{\vec{q}}\theta_{\vec{q}}\right)^2,\\
f^0_\lambda(\vec{p}+\vec{q}) &\approx f^0_\lambda(\vec{q})+\vec{p}\cdot\vec{\nabla}_{\vec{q}}f^0_\lambda(\vec{q}),\\
\epsilon_\lambda(\vec{p}+\vec{q}) &\approx \epsilon_\lambda(\vec{q})+\vec{p}\cdot\vec{\nabla}_{\vec{q}}\epsilon_\lambda(\vec{q}).
\end{aligned} \tag{2.76}$$

Let us first calculate the real part of the polarization in Eq.(2.70). The intraband contribution, when $\lambda=\lambda'$, gives

$$\begin{aligned}
&\mathrm{Re}\,\Pi(\vec{q},\omega)\\
\approx\;& N\sum_{\lambda=\pm1}\int\frac{d\vec{p}}{(2\pi)^2}\frac{-\vec{q}\cdot\vec{\nabla}_{\vec{p}}f^0_\lambda(\vec{p})}{\omega}\Big[1+\frac{\vec{q}\cdot\vec{\nabla}_{\vec{p}}\epsilon_\lambda(\vec{p})}{\omega}\Big],\\
=\;& \frac{N}{\omega^2}\int\frac{d\vec{p}}{(2\pi)^2}\Big[f^0_+(\vec{p})(\vec{q}\cdot\vec{\nabla}_{\vec{p}})^2\epsilon_+(\vec{p})\\
&\qquad -\left(1-f^0_-(\vec{p})\right)(\vec{q}\cdot\vec{\nabla}_{\vec{p}})^2\epsilon_-(\vec{p})\Big],\\
=\;& \frac{Nq^2}{\omega^2}\int\frac{pdpd\theta}{(2\pi)^2}\Big[f^0_+(\vec{p})+\left(1-f^0_-(\vec{p})\right)\Big]\frac{\sin^2\theta}{p}\\
=\;& \frac{Nq^2}{4\pi\omega^2}\int dp\Big[f^0_+(\vec{p})+(1-f^0_-(\vec{p}))\Big]\\
=\;& -\frac{Nq^2}{4\pi\omega^2}T\Big[\mathrm{Li}_1\left(-e^{\mu/T}\right)+\mathrm{Li}_1\left(-e^{-\mu/T}\right)\Big]\\
=\;& \frac{Nq^2}{4\pi\omega^2}T\Big[\log\left(1+e^{\mu/T}\right)+\log\left(1+e^{-\mu/T}\right)\Big]\\
=\;& \frac{Nq^2}{4\pi\omega^2}T\Big[\log\left(2+2\cosh\mu/T\right)\Big].
\end{aligned} \tag{2.77}$$

In contrast, the interband contribution, when $\lambda=-\lambda'$, gives a logarithmic correction which will be neglected in evaluating the plasmon energy dispersion. For the case of non-zero dopings, at zero temperature, this interband contribution reads $\frac{Np^2}{16\pi\omega}\log\left(\left|\frac{\omega-2\mu}{\omega+2\mu}\right|\right)$. By substituting Eq.(2.77) into Eq.(2.74), we can derive the dispersion

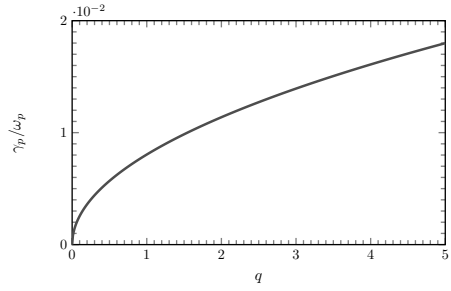

Figure 2.11: The plot shows the ratio of the plasmon decay rate evaluated in Eq.(2.81) to the energy dispersion evaluated in Eq.(2.78) for small momenta. It can be observed that, within the low-momentum approximation, the ratio is small. As a result, the plasmon is a well-defined excitation. Here we use $\mu/T = 3$, but it should be noted that this feature is generic for any μ/T.

relation for plasmon. It reads as

$$\omega_p(\vec{q}) = \pm\sqrt{\frac{N}{2}\alpha T q \log\left(2 + 2\cosh(\mu/T)\right)}. \tag{2.78}$$

Note that this is the same result as we obtained from the Boltzmann approach in the main text.

Next, we consider the imaginary part of the polarization function. The main contribution to the imaginary part is from the interband transition, when $\lambda = -\lambda'$. This gives

$$\begin{aligned}
&\mathrm{Im}\,\Pi(\vec{q},\omega) \\
&\approx -N\pi \sum_{\lambda=\pm 1} \int \frac{d\vec{p}}{(2\pi)^2}\frac{1}{4}\left(\vec{q}\cdot\vec{\nabla}_{\vec{p}}\theta_{\vec{p}}\right)^2 \left[f^0_{\lambda}(\vec{p}) - f^0_{-\lambda}(\vec{p})\right] \\
&\qquad\qquad \delta(\omega + \epsilon_{\lambda}(\vec{p}) - \epsilon_{-\lambda}(\vec{p})), \\
&= -N\pi \int \frac{d\vec{p}}{(2\pi)^2}\frac{1}{4}\frac{q^2}{p^2}\sin^2(\theta) \\
&\qquad\qquad \Big[\Big(f^0_{+}(\vec{p}) - f^0_{-}(\vec{p})\Big)\delta(\omega + \epsilon_{+}(\vec{p}) - \epsilon_{-}(\vec{p})) \\
&\qquad\qquad +\Big(f^0_{-}(\vec{p}) - f^0_{+}(\vec{p})\Big)\delta(\omega + \epsilon_{-}(\vec{p}) - \epsilon_{+}(\vec{p}))\Big].
\end{aligned}$$

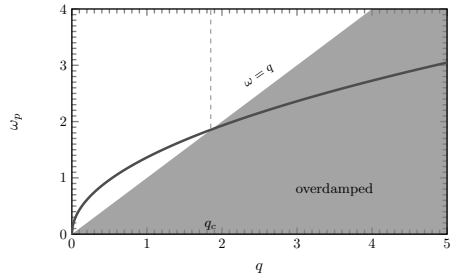

Figure 2.12: The plot shows the energy dispersion of plasmon. Here we use $\mu/T = 3$.

Since $f^0_\pm(\vec{p})$ depends only on the magnitude of the momentum $\vec{p}$, let us now denote it by $f^0_\pm(p)$. The angular integral can be performed straighforwardly, this gives

$$\begin{aligned}
&\mathrm{Im}\,\Pi(\vec{q},\omega) \\
&\approx -\frac{N}{16}q^2\int_0^\infty \frac{dp}{p}\Big[\Big(f^0_+(p)-f^0_-(p)\Big)\delta(\omega+2p)+ \\
&\qquad\qquad \Big(f^0_-(p)-f^0_+(p)\Big)\delta(\omega-2p)\Big], \\
&= -\frac{N}{16}q^2\int_0^\infty \frac{dp}{p}\Big(f^0_+(p)-f^0_-(p)\Big)\Big(\delta(\omega+2p)-\delta(\omega-2p)\Big), \\
&= -\frac{N}{16}q^2\int_0^\infty \frac{dp}{p}\Big(f^0_+(p)-f^0_-(p)\Big)\frac{1}{2}\Big(\delta(p+\omega/2)-\delta(p-\omega/2)\Big), \\
&= \frac{N}{16}\frac{q^2}{\omega}\left(\frac{1}{e^{\frac{|\omega|/2-\mu}{T}}+1}-\frac{1}{e^{\frac{-|\omega|/2-\mu}{T}}+1}\right). \qquad (2.79)
\end{aligned}$$

In the limit of zero temperature, this becomes

$$\mathrm{Im}\,\Pi^R(\vec{q},\omega) \approx -\frac{N}{16}\frac{q^2}{\omega}\Theta(|\omega|-2|\mu|), \qquad (2.80)$$

which was found previously in [54]. It vanishes when $|\omega| < 2|\mu|$, consequently, the long-lived plasmon mode exists in this region. By substituting the real part in Eq.(2.77) and the imaginary part in Eq.(2.79) into Eq.(2.75), we find the decay rate of plasmon which

reads as

$$\gamma_p(\vec{q}) = -\frac{\pi\omega_p(\vec{q})^2}{8T\log(2+2\cosh\mu/T)} \times \left(\frac{1}{e^{\frac{|\omega_p(\vec{q})|/2-\mu}{T}}+1} - \frac{1}{e^{\frac{-|\omega_p(\vec{q})|/2-\mu}{T}}+1}\right). \quad (2.81)$$

In Fig.(2.11), we shows the ratio of the decay rate to the energy evaluated above in Eqs.(2.81) and (2.78). We find that $\gamma_p/\omega_p \ll 1$, so, within the low-momentum approximation, the plasmon is a well-defined excitation. However, as we show in Fig.(2.12), the square-root q energy dispersion enters the region $\omega < q$ where the plasmon becomes an over-damped mode. This defined a momentum cutoff above which the plasmon is unstable mode. The momentum cutoff satisfies

$$\omega_p(q_c)/q_c = 1 \,, \quad (2.82)$$

so we find that

$$q_c = \frac{N}{2}\alpha T\log(2+2\cosh(\mu/T)) \,. \quad (2.83)$$

2.6.3 Relaxation time of plasmon

In this section, we are going to derive the relaxation time τ_b for the plasmon used in the main text. To this end, let us consider the Boltzmann equation for the plasmon.

$$\partial_t b(\vec{x},\vec{p},t) + \vec{v}_b\cdot\vec{\nabla}_{\vec{x}} b(\vec{x},\vec{p},t) = -\frac{2\alpha\pi^2 N\omega_p(\vec{p})}{p}\int\frac{d\vec{q}}{(2\pi)^2}\mathcal{F}_{\lambda\lambda'}(\vec{p}+\vec{q},\vec{q})\delta(\omega_p(\vec{p})+\epsilon_\lambda(\vec{q})-\epsilon_{\lambda'}(\vec{p}+\vec{q})) \Big[f_\lambda(\vec{q})\Big(1-f_{\lambda'}(\vec{p}+\vec{q})\Big)b(\vec{p}) - \Big(1-f_\lambda(\vec{q})\Big)f_{\lambda'}(\vec{p}+\vec{q})\Big(1+b(\vec{p})\Big)\Big]. \quad (2.84)$$

The derivation of this equation will be given in detail in the subsequent chapter. By substituting $f = f^0$ and $b = b^0 + \delta b$ to the Boltzmann equation above, the left-hand-side becomes

$$\partial_t\delta b(\vec{x},\vec{p},t) + \vec{v}_b\cdot\vec{\nabla}T\partial_T b^0(\vec{p}), \quad (2.85)$$

and the collision integral becomes

$$-\frac{2\alpha\pi^2 N\omega_p(\vec{p})}{p}\int\frac{d\vec{q}}{(2\pi)^2}\mathcal{F}_{\lambda\lambda'}(\vec{p}+\vec{q},\vec{q})\delta(\omega_p(\vec{p})+\epsilon_\lambda(\vec{q})-\epsilon_{\lambda'}(\vec{p}+\vec{q}))$$
$$\left(f^0_\lambda(\vec{q})-f^0_{\lambda'}(\vec{p}+\vec{q})\right)\delta b(\vec{p})$$
$$=\frac{2\alpha\pi\omega_p(\vec{p})}{p}\,\mathrm{Im}\,\Pi\delta b$$
$$=-2\gamma_p\delta b, \tag{2.86}$$

where γ_p is the decay rate for plasmon in Eq.(2.81). To obtain the result above, we approximate the imaginary part of the polarization function at the same level as we did in the previous section. Let us note that in principle there are contributions of the form $-\delta f_+/\tau_{+b}$ and $-\delta f_-/\tau_{-b}$ to the collision integral above. However, evaluation the $1/\tau_{\pm b}$ is equivalent to solving the Boltzmann equation, so we will postpone it until the last chapter.

Chapter 3

Keldysh quantum-field theory of Coulomb interacting Dirac electrons in two dimensions

In the subsequent chapters, we employ a quantum-field theory to study transport properties of the Dirac electrons interacting via Coulomb interactions. In order to set down the preliminaries, Keldysh quantum-field theory for the Coulomb-interacting Dirac electrons is developed in this chapter. The central object of the theory is a partition function from which physical observables can be determined. We write the partition function by means of the functional-integral over time-dependent fields along the closed time-contour. This is typically referred to as a Keldysh contour. This partition function is the starting point for our analysis in subsequent chapters.

The organization of the chapter is as follows. In section 3.1, the model for Coulomb-interacting charged Dirac electrons in two dimensions is introduced. This model is the main object of our analysis in this thesis. Furthermore, we assume that the effect of the underlying lattice is taken into account by a jellium model, meaning that electrons move in a uniform and positively charged background. We then proceed to a technical section, Sec. 3.2, where we derive the functional-integral representation of the partition function. Next, the formalism of real-time quantum field theory based on this partition function is reviewed. It is a summary of the most important steps that lead from a fully quantum mechanical treatment towards

the semiclassical Boltzmann equation. This includes the structure of the Green's functions on the closed-time contour in Sec. 3.3. We then discuss the Dyson equation, including the Keldysh or quantum-kinetic equation in Sec. 3.5. We proceed to introduce the Wigner transform and the Moyal product in Sec. 3.6 which allows to perform the gradient expansion on the Keldysh equation in Sec. 3.7 and obtain the Boltzmann equation.

3.1 The model

We study a theory of Dirac electrons in two spatial dimensions interacting via long-range Coulomb interactions. This model is applicable to low-energy interacting electrons in graphene where momenta are measured with respect to the K and K' points in the Brillouin zone.

In coordinate space, the Hamiltonian is given by

$$\hat{H} = \hat{H}_0 + \hat{H}_{\text{ex}} + \hat{H}_I \ , \tag{3.1}$$

with the non-interacting part being

$$\hat{H}_0 = \sum_{i=1}^{N} \sum_{\lambda,\lambda'=\pm} \int d\vec{x} \ \hat{\Psi}^\dagger_{i,\lambda}(\vec{x}) \hat{H}_{D,\lambda\lambda'}(\vec{x}) \hat{\Psi}_{i,\lambda'}(\vec{x}) \ , \tag{3.2}$$

where $\hat{H}_{D,\lambda\lambda'}(\vec{x}) = \left(-i\hbar v_F \vec{\sigma}\cdot\vec{\nabla} - \mu\right)_{\lambda\lambda'}$ is the Dirac Hamiltonian with a Fermi velocity v_F and chemical potential μ. Here $\hat{\Psi}^\dagger_{i,\lambda}(\vec{x})$ ($\hat{\Psi}_{i,\lambda}(\vec{x})$) creates (annihilates) an electron at a position $\vec{x}$. The flavor index denoted by i ranging from $i = 1, ..., N$ and $\lambda, \lambda' \in \{+, -\}$ denote spinor indices.

The electrons interact via the long-range Coulomb interaction. This effect is included into our model by the interaction Hamiltonian $\hat{H}_I$. It is given by

$$\hat{H}_I = \sum_{i=1}^{N} \sum_{\lambda,\lambda'=\pm} \frac{1}{2} \int d\vec{x} d\vec{x}' \ \hat{\Psi}^\dagger_{i,\lambda}(\vec{x}) \hat{\Psi}^\dagger_{i,\lambda'}(\vec{x}') V(\vec{x}-\vec{x}') \hat{\Psi}_{i,\lambda'}(\vec{x}') \hat{\Psi}_{i,\lambda}(\vec{x}), \tag{3.3}$$

where the Coulomb potential between two electrons of charge e separated by a distance $|\vec{x}-\vec{x}'|$ reads

$$V(\vec{x}-\vec{x}') = \frac{e^2}{4\pi\epsilon|\vec{x}-\vec{x}'|}. \tag{3.4}$$

Here ϵ defines the average dielectric constant.

In addition, the static potential energy $V_{\rm ex}(\vec{x})$ is added to take into account the positively charge background in which electrons move.

$$V_{\rm ex}(\vec{x}) = -n_0 \int d\vec{x}' V(\vec{x}-\vec{x}'), \tag{3.5}$$

where n_0 is the average density of the background which is identical to electron density in thermal equilibrium. The interaction of the electrons with the inert positively charged background is explained by

$$\hat{H}_{\rm ex} = \sum_{i=1}^{N} \sum_{\lambda=\pm} \int d\vec{x}\ \hat{\Psi}^{\dagger}_{i,\lambda}(\vec{x}) V_{\rm ex}(\vec{x}) \hat{\Psi}_{i,\lambda}(\vec{x}). \tag{3.6}$$

One may transform the Hamiltonian into a Fourier space. The non-interacting Hamiltonian acquires the form

$$\hat{H}_0 = \sum_{i=1}^{N} \sum_{\lambda,\lambda'=1,2} \int \frac{d\vec{p}}{(2\pi)^2}\ \hat{\Psi}^{\dagger}_{i,\lambda}(\vec{p}) \hat{\mathcal{H}}_{D,\lambda\lambda'}(\vec{p}) \hat{\Psi}_{i,\lambda'}(\vec{p})\ , \tag{3.7}$$

where $\hat{\mathcal{H}}_{D,\lambda\lambda'}(\vec{p}) = (\hbar v_F \vec{\sigma}\cdot\vec{p} - \mu)_{\lambda\lambda'}$. This Hamiltonian consists of two-energy band given by

$$\epsilon_{\pm}(\vec{p}) = \pm\hbar v_F p - \mu, \tag{3.8}$$

where $p = |\vec{p}|$ denotes the norm of the two-dimensional momentum vector. The Fourier transform of the external potential term is straightforward but will not be important in our discussion. We therefore are not discussing it here. The interacting Hamiltonian becomes

$$\begin{aligned}\hat{H}_I \quad = \quad & \sum_{i=1}^{N} \sum_{\lambda,\lambda'=\pm} \frac{1}{2} \int \frac{d\vec{p}}{(2\pi)^2} \frac{d\vec{k}}{(2\pi)^2} \frac{d\vec{q}}{(2\pi)^2}\ \hat{\Psi}^{\dagger}_{i,\lambda}(\vec{k}-\vec{q}) \\ & \times \hat{\Psi}^{\dagger}_{i,\lambda'}(\vec{p}+\vec{q}) V(\vec{q}) \hat{\Psi}_{i,\lambda'}(\vec{k}) \hat{\Psi}_{i,\lambda}(\vec{p}).\end{aligned} \tag{3.9}$$

Hereafter we set $\hbar = 1$. The Fourier transformation of the $1/r$ Coulomb interaction between electrons in two dimensions reads

$$V(\vec{p}) = \frac{e^2}{2\epsilon p} = \frac{2\pi\alpha v_F}{p}. \tag{3.10}$$

The strength of the Coulomb interaction is usually characterised by the ratio of the potential energy to the kinetic energy. For the Dirac fermion, this ratio boils down to the fine structure constant $\alpha = e^2/4\pi\epsilon\hbar v_F$. We note that electrons of different flavors are decoupled, as a result, we can focus only on one of them and suppress the flavor index from now on. The contribution of the rest sectors are accounted for by multiplying the number of degeneracy N to the final result. For graphene, λ, λ' denote the pseudo-spin resulting from sub-lattices A and B. The number of fermion flavors $N = 4$ counts spin and valley degrees of freedom. It was found that $v_F \approx 10^6$ m/s. Here ϵ measures the average value of the dielectric constant of materials above and below it, *e.g.*, $\epsilon = 1$ for suspended graphene in vacuum and $\epsilon \approx 7$ for graphene sandwiched in hBN layers. For these two cases $\alpha = 2.2$ and $\alpha \approx 0.3$, respectively. Thus, graphene can be a playground for both weak and strong interaction effects.

3.2 The partition function

The central object in the Keldysh formalism is the partition function. It allows for the derivation of Green's functions and associated physical observables by means of functional differentiation. In this section we review the construction of the partition function for the model introduced in Eq. (3.1). We follow closely the presentation given in [81, 82]. The idea is that we assume in the distant past ($t = -\infty$) the system was in thermal equilibrium at a temperature T. Its state is specified by the density matrix operator associated with the non-interacting Hamiltonian according to

$$\hat{\rho} = e^{-\beta \hat{H}_0}, \tag{3.11}$$

where $1/\beta = k_B T$ defines the thermal energy associated with the temperature T where k_B is the Boltzmann constant. The interaction will be switched on adiabatically later and reach its actual

strength before the observation. In addition, external perturbations might be subsequently established and drive the system away from equilibrium.

The partition function is defined in terms of the traces of the operators according to

$$Z = \frac{\mathrm{Tr}\left[\hat{U}_C \hat{\rho}\right]}{\mathrm{Tr}[\hat{\rho}]}, \tag{3.12}$$

where $\hat{U}_C = \mathcal{T}_C \exp\left(-i \oint_C \hat{H}(t)dt\right)$ is the evolution operator along the closed time-integration contour $C = C_+ \cup C_-$ depicted in Fig. (3.1). Here $\mathcal{T}_C$ orders the operators according to the position of their time arguments on the contour C. The evolution operator describes evolution of the system from $t = -\infty$, where the system is non-interacting and in equilibrium, towards $t = \infty$ then return to the equilibrium state at $t = -\infty$. The traces are evaluated with respect to the equilibrium states at $t = -\infty$.

Our goal in this section is to write the partition function defined in Eq.(3.12) as a functional integral over time-dependent fields. It turns out that these fields are the eigenvalues of the coherent states. To this end, it is convenient to expand the field operators in terms of a complete set of basis vectors that is formed by the eigenstates of the Dirac Hamiltonian $\hat{H}_{D,\lambda\lambda'}$, namely

$$\begin{aligned} \hat{\Psi}_\lambda(\vec{x}) &= \sum_{\vec{n},\alpha} \phi^\alpha_{\vec{n},\lambda}(\vec{x}) \hat{\Psi}_{\vec{n},\alpha}, \\ \hat{\Psi}^\dagger_\lambda(\vec{x}) &= \sum_{\vec{n},\alpha} (\phi^\dagger)^\alpha_{\vec{n},\lambda}(\vec{x}) \hat{\Psi}^\dagger_{\vec{n},\alpha}, \end{aligned} \tag{3.13}$$

where $\phi^\alpha_{\vec{n},\lambda}$ is the α^{th} eigenvector of the Dirac Hamiltonian with the corresponding eigenenergy $\epsilon_{\vec{n},\alpha}$ satisfying

$$\sum_{\lambda'} \hat{H}_{D,\lambda\lambda'}(\vec{x}) \phi^\alpha_{\vec{n},\lambda'}(\vec{x}) = \epsilon_{\vec{n},\alpha} \phi^\alpha_{\vec{n},\lambda}(\vec{x}). \tag{3.14}$$

The eigenstates are orthonormal to each other, *i.e.*,

$$\sum_\lambda \int d\vec{x}\, (\phi^\dagger)^\alpha_{\vec{n},\lambda}(\vec{x}) \phi^{\alpha'}_{\vec{n}',\lambda}(\vec{x}) = \delta_{\vec{n}\vec{n}'} \delta_{\alpha\alpha'}. \tag{3.15}$$

We find that due to the invariance under spatial translation the eigenstates of the Dirac Hamiltonian take the form of a product of the propagating plane wave and the spinor representing the pseudo-spin degree of freedom, namely

$$\phi^{\pm}_{\vec{p},\lambda}(\vec{x}) = \frac{1}{\sqrt{2}} \begin{pmatrix} \pm e^{-i\theta_{\vec{p}}} \\ 1 \end{pmatrix}_{\lambda} e^{i\vec{p}\cdot\vec{x}}. \tag{3.16}$$

Here $\vec{p}$ is the momentum a Dirac electron and $\theta_{\vec{p}} = \arctan(p_y/p_x)$ is the angle of the two-dimensional momentum vector. Recall that p is the magnitude of the momentum vector. The corresponding eigenenergies are given by

$$\epsilon_{\vec{p},\pm} = \pm\hbar v_F p - \mu. \tag{3.17}$$

Let us note that the plane-wave solution is not always a useful starting point, for example, in the case of electrons moving in a strong and constant magnetic field $B\hat{z}$. By employing the Laudau gauge $\vec{A} = xB\hat{y}$, the eigenstates of this problem is labeled by n and p_y where n is the so-called Landau level and p_y is the y-component of the momentum $\vec{p}$. With a slight modification, the formalism we are developing is applicable to this case too. Having this in mind, in what follows, we will keep the notation general as much as possible.

We insert Eq.(3.13) into the Dirac Hamiltonian and obtain

$$\hat{H}_0 = \sum_{\vec{n},\alpha} \hat{\Psi}^{\dagger}_{\vec{n},\alpha} \epsilon_{\vec{n},\alpha} \hat{\Psi}_{\vec{n},\alpha}. \tag{3.18}$$

The non-interacting part of the Hamiltonian becomes diagonal. On the other hand, the interaction part of the Hamiltonian is transformed into

$$H_I = \frac{1}{2} \sum_{\vec{n}_1,\vec{n}_2,\vec{n}_3,\vec{n}_4} \sum_{\alpha_1,\alpha_2,\alpha_3,\alpha_4} \mathcal{V}^{\alpha_1,\alpha_2,\alpha_3,\alpha_4}_{\vec{n}_1,\vec{n}_2,\vec{n}_3,\vec{n}_4} \hat{\Psi}^{\dagger}_{\vec{n}_1,\alpha_1} \hat{\Psi}^{\dagger}_{\vec{n}_2,\alpha_2} \hat{\Psi}_{\vec{n}_3,\alpha_3} \hat{\Psi}_{\vec{n}_4,\alpha_4}, \tag{3.19}$$

where the interaction matrix reads as

$$\mathcal{V}^{\alpha_1,\alpha_2,\alpha_3,\alpha_4}_{\vec{n}_1,\vec{n}_2,\vec{n}_3,\vec{n}_4} = \sum_{\lambda,\lambda'} \int d\vec{x} d\vec{x}' \; (\phi^{\dagger})^{\alpha_1}_{\vec{n}_1,\lambda}(\vec{x}) (\phi^{\dagger})^{\alpha_2}_{\vec{n}_2,\lambda'}(\vec{x}') V(\vec{x}-\vec{x}') \phi^{\alpha_3}_{\vec{n}_3,\lambda'}(\vec{x}') \phi^{\alpha_4}_{\vec{n}_4,\lambda}(\vec{x}). \tag{3.20}$$

Similarly, the Hamiltonian describing the interaction between Dirac eletrons and jellium background is transformed into

$$\hat{H}_{\rm ex} = \sum_{\vec{n}_1,\vec{n}_2} \sum_{\alpha_1,\alpha_2} \hat{\Psi}^{\dagger}_{\vec{n}_1,\alpha_1} \mathcal{V}^{\alpha_1,\alpha_2}_{{\rm ex};\vec{n}_1,\vec{n}_2} \hat{\Psi}_{\vec{n}_2,\lambda_2}. \tag{3.21}$$

where the matrix representing the external potential is given by

$$\mathcal{V}^{\alpha_1,\alpha_2}_{{\rm ex};\vec{n}_1,\vec{n}_2} = \sum_{\lambda} \int d\vec{x}\ (\phi^{\dagger})^{\alpha_1}_{\vec{n}_1,\lambda}(\vec{x}) V_{\rm ex}(\vec{x}) \phi^{\alpha_2}_{\vec{n}_2,\lambda}(\vec{x}). \tag{3.22}$$

The advantage of this basis is that it simplifies the evaluation of the partition function. Let us return to the partition function in Eq.(3.12) and first evaluate the trace of the density operator in the denominator. The trace of an arbitrary operator can be evaluated by means of a functional integral over coherent states according to

$$\mathrm{Tr}[\hat{O}] = \int d\psi^{\dagger} d\psi\ e^{-(\psi|\psi)} \left\langle \psi \right| \hat{O} \left| -\psi \right\rangle . \tag{3.23}$$

By applying this formula to the trace of the density matrix operator, one can straightforwardly show that

$$\begin{aligned}
\mathrm{Tr}[\hat{\rho}] &= \int d\psi^{\dagger} d\psi\ e^{-(\psi|\psi)} \left\langle \psi \right| \hat{\rho} \left| -\psi \right\rangle \\
&= \int d\psi^{\dagger} d\psi\ e^{-(\psi|\psi)} \left\langle \psi \right| e^{-\beta \sum_{\vec{n},\alpha} (\epsilon_{\vec{n},\alpha} - \mu) \hat{\Psi}^{\dagger}_{\vec{n},\alpha} \hat{\Psi}_{\vec{n},\lambda}} \left| -\psi \right\rangle \\
&= \int d\psi^{\dagger} d\psi\ e^{-\sum_{\vec{n},\lambda} (1 + e^{-\beta(\epsilon_{\vec{n},\alpha} - \mu)}) \psi^{\dagger}_{\vec{n},\lambda} \psi_{\vec{n},\lambda}} \\
&= \prod_{\vec{n},\lambda} (1 + e^{-\beta(\epsilon_{\vec{n},\alpha} - \mu)}).
\end{aligned} \tag{3.24}$$

Next, we consider the numerator and evaluate the trace of the evolution operator on the close time contour depicted in Fig. (3.1). To this end, as the first step, we split the closed time contour into $2M$ discrete points such that $t_1 = -\infty$ and $t_M = \infty$ and each time interval is of length δ_t as depicted in Fig.(3.1). For the pedagogical reason, we take $M = 3$. Generalization to an arbitrary value of M is straightforward. We have that

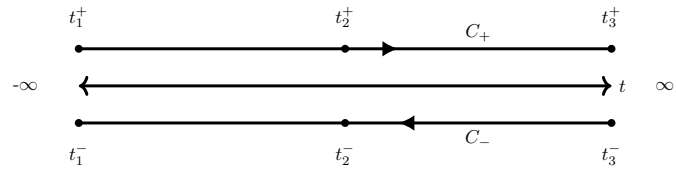

Figure 3.1

$$\mathrm{Tr}\left[\hat{U}_C\hat{\rho}\right] = \int d\psi^\dagger_{t_1^-} d\psi_{t_1^-} e^{(\psi_{t_1^-}|\psi_{t_1^-})} \left\langle \psi_{t_1^-}\right| \hat{U}_C\hat{\rho} \left|-\psi_{t_1^-}\right\rangle, \qquad (3.25)$$

where the trace is evaluated at $t_1^- = -\infty$ when the system is non-interacting and in equilibrium. The system evolve form $t_1^+ = -\infty$ along the contour towards $t_3^+ = \infty$ before returning to $t_1^- = -\infty$. Thus, the evolution operator is decomposed as

$$\hat{U}_C = \hat{U}_{t_1^-,t_1^+} = \hat{U}_{t_1^-,t_2^-}\hat{U}_{t_2^-,t_3^-}\hat{U}_{t_3^-,t_3^+}\hat{U}_{t_3^+,t_2^+}\hat{U}_{t_2^+,t_1^+} = \hat{U}_{-\delta_t}\hat{U}_{-\delta_t}\hat{1}\hat{U}_{\delta_t}\hat{U}_{\delta_t}. \qquad (3.26)$$

The superscripts $\pm$ of the time variables indicate either they are on the forward or backward branches. Here $U_{t,t'} = e^{-i\hat{H}(t-t')}$ is the evolution operator during the time interval $t - t'$ by the total Hamiltonian $\hat{H} = \hat{H}_0 + \hat{H}_I + \hat{H}_{\mathrm{ex}}$. It reduces to $U_{\pm\delta_t} = e^{\mp i\hat{H}\delta_t}$ which explains the evolution during the time interval δ_t along the forward and backward of time directions, respectively.

For the second step, we insert the resolution of unity in the coherent state basis at each intermediate point along the contour. The resolution of unity is given by

$$\hat{1} = \int d\psi^\dagger d\psi\, e^{-(\psi|\psi)} \left|\psi\right\rangle \left\langle\psi\right|. \qquad (3.27)$$

One finds the following product in the expression for $\mathrm{Tr}\left[\hat{U}_C\hat{\rho}\right]$:

$$\begin{aligned}\left\langle \psi_{t_1^-}\right|\hat{U}_C\hat{\rho}\left|-\psi_{t_1^-}\right\rangle = \\ \left\langle \psi_{t_{1-}}\right|\hat{U}_{t_1^-,t_2^-}\left|\psi_{t_2^-}\right\rangle\left\langle \psi_{t_2^-}\right|\hat{U}_{t_2^-,t_3^-}\left|\psi_{t_3^-}\right\rangle\left\langle \psi_{t_3^-}\middle|\psi_{t_3^+}\right\rangle \\ \left\langle \psi_{t_{3+}}\right|\hat{U}_{t_3^+,t_2^+}\left|\psi_{t_2^+}\right\rangle\left\langle \psi_{t_2^+}\right|\hat{U}_{t_2^+,t_1^+}\left|\psi_{t_1^+}\right\rangle\left\langle \psi_{t_1^+}\right|\hat{\rho}\left|-\psi_{t_1^-}\right\rangle .\end{aligned} \tag{3.28}$$

Note that as t_3^+ and t_3^- are physically the same point, there is no evolution operator inserted in between them. The matrix element of the density matrix operator is given by

$$\left\langle \psi_{t_1^+}\right|\hat{\rho}\left|-\psi_{t_1^-}\right\rangle = \exp\left(-\sum_{\vec{n},\alpha} e^{-\beta(\epsilon_{\vec{n},\alpha}-\mu)}\psi^\dagger_{\vec{n},\alpha;t_1^+}\psi_{\vec{n},\alpha;t_1^-}\right). \tag{3.29}$$

On the other hand, the matrix elements of the evolution operator are given by

$$\begin{aligned}\left\langle \psi_{t_j\pm\delta_t}\right|\hat{U}_{\pm\delta_t}\left|\psi_{t_j}\right\rangle &= \left\langle \psi_{t_j\pm\delta_t}\right| e^{\mp i\hat{H}[\hat{\Psi}^\dagger,\hat{\Psi}]\delta_t}\left|\psi_{t_j}\right\rangle \\ &\approx \left\langle \psi_{t_j\pm\delta_t}\right|1\mp i\hat{H}[\psi^\dagger_{t_j\pm\delta t},\psi_{t_j}]\delta_t\left|\psi_{t_j}\right\rangle \\ &\approx e^{(\psi_{t_j\pm\delta_t}|\psi_{t_j})\mp i\hat{H}[\psi^\dagger_{t_j\pm\delta_t},\psi_{t_j}]\delta_t}.\end{aligned} \tag{3.30}$$

By collecting all the exponential factor along the contour, the partition function becomes

$$Z = \int \mathcal{D}\psi^\dagger\mathcal{D}\psi\ \exp\left(iS_0 + iS_{\mathrm{ex}} + iS_I\right). \tag{3.31}$$

where the measure of the functional integration takes the form of

$$\mathcal{D}\psi^\dagger\mathcal{D}\psi = \frac{1}{\mathrm{Tr}[\hat{\rho}]}\prod_{\vec{n},\alpha}\prod_{j=1}^{M}\prod_{\xi\pm} d\psi^\dagger_{\vec{n},\alpha;t_j^\xi}d\psi_{\vec{n},\alpha;t_j^\xi}. \tag{3.32}$$

Note that the trace of the density matrix operator evaluated in Eq.(3.24) provides solely an irrelevant factor and therefore is absorbed into the measure. The interaction part of the action is given

by

$$S_I = -\frac{1}{2}\sum_{j=1}^{M-1}\sum_{\xi=\pm}\sum_{\vec{n}_1,\vec{n}_2,\vec{n}_3,\vec{n}_4}\sum_{\alpha_1,\alpha_2,\alpha_3,\alpha_4}\xi\delta_t \mathcal{V}^{\alpha_1,\alpha_2,\alpha_3,\alpha_4}_{\vec{n}_1,\vec{n}_2,\vec{n}_3,\vec{n}_4} \psi^{\dagger}_{\vec{n}_1,\alpha_1;t_j^{\xi}+\delta_t}\psi^{\dagger}_{\vec{n}_2,\alpha_2;t_j^{\xi}+\delta_t}\psi_{\vec{n}_3,\alpha_3;t_j^{\xi}}\psi_{\vec{n}_4,\alpha_4;t_j^{\xi}}. \quad (3.33)$$

Similarly, the external interaction part of the action is given by

$$S_{\rm ex} = -\sum_{j=1}^{M-1}\sum_{\xi=\pm}\sum_{\vec{n}_1,\vec{n}_2}\sum_{\alpha_1,\alpha_2}\xi\delta_t\psi^{\dagger}_{\vec{n}_1,\alpha_1;t_j^{\xi}+\delta_t}\mathcal{V}^{\alpha_1,\alpha_2}_{{\rm ex};\vec{n}_1,\vec{n}_2}\psi_{\vec{n}_2,\alpha_2;t_j^{\xi}}. \quad (3.34)$$

Note that the evolution operator on the backward branch moves in the opposite directions to the time axis. As a result, it gives a global multiplicative factor ξ in the action. Thus, we have $\xi = 1$ for forward branch and $\xi = -1$ for backward branch in Eqs. (3.33) and (3.34).

The non-interacting part of the action reads

$$S_0 = \sum_{j,j'=1}^{M}\sum_{\xi,\xi'=\pm}\sum_{\vec{n},\alpha}\sum_{\vec{n}',\alpha'}\psi^{\dagger}_{\vec{n},\alpha;t_j^{\xi}}(-\hat{G}_0^{-1})_{\vec{n},\vec{n}',\alpha,\alpha';t_j^{\xi},t_{j'}^{\xi'}}\psi_{\vec{n}',\alpha';t_{j'}^{\xi'}}, \quad (3.35)$$

where, for $M = 3$, the inverse Green's function reads as

$$(-i\hat{G}_0^{-1})_{\vec{n},\vec{n}',\alpha,\alpha';t_j^{\xi},t_{j'}^{\xi'}} = \begin{array}{c} \\ t_1^+ \\ t_2^+ \\ t_3^+ \\ t_3^- \\ t_2^- \\ t_1^- \end{array} \begin{array}{c} \begin{array}{cccccc} t_1^+ & t_2^+ & t_3^+ & t_3^- & t_2^- & t_1^- \end{array} \\ \begin{pmatrix} -1 & 0 & 0 & 0 & 0 & -\rho(\epsilon_{\vec{n},\alpha}) \\ h_+ & -1 & 0 & 0 & 0 & 0 \\ 0 & h_+ & -1 & 0 & 0 & 0 \\ 0 & 0 & 1 & -1 & 0 & 0 \\ 0 & 0 & 0 & h_- & -1 & 0 \\ 0 & 0 & 0 & 0 & h_- & -1 \end{pmatrix} \end{array} \delta_{\vec{n}\vec{n}'}\delta_{\alpha\alpha'}. \quad (3.36)$$

Here $h_{\pm} = 1 \mp i(\epsilon_{\vec{n},\alpha} - \mu)\delta_t$ originate from the matrix elements of the time evolution operator given by Eq.(3.30) and $\rho(\epsilon_{\vec{n},\alpha}) = \exp(-\beta(\epsilon_{\vec{n},\alpha}))$ comes from the matrix elements of the density matrix

operator evaluated in Eq.(3.29). The main diagonal elements comes from the resolution of unity, Eq.(3.27). Note that as we choose to work with the basis that diagonalises the non-interacting part of the Hamiltonain, iG^{-1} is diagonal in this basis too. The inverse Green's function is thus proportional to $\delta_{\vec{n},\vec{n}'}\delta_{\alpha\alpha'}$. Another remark that should be pointed out is that the structure of iG^{-1} given above is general for any values of M. Generalization to an arbitrary value of M is straightforward.

In the end, we are interested in the continuum limit of the above action. This is achieved by taking the limit $M \to \infty$ while keeping $M\delta_t$ constant. According to Eq.(3.35) and Eq.(3.36), the non-interacting part of the action reads

$$\begin{aligned} S_0 &= i\psi^{\dagger}_{\vec{n},\alpha;t_1^+}\left(\psi_{\vec{n},\alpha;t_1^+} + \rho(\epsilon_{\vec{n},\alpha})\psi_{\vec{n},\alpha;t_1^-}\right) - i\psi^{\dagger}_{\vec{n},\alpha;t_N^-}\psi_{\vec{n},\alpha;t_N^-} \\ &+ i\sum_{j=1}^{N-1}\sum_{\vec{n},\alpha}\psi^{\dagger}_{\vec{n},\alpha;t_j^+ +\delta_t}\left[\frac{\psi_{\vec{n},\alpha;t_j^+ +\delta_t} - \psi_{\vec{n},\alpha;t_j^+}}{\delta_t} + i\epsilon_{\vec{n},\alpha}\psi_{\vec{n},\alpha;t_j^+}\right]\delta_t \\ &+ i\sum_{j=1}^{N-1}\sum_{\vec{n},\alpha}\psi^{\dagger}_{\vec{n},\alpha;t_j^-}\left[\frac{\psi_{\vec{n},\alpha;t_j^-} - \psi_{\vec{n},\alpha;t_j^- +\delta_t}}{\delta_t} - i\epsilon_{\vec{n},\alpha}\psi_{\vec{n},\alpha;t_j^-}\right]\delta_t \ . \end{aligned} \tag{3.37}$$

Hence, after taking the continuum limit, we find that

$$\begin{aligned} S_0 &= \sum_{\vec{n},\alpha}\int_{-\infty}^{\infty} dt\psi^{\dagger}_{\vec{n},\alpha;+}(t)\left(i\partial_t - \epsilon_{\vec{n},\alpha} + \mu\right)\psi_{\vec{n},\alpha;+}(t) \\ &\quad - \sum_{\vec{n},\alpha}\int_{-\infty}^{\infty} dt\psi^{\dagger}_{\vec{n},\alpha;-}(t)\left(i\partial_t - \epsilon_{\vec{n},\alpha} + \mu\right)\psi_{\vec{n},\alpha;-}(t). \end{aligned} \tag{3.38}$$

Here we employed the notation $\psi_{\vec{n},\alpha;t^{\xi}} \equiv \psi_{\vec{n},\alpha;\xi}(t)$; We neglected the boundary terms and obtained the action describing two duplicate copies of fermions, one lives on the forward contour and another lives on the backward contour. It is important to note that the continuum limit of the action written above is correct up to the boundary terms. Although the fermions on the backward and forward branches look

seemingly independent, they are actually coupled by the disregarded boundary terms. Therefore, calculating the non-interacting Green's function from this action is already not straightforward. One needs to resort to the discretized version of the theory, determine the inverse of the matrix in Eq.(3.36) and at the last step taking the limit $M \to \infty$ to obtain the Green's function in the continuum limit. This will be the topic of next section.

One may transform the action back to the coordinate space by employing Eqs.(3.13), (3.14), and (3.15), this yields

$$S_0 = \sum_{\xi=\pm} \sum_{\lambda\lambda'} \xi \int_{-\infty}^{\infty} dt \int d\vec{x} \psi^{\dagger}_{\lambda;\xi}(\vec{x},t) \Big(i\partial_t - \hat{H}_{D,\lambda\lambda'}(\vec{x}) \Big)_{\lambda\lambda'} \psi_{\lambda';\xi}(\vec{x},t). \tag{3.39}$$

Let us finish this section with the continuum limit of the interaction part of the action. We find that

$$\begin{aligned} S_I \quad = \quad & -\sum_{\xi=\pm} \sum_{\vec{n}_1,\vec{n}_2,\vec{n}_3,\vec{n}_4} \sum_{\alpha_1,\alpha_2,\alpha_3,\alpha_4} \frac{1}{2} \int_{-\infty}^{\infty} dt \xi \mathcal{V}^{\alpha_1,\alpha_2,\alpha_3,\alpha_4}_{\vec{n}_1,\vec{n}_2,\vec{n}_3,\vec{n}_4} \\ & \psi^{\dagger}_{\vec{n}_1,\alpha_1;\xi}(t) \psi^{\dagger}_{\vec{n}_2,\alpha_2;\xi}(t) \psi_{\vec{n}_3,\alpha_3;\xi}(t) \psi_{\vec{n}_4,\alpha_4;\xi}(t). \end{aligned} \tag{3.40}$$

and

$$S_{\rm ex} = -\sum_{\xi=\pm} \sum_{\vec{n}_1,\vec{n}_2} \sum_{\alpha_1,\alpha_2} \int_{-\infty}^{\infty} dt \xi \psi^{\dagger}_{\vec{n}_1,\alpha_1;\xi}(t) \mathcal{V}^{\alpha_1,\alpha_2}_{{\rm ex};\vec{n}_1,\vec{n}_2} \psi_{\vec{n}_2,\alpha_2;\xi}(t). \tag{3.41}$$

Recall that here we slightly modify the notation, $\psi_{\vec{n},\alpha;t^{\xi}} \equiv \psi_{\vec{n},\alpha;\xi}(t)$. Furthermore, one may rotate them back to the coordinate space and find that

$$\begin{aligned} S_I = -\frac{1}{2} \sum_{\xi=\pm} \sum_{\lambda,\lambda'} \int_{-\infty}^{\infty} dt d\vec{x} d\vec{x}' \; & \xi \psi^{\dagger}_{\lambda;\xi}(\vec{x},t) \psi^{\dagger}_{\lambda';\xi}(\vec{x}',t) V(\vec{x}-\vec{x}') \\ & \psi_{\lambda';\xi}(\vec{x}',t) \psi_{\lambda;\xi}(\vec{x},t). \end{aligned} \tag{3.42}$$

and

$$S_{\rm ex} = -\sum_{\xi=\pm} \sum_{\lambda} \int_{-\infty}^{\infty} dt \xi \psi^{\dagger}_{\lambda;\xi}(\vec{x}',t) V_{\rm ex}(\vec{x}) \psi_{\lambda;\xi}(\vec{x},t). \tag{3.43}$$

3.3 Non-interacting Green's functions

This section is about the Green's functions. Given an action S, the Green's function denoted by $G^{\xi\xi'}_{\vec{n},\vec{n}',\alpha,\alpha'}(t_j,t_{j'})$ can be calculated by means of

$$\begin{aligned} iG^{\xi\xi'}_{\vec{n},\vec{n}',\alpha,\alpha'}(t_j,t_{j'}) &\equiv \langle\psi_{\vec{n},\alpha;\xi}(t_j)\psi^{\dagger}_{\vec{n}',\alpha';\xi'}(t_{j'})\rangle \\ &= \int \mathcal{D}\psi^{\dagger}\mathcal{D}\psi\ \psi_{\vec{n},\alpha;\xi}(t_j)\psi^{\dagger}_{\vec{n}',\alpha';\xi'}(t_{j'})e^{iS}. \end{aligned} \tag{3.44}$$

First, we consider the non-interacting Dirac theory described by the action in Eq. (3.35). The Green's function for this case can be calculated exactly by employing the basic properties of Gaussian integral. We find that

$$iG^{\xi\xi'}_{0;\vec{n},\vec{n}',\alpha,\alpha'}(t_j,t_{j'}) = \left(iG_0^{-1}\right)^{-1}_{\vec{n},\vec{n}',\alpha,\alpha',t_j^{\xi},t_{j'}^{\xi'}}. \tag{3.45}$$

The non-interacting Green's function is essentially obtained from the inverse of the matrix $G^{-1}_{0;\vec{n},\vec{n}',\alpha,\alpha',t_j^{\xi},t_{j'}^{\xi'}}$ in Eq.(3.36). By inverting the matrix in Eq.(3.36), we obtain the Green's function for the non-interaction Dirac theory reading as

$$i\hat{G}^{\xi\xi'}_{0;\vec{n},\vec{n}',\alpha,\alpha'}(t_j,t_{j'}) = -\delta_{\vec{n}\vec{n}'}\delta_{\alpha\alpha'}\frac{1}{1+\rho(h_+h_-)^2}\times$$

$$\begin{array}{c} \\ t_1^+ \\ t_2^+ \\ t_3^+ \\ t_3^- \\ t_2^- \\ t_1^- \end{array} \begin{array}{c} \begin{array}{cccccc} t_1^+ & t_2^+ & t_3^+ & t_3^- & t_2^- & t_1^- \end{array} \\ \begin{pmatrix} 1 & -h_-h_+^2\rho & -h_+^2\rho & -h_+^2\rho & -h_+\rho & -\rho \\ h_- & 1 & -h_-h_+^2\rho & -h_-h_+^2\rho & -h_-h_+\rho & -h_-\rho \\ h_-^2 & h_- & 1 & -h_-^2h_+^2\rho & -h_-^2h_+\rho & -h_-^2\rho \\ h_-^2 & h_- & 1 & 1 & -h_-^2h_+\rho & -h_-^2\rho \\ h_-^2h_+ & h_-h_+ & h_+ & h_+ & 1 & -h_-^2h_+\rho \\ h_-^2h_+^2 & h_-h_+^2 & h_+^2 & h_+^2 & h_+ & 1 \end{pmatrix} \end{array}. \tag{3.46}$$

Here we introduced the shorthand notation $\rho \equiv \rho(\epsilon_{\vec{n},\alpha})$. The structure of the Green's function is indeed general and generalization to an arbitrary number of time intervals on the closed time contour is

straightforward. We find that the Green's function may be partitioned into fours submatrices, namely

$$i\hat{G}_{0;\vec{n},\vec{n}',\alpha,\alpha'}(t_j,t_{j'}) = \begin{pmatrix} iG^{++}_{0;\vec{n},\vec{n}',\alpha,\alpha'}(t_j,t_{j'}) & iG^{+-}_{0;\vec{n},\vec{n}',\alpha,\alpha'}(t_j,t_{j'}) \\ iG^{-+}_{0;\vec{n},\vec{n}',\alpha,\alpha'}(t_j,t_{j'}) & iG^{--}_{0;\vec{n},\vec{n}',\alpha,\alpha'}(t_j,t_{j'}) \end{pmatrix}, \tag{3.47}$$

where

$$\begin{aligned} iG^{+-}_{0;\vec{n},\vec{n}',\alpha,\alpha'}(t_j,t_{j'}) &= -\delta_{\vec{n}\vec{n}'}\delta_{\alpha\alpha'}\frac{\rho h_+^{j'-1}h_-^{j-1}}{1+\rho(h_+h_-)^{N-1}}, \\ iG^{-+}_{0;\vec{n},\vec{n}',\alpha,\alpha'}(t_j,t_{j'}) &= \delta_{\vec{n}\vec{n}'}\delta_{\alpha\alpha'}\frac{h_+^{N-j}h_-^{N-j'}}{1+\rho(h_+h_-)^{N-1}}, \end{aligned}$$

$$\begin{aligned} &iG^{++}_{0;\vec{n},\vec{n}',\alpha,\alpha'}(t_j,t_{j'}) \\ &\qquad = \delta_{\vec{n}\vec{n}'}\delta_{\alpha\alpha'}\frac{h_-^{j-j'}}{1+\rho(h_+h_-)^{N-1}}\begin{cases} 1 & \text{if } j \geq j' \\ -\rho(h_-h_+)^{N-1} & \text{if } j < j' \end{cases}, \\ &iG^{--}_{0;\vec{n},\vec{n}',\alpha,\alpha'}(t_j,t_{j'}) \\ &\qquad = \delta_{\vec{n}\vec{n}'}\delta_{\alpha\alpha'}\frac{h_+^{j'-j}}{1+\rho(h_+h_-)^{N-1}}\begin{cases} 1 & \text{if } j \leq j' \\ -\rho(h_-h_+)^{N-1} & \text{if } j > j' \end{cases}. \end{aligned} \tag{3.48}$$

Next, we obtain the Green's functions in the continuum limit by taking the limit of $M \to \infty$. To this end, recall that $h_\pm = 1 \mp i(\epsilon_{\vec{n},\alpha})\delta_t$. This implies that

$$(h_+h_-)^{M-1} = (1+(\epsilon_{\vec{n},\alpha})^2\delta_t^2)^{M-1} \approx e^{(\epsilon_{\vec{n},\alpha})^2\delta_t^2)(M-1)} \xrightarrow{M\to\infty} 1, \tag{3.49}$$

while

$$h_\pm^j = (1 \mp i(\epsilon_{\vec{n},\alpha})\delta_t)^j \approx e^{\mp i(\epsilon_{\vec{n},\alpha})t}, \tag{3.50}$$

where we denote $t = j\delta_t$. This gives

$$
\begin{aligned}
iG^{+-}_{0;\vec{n},\vec{n}',\alpha,\alpha'}(t,t') &= -\delta_{\vec{n}\vec{n}'}\delta_{\alpha\alpha'}\frac{\rho}{1+\rho}e^{-i(\epsilon_{\vec{n},\alpha})(t-t')}, \\
&= -\delta_{\vec{n}\vec{n}'}\delta_{\alpha\alpha'}f^0(\epsilon_{\vec{n},\alpha})e^{-i(\epsilon_{\vec{n},\alpha})(t-t')}, \\
iG^{-+}_{0;\vec{n},\vec{n}',\alpha,\alpha'}(t,t') &= \delta_{\vec{n}\vec{n}'}\delta_{\alpha\alpha'}\frac{1}{1+\rho}e^{-i(\epsilon_{\vec{n},\alpha})(t-t')}, \\
&= \delta_{\vec{n}\vec{n}'}\delta_{\alpha\alpha'}(1-f^0(\epsilon_{\vec{n},\alpha}))e^{-i(\epsilon_{\vec{n},\alpha})(t-t')}, \\
&iG^{++}_{0;\vec{n},\vec{n}',\alpha,\alpha'}(t,t') \\
&\quad = \theta(t-t')iG^{-+}_{0;\vec{n},\vec{n}',\alpha,\alpha'}(t,t') + \theta(t'-t)iG^{+-}_{0;\vec{n},\vec{n}',\alpha,\alpha'}(t,t'), \\
&iG^{--}_{0;\vec{n},\vec{n}',\alpha,\alpha'}(t,t') \\
&\quad = \theta(t-t')iG^{+-}_{0;\vec{n},\vec{n}',\alpha,\alpha'}(t,t') + \theta(t'-t)iG^{-+}_{0;\vec{n},\vec{n}',\alpha,\alpha'}(t,t').
\end{aligned}
\tag{3.51}
$$

Here $f^0(\epsilon_{\vec{n},\alpha}) = \frac{\rho}{1+\rho} = \frac{1}{e^{\beta(\epsilon_{\vec{n},\alpha})}+1}$ denotes the Fermi-Dirac distribution function. Note that we modified again the notation for the Green's functions as

$$
iG^{\xi\xi'}_{0;\vec{n},\vec{n}',\alpha,\alpha'}(t,t') \equiv iG^{\xi\xi'}_{0;\vec{n},\vec{n}',\alpha,\alpha'}(t_j,t_{j'}); \tag{3.52}
$$

We dropped the subscripts j and j' of the time variables.

The Green's functions defined in Eq.(3.51) are not independent. It is easy to show that

$$
\begin{aligned}
&iG^{+-}_{0;\vec{n},\vec{n}',\alpha,\alpha'}(t,t') + iG^{+-}_{0;\vec{n},\vec{n}',\alpha,\alpha'}(t,t') = \\
&\qquad iG^{--}_{0;\vec{n},\vec{n}',\alpha,\alpha'}(t,t') + iG^{++}_{0;\vec{n},\vec{n}',\alpha,\alpha'}(t,t').
\end{aligned}
\tag{3.53}
$$

This leads to the idea that, instead of $\psi^{(\dagger)}_{\vec{n},\alpha,\pm}(t)$, one may define a pair of new fields in such a way that the resulting Green's function contains a zero block due to the above relation while the other blocks are non-zero and independent. For fermions, it is customary to employ Larkin-Ovchinnikov transformation reading as

$$
\begin{aligned}
\psi_{\vec{n},\alpha;\xi}(t) &= \sum_{a=1}^{2} L_{\xi a}\psi_{\vec{n},\alpha;a}(t) \\
\psi^{\dagger}_{\vec{n},\alpha;\xi}(t) &= \sum_{a=1}^{2} \psi^{\dagger}_{\vec{n},\alpha;a}(t)\tilde{L}_{a\xi}.
\end{aligned}
\tag{3.54}
$$

The newly introduced fields $\psi_{\vec{n},\alpha;a}$ and $\psi^{\dagger}_{\vec{n},\alpha;a}$ are transformed to the old fields $\psi_{\vec{n},\alpha;\xi}$ and $\psi^{\dagger}_{\vec{n},\alpha;\xi}$ by transformation matrices

$$L_{\xi a} = \frac{1}{\sqrt{2}} \begin{pmatrix} 1 & 1 \\ 1 & -1 \end{pmatrix}_{\xi a} \quad \text{and} \quad \tilde{L}_{a\xi} = \frac{1}{\sqrt{2}} \begin{pmatrix} 1 & -1 \\ 1 & 1 \end{pmatrix}_{a\xi}. \tag{3.55}$$

The latin alphabet a takes on the value 1 and 2 denoting the so-called Keldysh index of the fermion. It should be noted that $L_{\xi a} \neq (\tilde{L}_{\xi a})^{\dagger}$ as the Grassmann field $\psi^{\dagger}$ are not conjugated to ψ. They are actually completely different Grassmann fields and hence they can be transformed in an arbitrary manner.

In the Larkin-Ovchinnikov basis, the Green's function takes the form of

$$i\hat{G}_{\vec{n},\vec{n}',\alpha,\alpha'}(t,t') = \begin{pmatrix} iG^{11}_{\vec{n},\vec{n}',\alpha,\alpha'}(t,t') & iG^{12}_{\vec{n},\vec{n}',\alpha,\alpha'}(t,t') \\ iG^{21}_{\vec{n},\vec{n}',\alpha,\alpha'}(t,t') & iG^{22}_{\vec{n},\vec{n}',\alpha,\alpha'}(t,t') \end{pmatrix}, \tag{3.56}$$

where

$$\begin{aligned}
iG^{11}_{\vec{n},\vec{n}',\alpha,\alpha'}(t,t') &= \frac{i}{2}\left(G^{++} + G^{-+} - G^{+-} - G^{--}\right)_{\vec{n},\vec{n}',\alpha,\alpha'}(t,t'), \\
iG^{12}_{\vec{n},\vec{n}',\alpha,\alpha'}(t,t') &= \frac{i}{2}\left(G^{++} + G^{-+} + G^{+-} + G^{--}\right)_{\vec{n},\vec{n}',\alpha,\alpha'}(t,t'), \\
iG^{21}_{\vec{n},\vec{n}',\alpha,\alpha'}(t,t') &= \frac{i}{2}\left(G^{++} - G^{-+} - G^{+-} + G^{--}\right)_{\vec{n},\vec{n}',\alpha,\alpha'}(t,t'), \\
iG^{22}_{\vec{n},\vec{n}',\alpha,\alpha'}(t,t') &= \frac{i}{2}\left(G^{++} - G^{-+} + G^{+-} - G^{--}\right)_{\vec{n},\vec{n}',\alpha,\alpha'}(t,t').
\end{aligned} \tag{3.57}$$

The superscripts taken on the values 1 and 2 label the so-called Keldysh indices of the fermionic Green's function. By employing the relation given in Eq.(3.53) together with the expressions given

in Eq.(3.51), we find that

$$\begin{aligned}
iG^{11}_{\vec{n},\vec{n}',\alpha,\alpha'}(t,t') &= \theta(t-t')\left(iG^{-+}-iG^{+-}\right)_{\vec{n},\vec{n}',\alpha,\alpha'}(t,t'),\\
&= \theta(t-t')\delta_{\vec{n}\vec{n}'}\delta_{\alpha\alpha'}e^{-i(\epsilon_{\vec{n},\alpha}-\mu)(t-t')},\\
iG^{12}_{\vec{n},\vec{n}',\alpha,\alpha'}(t,t') &= \left(iG^{-+}+iG^{+-}\right)_{\vec{n},\vec{n}',\alpha,\alpha'}(t,t'),\\
&= (1-2f^0(\epsilon_{\vec{n},\alpha}))\delta_{\vec{n}\vec{n}'}\delta_{\alpha\alpha'}e^{-i(\epsilon_{\vec{n},\alpha}-\mu)(t-t')},\\
iG^{21}_{\vec{n},\vec{n}',\alpha,\alpha'}(t,t') &= 0\,,\\
iG^{22}_{\vec{n},\vec{n}',\alpha,\alpha'}(t,t') &= \theta(t'-t)\left(iG^{+-}-iG^{-+}\right)_{\vec{n},\vec{n}',\alpha,\alpha'}(t,t')\,,\\
&= -\theta(t'-t)\delta_{\vec{n}\vec{n}'}\delta_{\alpha\alpha'}e^{-i(\epsilon_{\vec{n},\alpha}-\mu)(t-t')}. \qquad (3.58)
\end{aligned}$$

As a result of the relation in Eq.(3.53), $iG^{21}_{\vec{n},\vec{n}',\alpha,\alpha'}(t,t')$ vanishes. Furthermore, we observe that $iG^{11}_{\vec{n},\vec{n}',\alpha,\alpha'}(t,t')$ is proportional to $\theta(t-t')$. Since it is non-zero only when $t>t'$, it is dubbed as a retarded Green's function and hereafter denoted by $iG^{R}_{\vec{n},\vec{n}',\alpha,\alpha'}(t,t')$. In contrast, $iG^{22}_{\vec{n},\vec{n}',\alpha,\alpha'}(t,t')$ is proportional to $\theta(t'-t)$ which is non-zero if and only if $t<t'$. It is therefore dubbed as an advanced Green's function and denoted by $iG^{A}_{\vec{n},\vec{n}',\alpha,\alpha'}(t,t')$.

Moreover, we have $iG^{22}_{\vec{n},\vec{n}',\alpha,\alpha'}(t,t')$ which is usually called a Keldysh Green's function and hereafter denoted by $iG^{K}_{\vec{n},\vec{n}',\alpha,\alpha'}(t,t')$. We find that the Keldysh Green's function is related to the retarded and advanced Green's functions by means of

$$G^{K}_{\vec{n},\vec{n}',\alpha,\alpha'}(t,t') = G^{R}_{\vec{n},\vec{n}',\alpha,\alpha'}(t,t')F(\epsilon_{\vec{n},\alpha}) - F(\epsilon_{\vec{n},\alpha})G^{A}_{\vec{n},\vec{n}',\alpha,\alpha'}(t,t'), \qquad (3.59)$$

where we introduced $F(\epsilon_{\vec{n},\alpha}) = 1-2f^0(\epsilon_{\vec{n},\alpha})$.

Notice that the Keldysh Green's function contains information about the energy spectrum as well as the occupation number, while the retarded and advanced Green's functions depend only on the energy spectrum.

In addition, we find that, for a non-interacting theory, the Green's functions depend solely on the relative time coordinate, $t-t'$, but not the center-of-mass coordinate $(t+t')/2$. Therefore, the Fourier transforms of the Green's function with respect to $t-t'$ may be performed and are given by

$$iG^{R}(\epsilon) = \frac{i\delta_{\vec{n}\vec{n}'}\delta_{\alpha\alpha'}}{\epsilon+i0^+-\epsilon_{\vec{n},\alpha}}, \qquad (3.60)$$

$$iG^A(\epsilon) = \frac{i\delta_{\vec{n}\vec{n}'}\delta_{\alpha\alpha'}}{\epsilon - i0^+ - \epsilon_{\vec{n},\alpha}}, \tag{3.61}$$

$$iG^K(\epsilon) = 2\pi\delta_{\vec{n}\vec{n}'}\delta_{\alpha\alpha'}\delta(\epsilon - \epsilon_{\vec{n},\alpha} + \mu)(1 - 2f^0(\epsilon_{\vec{n},\alpha})). \tag{3.62}$$

As one might expect, we see that $iG^{R/A}(\epsilon)$ have poles precisely at $\epsilon = \epsilon_{\vec{n},\alpha} - \mu$ which correspond to the energies of the elementary excitations. Recall that for a homogeneous and non-interacting Dirac electron gas, the energies of the single-particle states are given by $\epsilon^{\pm}_{\vec{p},\alpha} = \pm\hbar v_F p - \mu$.

3.4 Keldysh action

We find that the Larkin-Ovchinnikov basis is the basis that the condition in Eq. (3.53) is implemented explicitly such that one component of the Green's function vanishes and the remaining components are independent. Hence, it is convenient to rotate the action also by the same transformation.

We first consider the non-interacting part of the action given by Eq.(3.38). By employing the Larkin-Ovchinnikov transformation, we find that

$$\begin{aligned} S_0 &= \sum_{\xi=\pm}\sum_{\vec{n},\alpha}\xi\int_{-\infty}^{\infty} dt\ \psi^{\dagger}_{\vec{n},\alpha;\xi}(t)\left(i\partial_t - \epsilon_{\vec{n},\alpha}\right)\psi_{\vec{n},\alpha;\xi}(t), \\ &= \sum_{a,b=1}^{2}\sum_{\xi=\pm}\sum_{\vec{n},\alpha}\xi\int_{-\infty}^{\infty} dt\ \psi^{\dagger}_{\vec{n},\alpha;a}(t)\tilde{L}_{a\xi}\left(i\partial_t - \epsilon_{\vec{n},\alpha}\right) \\ &\qquad\qquad L_{\xi,b}\psi_{\vec{n},\alpha;b}(t), \\ &= \sum_{a=1}^{2}\sum_{\vec{n},\alpha}\int_{-\infty}^{\infty} dt\ \psi^{\dagger}_{\vec{n},\alpha;a}(t)\left(i\partial_t - \epsilon_{\vec{n},\alpha}\right)\psi_{\vec{n},\alpha;a}(t). \end{aligned} \tag{3.63}$$

The interaction parts of the action can be transformed into the Larkin-Ovchinnikov basis. They read as

$$S_{\rm ex} = -\sum_{a=1}^{2}\sum_{\vec{n}_1,\vec{n}_2}\sum_{\alpha_1,\alpha_2}\int_{-\infty}^{\infty} dt\psi^{\dagger}_{\vec{n},\alpha;a}(t)\mathcal{V}^{\alpha_1,\alpha_2}_{{\rm ex};\vec{n}_1,\vec{n}_2}\psi_{\vec{n},\alpha;a}(t), \tag{3.64}$$

and

$$S_I = -\sum_{a,b,c,d,e,f=1}^{2}\sum_{\vec{n}_1,\vec{n}_2,\vec{n}_3,\vec{n}_4}\sum_{\alpha_1,\alpha_2,\alpha_3,\alpha_4}\frac{1}{2}\int_{-\infty}^{\infty}dt\psi^{\dagger}_{\vec{n}_1,\alpha_1;a}$$
$$\gamma^{e}_{ab}(t)\psi_{\vec{n}_4,\alpha_4;b}(t)\frac{\mathcal{V}^{\alpha_1,\alpha_2,\alpha_3,\alpha_4}_{\vec{n}_1,\vec{n}_2,\vec{n}_3,\vec{n}_4}}{2}\sigma^{x}_{ef}\psi^{\dagger}_{\vec{n}_2,\alpha_2;c}(t)\gamma^{f}_{cd}\psi_{\vec{n}_3,\alpha_3;d}(t). \tag{3.65}$$

Here The vertex operators γ are third rank tensors operating on the Keldysh space of fermion as well as boson. They are defined as $\gamma^1_{ab} = 1_{ab}$ and $\gamma^2_{ab} = \sigma^x_{ab}$.

Finally, we transform the actions back to the coordinate space by using Eqs. (3.13), (3.14), and (3.15), this yields

$$S_0 = \sum_{a=1}^{2}\sum_{\lambda\lambda'}\int_{-\infty}^{\infty}dt\int d\vec{x}\psi^{\dagger}_{\lambda;a}(\vec{x},t)\Big(i\partial_t - \hat{H}_{D,\lambda\lambda'}(\vec{x})\Big)_{\lambda\lambda'}\psi_{\lambda';a}(\vec{x},t)\ , \tag{3.66}$$

$$S_{\rm ex} = -\sum_{a=1}^{2}\sum_{\lambda}\int_{-\infty}^{\infty}dt\psi^{\dagger}_{\lambda;a}(\vec{x}',t)V_{\rm ex}(\vec{x})\psi_{\lambda;a}(\vec{x},t)\ , \tag{3.67}$$

and

$$S_I = -\frac{1}{2}\sum_{a,b,c,d,e,f=1}^{2}\sum_{\lambda,\lambda'}\int_{-\infty}^{\infty}dtd\vec{x}d\vec{x}'\ \psi^{\dagger}_{\lambda;a}(\vec{x},t)\gamma^{e}_{ab}\psi_{\lambda;b}(\vec{x},t)$$
$$\frac{V(\vec{x}-\vec{x}')}{2}\sigma^{x}_{ef}\psi^{\dagger}_{\lambda';c}(\vec{x}',t)\gamma^{f}_{cd}\psi_{\lambda';d}(\vec{x}',t). \tag{3.68}$$

This theory will be the starting point for our analysis in the next chapter.

3.5 Interacting Green's function

In this section, we discuss Green's function of the interacting theory. In the Larkin-Ovchinnikov basis, by implementing the condition in

Eq. (3.53). The interacting Green's function also has the same structure as the Green's function in the non-interacting theory, namely

$$\begin{aligned} iG_{ab;\lambda\lambda'}(\vec{x},\vec{x}',t,t') &= \left\langle \begin{pmatrix} \psi_1(\vec{x},t) \\ \psi_2(\vec{x},t) \end{pmatrix} \begin{pmatrix} \psi_1^\dagger(\vec{x}',t') & \psi_2^\dagger(\vec{x}',t') \end{pmatrix} \right\rangle \\ &= \begin{pmatrix} iG^R(\vec{x},\vec{x}',t,t') & iG^K(\vec{x},\vec{x}',t,t') \\ 0 & iG^A(\vec{x},\vec{x}',t,t') \end{pmatrix}_{ab}. \end{aligned} \tag{3.69}$$

The superscripts R, A and K stand for the retarded, advanced and Keldysh components of the Green's function, respectively. The Green's functions are calculable within the functional integral formalism according to

$$iG_{ab}(\vec{x},\vec{x}',t,t') = \frac{1}{Z}\int \mathcal{D}\psi^\dagger \mathcal{D}\psi \; \psi_a(\vec{x},t)\psi_b^\dagger(\vec{x}',t') \exp\bigl(iS[\psi^\dagger,\psi]\bigr), \tag{3.70}$$

with the action given in Eqs.(3.66), (3.67), and (3.68). It can be seen that the inverse Green's function is given by

$$G_{ab}^{-1}(\vec{x},\vec{x}';t,t') = \begin{pmatrix} (G^{-1})^R(\vec{x},\vec{x}',t,t') & (G^{-1})^K(\vec{x},\vec{x}',t,t') \\ 0 & (G^{-1})^A(\vec{x},\vec{x}',t,t') \end{pmatrix}_{ab},$$

where

$$(G^{-1})^{R/A} = (G^{R/A})^{-1}, \tag{3.71}$$

and

$$G^R \circ (G^{-1})^K = -G^K \circ (G^{-1})^A. \tag{3.72}$$

The convolution operator $\circ$ is short for the integration over space and time coordinates as well as the summation over the spinor indices. By a symmetry argument, the Keldysh component ($G_{12;\lambda\lambda'} \equiv G^K_{\lambda\lambda'}$) is usually parametrized in terms of the retarded and advanced components according to

$$G^K_{\lambda\lambda'}(\vec{r},\vec{r'};t,t') \equiv (G^R \circ F - F \circ G^A)_{\lambda\lambda'}(\vec{r},\vec{r'};t,t'). \tag{3.73}$$

Here F is a Hermitian two-point function. By inserting this equation into Eq.(3.72), we find

$$(G^{-1})^K = (G^R)^{-1} \circ F - F \circ (G^A)^{-1}. \tag{3.74}$$

This shows that the Keldysh component of the Green function and its inverse can be parametrized in the same way.

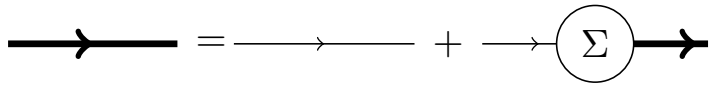

Figure 3.2: Diagrammatic representation of the Dyson equation for the fermion Green's function.

Dyson equation

In the presence of interactions, the Green's function obeys a Dyson equation (pictorially represented in Fig. 3.2). It reads as

$$G = G_0 + G_0 \otimes \Sigma \otimes G. \tag{3.75}$$

Here Σ denotes the self-energy which is evaluated order by order from a perturbative expansion in the interaction. It is represented diagrammatically by a set of one-particle irreducible diagrams. The convolution $\otimes$ denotes integration over time and space, as well as summation of internal indices, including the Keldysh indices. One can rewrite Eq. (3.75) as

$$G^{-1} = G_0^{-1} - \Sigma. \tag{3.76}$$

The fermion self-energy inherits the Keldysh matrix structure of the inverse Green function.

$$\Sigma_{ab;\lambda\lambda'}(\vec{x},\vec{x}',t,t') = \begin{pmatrix} \Sigma^R_{\lambda\lambda'}(\vec{x},\vec{x}',t,t') & \Sigma^K_{\lambda\lambda'}(\vec{x},\vec{x}',t,t') \\ 0 & \Sigma^A_{\lambda\lambda'}(\vec{x},\vec{x}',t,t') \end{pmatrix}_{ab}. \tag{3.77}$$

For the retarded and advanced components, it consequently enters according to

$$(G^{-1})^{R/A} = (G_0^{-1})^{R/A} - \Sigma^{R/A}\,. \tag{3.78}$$

The self-energy plays two major roles: It can affect the dispersion relation and lead to a finite-lifetime. This is most easily seen in frequency-momentum space. The modified pole $\omega = \omega(\vec{p}) - i\gamma(\vec{p})$ is the solution of $(G_0^{-1})^R(\vec{p},\omega) - \Sigma^R(\vec{p},\omega) = 0$. It gives a new dispersion relation, $\omega(\vec{p})$, as well as a decay rate, $\gamma(\vec{p})$, of the excitation. When the decay rate is sufficiently small, this excitation is called a quasi-particle.

The Keldysh component of the Dyson equation leads to a kinetic equation that governs the time evolution of the fermion occupation function. We find that

$$-\Sigma^K = (G^{-1})^K = (G^R)^{-1} \circ F - F \circ (G^A)^{-1} \,, \tag{3.79}$$

where we used the fact that $(G_0^{-1})^K = 0$. To arrive at the second equality, we use Eq. (3.66) and parametrize the Keldysh component of the inverse Green function in terms of the Hermitian function F. Subsequently, by substituting Eq. (3.78) into Eq.(3.79), one finds

$$G_0^{-1} \circ F - F \circ G_0^{-1} = -\Sigma^K + \Sigma^R \circ F - F \circ \Sigma^A. \tag{3.80}$$

The regularization $\pm i\delta$ can be omitted from the retarded and advanced components in the presence of a non-zero self-energy. The above equation is called the quantum-kinetic equation for the distribution matrix F. It has an interpretation that becomes obvious upon comparison with the Boltzmann equation: its left-hand side forms a streaming term, whereas the right-hand side gives a collision integral. The solution of the full quantum kinetic equation, Eq. (3.80) is usually exceedingly difficult, However, after some approximations, discussed below, the quantum kinetic equation reduces to a Boltzmann equation. The latter can be solved by, for instance, a variational method [77].

3.6 The Wigner transform and the gradient expansion

In equilibrium quantum-field theory, diagrammatic approaches are, because of homogeneity, usually carried out in momentum- and energy-space instead of coordinate-space and time, meaning it is a simple Fourier transform. The semiclassical limit, however, is most conveniently accessed using the Wigner transform, which is a mixed representation. We briefly summarize it here for convenience. A generic space-time function, $g(\vec{x}_1, \vec{x}_2, t_1, t_2)$, can be rewritten in terms of center-of-mass $(\vec{r}, t) = ((\vec{x}_1 + \vec{x}_2)/2, (t_1 + t_2)/2)$ and relative coordinates $(\vec{x}, \tau) = (\vec{x}_1 - \vec{x}_2, t_1 - t_2)$. The Wigner transform is now a Fourier transform over the relative coordinates while the

center-of-mass coordinates are kept intact. Consequently, one obtains a function of center-of-mass spacetime, momentum, and frequency, *i.e.*, $\tilde{g}(\vec{r},t,\vec{p},\omega) = \int d\vec{x}d\tau\ g(\vec{r},t,\vec{x},\tau)\ e^{-i\vec{p}\cdot\vec{x}+i\omega\tau}$. There are two important Wigner transforms that will be needed later for our derivation of the Boltzmann equation.

(i) For a two-point function which can be decompose into an algebraic product of other two-point functions, *i.e.*, $C(\vec{r}_1,\vec{r}_2;t_1,t_2) = A(\vec{r}_1,\vec{r}_2;t_1,t_2)B(\vec{r}_1,\vec{r}_2;t_1,t_2)$, one can show that its Wigner transform is given by the momentum-frequency convolution

$$C(\vec{r},t,\vec{p},\omega) = \int \frac{d\vec{p}_1}{(2\pi)^d}\frac{d\omega_1}{2\pi}\ A(\vec{r},t,\vec{p}_1,\omega_1)B(\vec{r},t,\vec{p}-\vec{p}_1,\omega-\omega_1). \tag{3.81}$$

(ii) The Wigner transform of the space-time convolution of two two-point functions *i.e.*, $D(\vec{r}_1,\vec{r}_2;t_1,t_2) = (A\circ B)(\vec{r}_1,\vec{r}_2;t_1,t_2)$ is given by their Moyal product reading as

$$\begin{aligned} D(\vec{r},t,\vec{p},\omega) &= A(\vec{r},t,\vec{p},\omega)\star B(\vec{r},t,\vec{p},\omega) \\ &= A(\vec{r},t,\vec{p},\omega)e^{\frac{i}{2}\left(\overleftarrow{\partial}_{\vec{r}}\overrightarrow{\partial}_{\vec{p}}-\overleftarrow{\partial}_{\vec{p}}\overrightarrow{\partial}_{\vec{r}}-\overleftarrow{\partial}_{t}\overrightarrow{\partial}_{\omega}+\overleftarrow{\partial}_{\omega}\overrightarrow{\partial}_{t}\right)}B(\vec{r},t,\vec{p},\omega)\ . \end{aligned} \tag{3.82}$$

In the cases we are interested in, the function varies slowly with the center-of-mass coordinates and fast with the relative coordinates. Consequently, it is legitimate to keep only the lowest-order gradient terms according to

$$\begin{aligned} D(\vec{r},t,\vec{p},\omega) \approx\ & A(\vec{r},t,\vec{p},\omega)B(\vec{r},t,\vec{p},\omega) \\ & -\frac{i}{2}\Big[\partial_{\vec{p}}A(\vec{r},t,\vec{p},\omega)\partial_{\vec{r}}B(\vec{r},t,\vec{p},\omega) \\ & -\partial_{\vec{R}}A(\vec{r},t,\vec{p},\omega)\partial_{\vec{p}}B(\vec{r},t,\vec{p},\omega)\Big] \\ & +\frac{i}{2}\Big[\partial_{\omega}A(\vec{r},t,\vec{p},\omega)\partial_{t}B(\vec{r},t,\vec{p},\omega) \\ & -\partial_{t}A(\vec{r},t,\vec{p},\omega)\partial_{\omega}B(\vec{r},t,\vec{p},\omega)\Big] + \dots\ . \end{aligned} \tag{3.83}$$

3.7 Gradient expansion of the Keldysh equation

The Wigner transform of the Keldysh equation in Eq. (3.80), reads

$$\left[G_0^{-1} - \mathrm{Re}\,\Sigma_\star^{R\star}; F\right]_- \quad = \quad -\Sigma_\star^K + i\{\mathrm{Im}\,\Sigma_\star^{R\star}; F\}_+ \,. \tag{3.84}$$

In writing the above equation, we introduced the notation $\Sigma_\star$. It accounts for the fact that the self-energy itself has a gradient expansion according to

$$\Sigma_\star \approx \Sigma + \Sigma_\times + ... \tag{3.85}$$

where Σ involves no gradients, while $\Sigma_\times$ involves both one spatial and momentum gradient (or, equivalently, frequency and time) [83, 84]. To leading order in non-vanishing gradients we find

$$\begin{aligned}
&\left[G_0^{-1} - \mathrm{Re}\,\Sigma^R, F\right] + i\Big\{\partial_{\vec{x}}\left(G_0^{-1} - \mathrm{Re}\,\Sigma^R\right)\cdot\partial_{\vec{p}}F \\
&-\partial_{\vec{p}}\left(G_0^{-1} - \mathrm{Re}\,\Sigma^R\right)\cdot\partial_{\vec{x}}F - \partial_t\left(G_0^{-1} - \mathrm{Re}\,\Sigma^R\right)\partial_\epsilon F \\
&+\partial_\epsilon\left(G_0^{-1} - \mathrm{Re}\,\Sigma^R\right)\partial_t F\Big\} = -\Sigma^K + i\{\mathrm{Im}\,\Sigma^R, F\} \\
&-\Sigma_\times^K + i\{\mathrm{Im}\,\Sigma_\times^R, F\}.
\end{aligned} \tag{3.86}$$

It turns out that the contributions due to $\Sigma_\times$ are of the non-quasi-particle type and vanish once we perform the quasi-particle approximation. Consequently, we drop them form our following discussion.

In order to set up a formalism that accommodates for a two- or even multi-band scenario we make the following assumption: There is a transformation $\mathcal{U}_{\vec{p}}$ (in the case of a Dirac-type theory we specify it later) that projects the Green's function into a diagonal basis according to

$$g_0^{R/A}(\vec{x},\vec{p},\omega) \quad = \quad \mathcal{U}_{\vec{p}}^\dagger G_0^{R/A}(\vec{x},\vec{p},\omega)\mathcal{U}_{\vec{p}} \tag{3.87}$$

with $g_0^{R/A}(\vec{x},\vec{p},\omega)$ being a diagonal matrix. While in the following we present matrix equations, we only concentrate on the diagonal

elements. Equivalently, we project the self-energies into the quasi-particle basis according to

$$\sigma^{R/A}(\vec{x},\vec{p},\omega) \quad = \quad \mathcal{U}^{\dagger}_{\vec{p}}\Sigma^{R/A}(\vec{x},\vec{p},\omega)\mathcal{U}_{\vec{p}}. \tag{3.88}$$

This leads to

$$\begin{aligned} & i\partial_{\vec{x}}\left(g_0^{-1}-\operatorname{Re}\sigma^R\right)\cdot\left(\partial_{\vec{p}}F+i\left[\mathcal{A}_{\vec{p}},F\right]\right) \\ & -\left(\partial_{\vec{p}}\left(g_0^{-1}-\operatorname{Re}\sigma^R\right)+i\left[\mathcal{A}_{\vec{p}},g_0^{-1}-\operatorname{Re}\sigma^R\right]\right)\cdot\partial_{\vec{x}}F \\ & -\partial_t\left(g_0^{-1}-\operatorname{Re}\sigma^R\right)\partial_\epsilon F+\partial_\epsilon\left(g_0^{-1}-\operatorname{Re}\sigma^R\right)\partial_t F \\ & \qquad\qquad = -\sigma^K+2i\operatorname{Im}\sigma^R F\ . \end{aligned} \tag{3.89}$$

We observe that two additional terms which involve the Berry connection $\mathcal{A}_{\vec{p}}=-i\mathcal{U}^{\dagger}_{\vec{p}}\partial_{\vec{p}}\mathcal{U}_{\vec{p}}$ are obtained. We are interested here in the solution to zeroth order in $\mathcal{A}_{\vec{p}}$ that is

$$F_{\lambda\lambda'}=F^{(0)}_{\lambda\lambda'}+\mathcal{O}(\mathcal{A}_{\vec{p}})=(1-2f_\lambda(\vec{r},\vec{p},t))\delta_{\lambda\lambda'}+\mathcal{O}(\mathcal{A}_{\vec{p}}), \tag{3.90}$$

containing only the diagonal elements of the distribution function. The function f introduce above will later play the role of the fermionic distribution function and, in equilibrium, it reduces to the Fermi-Dirac distribution. Within the quasi-particle approximation, f_λ is independent of the frequency variable. Moreover, it is assumed to be diagonal in the spinor space, consequently, only the main diagonal elements of the self-energies are important. In total, this leads to

$$\begin{aligned} & \partial_\epsilon\left(g^{-1}_{0,\lambda\lambda}(\vec{x},t,\vec{p},\epsilon)-\operatorname{Re}\sigma^R_{\lambda\lambda}(\vec{x},t,\vec{p},\epsilon)\right)\partial_t f_\lambda(\vec{x},t,\vec{p}) \\ & +\partial_{\vec{x}}\left(g^{-1}_{0,\lambda\lambda}(\vec{x},t,\vec{p},\epsilon)-\operatorname{Re}\sigma^R_{\lambda\lambda}(\vec{x},t,\vec{p},\epsilon)\right)\cdot\partial_{\vec{p}}f_\lambda(\vec{x},t,\vec{p}) \\ & -\partial_{\vec{p}}\left(g^{-1}_{0,\lambda\lambda}(\vec{x},t,\vec{p},\epsilon)-\operatorname{Re}\sigma^R_{\lambda\lambda}(\vec{x},t,\vec{p},\epsilon)\right)\cdot\partial_{\vec{x}}f_\lambda(\vec{x},t,\vec{p}) \\ & =-\frac{i}{2}\sigma^K_{\lambda\lambda}(\vec{x},t,\vec{p},\epsilon)-\operatorname{Im}\sigma^R(\vec{x},\vec{p},t,\epsilon)(1-2f(\vec{x},t,\vec{p}))\ . \end{aligned} \tag{3.91}$$

The left-hand side will contain the so-called streaming terms, consisting of three contributions. The first term describes the time

derivative of the distribution function with the quasi-particle weight $\partial_\epsilon \left(g_0^{-1} - \mathrm{Re}\,\sigma^R\right) = 1 - \partial_\epsilon \,\mathrm{Re}\,\sigma^R$. The second term accounts for the change of the distribution function due to a force $\partial_{\vec{x}} \left(g_0^{-1} - \mathrm{Re}\,\sigma^R\right)$, whereas the last term tracks the change of the distribution function due to the diffusion of excitations with the velocity $\partial_{\vec{p}} \left(g_0^{-1} - \mathrm{Re}\,\sigma^R\right)$. The right-hand side describes collisions that drive the system towards equilibrium.

The missing piece to transform Eqs. (3.91) into Boltzmann equations is to integrate them over the respective spectral functions, as we will discuss in the subsequent chapter.

Chapter 4

Electron-hole hydrodynamics: the weak coupling limit

Hereafter, we study the hydrodynamic properties of ultraclean interacting two-dimensional Dirac electrons with Keldysh quantum field theory set up in the previous chapter. We study it in this chapter from a weak-coupling and in the next chapter a strong-coupling perspective. In these chapters, we demonstrate that long-range Coulomb interactions play two independent roles. (i) They provide the inelastic and momentum-conserving scattering mechanism that leads to fast local equilibration; This is the subject discussed in this chapter. (ii) The long-range component of the Coulomb interaction facilitates the emergence of collective excitations, for instance plasmons, that contribute to transport properties on equal footing with electrons. This will be the subject discussed in the next chapter. This chapter is based on part of K. Pongsangangan, T. Ludwig, H.T.C. Stoof, and L. Fritz, *Hydrodynamics of charged Dirac electrons in two dimensions. II. Role of collective modes.* (accepted at PRB) (2022).

4.1 introduction

The conventional theory of electronic transport in a solid-state setting describes the motion of electrons in the following way: individual electrons diffuse on the background of a disordered lattice, primarily scattering from impurities and/or lattice vibrations [1, 4, 77].

However, recent years have seen tremendous progress in realizing electronic transport that follows a different paradigm: hydrodynamic electrons, meaning electrons flowing collectively like a viscous liquid, such as water or honey. This idea has first been discussed in the 1960s by Gurzhi [44]. However, the subject has only recently picked up a lot of pace. This is mostly due to recent advances in the preparation of ultrapure mono- and bilayer graphene samples with sufficiently strong interactions [16, 17, 36, 37, 38, 39]. The prerequisite for the experimental observation of electron hydrodynamics is that microscopic momentum-conserving electron-electron collisions due to Coulomb interactions must be considerably faster than momentum-relaxing scatterings of electrons from impurities and/or phonons. This allows the electrons to locally establish equilibrium. In that situation, it is justified to speak of approximate conservation laws, sufficient to open the door for the observation of electron hydrodynamics [33, 34, 12, 85, 48, 49]. The theoretical method used to investigate this hydrodynamic flow is usually based on the traditional Navier-Stokes equation which expresses conservation of momentum, energy and electric charge [45, 48, 66]. One way to derive these hydrodynamic equations from microscopics starts from the Boltzmann equation [78, 49]. There, usually, the effect of the Coulomb interactions enters only through electron-electron collisions leading to local equilibrium. This effect is usually calculated from a weak-coupling perspective within second-order perturbation theory in the interaction strength, referred to as the Born approximation for the cross-section [12, 33, 32, 59]. This will be discussed in this chapter.

Background and main idea: Strongly correlated many-particle systems can often be regarded as a collection of weakly interacting excitations. One of the prime examples of this kind is the Landau Fermi liquid [9]. Its excitations behave as well-defined entities, called quasi-particles. This means, the following conditions must be fulfilled: (i) an excitation with momentum $\vec{p}$ possesses a well-defined complex energy spectrum, say $\hbar\omega(\vec{p}) = \epsilon(\vec{p}) - i\gamma(\vec{p})$, where the imaginary part of the energy $\gamma(\vec{p})$ describes the decay rate of the particle, inversely proportional to the lifetime of the excitation; (ii) an excitation must be long-lived which means that the decay must be at least

underdamped $\gamma(\vec{p}) \ll \epsilon(\vec{p})$. These requirements usually limit one to the low-frequency and/or long-wavelength behavior of the system. Under such circumstances, it is justified to consider the complicated interacting system as a collection of independent elementary quasi-particles [70]. Once this paradigm is adopted for a given many-body system, there are two main questions in need of answer: (i) what are the quasi-particles involved in physical phenomena of interest at the relevant energy scale and (ii) what is the population of these quasi-particles in each momentum state especially when the system is exposed to external disturbances? The latter is quantified by a distribution function $f(\vec{x}, t, \vec{p})$ which gives a probability that the particle in a momentum state $\vec{p}$ is found in a neighborhood of a spatial position $\vec{x}$ at time t. For a given non-equilibrium situation, the distribution function is governed by the Boltzmann equation. The knowledge of the distribution function and the energy spectrum is vital to determine all thermodynamic as well as transport properties of the system in a straightforward fashion.

In this chapter, we discuss two-component hydrodynamics as currently used for the description of graphene. We derive all the equations from the Schwinger-Keldysh approach and show how the two-component fluid picture emerges within a weak-coupling approach to second order in the Coulomb interaction. The organization of the rest of this chapter is as follows. We start with a brief summary of the non-interacting Green's functions in Sec. 4.2. Within weak coupling, Coulomb interactions play two different roles: (i) It is seen by an electron as an internal potential produced by all the other particles in the system. This is the result of perturbation theory to first order, called the Hartree-Fock scheme [56], where the Fock term leads to a renormalization of the Fermi velocity [57, 58]. The potential energy, on the other hand, is referred to as the Hartree potential. In thermal equilibrium, it is canceled by a potential from the underlying positively charged background in which the particles move. However, it builds the basis for a derivation of the collective excitations of the fluid [13, 70]. This aspect is discussed in Sec. 4.3; (ii) The Coulomb interaction manifests itself as an inelastic and momentum conserving scattering mechanism [33, 34, 32, 59, 12]. This process is an important requirement for observing the electron hy-

drodynamical regime since it leads to local equilibration. We discuss this in Sec. 4.4 where we discuss the scattering process in some detail. We then derive the ensuing conservation laws starting from the Boltzmann equation in Sec. 4.5 and finish the chapter with a discussion of collective modes in Sec. 4.6. We find a collective mode that we later identify with the plasmon.

4.2 The non-interacting limit

From the previous chapter, we consider a model of interacting Dirac fermions according to Eqs. (3.66), (3.67), (3.68). We first neglect the Coulomb interactions; We find the retarded Green's function of the non-interacting Dirac theory reading as

$$G_0^{R/A}(\vec{x},\vec{p},\omega) = \left(\omega \pm i\delta - v_F\vec{\sigma}\cdot\vec{p} + \mu - V_{\rm ex}(\vec{x})\right)^{-1} . \tag{4.1}$$

It is convenient to work in the quasi-particle basis. There, the Dirac Hamiltonian as well as the Green's function are diagonal. This leads to

$$\begin{aligned} g^{R/A}_{0,\lambda\lambda',ij}(\vec{x},\vec{p},\omega) &= \left(\mathcal{U}^\dagger_{\vec{p}} G^{R/A}_{0,ij}(\vec{x},\vec{p},\omega)\mathcal{U}_{\vec{p}}\right)_{\lambda\lambda'} \\ &= \left(\omega \pm i\delta - \lambda v_F p + \mu - V_{\rm ex}(\vec{x})\right)^{-1}\delta_{\lambda\lambda'}\delta_{ij} , \end{aligned} \tag{4.2}$$

with

$$\mathcal{U}_{\vec{p}} = \frac{1}{\sqrt{2}}\begin{pmatrix} -\exp(-i\theta_{\vec{p}}) & \exp(-i\theta_{\vec{p}}) \\ 1 & 1 \end{pmatrix} . \tag{4.3}$$

Here, p denotes the magnitude of the momentum $\vec{p}$ and $\tan(\theta_{\vec{p}}) = p_y/p_x$. The dispersion relation can be extracted from the poles of the Green's function in Eq. (4.2): the non-interacting Dirac theory has two linear dispersing energy bands $\epsilon_\pm(\vec{x},\vec{p}) = \pm v_F p + V_{\rm ex}(\vec{x}) - \mu$ with the effective local chemical potential given by $\mu - V_{\rm ex}(\vec{x})$. The spectral function, defined by $\mathrm{Im}\, g^R_{0,\lambda\lambda'}(\vec{x},\vec{p},\omega) = -\pi\delta(\omega - \epsilon_\lambda(\vec{x},\vec{p}))\delta_{\lambda\lambda'}$, exhibits resonances at $\omega = \epsilon_\pm(\vec{x},\vec{p})$. The Wigner transform of the

Keldysh Green's function of Eq.(3.73) reads

$$\begin{aligned} g^K_{0,\lambda\lambda'}(\vec{x},t,\vec{p},\omega) &= 2i\,\mathrm{Im}\, g^R_{0,\lambda\lambda''}(\vec{x},\vec{p},\omega)F_{\lambda''\lambda'}(\vec{x},\vec{p},\omega) \\ &= -2\pi i\delta(\omega-\epsilon_\lambda(\vec{x},\vec{p}))\,(1-2f_\lambda(\vec{x},\vec{p},t))\,\delta_{\lambda\lambda'}. \end{aligned} \tag{4.4}$$

where $f(\vec{x},\vec{p},t)$ is the Fermi Dirac distribution in equilibrium. The Keldysh component thus contains the information about the occupation numbers, whereas the retarded and advanced components only contain information about the resonances and the energy level.

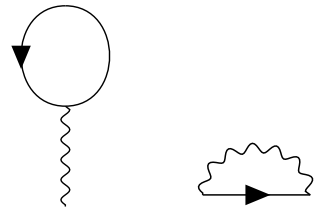

(a) (b)

Figure 4.1: The self-energies at first order in the interaction. The left diagram is known as the direct or Hartree contribution and the right diagram is known as the Fock or exchange contribution.

4.3 Hartree-Fock approximation: The collisionless limit

In what follows, we will discuss the corrections of the energy spectrum due to the Coulomb interaction. To this end, we study the Hartree and Fock self-energies [27] depicted in Fig. 4.1a and Fig. 4.1b.

4.3.1 The Hartree diagram

The Hartree diagram, in Fig. 4.1a, has the following algebraic expression:

$$-i\Sigma^H_{ab;\lambda\lambda'}(\vec{x},\vec{x}';t,t') = -\delta_{\lambda\lambda'}\delta(\vec{x}-\vec{x}')\delta(t-t') \int dt''d\vec{x}''\ \gamma^e_{ab}D_{0,ef}(\vec{x}',\vec{x}'',t',t'')\gamma^f_{cd}G_{0,dc;\lambda''\lambda'';ii}(\vec{x}'',\vec{x}'',t'',t'')\ . \tag{4.5}$$

Since $D_{0,ef}(\vec{x},\vec{x}',t,t') = \sigma^x_{ef}\delta(t-t')\frac{V(|\vec{x}-\vec{x}'|)}{2}$ is off-diagonal in Keldysh space, only two terms survive when we sum over e and f subscripts. This gives

$$\begin{aligned} -i\Sigma^H_{ab;\lambda\lambda'}&(\vec{x},\vec{x}';t,t') \\ &= -\delta_{\lambda\lambda'}\delta(\vec{x}-\vec{x}')\delta(t-t')\int dt''d\vec{x}''\frac{V(|\vec{x}'-\vec{x}''|)}{2}\gamma^1_{ab}\gamma^2_{cd} \\ &\qquad G_{0,dc;\lambda''\lambda'',ii}(\vec{x}'',\vec{x}'',t'',t'') \\ &\quad -\delta_{\lambda\lambda'}\delta(\vec{x}-\vec{x}')\delta(t-t')\int dt''d\vec{x}''\frac{V(|\vec{x}'-\vec{x}''|)}{2}\gamma^2_{ab}\gamma^1_{cd} \\ &\qquad G_{0,dc;\lambda\lambda,ii}(\vec{x}'',\vec{x}'',t'',t'')\ . \end{aligned} \tag{4.6}$$

We find that the second term vanishes as

$$\begin{aligned} \gamma^2_{ab}\gamma^1_{cd}&G_{0,dc;\lambda''\lambda'',ii}(\vec{x}',\vec{x}',t',t') \\ &= G^R_{0;\lambda''\lambda'',ii}(\vec{x}',\vec{x}',t',t') + G^A_{0;\lambda''\lambda'',ii}(\vec{x}',\vec{x}',t',t') \\ &= \int\frac{d\omega}{2\pi}\frac{d\vec{p}}{(2\pi)^2}\,\mathrm{Re}\,G^R_{0;\lambda''\lambda'',ii}(\vec{x}',t',\vec{p},\omega) = 0\ . \end{aligned} \tag{4.7}$$

The last equality follows because $\mathrm{Re}\,G^R_{0;\sigma\sigma}(\vec{x}',t',\vec{p},\omega)$ is an analytic function in either the upper or the lower complex frequency halfplane. Consequently, we have

$$-i\Sigma^H_{ab;\lambda\lambda'}(\vec{x},\vec{x}',t,t') = -\delta_{\lambda\lambda'}\delta(\vec{x}-\vec{x}')\delta(t-t')\delta_{ab} \int d\vec{x}''\frac{V(|\vec{x}'-\vec{x}''|)}{2}G^K_{0;\lambda''\lambda'',ii}(\vec{x}'',\vec{x}'';t,t). \tag{4.8}$$

Finally, after a Wigner transformation, we rotate the self-energy into the quasi-particle basis. This gives

$$\begin{aligned} -i\sigma^{H}_{ab;\lambda\lambda'}(\vec{x},t,\vec{p},\omega) &= -i\left(\mathcal{U}^{\dagger}_{\vec{p}}\Sigma^{H}(\vec{x},t,\vec{p},\omega)\mathcal{U}_{\vec{p}}\right)_{\lambda\lambda'} \\ &= -\delta_{\lambda\lambda'}\delta_{ab}\int d\vec{x}''\frac{V(|\vec{x}'-\vec{x}''|)}{2}g^{K}_{0;\lambda''\lambda'',ii}(\vec{x}'',\vec{x}';t,t)\ , \end{aligned} \tag{4.9}$$

where the Wigner transformation of the Keldysh Green's function, $g^{K}_{0;\lambda''\lambda'',ii}(\vec{x}'',\vec{x}';t,t)$, with the same time and spatial argument is associated with the electron density according to

$$g^{K}_{0;\lambda''\lambda'',ii}(\vec{x}'',\vec{x}'';t,t) = 2in(\vec{x}'',t). \tag{4.10}$$

Here $n(\vec{x}'',t) = n_{+}(\vec{x}'',t)+n_{-}(\vec{x}'',t)$ defines the total charge density at position $\vec{x}''$ and time t, where $n_{+}(\vec{x'},t) = N\int\frac{d\vec{k}}{(2\pi)^2}f_{+}(\vec{x}',\vec{k},t)$ is electron charge density and $n_{-}(\vec{x}',t) = N\int\frac{d\vec{k}}{(2\pi)^2}\left(f_{-}(\vec{x}',\vec{k},t)-1\right)$ is the hole charge density. The electron charge $-e$ is henceforth set to 1. In total, the Hartree self-energy produces the classical Coulomb potential of all electrons in the system exerted on an electron located at a position $\vec{x}$ according to

$$\sigma^{H}_{ab;\lambda\lambda'}(\vec{x},t,\vec{p},\omega) = \delta_{\lambda\lambda'}\delta_{ab}\int d\vec{x}'V(\vec{x}-\vec{x}')n(\vec{x}',t). \tag{4.11}$$

The Hartree term is real-valued and independent of the momentum and frequency variables. Furthermore, it is diagonal in Keldysh space, meaning its Keldysh component is zero.

4.3.2 The Fock diagram

Next, we are going to sketch the calculation of the Fock self-energy diagram depicted in Fig.(4.1b). It reads

$$-i\Sigma^{F}_{ab;\lambda\lambda'}(\vec{x},\vec{x}';t,t') = \gamma^{\alpha}_{ac}D_{0,\alpha\beta}(\vec{x},\vec{x}';t,t')G_{0,cd;\lambda\lambda'}(\vec{x},\vec{x}';t,t')\gamma^{\beta}_{db}. \tag{4.12}$$

After a Wigner transformation followed by a few steps of algebraic manipulations, we find that

$$-i\Sigma^F_{ab;\lambda\lambda'}(\vec{x},\vec{p};t,\nu) = \delta_{ab}\int\frac{d\vec{p}_1}{(2\pi)^2}\frac{V(\vec{p}-\vec{p}_1)}{2}\int\frac{d\nu_1}{2\pi}G^K_{0,\lambda\lambda'}(\vec{x},\vec{p}_1;t,\nu_1). \tag{4.13}$$

Subsequently, we transform it into the quasi-particle basis according to $-i\sigma^F_{ab;\lambda\lambda'}(\vec{x},\vec{p};t,\nu) = -i\left(\mathcal{U}^\dagger_{\vec{p}}\Sigma^F_{ab}(\vec{x},\vec{p};t,\nu)\mathcal{U}_{\vec{p}}\right)_{\lambda\lambda'}$. We are interested in elements on the main diagonal of the spinor space. They are given by

$$\sigma^F_{ab;\lambda\lambda}(\vec{x},\vec{p};t,\nu) = \sigma^{F,1}_{ab;\lambda\lambda}(\vec{x},\vec{p};t,\nu) + \sigma^{F,2}_{ab;\lambda\lambda}(\vec{x},\vec{p};t,\nu), \tag{4.14}$$

where

$$\sigma^{F,1}_{ab;\lambda\lambda}(\vec{x},\vec{p};t,\nu) = \delta_{ab}\lambda\int\frac{d\vec{p}_1}{(2\pi)^2}\cos(\theta_{\vec{p}_1}-\theta_{\vec{p}})\frac{V(\vec{p}-\vec{p}_1)}{2}, \tag{4.15}$$

and

$$\begin{aligned}\sigma^{F,2}_{ab;\lambda\lambda}(\vec{x},\vec{p};t,\nu) &= \delta_{ab}\int\frac{d\vec{p}_1}{(2\pi)^2}\frac{1+\lambda\lambda_1\cos(\theta_{\vec{p}_1}-\theta_{\vec{p}})}{2}\frac{V(\vec{p}-\vec{p}_1)}{2}\\ &\quad\times\left((1-\lambda_1)-2f_{\lambda_1}(\vec{x},t,\vec{p}_1)\right).\end{aligned} \tag{4.16}$$

The first term diverges logarithmically and is responsible for the renormalization of the Fermi velocity. To see this, we explicitly substitute the Coulomb potential in Eq. (3.10) followed by a transformation of the momentum variable from Cartesian to polar coordinates. This gives

$$\begin{aligned}\sigma^{F,1}_{ab;\lambda\lambda}(\vec{x},\vec{p};t,\nu) &= \lambda\frac{\alpha v_F}{4\pi}\int p_1dp_1d\theta\frac{\cos\theta}{\sqrt{p^2+p_1^2-2pp_1\cos\theta}}\\ &\approx \lambda\frac{\alpha v_F p}{4}\int_p^{\mathcal{K}}dp_1\frac{1}{p_1} = \frac{\alpha}{4}\ln(\mathcal{K}/p)\lambda v_F p.\end{aligned} \tag{4.17}$$

$\theta = \theta_{\vec{p}_1} - \theta_{\vec{p}}$ is the angle of the momentum $\vec{p}_1$ measured with respect to $\vec{p}$. In order to extract the logarithmic divergence of the above integral, we expanded the square root to the first power in p/p_1, *i.e.*, $1/\sqrt{p^2 + p_1^2 - 2pp_1\cos\theta} \approx 1/p_1\,(1 + p\cos\theta/p_1)$. After the angular integral, we find the result in the second line of Eq.(4.17). The divergence of the integral is cut off at the inverse lattice spacing $\mathcal{K}$. The lower boundary of integration is consistently set to p (we require $p/p_1 \ll 1$). When substituting Eq.(4.17) into the Dyson equation, we find

$$g_0^{-1} - \sigma^F = \omega - \lambda\,(1 + \alpha\ln(\mathcal{K}/p)/4)\,v_F p. \tag{4.18}$$

the Fermi velocity is renormalized accordingly to

$$v_F^R = (1 + \alpha\ln(\mathcal{K}/p)/4)\,v_F.$$

Such logarithmic renormalization was first discussed within the renormalization group approach in Ref. [57] and measured in graphene in Ref. [58]. The second contribution, Eq. (4.16), describes the conventional exchange energy coming from both electrons and holes. It varies with the doping μ and the temperature T of the system. Moreover, different from the exchange energy of a conventional two dimensional electron gas, there is a factor $(1 + \lambda\lambda_1\cos(\theta_{\vec{p}_1} - \theta_{\vec{p}}))/2$ arising from the wavefunction overlap, where $\theta_{\vec{p}_1} - \theta_{\vec{p}}$ is the angle between $\vec{p}$ and $\vec{p}_1$ [86]. In total, it reads

$$\begin{aligned}
&(\sigma^{F,2})^R_{\pm\pm}(\vec{p}) \\
&\quad = -\int \frac{d\vec{p}_1}{(2\pi)^2}\,\frac{1 \pm \cos(\theta_{\vec{p}_1} - \theta_{\vec{p}})}{2}\,V(\vec{p} - \vec{p}_1)\,f_+^0(\vec{p}_1) \\
&\qquad + \int \frac{d\vec{p}_1}{(2\pi)^2}\,\frac{1 \mp \cos(\theta_{\vec{p}_1} - \theta_{\vec{p}})}{2}\,V(\vec{p} - \vec{p}_1)(1 - f_-^0(\vec{p}_1)).
\end{aligned} \tag{4.19}$$

After a series of manipulations, we find

$$
\begin{aligned}
&(\sigma^{F,2})^R_{\pm\pm}(\vec{p}) \\
&= -\frac{\alpha v_F}{4\pi}\int dp_1 \sqrt{\frac{p_1}{2p}}\left(g\left(\frac{p^2+p_1^2}{2pp_1}\right) \pm h\left(\frac{p^2+p_1^2}{2pp_1}\right)\right) f^0_+(\vec{p}_1) \\
&+\frac{\alpha v_F}{4\pi}\int dp_1 \sqrt{\frac{p_1}{2p}}\left(g\left(\frac{p^2+p_1^2}{2pp_1}\right) \mp h\left(\frac{p^2+p_1^2}{2pp_1}\right)\right) (1-f^0_-(\vec{p}_1)),
\end{aligned}
\tag{4.20}
$$

with

$$
\begin{aligned}
g(x) &= \int_0^{2\pi} \frac{d\theta}{\sqrt{x-\cos\theta}} \\
h(x) &= \int_0^{2\pi} \frac{d\theta\ \cos\theta}{\sqrt{x-\cos\theta}}\ .
\end{aligned}
\tag{4.21}
$$

We proceed by evaluating the p_1-integral numerically. We show in Fig. 4.2 the exchange energies for electrons, $(\sigma^{F,2})^R_{++}$, and holes, $(\sigma^{F,2})^R_{++}$, at the chemical potential $\mu/T = 1$ for various values of momenta. We see that the self-energy becomes less important at high momenta. In Fig. 4.3 (b) we show the spectral function of the electrons with and without the Fock correction. Since the exchange energy is a real-valued function, there remains the Delta-peak feature manifested as the blue line in the middle of the plot. Compare to the spectral function of the non-interacting theory in Fig. 4.3 (a), the exchange energy plays two roles: (i) it shifts the chemical potential and (ii) it increases the Fermi velocity [86]. However, its effect is relatively small compared to the Fermi velocity renormalization coming from the logarithmic divergence. Therefore, we keep only the latter effect in the following. In practice, this leads to replacing v_F with v_F^R, the renormalized Fermi velocity, in all expressions.

4.3.3 Energy spectrum

We are now ready to evaluate the energy spectrum of quasi-electrons and quasi-holes in equilibrium within the Hartree-Fock approximation. The dispersion relation of the excitations can be found from

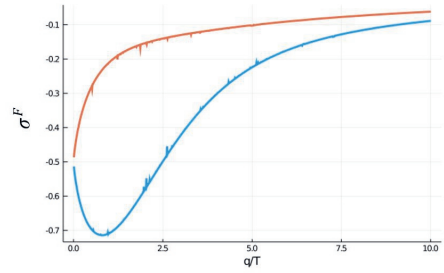

Figure 4.2: Exchange self-energies for Dirac fermions with the chemical potential $\mu/T = 1$ as functions of wave vector q/T. The fine structure constant α is chosen to be 1. The blue curve represents $(\sigma^{F,2})^R_{++}$ showing the exchange energy correction of the electrons. The orange curve shows $(\sigma^{F,2})^R_{--}$ the exchange energy of the holes.

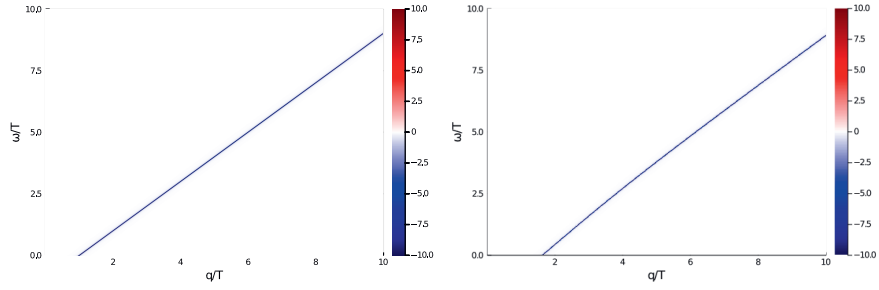

Figure 4.3: Spectral function at $\mu/T = 1$ and $\alpha = 1$. (a) The spectral function of the non-interacting electrons follows $\mathrm{Im}\, g_0^R(\vec{q}, \omega) = -2\pi i\delta(\omega - v_F q + \mu)$. The blue line in the middle of the plot manifests the Delta peak at $\omega = v_F q - \mu$ (v_F is set to 1 in the plot). (b) The spectral function with the inclusion of the exchange conventional energy in Eq.(4.19). Since the exchange energy is a real-valued function, the spectral function still has the Delta-peak feature as shown by the blue line in the middle of the plot.

the roots of the inverse Green's function. In the presence of the interaction, the inverse Green's function is the solution of the Dyson equation in Eq. (3.78). We first transform the Dyson equation into

the quasi-particle basis, which leads to

$$(g^{-1})^R_{\lambda\lambda'} = (g_0^{-1})^R_{\lambda\lambda'} - (\sigma^H)^R_{\lambda\lambda'}. \tag{4.22}$$

where the retarded component of the Hartree self-energy is given by the first row and first column element of Eq.(4.11) that is $(\sigma^H)^R_{\lambda\lambda'} = \sigma^H_{11,\lambda\lambda'}$. This gives

$$\begin{aligned}(g^{-1})^R_{\lambda\lambda'}(\vec{x},t,\vec{p},\omega) &= \Big(\omega + i\delta \mp \lambda v_F^R p + \mu \\ &- V_{\rm ex}(\vec{x}) - \int d\vec{x}' V(\vec{x}-\vec{x}')n(\vec{x}',t)\Big)\delta_{\lambda\lambda'}\ ,\end{aligned} \tag{4.23}$$

where $n(\vec{x},t)$ is the total electron density. By inserting $V_{\rm ex}(\vec{x})$ from Eq. (3.5), we find that

$$(g^{-1})^{R/A}_{\lambda\lambda'}(\vec{x},t,\vec{p},\omega) = \omega \pm i\delta - \lambda v_F^R p + \mu - V^H(\vec{x}), \tag{4.24}$$

where the Hartree potential $V^H(\vec{x})$ is defined as

$$V^H(\vec{x}) = \int d\vec{x}' V(\vec{x}-\vec{x}')\left(n(\vec{x}',t) - n_0\right). \tag{4.25}$$

The Hartree term represents the static potential energy of an electron at a position $\vec{x}$. This potential is produced by all other electrons with the density $n(\vec{x}',t)$ at the other positions $\vec{x}'$ through Coulomb interaction. This contribution is partially canceled by the potential $V_{\rm ex}(\vec{x})$ arising from the interaction between electrons and the underlying jellium background. This fixed uniformly distributed positively charged background guarantees the over-all electrical neutrality of the system. Here n_0 is the ion charge density which is identical to the electron charge density in thermal equilibrium. Hence, in global thermal equilibrium, the Hartree potential vanishes and thus the energy spectrum of electrons is given by

$$\epsilon_\lambda(\vec{p}) = \lambda v_F^R p\ , \tag{4.26}$$

as expected.

4.3.4 The kinetic equation for Dirac fermions

Next, we derive the Bolzmann equation within the Hartree-Fock approximation. To this end, we consider Eq. (3.91). The left-hand side will contain the so-called streaming terms, consisting of three contributions. The first term describes the time derivative of the distribution function with the quasi-particle weight $\partial_\epsilon \left(g_0^{-1} - \mathrm{Re}\,\sigma^R\right) = 1 - \partial_\epsilon \,\mathrm{Re}\,\sigma^R$. The second term accounts for the change of the distribution function due to a force $\partial_{\vec{x}} \left(g_0^{-1} - \mathrm{Re}\,\sigma^R\right)$, whereas the last term tracks the change of the distribution function due to the diffusion of excitations with the velocity $\partial_{\vec{p}} \left(g_0^{-1} - \mathrm{Re}\,\sigma^R\right)$. The right-hand side describes collisions that drive the system towards equilibrium. Using the Hartree-Fock approximation in Eq.(4.24), we find

$$\begin{aligned} \partial_\epsilon \left(g_0^{-1} - (\mathrm{Re}\,\sigma^H)^R\right) &= 1, \\ \partial_{\vec{p}} \left(g_0^{-1} - (\mathrm{Re}\,\sigma^H)^R\right) &= -\lambda v_F^R \hat{p}, \\ \partial_{\vec{x}} \left(g_0^{-1} - (\mathrm{Re}\,\sigma^H)^R\right) &= -\partial_{\vec{x}} V^H(\vec{x}). \end{aligned} \tag{4.27}$$

We first substitute these derivatives into Eq.(3.91) followed by a multiplication of the resulting equation with the spectral function $\mathrm{Im}\, g^{-1}_{\lambda\lambda}(\vec{p},\epsilon) = -2\pi i \delta(\epsilon - \lambda v_F^R p)$. Subsequently, we integrate it over the frequency which amounts to the quasi-particle approximation. In the end, we obtain the mean-field collisionless Boltzmann equation, also known as the Vlasov equation [13], for electrons ($\lambda = +$) and holes ($\lambda = -$)

$$\partial_t f_\lambda(\vec{x},t,\vec{p}) + \lambda v_F^R \hat{p}\cdot\partial_{\vec{x}} f_\lambda(\vec{x},t,\vec{p}) - \partial_{\vec{x}} V^H(\vec{x})\cdot\partial_{\vec{p}} f_\lambda(\vec{x},t,\vec{p}) = 0, \tag{4.28}$$

where $\hat{p}$ denotes the unit vector in the direction of the momentum $\vec{p}$. In the above equation, the equilibrium value of the distribution functions is given by $f^0_\lambda(\vec{p}) = (1 + \exp\left(\frac{\lambda v_F^R p - \mu}{T}\right))^{-1}$. The potential $V^H(\vec{x}) = \int d\vec{x}' V(\vec{x} - \vec{x}')\delta n(\vec{x}', t)$ results from the Hartree self-energy, where $\delta n = n - n_0$ is the density fluctuation. This potential is also the solution of the classical Poisson equation for the internal electric field.

To summarize, we found that the Hartree-Fock diagrams lead to the Vlasov equation.

4.4 Second-order perturbation theory: - Born approximation

An important role in hydrodynamic systems is the relaxation process towards local equilibrium by means of interactions that conserve particle number, momentum, and energy. These collisions occur beyond first order in the Coulomb interaction. The lowest non-vanishing order is second order and the contributions are pictorially shown in Fig.(4.4). This is called the Born approximation for the cross section [33, 32, 12, 59]. In principle, these diagrams play two roles: (i) they describe the aforementioned relaxations due to collisions and (ii) they renormalize the quasi-particle properties [27, 87].

The calculation of these diagrams is tedious but straightforward. Here we summarize our final results and present the full derivation in Appendix 4.8. The Boltzmann equation reads

$$\begin{aligned}
&\partial_t f_\lambda(\vec{x},t,\vec{p}) + \lambda v_F^R \hat{p}\cdot\partial_{\vec{x}} f_\lambda(\vec{x},t,\vec{p}) - \ \partial_{\vec{x}} V^H(\vec{x},t)\cdot\partial_{\vec{p}} f_\lambda(\vec{x},t,\vec{p}) \\
&\quad = -\int \frac{d\vec{k}_1}{(2\pi)^2}\frac{d\vec{q}}{(2\pi)^2} R_{\lambda\lambda_1\lambda_3\lambda_2}(\vec{k},\vec{k}_1,\vec{q}) \\
&\qquad 2\pi\delta(\lambda\epsilon_{\vec{k}} - \lambda_1\epsilon_{\vec{k}-\vec{q}} - \lambda_2\epsilon_{\vec{k}_1+\vec{q}} + \lambda_3\epsilon_{\vec{k}_1}) \\
&\qquad \Big[f_\lambda(\vec{k}) f_{\lambda_3}(\vec{k}_1)(1-f_{\lambda_1}(\vec{k}-\vec{q}))(1-f_{\lambda_2}(\vec{k}_1+\vec{q})) \\
&\qquad -(1-f_\lambda(\vec{k}))(1-f_{\lambda_3}(\vec{k}_1)) f_{\lambda_1}(\vec{k}-\vec{q}) f_{\lambda_2}(\vec{k}_1+\vec{q}) \Big],
\end{aligned} \tag{4.29}$$

where we introduced the shorthand notation

$$\begin{aligned}
&R_{\lambda\lambda_1\lambda_3\lambda_2}(\vec{k},\vec{k}_1,\vec{q}) = \\
&\quad 2\Big[|T_{\lambda\lambda_1\lambda_3\lambda_2} - T_{\lambda\lambda_2\lambda_1\lambda_3}|^2 + (N-1)\left(|T_{\lambda\lambda_1\lambda_3\lambda_2}|^2 + |T_{\lambda\lambda_2\lambda_1\lambda_3}|^2 \right) \Big].
\end{aligned} \tag{4.30}$$

In this expression, we have used

$$T_{\lambda\lambda_1\lambda_2\lambda_3}(\vec{k},\vec{k}_1,\vec{q}) = \frac{V(\vec{q})}{2} M^{\lambda\lambda_1}_{\vec{k},\vec{k}-\vec{q}} M^{\lambda_2\lambda_3}_{\vec{k}_1,\vec{k}_1+\vec{q}}\,, \tag{4.31}$$

where the coherence factor M comes from the overlap of the single-particle wavefunctions. It is defined according to

$$M^{\lambda\lambda_1}_{\vec{k},\vec{k}_1} = \left(\mathcal{U}^{\dagger}_{\vec{k}}\mathcal{U}_{\vec{k}_1}\right)_{\lambda\lambda_1} . \tag{4.32}$$

For brevity, we suppress the space and time variables of the distribution functions in the collision terms and have in mind that they all depend on the same set of variables that is $(\vec{x}, t)$. The collision does not shift the center-of-mass and time coordinates. This effect indeed exists, but it will show up at higher order in the gradient expansion [88]. We can understand this collision integral in the following way: an electron in band λ with momentum $\vec{k}$ is scattered into band λ_1 and momentum $\vec{k}+\vec{q}$ by a collision with another electron in band λ_3 and state $\vec{k}_1$ which is itself scattered into the energy band λ_2 and state $\vec{k}_1 - \vec{q}$. For this event to take place, the initial states $\vec{k}$ and $\vec{k}_1$ have to be filled and the final states $\vec{k}-\vec{q}$ and $\vec{k}_1+\vec{q}$ must be empty. Thus the factors $f_\lambda(\vec{k})$ and $f_{\lambda_3}(\vec{k}_1)$ are the occupation number of these state and $1 - f_{\lambda_1}(\vec{k}-\vec{q})$ and $1 - f_{\lambda_2}(\vec{k}_1+\vec{q})$ describes the probability that the final states are unoccupied. The conservation of energy is taken into account by the delta-function. The transition probability of this event is $R_{\lambda\lambda_1\lambda_3\lambda_2}$.

In total, we find that, up to second order in the perturbation theory, Coulomb interaction enters the Boltzmann transport equation in two ways: (i) as the Hartree potential produced by all the other particles in the system and (ii) inelastic and momentum-conserving electron-electron scatterings leading to local equilibration. Let us note that within this approximation, the contribution from the real part of the second-order diagrams to the left-hand side of Eq. (4.29) is neglected.

Finally, let us note that the Born approximation is valid only when the kinetic energy of the electrons is large compared to the Coulomb interaction potential [77]. For the Dirac system, the ratio of the potential energy to the kinetic energy is characterized by the fine structure constant $\alpha = e^2/4\pi\epsilon v_F$. In condensed-matter systems, this constant is not necessarily small (for graphene $\alpha \approx 0.3 - 2.2$). In such a strong interaction limit, a perturbative series expansion in α may break down. Instead one can employ an alternative perturbative expansion in the other parameters. In the subsequent chapter,

we will employ the random-phase approximation (RPA) and show that it gives a different, more complicated picture from the Hartree-Fock-Born result presented in this section.

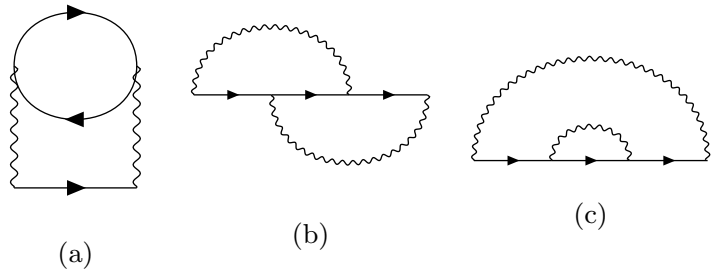

Figure 4.4: Self-energy to second order in the interaction.

4.5 Conservation laws

The collision integral on the right-hand side of the Boltzmann equation in Eq. (4.29), henceforth denoted $C_\lambda[f](\vec{k})$, has conservation laws encoded in it. These conservation laws are important for two reasons: (i) They allow for an identification or derivation of physical quantities such as charge and current densities; (ii) it provides the basis of the derivation of conservation laws and even transport phenomena. When a system is driven away from equilibrium, the first thing that happens is that collisions drive the system to local equilibrium. Afterwards, there is a much slower return to global equilibrium. The latter describes transport processes and is governed by the conservation laws. The conserved quantities in the system under consideration are particle number, momentum, and energy. The conservation laws of electric charge, momentum, and energy are obtained by multiplying the Boltzmann equation in Eq. (4.29), by 1, $\vec{p}$ and $\epsilon_\lambda(\vec{x},\vec{p}) = \lambda v_F^R p + V^H(\vec{x})$ and then integrating the resulting equations over all momentum $\vec{p}$ as well as summing over energy bands $\pm$ and flavors. This leads to the following collisional invariants

$$N \sum_{\lambda=\pm} \int \frac{d\vec{p}}{(2\pi)^2}\, C_\lambda[f](\vec{p}) = 0, \tag{4.33}$$

$$N \sum_{\lambda=\pm} \int \frac{d\vec{p}}{(2\pi)^2}\ \vec{p} C_\lambda[f](\vec{p}) = 0, \tag{4.34}$$

and

$$N \sum_{\lambda=\pm} \int \frac{d\vec{p}}{(2\pi)^2}\ \epsilon_\lambda(\vec{x},\vec{p}) C_\lambda[f](\vec{p}) = 0. \tag{4.35}$$

(i) The continuity equation of charge can be obtained by integrating the Boltzmann equation in Eq. (4.29), over momentum $\vec{p}$ followed by a summation over the band index and flavor index, see Eq. (4.33). In contrast to the case of one band system, there is a subtle point here relating to the infinite number of particles in the filled band which is unbound from below. This infinite constant vanishes upon differentiation and does not contribute to the continuity equation. Therefore, we can subtract the infinite contribution coming from the Dirac sea and instead consider the population of holes defined as $f(\vec{x},t,\vec{k})-1$. First, we consider the time-derivative term. Integrating this term over all states gives

$$\begin{aligned} & N \sum_{\lambda=\pm} \int \frac{d\vec{p}}{(2\pi)^2} \partial_t f_\lambda(\vec{x},t,\vec{p}) \\ & \quad = \partial_t\ N \int \frac{d\vec{p}}{(2\pi)^2} \Big[f_+(\vec{x},t,\vec{p}) + (f_-(\vec{x},t,\vec{p}) - 1) \Big]. \end{aligned} \tag{4.36}$$

We denote the charge density by

$$n(\vec{x},t) = N \int \frac{d\vec{p}}{(2\pi)^2}\ \left[f_+(\vec{x},t,\vec{p}) + (f_-(\vec{x},t,\vec{p}) - 1) \right]. \tag{4.37}$$

The second term can be integrated in a similar fashion and gives

$$\begin{aligned} & N \sum_{\lambda=\pm} \int \frac{d\vec{p}}{(2\pi)^2} \lambda v_F^R \hat{p} \cdot \partial_{\vec{x}} f_\lambda(\vec{x},t,\vec{p}) \\ & \quad = \partial_{\vec{x}} \cdot\ N \int \frac{d\vec{p}}{(2\pi)^2} v_F^R \hat{p} \Big[f_+(\vec{x},t,\vec{p}) - (f_-(\vec{x},t,\vec{p}) - 1) \Big]. \end{aligned} \tag{4.38}$$

This term can be identified with the charge current density

$$\vec{j}(\vec{x},t) = N \int \frac{d\vec{p}}{(2\pi)^2}\ v_F^R \hat{p} \Big[f_+(\vec{x},t,\vec{p}) - (f_-(\vec{x},t,\vec{p}) - 1) \Big]. \tag{4.39}$$

The momentum-derivative term vanishes upon integration

$$-N\sum_{\lambda=\pm}\int\frac{d\vec{p}}{(2\pi)^2}\partial_{\vec{x}}V^H(\vec{x})\cdot\partial_{\vec{p}}f_\lambda(\vec{x},t,\vec{p})$$
$$=-N\sum_{\lambda=\pm}\int\frac{d\vec{p}}{(2\pi)^2}\partial_{\vec{p}}\cdot\Big[\partial_{\vec{x}}V^H(\vec{x})f_\lambda(\vec{x},t,\vec{p})\Big]=0\,, \tag{4.40}$$

since it is a total derivative. Combining the above equations together with Eq. (4.33), we find the continuity equation for the electric charge according to

$$\partial_t n(\vec{x},t)+\partial_{\vec{x}}\cdot\vec{j}(\vec{x},t)=0. \tag{4.41}$$

It is worthwhile noting here that the charge density is conserved locally.

(ii) Momentum conservation can be obtained by multiplying the Boltzmann equation in Eq. (4.29) by momentum before integrating the resulting equation over all states, see Eq. (4.34). The time-derivative term yields

$$N\sum_{\lambda=\pm}\int\frac{d\vec{p}}{(2\pi)^2}\vec{p}\partial_t f_\lambda(\vec{x},t,\vec{p})=$$
$$\partial_t\ N\int\frac{d\vec{p}}{(2\pi)^2}\vec{p}\Big[f_+(\vec{x},t,\vec{p})+(f_-(\vec{x},t,\vec{p})-1)\Big]. \tag{4.42}$$

This allows to define the momentum density,

$$\vec{n}^{\vec{p}}(\vec{x},t)=N\int\frac{d\vec{p}}{(2\pi)^2}\vec{p}\Big[f_+(\vec{x},t,\vec{p})+(f_-(\vec{x},t,\vec{p})-1)\Big]. \tag{4.43}$$

The space-derivative term can be similarly integrated and gives

$$N\sum_{\lambda=\pm}\int\frac{d\vec{p}}{(2\pi)^2}\vec{p}\,\lambda v_F^R\hat{p}\cdot\partial_{\vec{x}}f_\lambda(\vec{x},t,\vec{p})$$
$$=\partial_{\vec{x}}\cdot\ N\int\frac{d\vec{p}}{(2\pi)^2}v_F^R\vec{p}\hat{p}\Big[f_+(\vec{x},t,\vec{p})-(f_-(\vec{x},t,\vec{p})-1)\Big]. \tag{4.44}$$

From this result, we define the momentum-flux tensor,

$$\vec{\vec{\Pi}}(\vec{x},t) = N\int \frac{d\vec{p}}{(2\pi)^2}\; v_F^R \vec{p}\hat{p}\Big[f_+(\vec{x},t,\vec{p}) - (f_-(\vec{x},t,\vec{p})-1)\Big]. \quad (4.45)$$

The momentum-derivative term yields

$$\begin{aligned} -N\sum_{\lambda=\pm}\int \frac{d\vec{p}}{(2\pi)^2}\vec{p}\partial_{\vec{x}}V^H(\vec{x})\cdot\partial_{\vec{p}}f_\lambda(\vec{x},t,\vec{p}) \\ = \partial_{\vec{x}}V^H(\vec{x})N\int\frac{d\vec{p}}{(2\pi)^2}\;[f_+(\vec{x},t,\vec{p}) + (f_-(\vec{x},t,\vec{p})-1)] \\ = \partial_{\vec{x}}V^H(\vec{x})n(\vec{x},t). \end{aligned} \quad (4.46)$$

which defines a force term. Finally, combining the above equations, we find the momentum equation according to

$$\partial_t \vec{n}^{\vec{p}}(\vec{x},t) + \partial_{\vec{x}}\cdot\vec{\vec{\Pi}}(\vec{x},t) = -\partial_{\vec{x}}V^H(\vec{x},t)n(\vec{x},t). \quad (4.47)$$

This has a straightforward interpretation. The momentum of the electron fluid in any given volume element can be changed in two ways: (i) by means of momentum flow through the volume boundary accounting for the space-gradient term and (ii) by the internal electric field. Locally, the momentum density is not conserved and changed by the internal electric force $-\partial_{\vec{x}}V^H(\vec{x},t)$. This internal force, however, does not affect the total momentum of the entire system. We still expect that the total momentum of the system is conserved. This can be shown explicitly by integrating the momentum equation over all space. The integration of the momentum-flux gradient results in a surface term which vanishes. The Hartree force term also vanishes. To see this, we consider the property of the Coulomb potential

$$\partial_{\vec{x}}\frac{1}{|\vec{x}-\vec{x}'|} = -\frac{\vec{x}-\vec{x}'}{|\vec{x}-\vec{x}'|^3} = -\partial_{\vec{x}'}\frac{1}{|\vec{x}-\vec{x}'|}. \quad (4.48)$$

Based on this, one can show explicitly that

$$\begin{aligned} \int d\vec{x}\partial_{\vec{x}}V^H(\vec{x},t)n(\vec{x},t) &= \int d\vec{x}d\vec{x}'\partial_{\vec{x}}V(\vec{x}-\vec{x}')(n(\vec{x}',t)-n_0)n(\vec{x},t) \\ &= 0. \end{aligned} \quad (4.49)$$

Combining all the above equations, we obtain

$$\partial_t \vec{P} = 0, \tag{4.50}$$

where the total momemtum of the entire system is given by

$$\vec{P}(t) = \int d\vec{r}\, \vec{n}^{\vec{p}}(\vec{r}, t). \tag{4.51}$$

(iii) Similarly, energy conservation is obtained by multiplying the Boltzmann equation, Eq. (4.29) by energy $\epsilon(\vec{x}, \vec{p})$ followed by integrating and summing the equation over all states, see Eq. (4.35). The time-derivative term yields

$$N \sum_{\lambda=\pm} \int \frac{d\vec{p}}{(2\pi)^2} \epsilon_\lambda(\vec{x}, \vec{p}) \partial_t f_\lambda(\vec{x}, t, \vec{p}) \;=\; \partial_t \; N \int \frac{d\vec{p}}{(2\pi)^2} \Big[\epsilon_+(\vec{x}, \vec{p}) f_+(\vec{x}, t, \vec{p}) + \epsilon_-(\vec{x}, \vec{p})(f_-(\vec{x}, t, \vec{p}) - 1) \Big]. \tag{4.52}$$

This defines the energy density according to

$$n^\epsilon(\vec{x}, t) = N \int \frac{d\vec{p}}{(2\pi)^2} \Big[\epsilon_+(\vec{x}, \vec{p}) f_+(\vec{x}, t, \vec{p}) + \epsilon_-(\vec{x}, \vec{p})(f_-(\vec{x}, t, \vec{p}) - 1) \Big]. \tag{4.53}$$

The spatial derivative leads to

$$\begin{aligned} N \sum_{\lambda=\pm} \int \frac{d\vec{p}}{(2\pi)^2} \epsilon_\lambda(\vec{x}, \vec{p}) \; \lambda v_F^R \hat{p} \cdot \partial_{\vec{x}} f_\lambda(\vec{x}, t, \vec{p}) \\ = \partial_{\vec{x}} \cdot \; N \int \frac{d\vec{p}}{(2\pi)^2} v_F^R \hat{p} \Big[\epsilon_+(\vec{x}, \vec{p}) f_+(\vec{x}, t, \vec{p}) \\ - \epsilon_-(\vec{x}, \vec{p})(f_-(\vec{x}, t, \vec{p}) - 1) \Big] - \partial_{\vec{x}} V^H(\vec{x}) \cdot \vec{j}. \end{aligned} \tag{4.54}$$

We find that it consists of two terms. The first term describes a divergence of an energy current density defined as

$$\vec{j}^\epsilon(\vec{x}, t) = N \int \frac{d\vec{p}}{(2\pi)^2} \; v_F^R \hat{p} \Big[\epsilon_+(\vec{x}, \vec{p}) f_+(\vec{x}, t, \vec{p}) - \epsilon_-(\vec{x}, \vec{p})(f_-(\vec{x}, t, \vec{p}) - 1) \Big], \tag{4.55}$$

whereas the second term describes Joule heating due to the internal force. Next, we consider the momentum-derivative term and find that it can also be rewritten as Joule heating due to the internal Coulomb force.

$$-N\sum_{\lambda=\pm}\int\frac{d\vec{p}}{(2\pi)^2}\epsilon_\lambda(\vec{x},\vec{p})\;\partial_{\vec{x}}V^H(\vec{x})\cdot\partial_{\vec{p}}f_\lambda(\vec{x},t,\vec{p})=\partial_{\vec{x}}V^H(\vec{x})\cdot\vec{j}\;. \tag{4.56}$$

This term will thus be canceled by the second term on the right-hand side of Eq. (4.54). Combining these equations, we find the continuity equation of energy:

$$\partial_t n^\epsilon(\vec{x},t)+\partial_{\vec{x}}\cdot\vec{j}^\epsilon(\vec{x},t)=0. \tag{4.57}$$

Eqs.(4.41), (4.47), and (4.57) constitute the main equations of electron hydrodynamics and can be used to derive the Navier-Stokes equations. Let us emphasize once again that, in contrast to the hydrodynamic equations of usual fluids, electrons interact among themselves via long-range Coulomb interactions and this effect shows up on the right-side of the momentum equation in Eq.(4.47)

4.6 Collective modes

Now that we have the fundamental equations of hydrodynamics of weakly interacting charged Dirac electrons, let us study some of its properties. There are three independent hydrodynamic variables. Here we choose the set of independent variables consisting of the charge density (n), the energy density (n^ϵ) and the hydrodynamic velocity $\vec{u}$ in terms of which the other quantities can be written. To linear order in $\vec{u}$, we find that the charge current density is given by $\vec{j}=n\vec{u}$. The momentum flux is associated with the pressure by means of $\Pi_{ij}=P\delta_{ij}$ where the pressure is in turn proportional to the energy density according to $P=n^\epsilon/2$. One of the consequences of the linear spectrum of Dirac electrons is that the momentum density is decoupled from the charge current. Instead, it is proportional to the energy currents according to $n^{\vec{p}}=\vec{j}^\epsilon/v_F^2$ where the energy current is given by $j^\epsilon=(P+n^\epsilon)\vec{u}$. We now consider an electron fluid at rest with constant $n=n_0$, $n^\epsilon=n_0^\epsilon$, and $\vec{u}=0$. We are

interested in small fluctuations around constant and homogeneous solution, and put $n = n_0 + \delta n$, $n^\epsilon = n_0^\epsilon + \delta n^\epsilon$ and small $\vec{u}$. We insert this solution into the hydrodynamic equations in Eqs. (4.41, (4.47), and (4.57). By keeping terms up to linear order in the fluctuations, we obtain

$$\begin{aligned} \partial_t \delta n(\vec{x},t) + n_0 \partial_{\vec{x}} \cdot \vec{u}(\vec{x},t) &= 0, \\ (P_0 + n_0^\epsilon)/v_F^2 \partial_t \vec{u}(\vec{x},t) + \partial_{\vec{x}} \delta P(\vec{x},t) &= -\partial_{\vec{x}} V^H(\vec{x},t) n_0, \\ \partial_t \delta n^\epsilon(\vec{x},t) + (P_0 + n_0^\epsilon) \partial_{\vec{x}} \cdot \vec{u}(\vec{x},t) &= 0. \end{aligned} \tag{4.58}$$

The solutions to these equations are propagating waves. As an ansatz, we insert

$$\begin{pmatrix} \delta n(\vec{x},t) \\ \vec{u}(\vec{x},t) \\ \delta n^\epsilon(\vec{x},t) \end{pmatrix} = \begin{pmatrix} \delta n(\vec{p},\omega) \\ \vec{u}(\vec{p},\omega) \\ \delta n^\epsilon(\vec{p},\omega) \end{pmatrix} e^{i\vec{p}\cdot\vec{x} - i\omega t} \tag{4.59}$$

into the linearized hydrodynamic equations in Eq. (4.58). This leads to

$$\begin{aligned} -i\omega \delta n(\vec{p},\omega) + i n_0 p u_\parallel(\vec{p},\omega) &= 0\ , \\ -i\omega \frac{P_0 + n_0^\epsilon}{v_F^2} \vec{u}(\vec{p},\omega) + i\vec{p}\, \delta P(\vec{p},\omega) &= -\frac{i 2\pi\alpha v_F \vec{p}}{p} \delta n(\vec{p},\omega) n_0\ , \\ -i\omega \delta n^\epsilon(\vec{p},\omega) + (P_0 + n_0^\epsilon) i p u_\parallel(\vec{p},\omega) &= 0\ . \end{aligned} \tag{4.60}$$

Here, we define $u_\parallel = \vec{u} \cdot \vec{p}/p$ which gives the component of the hydrodynamic velocity in the direction of the momentum $\vec{p}$. We are interested in the longitudinal propagating modes, so we project the momentum equation on the momentum $\vec{p}/p$. This gives

$$-i\omega \frac{P_0 + n_0^\epsilon}{v_F^2} u_\parallel(\vec{p},\omega) + ip\ \delta P(\vec{p},\omega) = -i 2\pi\alpha v_F \delta n(\vec{p},\omega) n_0. \tag{4.61}$$

Together with the other two equations, we find that

$$\begin{pmatrix} -i\omega & i n_0 p & 0 \\ i 2\pi\alpha v_F n_0 & -i\omega \frac{P_0 + n_0^\epsilon}{v_F^2} & ip/2 \\ 0 & ip(P_0 + n_0^\epsilon) & -i\omega \end{pmatrix} \begin{pmatrix} \delta n(\vec{p},\omega) \\ u_\parallel(\vec{p},\omega) \\ \delta n^\epsilon(\vec{p},\omega) \end{pmatrix} = \begin{pmatrix} 0 \\ 0 \\ 0 \end{pmatrix}. \tag{4.62}$$

For this equation to have non-trivial solutions, the frequency of the fluctuations has to satisfy the dispersion relations

$$\begin{aligned} \omega(\vec{p}) &= 0 \\ \omega_{\pm}(\vec{p}) &= \pm\sqrt{2\pi\alpha v_F^3 n_0^2 p/(P_0+n_0^{\epsilon})+v_F^2 p^2/2}. \end{aligned} \tag{4.63}$$

We observe, that in the long wavelength limit, there is a square-root dispersion which represents the hydrodynamic plasmon. At charge neutrality, $n_0 = 0$, the dispersion becomes linear with the speed given by $v_F/\sqrt{2}$.

This result, as we will see later, is in disagreement with the calculation within the RPA. The RPA calculation predicts the existence of thermal plasmons at charge neutrality and at non-zero temperature. The key step to reconcile these results relies on the observation that, for Dirac electrons, the momentum density and charge current are decoupled. This is in stark contrast to one-band systems with a parabolic dispersion where the momentum density is proportional to the charge current. To this end, let us additionally consider an equation of motion for the charge current, which is obtained by multiplying the Boltzmann equation, Eq. (4.29), by the corresponding group velocity $\partial_{\vec{p}}\epsilon_{\lambda}(\vec{x},\vec{p}) = \lambda v_F^R \hat{p}$ and integrating the resulting equation over all states. The time-derivative term yields

$$N\sum_{\lambda=\pm}\int\frac{d\vec{p}}{(2\pi)^2}\lambda v_F^R\hat{p}\partial_t f_{\lambda}(\vec{x},t,\vec{p}) = \partial_t\vec{j}(\vec{x},t). \tag{4.64}$$

The space-derivative term can be similarly integrated and gives

$$N\sum_{\lambda=\pm}\int\frac{d\vec{p}}{(2\pi)^2}\left(v_F^R\right)^2\hat{p}\hat{p}\cdot\partial_{\vec{x}}f_{\lambda}(\vec{x},t,\vec{p}) = \partial_{\vec{x}}\cdot\vec{\vec{\Xi}}(\vec{x},t)\ , \tag{4.65}$$

where we define a second-rank tensor according to

$$\vec{\vec{\Xi}}(\vec{x},t) = N\sum_{\lambda=\pm}\int\frac{d\vec{p}}{(2\pi)^2}v_F^2\hat{p}\hat{p}\Big[f_+(\vec{x},t,\vec{p})+(f_-(\vec{x},t,\vec{p})-1)\Big]. \tag{4.66}$$

The momentum-derivative term yields

$$-N\sum_{\lambda=\pm}\int\frac{d\vec{p}}{(2\pi)^2}\lambda v_F^R\hat{p}\partial_{\vec{x}}V^H(\vec{x})\cdot\partial_{\vec{p}}f_\lambda(\vec{x},t,\vec{p})=\partial_{\vec{x}}V^H(\vec{x})\cdot\vec{\vec{\Lambda}}(\vec{x},t) \tag{4.67}$$

where another second rank tensor has components given by

$$\vec{\vec{\Lambda}}_{ij}(\vec{x},t)=N\int\frac{d\vec{p}}{(2\pi)^2}\left(\frac{\delta_{ij}}{p}-\frac{p_ip_j}{p^3}\right)\left[f_+(\vec{x},t,\vec{p})+(f_-(\vec{x},t,\vec{p})-1)\right]. \tag{4.68}$$

In contrast to the conserved quantities discussed in the previous section, the group velocity is not a collisional invariant. Therefore, the current density is not conserved by electron-electron interactions. This is particularly true at charge neutrality. The integration of the collision term is, in general, very complicated, especially, since the distribution function is unknown. For the purpose of this discussion, we resort to the relaxation time approximation and assume that

$$\sum_{\lambda=\pm}\int\frac{d\vec{p}}{(2\pi)^2}\,\lambda v_F^R pC_\lambda[f](\vec{p})\approx-\frac{\vec{j}}{\tau}\,. \tag{4.69}$$

The value of the relaxation time τ may be approximated by the corresponding element of the collision operator in the Boltzmann equation (see for example in [33]). Finally, combining the above calculations, we find the equation of motion for the charge current.

$$\partial_t\vec{j}_k(\vec{x},t)+\partial_{\vec{x}_i}\vec{\vec{\Xi}}_{ik}(\vec{x},t)+\partial_{\vec{x}_i}V^H(\vec{x},t)\vec{\vec{\Lambda}}_{ik}(\vec{x},t)=-\frac{\vec{j}_k(\vec{x},t)}{\tau}. \tag{4.70}$$

To linear order in $\vec{u}$, we find that $\vec{\vec{\Xi}}_{ij}=nv_F^2/2\;\delta_{ij}$ which is proportional to the charge density and $\vec{\vec{\Lambda}}_{ij}=\frac{N}{4\pi}\mathcal{N}\delta_{ij}$ where $\mathcal{N}=\int dp\left[f_+^0(\vec{p})-(f_-^0(\vec{p})-1)\right]=T\log(2+2\cosh\mu/T)$. Here $f_\lambda^0(\vec{p})=(1+\exp\left(\frac{\lambda v_F p-\mu}{T}\right))^{-1}$ is the Fermi-Dirac distribution function. We are interested in small density fluctuations around the constant and homogeneous value. The solution is $n=n_0+\delta n$ and small $\vec{u}$. We insert this solution into the current equation (4.70) and keep the

terms to linear order in the fluctuations. This gives

$$n_0 \partial_t \vec{u}_k(\vec{x},t) + \frac{v_F^2}{2}\partial_{\vec{x}_k}\delta n(\vec{x},t) + \partial_{\vec{x}_k} V^H(\vec{x},t)\frac{N}{4\pi}\mathcal{N} = -\frac{n_0 \vec{u}_k(\vec{x},t)}{\tau}. \tag{4.71}$$

The solution to this equation are propagating waves of the form

$$\begin{pmatrix} \delta n(\vec{x},t) \\ \vec{u}(\vec{x},t) \end{pmatrix} = \begin{pmatrix} \delta n(\vec{p},\omega) \\ \vec{u}(\vec{p},\omega) \end{pmatrix} e^{i\vec{p}\cdot\vec{x}-i\omega t}. \tag{4.72}$$

We insert this solution into the linearized current equation (4.71) and obtain

$$-i\omega n_0 \vec{u}(\vec{p},\omega) + i\frac{v_F^2}{2}\vec{p}\delta n(\vec{p},\omega) + i\frac{2\pi\alpha v_F \vec{p}}{p}\delta n(\vec{p},\omega)\frac{N}{4\pi}\mathcal{N} = -\frac{n_0 \vec{u}(\vec{p},\omega)}{\tau}. \tag{4.73}$$

Next, we project the equation on the momentum $\vec{p}/p$, This gives

$$-i\omega n_0 u_\parallel(\vec{p},\omega) + i\frac{v_F^2}{2}p\delta n(\vec{p},\omega) + i2\pi\alpha v_F \delta n(\vec{p},\omega)\frac{N}{4\pi}\mathcal{N} = -\frac{n_0 u_\parallel(\vec{p},\omega)}{\tau}. \tag{4.74}$$

Together with the continuity equation, we find that

$$\begin{pmatrix} -i\omega & in_0 p \\ i\alpha v_F \frac{N}{2}\mathcal{N} + i\frac{v_F^2}{2}p & -i\omega n_0 + n_0/\tau \end{pmatrix} \begin{pmatrix} \delta n(\vec{p},\omega) \\ u_\parallel(\vec{p},\omega) \end{pmatrix} = \begin{pmatrix} 0 \\ 0 \end{pmatrix}. \tag{4.75}$$

For this equation to be valid, the frequency of the density fluctuations has to satisfy the dispersion relation

$$\omega_\pm(\vec{p}) = \pm\sqrt{\frac{N}{2}\alpha v_F T p \log(2+2\cosh\mu/T) + \frac{v_F^2 p^2}{2} - \frac{1}{4\tau^2}} - \frac{i}{2\tau}. \tag{4.76}$$

Note that, in the long-wavelength limit, we recover the previous hydrodynamic result.

4.7 Conclusion and Outlook

In this chapter we have studied the basic equations of hydrodynamics in ultraclean interacting two-dimensional Dirac systems. Our

approach was based on non-equilibrium quantum field theory. We first derived the hydrodynamic equations in weakly interacting systems, based on low-order perturbation theory. This allows to recover mostly known literature expressions. We go beyond a weak coupling analysis in the next chapter.

4.8 Appendices

Derivation of the collision integral of Eq.(4.29)

The algebraic expression for the diagram (4.4a) is given by

$$\begin{aligned} -i\Sigma^{(2a)}_{ah}(\vec{x},\vec{x}';t,t') &= -iN\int dt_1 dt_2 d\vec{x}_1 d\vec{x}_2\ \gamma^{a'}_{ab}\gamma^{b'}_{cd}\gamma^{c'}_{ef}\gamma^{d'}_{gh} \\ & D_{0,a'b'}(\vec{x},\vec{x}_1;t,t_1)D_{0,\gamma\delta}(\vec{x}_2,\vec{x'};t_2,t') \\ & G_{0,bg}(\vec{x},\vec{x'};t,t')G_{0,de}(\vec{x}_1,\vec{x}_2;t_1,t_2) \\ & G_{0,fc}(\vec{x}_2,\vec{x}_1;t_2,t_1). \end{aligned} \tag{4.77}$$

After a Wigner transformation, its Keldysh component in the quasiparticle basis reads

$$\begin{aligned} &(\sigma^{(2a)}_{\lambda\lambda})^K(\vec{x},\vec{k},t,\omega) = \\ &\quad iN\int\frac{d\vec{k}_1}{(2\pi)^2}\frac{d\vec{q}}{(2\pi)^2}2\pi\delta(\omega-\lambda_1\epsilon_{\vec{k}-\vec{q}}-\lambda_2\epsilon_{\vec{k}_1+\vec{q}}+\lambda_3\epsilon_{\vec{k}_1}) \\ &\quad |T_{\lambda\lambda_1\lambda_2\lambda_3}(\vec{k},\vec{k}_1,\vec{q})|^2\Big(F_{\lambda_3}(\vec{x},t,\vec{k}_1)-F_{\lambda_2}(\vec{x},t,\vec{k}_1+\vec{q}) \\ &\quad +F_{\lambda_1}(\vec{x},t,\vec{k}-\vec{q})\Big[F_{\lambda_2}(\vec{x},t,\vec{k}_1+\vec{q})F_{\lambda_3}(\vec{x},t,\vec{k}_1)-1\Big]\Big). \end{aligned} \tag{4.78}$$

Here we assume that the distribution function within the quasiparticle approximation has no off-diagonal elements in the spinor space. Furthermore, we introduce the shorthand notation for ihe Coulomb interaction transition probability amplitude

$$T_{\lambda\lambda_1\lambda_2\lambda_3}(\vec{k},\vec{k}_1,\vec{q}) = \frac{V(\vec{q})}{2}M^{\lambda\lambda_1}_{\vec{k},\vec{k}-\vec{q}}M^{\lambda_2\lambda_3}_{\vec{k}_1,\vec{k}_1+\vec{q}}\,, \tag{4.79}$$

where the coherent factor coming from the overlap of the wavefunction is defined according to

$$M^{\lambda\lambda_1}_{\vec{k},\vec{k}_1} = \left(\mathcal{U}^{\dagger}_{\vec{k}}\mathcal{U}_{\vec{k}_1}\right)_{\lambda\lambda_1} \quad . \tag{4.80}$$

The retarded component of the self-energy is given by

$$\begin{aligned} 2i\,\mathrm{Im}(\sigma^{(2a)}_{\lambda})^R(\vec{k},\omega) = \\ & iN\int \frac{d\vec{k}_1}{(2\pi)^2}\frac{d\vec{q}}{(2\pi)^2} 2\pi\delta(\omega - \lambda_1\epsilon_{\vec{k}-\vec{q}} - \lambda_2\epsilon_{\vec{k}_1+\vec{q}} + \lambda_3\epsilon_{\vec{k}_1}) \\ & |T_{\lambda\lambda_1\lambda_2\lambda_3}(\vec{k},\vec{k}_1,\vec{q})|^2\Big(F_{\lambda_2}(\vec{x},t,\vec{k}_1+\vec{q})F_{\lambda_3}(\vec{x},t,\vec{k}_1) - 1 \\ & + F_{\lambda_1}(\vec{x},t,\vec{k}-\vec{q})\Big[F_{\lambda_3}(\vec{x},t,\vec{k}_1) - F_{\lambda_2}(\vec{x},t,\vec{k}_1+\vec{q})\Big]\Big). \end{aligned} \tag{4.81}$$

The algebraic expression for the diagram (4.4b) is given by

$$\begin{aligned} -i\Sigma^{(b)}_{ah}(\vec{x},\vec{x}';t,t') &= i\int dt_1 dt_2 d\vec{x}_1 d\vec{x}_2 \gamma^{a'}_{ab}\ \gamma^{b'}_{cd}\gamma^{c'}_{ef}\gamma^{d'}_{gh} \\ & D_{0,a'c'}(\vec{x},\vec{x}_2;t,t_2)D_{0,b'd'}(\vec{x}_1,\vec{x}';t_1,t') \\ & G_{0,bc}(\vec{x},\vec{x}_1;t,t_1)G_{0,de}(\vec{x}_1,\vec{x}_2;t_1,t_2) \\ & G_{0,fg}(\vec{x}_2,\vec{x}';t_2,t'). \end{aligned} \tag{4.82}$$

After a Wigner transformation, the Keldysh component of the self-energy in the quasi-particle basis reads

$$\begin{aligned} (\sigma^{(2b)}_{\lambda})^K(\vec{x},\vec{k},t,\omega) = \\ & -i\int \frac{d\vec{k}_1}{(2\pi)^2}\frac{d\vec{q}}{(2\pi)^2} 2\pi\delta(\omega - \lambda_1\epsilon_{\vec{k}-\vec{q}} - \lambda_2\epsilon_{\vec{k}_1+\vec{q}} + \lambda_3\epsilon_{\vec{k}_1}) \\ & T_{\lambda\lambda_1\lambda_3\lambda_2}(\vec{k},\vec{k}_1,\vec{q})T^*_{\lambda\lambda_2\lambda_1\lambda_3}(\vec{k},\vec{k}_1,\vec{k}-\vec{q}-\vec{k}_1) \\ & \Big(F_{\lambda_3}(\vec{x},t,\vec{k}_1) - F_{\lambda_2}(\vec{x},t,\vec{k}_1+\vec{q}) + F_{\lambda_1}(\vec{x},t,\vec{k}-\vec{q})\times \\ & \Big[F_{\lambda_2}(\vec{x},t,\vec{k}_1+\vec{q})F_{\lambda_3}(\vec{x},t,\vec{k}_1) - 1\Big]\Big), \end{aligned} \tag{4.83}$$

whereas the retarded component of the self-energy is given by

$$
\begin{aligned}
2i\,\mathrm{Im}(\sigma_{\lambda}^{(2b)})^{R}(\vec{k},\omega) = & \\
& -i\int \frac{d\vec{k}_1}{(2\pi)^2}\frac{d\vec{q}}{(2\pi)^2} 2\pi\delta(\omega-\lambda_1\epsilon_{\vec{k}-\vec{q}}-\lambda_2\epsilon_{\vec{k}_1+\vec{q}}+\lambda_3\epsilon_{\vec{k}_1}) \\
& T_{\lambda\lambda_1\lambda_3\lambda_2}(\vec{k},\vec{k}_1,\vec{q})T^{*}_{\lambda\lambda_2\lambda_1\lambda_3}(\vec{k},\vec{k}_1,\vec{k}-\vec{q}-\vec{k}_1) \\
& \Big(F_{\lambda_2}(\vec{x},t,\vec{k}_1+\vec{q})F_{\lambda_3}(\vec{x},t,\vec{k}_1)-1+F_{\lambda_1}(\vec{x},t,\vec{k}-\vec{q})\times \\
& \Big[F_{\lambda_3}(\vec{x},t,\vec{k}_1)-F_{\lambda_2}(\vec{x},t,\vec{k}_1+\vec{q})\Big]\Big). \qquad (4.84)
\end{aligned}
$$

The algebraic expression for the diagram (4.4c) is given by

$$
\begin{aligned}
-i\Sigma^{(c)}_{ah}(\vec{x},\vec{x}';t,t') &= i\int dt_1dt_2d\vec{x}_1d\vec{x}_2\;\gamma^{a'}_{ab}\gamma^{b'}_{cd}\gamma^{c'}_{ef}\gamma^{d'}_{gh} \\
& D_{0,a'd'}(\vec{x},\vec{x}',t,t')D_{0,b'c'}(\vec{x}_1,\vec{x}_2;t_1,t_2) \\
& G_{0,bc}(\vec{x},\vec{x}_1;t,t_1)G_{0,de}(\vec{x}_1,\vec{x}_2;t_1,t_2) \\
& G_{0,fg}(\vec{x}_1,\vec{x}';t_2,t'). \qquad (4.85)
\end{aligned}
$$

This contribution to the collision intergral is omitted because $(\sigma_{\lambda}^{(2c)})^{K}$ and $2i\,\mathrm{Im}(\sigma_{\lambda}^{(2c)})^{R}$ are both zero. After combining these contributions from the diagram $(2a)$-$(2c)$ and substituting the distribution function to zero order in the Berry connection given by Eq.(3.90) , we find the collision integral for electron-electron scattering within the Born approximation. Hereafter we for brevity suppress space and time variables in the distribution function since the collision integral

is local in spacetime.

$$\begin{aligned}
&\sigma^K_\lambda(\vec{p}) - 2i\,\mathrm{Im}\,\sigma^R_\lambda(\vec{p})(1-2f_\lambda(\vec{p})) \\
&\quad = -8i\int \frac{d\vec{k}_1}{(2\pi)^2}\frac{d\vec{q}}{(2\pi)^2} 2\pi\delta(\omega - \lambda_1\epsilon_{\vec{k}-\vec{q}} - \lambda_2\epsilon_{\vec{k}_1+\vec{q}} + \lambda_3\epsilon_{\vec{k}_1}) \\
&\quad \Big[- T_{\lambda\lambda_1\lambda_3\lambda_2}(\vec{k},\vec{k}_1,\vec{q}) T^*_{\lambda\lambda_2\lambda_1\lambda_3}(\vec{k},\vec{k}_1,\vec{k}-\vec{q}-\vec{k}_1) \\
&\qquad\qquad + N|T_{\lambda\lambda_1\lambda_3\lambda_2}(\vec{k},\vec{k}_1,\vec{q})|^2\Big] \\
&\quad \Big[f_\lambda(\vec{k}) f_{\lambda_3}(\vec{k}_1)(1-f_{\lambda_1}(\vec{k}-\vec{q}))(1-f_{\lambda_2}(\vec{k}_1+\vec{q})) \\
&\quad - (1-f_\lambda(\vec{k}))(1-f_{\lambda_3}(\vec{k}_1)) f_{\lambda_1}(\vec{k}-\vec{q}) f_{\lambda_2}(\vec{k}_1+\vec{q})\Big].
\end{aligned} \tag{4.86}$$

We make connection to the Golden rule result by shifting the variables appropriately, This gives

$$\begin{aligned}
&\sigma^K_\lambda(\vec{p}) - 2i\,\mathrm{Im}\,\sigma^R_\lambda(\vec{p})(1-2f_\lambda(\vec{p})) = \\
&\quad -4i\int \frac{d\vec{k}_1}{(2\pi)^2}\frac{d\vec{q}}{(2\pi)^2} 2\pi\delta(\omega - \lambda_1\epsilon_{\vec{k}-\vec{q}} - \lambda_2\epsilon_{\vec{k}_1+\vec{q}} + \lambda_3\epsilon_{\vec{k}_1}) \\
&\quad \Big[|T_{\lambda\lambda_1\lambda_3\lambda_2}(\vec{k},\vec{k}_1,\vec{q}) - T_{\lambda\lambda_2\lambda_1\lambda_3}(\vec{k},\vec{k}_1,\vec{k}-\vec{q}-\vec{k}_1)|^2 \\
&\quad + (N-1)\Big(|T_{\lambda\lambda_1\lambda_3\lambda_2}(\vec{k},\vec{k}_1,\vec{q})|^2 + |T_{\lambda\lambda_2\lambda_1\lambda_3}(\vec{k},\vec{k}_1,\vec{k}-\vec{q}-\vec{k}_1)|^2\Big)\Big] \\
&\quad \Big[f_\lambda(\vec{k}) f_{\lambda_3}(\vec{k}_1)(1-f_{\lambda_1}(\vec{k}-\vec{q}))(1-f_{\lambda_2}(\vec{k}_1+\vec{q})) \\
&\quad - (1-f_\lambda(\vec{k}))(1-f_{\lambda_3}(\vec{k}_1)) f_{\lambda_1}(\vec{k}-\vec{q}) f_{\lambda_2}(\vec{k}_1+\vec{q})\Big].
\end{aligned} \tag{4.87}$$

We the multiply Eq.(4.87) by the spectral function followed by an integration over the frequency. In the end, we obtain a coupled system of Boltzmann equations for electrons ($\lambda = +$) and holes ($\lambda = -$).

Chapter 5

Electron-hole-plasmon hydrodynamics: the strong coupling limit

In the previous chapter, we study the hydrodynamic properties of ultraclean interacting two-dimensional Dirac electrons with Keldysh quantum field theory within the weak-coupling analysis. In this chapter, we study it from a strong-coupling perspective. We demonstrate that long-range Coulomb interactions play a role in facilitating the emergence of collective excitations, that is plasmons. We find that plasmons contribute to transport properties on equal footing with electrons. Our approach is based on an effective field theory of the collective field associated with the plasmon coupled to electrons. Within a conserving approximation for the coupled system we derive a set of coupled quantum-kinetic equations. This builds the foundation of the derivation of the Boltzmann equations for the interacting system of electrons and plasmons. From this, we explicitly derive all the conservation laws and identify the extra contributions of energy density and pressure from the plasmons. We demonstrate that plasmons show up in thermoelectric transport properties as well as quantities that enter the energy-momentum tensor, such as the viscosity[1].

[1]This chapter is based on part of K. Pongsangangan, T. Ludwig, H.T.C. Stoof, and L. Fritz, *Hydrodynamics of charged Dirac electrons in two dimensions. II. Role of collective modes.* (accepted at PRB) (2022).

5.1 Introduction

The main question we address in this chapter is what are the quasiparticles involved in hydrodynamical transport phenomena of ultraclean two-dimensional Dirac electrons at an accessible temperature and how do they equilibrate? The conventional theory for hydrodynamic behavior in two-dimensional Dirac systems is a version of a two-component hydrodynamics, consisting of electrons and holes [85, 66, 33]. This scenario is very popular and can formally be derived from a weak-coupling analysis using a Hartree-Fock-Born approximation. In that framework, Coulomb interaction plays two different roles: (i) It is seen by an electron as an internal potential produced by all the other particles in the system through the Hartree term; (ii) The Coulomb interaction manifests itself as an inelastic and momentum conserving scattering mechanism [33, 34, 32, 59, 12] which locally equilibrates the system. This process is an important requirement for observing the electron hydrodynamical regime with its fascinating transport properties [85, 48, 49].

Perturbation theory up to, in this case, second order in the coupling constant is unfortunately unable to describe many important physical phenomena, such as the emergence of collective modes. Collective modes, however, are the hallmark of interacting electronic systems. One such mode are plasma oscillations, also called plasmons. In conventional three-dimensional metals, plasmons are a gapped degree of freedom with a large energy gap, larger than the Fermi energy. This implies that thermal plasmons cannot be excited at realistic experimental temperatures and hence are largely irrelevant, both for thermodynamic as well as transport properties. As an example, aluminium at room temperature has a ratio of the plasmon gap to the thermal energy $\hbar\omega_p/k_BT \approx 16\text{ eV}/0.25\text{ eV} = 64$. Consequently, the plasmon occupation number is negligibly small, $n_B(\omega_p) \approx 10^{-28}$, where n_B is the equilibrium Bose-Einstein function distribution function [11]. In contrast, in two dimensions, plasmons are massless and follow a square-root dispersion, *i.e.*, $\omega \propto \sqrt{q}$ [55, 54, 53]. This is not only true for Dirac fermions but for a generic two-dimensional electronic system. Consequently, at accessible temperatures, plasmons can be excited and thus constitute proper low-energy elementary excitations. There might be various

effects that potentially destabilize the plasmon and broaden their spectral function such as disorder, electron-phonon, and electron-electron collision [89, 90]. However, it turns out that the plasmons are typically remarkably stable.

The main result in this chapter is that we offer a novel derivation of the equations of hydrodynamics from a strong-coupling perspective. This results in a combined description of electrons, holes, and plasmons, that are coupled to each other. In this description, plasmons enter on equal footing with the electronic degrees of freedom: we find that plasmons make a contribution of the same order of magnitude as the fermionic degrees of freedom to heat currents as well as the energy-momentum tensor and consequently should show up in measurements that measure thermal transport but also viscous effects.

The organization of the rest of the chapter is as follows. We start with a brief summary of the Keldysh formalism for a real bosonic field including the structure of the bosonic Green's function on the closed-time contour, the Dyson equation, the Keldysh or quantum-kinetic equation in Sec. 5.2. We proceed to perform the gradient expansion on the Keldysh equation and obtain the Boltzmann equation for a bosonic degree of freedom. Next, we study a formalized version of the random-phase approximation (RPA) in Sec. 5.3. To this end, we introduce a new quantum field associated with a plasmon excitation by means of a Hubbard-Stratonovich transformation [60, 61], which is an exact rewriting of the theory. After integrating out the fermions, the plasmons acquire their own dynamics, which is discussed in Sec. 5.5. An important side product is that we show that there is also a feedback effect, that renormalizes the fermions and provides scattering for them, despite having integrated them out. Importantly, we can show explicitly that this is not an instance of double counting, as one might suspect, but indeed required to preserve conservation laws. In Sec. 5.6 we find a set of coupled kinetic equations for electrons, holes, and the plasmons [72, 73, 91]. It is important that, within the conserving approximation, the electrons scatter from plasmons and vice versa. Using a series of approximations, we derive Boltzmann equations from this effective field theory. Based on this, we derive the conservation laws of the system

in Sec. 5.7 which indeed show that the fermion dynamics is strongly influenced by the plasmons. Furthermore, we observe, that the plasmons make an extra contribution to the heat current (this provides an alternative derivation of the heat-current operator starting from the quantum-kinetic equation) and energy density. Additionally, it makes similar contributions to the momentum flux and therefore shows up in quantities related to the viscosity. This section also confirms that RPA is indeed a conserving approximation. We conclude our results in Sec. 4.7 as well as provide an outlook for future work.

5.2 Green's function

In the subsequent section, we introduce a real bosonic field associated with the plasmon and proceed an analysis with the Keldysh quantum-field theory to obtain a quantum-kinetic equation. To this end, we start with a summary of the salient features of the Keldysh technique for a bosonic field. Similar to the fermion Green's function, the boson Green's function and its inverse have three non-vanishing components expressed in the following matrix structure

$$D_{ab}(\vec{x},\vec{x}',t,t') = \begin{pmatrix} D^K(\vec{x},\vec{x}',t,t') & D^R(\vec{x},\vec{x}',t,t') \\ D^A(\vec{x},\vec{x}',t,t') & 0 \end{pmatrix}_{ab}, \tag{5.1}$$

and

$$D^{-1}_{ab}(\vec{x},\vec{x}',t,t') = \begin{pmatrix} 0 & (D^{-1})^A(\vec{x},\vec{x}',t,t') \\ (D^{-1})^R(\vec{x},\vec{x}',t,t') & (D^{-1})^K(\vec{x},\vec{x}',t,t') \end{pmatrix}_{ab}, \tag{5.2}$$

together with the following relations

$$(D^{-1})^{R/A} = (D^{R/A})^{-1}, \tag{5.3}$$

and

$$D^R \circ (D^{-1})^K = -D^K \circ (D^{-1})^A. \tag{5.4}$$

The interacting Green's function is again determined from a Dyson equation (pictorially represented in Fig. 5.1)

$$D = D_0 + D_0 \otimes \Pi \otimes D, \tag{5.5}$$

Figure 5.1: Diagrammatic representation of the Dyson equation for the boson Green's function.

with a self-energy Π, which is, in general, approximated in a perturbative series. The self-energy assumes the same Keldysh matrix structure as the inverse Green function to preserve causality, namely

$$\Pi_{ab}(\vec{x},\vec{x}',t,t') = \begin{pmatrix} 0 & \Pi^A(\vec{x},\vec{x}',t,t') \\ \Pi^R(\vec{x},\vec{x}',t,t') & \Pi^K(\vec{x},\vec{x}',t,t') \end{pmatrix}_{ab}. \tag{5.6}$$

The poles of the retarded and advanced components are again shifted by interaction effects leading to a new energy dispersion and a lifetime for the dressed particles by means of

$$(D^{-1})^{R/A} = (D_0^{-1})^{R/A} - \Pi^{R/A}. \tag{5.7}$$

The Keldysh component of the Dyson equation leads to a kinetic equation for the boson distribution function B.

$$D_0^{-1} \circ B - B \circ D_0^{-1} = -\Pi^K + \Pi^R \circ B - B \circ \Pi^A. \tag{5.8}$$

The left-hand side again describes a streaming term, whereas the right-hand side accounts for collision events. The Hermitian function B is employed to parametrize the Keldysh Green function according to

$$D^K = D^R \circ B - B \circ D^A. \tag{5.9}$$

Before we continue, it is convenient to rewrite the Keldysh equations, Eq. (5.8). The rewriting seems arbitrary at this point, but later it will allow us to identify the left-hand sides with the streaming terms of a Boltzmann equation, whereas the right-hand sides will be the collision integrals. We can use the fact that we can decompose the self energies according to $\Pi^{R/A} = \operatorname{Re}\Pi^R \pm i \operatorname{Im}\Pi^R$. This allows to rewrite Eq. (5.8) as

$$\left[D_0^{-1} - \operatorname{Re}\Pi^R \circ, B\right] = -\Pi^K + i\{\operatorname{Im}\Pi^R \circ, B\}. \tag{5.10}$$

Here, we introduced the notation $[V \circ W] = V \circ W - W \circ V$ and $\{V \circ W\} = V \circ W + W \circ V$, defining the commutator and anticommutator of the functions V and W with $\circ$ as defined before. After a Wigner transformation and keeping the Moyal product to first non-trivial order, we obtain

$$\begin{aligned} i\Big\{ & \partial_{\vec{x}} \left(D_0^{-1} - \mathrm{Re}\,\Pi^R\right) \cdot \partial_{\vec{p}} B - \partial_{\vec{p}} \left(D_0^{-1} - \mathrm{Re}\,\Pi^R\right) \cdot \partial_{\vec{x}} B \\ & - \partial_t \left(D_0^{-1} - \mathrm{Re}\,\Pi^R\right) \partial_\omega B + \partial_\omega \left(D_0^{-1} - \mathrm{Re}\,\Pi^R\right) \partial_t B \Big\} \\ & = -\Pi^K + 2i\,\mathrm{Im}\,\Pi^R B. \end{aligned} \tag{5.11}$$

Next, we use the parametrization

$$B = 1 + 2b\,, \tag{5.12}$$

where b plays the role of the bosonic distribution function exactly in equilibrium reduces to the Bose-Einstein distribution. This leads to a Boltzmann equation for the boson reading as

$$\begin{aligned} & \partial_\epsilon \left(D_0^{-1}(\vec{x},t,\vec{p},\epsilon) - \mathrm{Re}\,\Pi^R(\vec{x},t,\vec{p},\epsilon)\right) \partial_t b(\vec{x},t,\vec{p}) \\ & + \partial_{\vec{x}} \left(D_0^{-1}(\vec{x},t,\vec{p},\epsilon) - \mathrm{Re}\,\Pi^R(\vec{x},t,\vec{p},\epsilon)\right) \cdot \partial_{\vec{p}} b(\vec{x},t,\vec{p}) \\ & - \partial_{\vec{p}} \left(D_0^{-1}(\vec{x},t,\vec{p},\epsilon) - \mathrm{Re}\,\Pi^R(\vec{x},t,\vec{p},\epsilon)\right) \cdot \partial_{\vec{x}} b(\vec{x},t,\vec{p}) \\ & = \frac{i}{2}\Pi^K(\vec{x},t,\vec{p},\epsilon) + \mathrm{Im}\,\Pi^R(\vec{x},\vec{p},t,\epsilon)(1 + 2b(\vec{x},t,\vec{p}))\,. \end{aligned} \tag{5.13}$$

5.3 The effective field theory: The random-phase approximation

In the previous chapter we focused on the weak-interaction limit of the action in Eqs. (3.66), (3.67), (3.68). We analyzed the theory by a straightforward pertubative expansion in the coupling constant. We now consider a system of fermions interacting strongly via long-range Coulomb interactions. It is well known that the interactions between electrons can generate plasma oscillations. Under certain circumstances, these plasma oscillations act as proper

quasi-particles, as we will show below. Describing these oscillations starting from Eqs. (3.66), (3.67), (3.68) requires to go beyond pure perturbation theory and to resort to a resummation scheme, such as the random-phase approximation (RPA) [5]. Formally, this can be achieved by a Hubbard-Stratonovich transformation [60] which is the formulation we choose here. The results in the following sections are the most important new results of this thesis.

We introduce a real scalar boson field $\phi_a(\vec{r},t)$ to decouple the quartic Coulomb interaction using the Hubbard-Stratonovich identity reading as

$$\exp\left(-\frac{i}{2}\int dtdt'd\vec{x}d\vec{x}'\rho^a(\vec{x},t)D_{0,ab}(\vec{x},\vec{x}',t,t')\rho^b(\vec{x}',t')\right) = \int \mathcal{D}\phi \exp\left(\frac{i}{2}\int dtdt'd\vec{x}d\vec{x}'\phi_a(\vec{x},t)D^{-1}_{0,ab}\phi_b(\vec{x}',t') - i\int dtd\vec{x}\phi_a(\vec{x},t)\rho^a(\vec{x},t)\right). \tag{5.14}$$

All the manipulations in this section are performed on the Schwinger-Keldysh closed time contour, meaning the indices a and b are the previously defined Keldysh indices. In writing down Eq. (5.14), we absorb an irrelevant normalization constant into the functional integration measure. The real scalar field is conjugate to the electron density and therefore directly captures the dynamics of the plasmons. Therefore, we henceforth refer to this boson field as plasmon field. Inserting the identity of Eq.(5.14) into the partition function of Eq. (3.31) leads to

$$Z = \int \mathcal{D}\psi^\dagger \mathcal{D}\psi \mathcal{D}\phi \exp\big(iS[\psi^\dagger,\psi,\phi]\big)\,, \tag{5.15}$$

where the action reads

$$\begin{aligned} S[\psi^\dagger,\psi,\phi] &= \int_{-\infty}^{\infty} dtdt' \Big[\int d\vec{x}d\vec{x}' \psi^\dagger_{a,\lambda}(\vec{x},t) \Big(G^{-1}_{0,ab;\lambda\lambda'} \\ &\quad -\gamma^c_{ab}\delta_{\lambda\lambda'}\phi_c(\vec{x},t)\delta(\vec{x}-\vec{x}')\delta(t-t') \Big) \psi_{b,\lambda'}(\vec{x}',t') \\ &\quad +\frac{1}{2}\int d\vec{x}d\vec{x}' \phi_a(\vec{x},t) D^{-1}_{0,ab}(\vec{x},\vec{x}',t,t')\phi_b(\vec{x}',t') \Big]. \end{aligned} \tag{5.16}$$

Philosophically, we have traded a theory of electrons interacting amongst themselves for a field theory where electrons interact with the plasmon field.

Green's functions

The bare inverse Green's function of the boson field reads

$$D^{-1}_{0,ab}(\vec{x},\vec{x}',t,t') = 4\epsilon\sigma^x_{ab}\delta(\vec{x}-\vec{x}')\delta(t-t')\sqrt{-\nabla^2}/e^2.$$

The square root of the Laplacian, $\sqrt{-\nabla^2}$, can be understood in the following way: it is the inverse Fourier transform of the absolute value of the momentum, $p \equiv |\vec{p}|$. The Fourier transform of $D^{-1}_{0,ab}(\vec{x},\vec{x}',t,t')$ consequently is given by

$$D^{-1}_{0,ab}(\vec{p},\omega) = \sigma^x_{ab}2V^{-1}(\vec{p}) = \sigma^x_{ab}2p/2\pi\alpha v_F \ . \tag{5.17}$$

There are two things worthwhile noting here. First, this zeroth-order Green's function has no dynamics. The dynamics will only be generated upon integrating out fermions or, equivalently, in perturbation theory. Second, it comes with a factor of $1/2$, *i.e.*, $D_{0,ab} \propto V(\vec{x}-\vec{x}')/2$, which is standard for a real-valued field. There also is the fermionic propagator, that we have to evaluate in the effective field theory of the plasmons. To obtain this field theory, we have to integrate out the fermions. This suggests that the fermionic propogator is given by the non-interacting one and all the renormalization effects are in the plasmon sector. This, however, is not true, and the generated dynamics feeds back into the fermion sector.

To see this, it proves advantageous to introduce source terms in the action in Eq. (5.16), according to

$$S_J[\psi^\dagger,\psi] = \int dtd\vec{x}\left(\psi_a^\dagger(\vec{x},t)J_a(\vec{x},t) + J_a^\dagger(\vec{x},t)\psi_a(\vec{x},t)\right). \quad (5.18)$$

This allows to recover the fermionic Green's function for any level of approximation of the plasmon field, even once the electrons are integrated out. This is very important in the section about the coupled quantum kinetic equations. The generating function for the fermionic Green's function reads

$$Z[J,J^\dagger] = \int \mathcal{D}\psi^\dagger\mathcal{D}\psi\mathcal{D}\phi\exp\left(iS[\psi^\dagger,\psi,\phi] + iS_J[\psi^\dagger,\psi]\right). \quad (5.19)$$

From this, we can determine the fermion Green's function by means of a functional derivative with respect to the source field, according to

$$iG(\vec{r},\vec{r}\,',t,t') = \frac{1}{Z[J,J^\dagger]}\frac{\delta}{\delta iJ(\vec{r}\,',t')}\frac{\delta}{\delta iJ^\dagger(\vec{r},t)}Z[J,J^\dagger]\Big|_{J=J^\dagger=0}. \quad (5.20)$$

We continue to integrate out the fermion fields, which gives an effective theory of the boson field associated with the density fluctuations. We find

$$Z[J,J^\dagger] = \int \mathcal{D}\phi\exp\left(iS_{\text{eff}}[\phi,J,J^\dagger]\right), \quad (5.21)$$

with the effective action given by

$$\begin{aligned} S_{\text{eff}}[\phi,J,J^\dagger] &= -i\text{Tr}\left[\ln\left(-iG^{-1}\right)\right] \\ &\quad +\frac{1}{2}\int dtdt'd\vec{x}d\vec{x}'\phi_a(\vec{x},t)D_{0,ab}^{-1}(\vec{x},\vec{x}'t,t')\phi_b(\vec{x}',t'). \\ &\quad -\int dtdt'd\vec{x}d\vec{x}'J^\dagger(\vec{x},t)G(\vec{x},\vec{x}',t,t';\phi)J(\vec{x}',t'). \end{aligned} \quad (5.22)$$

where the Green's function $G_{ab;\lambda\lambda'}(\vec{x},\vec{x}',t,t';\phi)$ is a functional of the plasmon field [82] as

$$\begin{aligned} &G_{ab;\lambda\lambda'}^{-1}(\vec{x},\vec{x}',t,t';\phi) = \\ &\quad G_{0,ab;\lambda\lambda'}^{-1}(\vec{x},\vec{x}',t,t') - \gamma_{ab}^c\phi_c(\vec{x},t)\delta_{\lambda\lambda'}\delta(\vec{x}-\vec{x}')\delta(t-t'). \end{aligned} \quad (5.23)$$

While this is formally exact, the presence of the dynamical field requires and approximation scheme to evaluate it. Using Eq. (5.20) and the generating function introduced in Eq. (5.21), we find that the fermion Green's function can be calculated according to

$$G_{ab;\lambda\lambda'}(\vec{r},\vec{r}\,',t,t') = \frac{1}{Z}\int \mathcal{D}\phi\; G_{ab;\lambda\lambda'}(\vec{r},\vec{r}\,',t,t';\phi)\exp\bigl(iS_{\rm eff}[\phi,J,J^\dagger]\bigr)\;\Big|_{J,J^\dagger=0}\,. \tag{5.24}$$

This equation consequently shows in a very explicit manner that the generated plasmon dynamics feeds back into the fermion dynamics through the field ϕ and its associated dynamics encoded in $S_{\rm eff}$. Consequently, the next step is to determine $S_{\rm eff}$.

5.4 The saddle-point equation

The effective action $S_{\rm eff}$, introduced formally in Eq. (5.22), can be obtained after integrating out the fermions. It is exact but also very complicated. The problem is that the trace cannot be evaluated in an easy manner due to the presence of the plasmon field in the Green's function of the fermions. Consequently, we require an approximation scheme. The saddle-point contribution to the partition function is given by the configuration that minimizes the action $S_{\rm eff}[\phi]$ (formally this manipulation is equivalent to Hartree or mean-field approximation). This can be obtained from the condition

$$\frac{\delta S_{\rm eff}[\phi]}{\delta\phi}\Big|_{\langle\phi\rangle} = 0 \tag{5.25}$$

This directly leads to

$$\langle\phi_c(\vec{x},t)\rangle = -i\int dt'd\vec{x}'D_{0,cd}(\vec{x},\vec{x}';t,t')G_{ab;\lambda\lambda}(\vec{x}';\vec{x}',t',t';\langle\phi\rangle)\gamma^d_{ba}. \tag{5.26}$$

It is a self-consistency equation for the local charge density. Philosophically, Eq. (5.26) corresponds to a self-consistent version of

the Hartree diagram previously discussed in Sec. 4.3. The fermion propagator on this level of approximation reads

$$\begin{aligned} G^{-1}_{ab;\lambda\lambda'}(\vec{x},\vec{x}',t,t';\langle\phi\rangle) &= G^{-1}_{0,ab;\lambda\lambda'}(\vec{x},\vec{x}',t,t') \\ &\quad -\gamma^c_{ab}\langle\phi_c(\vec{x},t)\rangle\delta_{\lambda\lambda'}\delta(\vec{x}-\vec{x}')\delta(t-t') \,. \end{aligned} \tag{5.27}$$

The expectation value of the plasmon can now be identified with the self-energy within the Hartree approximation, already given in Eq. (4.5). It thus recovers the dispersion of Eq. (4.26). We proceed to expand the plasmon field in deviations from the mean-field value, *i.e.*, $\phi_a(\vec{x},t) = \langle\phi_a(\vec{x},t)\rangle + \phi'_a(\vec{x},t)$ where $\langle\phi_a(\vec{x},t)\rangle$ is the saddle-point configuration and ϕ'_a is associated with fluctuations around the saddle point. As a result, we have

$$\begin{aligned} G^{-1}_{ab;\lambda\lambda'}(\vec{x},\vec{x}\,',t,t';\phi) &= G^{-1}_{ab;\lambda\lambda'}(\vec{x},\vec{x}',t,t';\langle\phi\rangle) \\ &\quad -\gamma^\alpha_{ab}\phi'_\alpha(\vec{x},t)\delta_{\lambda\lambda'}\delta(\vec{x}-\vec{x}')\delta(t-t') \,. \end{aligned} \tag{5.28}$$

We proceed to expand the effective action, Eq. (5.22), to second order in the fluctuations ϕ'. Substituting Eq. (5.28) into Eq.(5.22) and using the series expansion of logarithm, we suppress the Keldysh indices here, we find to second order in fluctuations that

$$\begin{aligned} S_{\rm eff}[\phi,0,0] &= -i\mathrm{Tr}\left[\ln -iG^{-1}(\langle\phi\rangle+\phi')\right] \\ &\quad +\frac{1}{2}\int dtdt'd\vec{x}d\vec{x}'\Big(\langle\phi_a(\vec{x},t)\rangle+\phi'_a(\vec{x},t)\Big) \\ &\quad D^{-1}_{0,ab}(\vec{x},\vec{x}'t,t')\left(\langle\phi_b(\vec{x}',t')\rangle+\phi'_b(\vec{x}',t')\right) \\ &\approx -i\mathrm{Tr}[\ln\big(-iG^{-1}(\langle\phi\rangle)\big)] + i\mathrm{Tr}[G(\langle\phi\rangle)\phi'] \\ &\quad +\int dtdt'd\vec{x}d\vec{x}'\langle\phi_a(\vec{x},t)\rangle D^{-1}_{0,ab}(\vec{x},\vec{x}';t,t')\phi'_b(\vec{x}',t') \\ &\quad +\frac{i}{2}\mathrm{Tr}[G(\langle\phi\rangle)\phi' G(\langle\phi\rangle)\phi']. \end{aligned} \tag{5.29}$$

Here, we use for brevity the shorthand notation

$$G^{-1}(\langle\phi\rangle) \equiv G^{-1}_{ab;\lambda\lambda'}(\vec{x},\vec{x}',t,t';\langle\phi\rangle).$$

The first term gives an irrelevant constant which will be absorbed in the functional integration measure. The linear terms in the fluctuations sum to zero at the saddle point. Their cancelation is equivalent to the saddle-point condition in Eq. (5.26). The remaining term, consequently, is the last term in Eq. (5.29). It is the term that accounts for quadratic fluctuations around the saddle point. At the same time, however, it determines the effective plasmon propagator with the the RPA approximation according to

$$S_{\rm eff}[\phi'] = \frac{1}{2} \sum_{\alpha,\beta=1,2} \int dt dt_1 d\vec{x} d\vec{x}' \phi'_\alpha(\vec{x},t) D^{-1}_{\alpha\beta}(\vec{x},\vec{x}';t,t') \phi'_\beta(\vec{x}',t') \ , \tag{5.30}$$

where the inverse plasmon Green's function satisfies

$$D^{-1}_{\alpha\beta}(\vec{x},\vec{x}',t,t') = D^{-1}_{0;\alpha\beta}(\vec{x},\vec{x}';t,t') - \Pi(\vec{x},\vec{x}',t,t'). \tag{5.31}$$

The self-energy Π has the diagrammatic representation shown in Fig. 5.3b. It is commonly referred to as the polarization diagram. The corresponding algebraic expression reads as

$$\Pi_{\alpha\beta} = -iN{\rm Tr}[\gamma^\alpha G(\vec{x},\vec{x}',t,t',\langle\phi\rangle)\gamma^\beta G_\phi(\vec{x}',\vec{x},t',t,\langle\phi\rangle)]. \tag{5.32}$$

The retarded component of Eq. (5.31) gives dynamics to the plasmon: it allows to determine the dispersion and decay rate of the plasmon in the next section. Its Keldysh components has the form of Eq. (5.8) which will be the starting point for the derivation of the Boltzmann equation for the plasmons. Now that we have the above effective action of the plasmon and its dynamics, it is time to return to the fermion Green's function $G_{ab;\lambda\lambda'}(\vec{x},\vec{x}',t,t')$ in Eq. (5.24). We can graphically represent the fermion Green's function expansion in terms of ϕ' according to Fig. 5.2. We now have to 'average' this fermion propagator over the Gaussian action of the bosons and resum it. It turns out that we have to choose the series corresponding to the Fock diagram, Fig. 5.3a, to obtain a conserving approximation [92]. The resulting Green's function is the solution of the Dyson equation

$$G^{-1}_{ab;\lambda\lambda'}(\vec{x},\vec{x}',t,t') = G^{-1}_{ab;\lambda\lambda'}(\vec{x},\vec{x}';t,t';\langle\phi\rangle) - \Sigma_{ab;\lambda\lambda'}(\vec{x},\vec{x}',t,t') \ ,$$

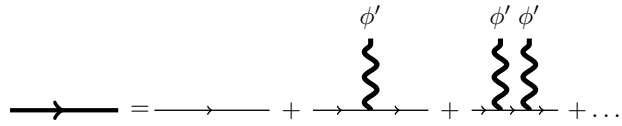

Figure 5.2: Diagram representing the solution of the Dyson equation (5.28) in terms of a series expansion of the quantum fluctuation ϕ'.

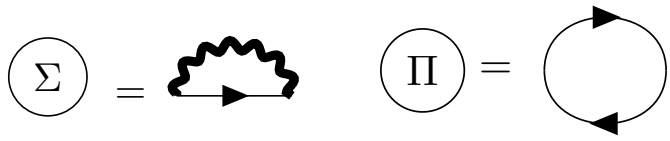

(a) electron self-energy

(b) Boson self-energy

Figure 5.3: Self-energy for electron and plasmon fields within the RPA approximation. The set of the GW-diagram and polarization function constitutes a conserving approximation.

where

$$\Sigma_{ab;\lambda\lambda'}(\vec{x},\vec{x}',t,t') = i\left(\gamma^{\alpha}G(\vec{x},\vec{x}',t,t';\langle\phi\rangle)\gamma^{\beta}\right)_{ab;\lambda\lambda'} D_{\alpha\beta}(\vec{x},\vec{x}',t,t') \,. \tag{5.33}$$

The Dyson equations in Eqs. (5.31)) and (5.33), together with the self-energies in Eqs. (5.32)) and (5.33), are the minimal set of equations that describes the interplay between the collective modes and the single-particle components of the interacting Dirac electron. This approximation can be derived from a single free energy diagram. It was shown in Ref. [92] that this implies that it constitutes a conserving approximation. As such, it respects the conservation laws of total energy and momentum in the combined system of electrons and plasmons, as we show explicitly in Sec. 5.7.

5.5 The plasmons

In this section we discuss the plasmon dynamics nonzero finite temperature and nonzero chemical potential. To this end, we analyze the polarization function numerically. We then proceed to find an approximate analytical description that we use to determine the plasmon spectrum and the quasi-particle lifetimes.

Nonzero temperature polarization function

Here, we consider the retarded component of the polarization function, Eq. (5.32), at nonzero temperature. After a Wigner transformation, we obtain

$$\Pi^R(\vec{p},\omega) = -iN\int \frac{d\vec{q}}{(2\pi)^2}\frac{d\nu}{2\pi}\Big[G^R_{\phi;\lambda\lambda'}(\vec{p}+\vec{q},\omega+\nu)G^K_{\phi;\lambda'\lambda}(\vec{q},\nu) + G^K_{\phi;\lambda\lambda'}(\vec{p}+\vec{q},\omega+\nu)G^A_{\phi;\lambda'\lambda}(\vec{q},\nu)\Big]. \tag{5.34}$$

Here, for brevity, we suppress the space and time variables of the functions involved. Next, we use the transformation matrix in Eq.-(4.3) to transform the objects within the polarization function into the quasi-particle basis. After that, we integrate over the frequency variable ν by making use of the Dirac delta function coming from g_0^K. Finally, by a straightforward algebraic manipulation, we find the polarization function expressed in the form of the Lindhard formula

$$\Pi^R(\vec{p},\omega) = 2N\sum_{\lambda\lambda'=\pm1}\int \frac{d\vec{q}}{(2\pi)^2}\frac{\mathcal{F}_{\lambda\lambda'}(\vec{p},\vec{q})\,(f_\lambda(\vec{q})-f_{\lambda'}(\vec{p}+\vec{q}))}{\omega+i0^+ +\lambda v_F^R q-\lambda' v_F^R|\vec{p}+\vec{q}|}\ .$$

The coherence factor is defined according to

$$\mathcal{F}_{\lambda\lambda'}(\vec{p},\vec{q}) = \frac{1}{2}(1+\lambda\lambda'\cos(\theta_{\vec{p}+\vec{q}}-\theta_{\vec{q}}))\ . \tag{5.35}$$

Let us note that, strictly speaking, compared to the conventional Lindard formula, there is an extra factor 2 in our result. This is consistent within our convention that the inverse bare boson Green's function comes with the same factor, *i.e.*, $D_0 \propto 2V(\vec{r}-\vec{r}\,')$.

The polarization function at zero temperature and arbitrary chemical potential ($\Pi_{\mu,0}$) can be calculated exactly. Here, we focus on nonzero temperatures. There is no analytical expression for the nonzero temperature polarization. However, there exists a relation between zero temperature and nonzero temperature polarization functions [55].

$$\Pi^R_{\mu,T}(\vec{p},\omega) = \int_0^\infty d\mu' \sum_{\lambda=\pm1} \frac{\Pi^R_{\mu',0}(\vec{p},\omega)}{4T\cosh^2\left(\frac{\mu'+\lambda\mu}{2T}\right)}. \tag{5.36}$$

Using this, we numerically solve the polarization function at arbitrary temperatures and subsequently replace it in the Dyson equation in Eq.(5.31). This allows us to determine the energy dispersion (ω_p) and the decay rate (γ_p) of the plasmon mode. The plasmon frequency ($\omega = \omega_p - i\gamma_p$) is obtained by equating the inverse Green's function to zero.

$$(D^{-1})^R(\vec{p},\omega) = (D_0^{-1})^R(\vec{p},\omega) - \Pi(\vec{p},\omega) = 0. \tag{5.37}$$

Defined this way, the decay rate γ_p is positive. If the damping is sufficiently weak ($\gamma_p \ll \omega_p$), one can expand the polarization function to leading order in γ_p

$$\Pi(\vec{p},\omega_p - i\gamma_p) \approx \operatorname{Re}\Pi(\vec{p},\omega_p) - i\gamma_p\partial_\omega \operatorname{Re}\Pi(\vec{p},\omega)\Big|_{\omega=\omega_p} + i\operatorname{Im}\Pi(\vec{p},\omega_p). \tag{5.38}$$

The energy of the plasmon can be determined from the real part of Eq. (5.37)

$$(D_0^{-1})^R(\vec{p},\omega_p) - \operatorname{Re}\Pi(\vec{p},\omega_p) = 0\ , \tag{5.39}$$

whereas the decay rate is a solution of imaginary part

$$\gamma_p = \frac{\operatorname{Im}\Pi(\vec{p},\omega)}{\partial_\omega \operatorname{Re}\Pi(\vec{p},\omega)}\bigg|_{\omega=\omega_p}. \tag{5.40}$$

In general, the non-interacting Green's function, D_0^{-1} can be a function of both momentum $\vec{p}$ and frequency ω. However, in our case, D_0^{-1} describes the bare Coulomb potential which is non-dynamical and hence does not depend on the frequency variable. Fig. 5.4 shows

the real part of the polarization function at nonzero chemical potential in the momentum-frequency plane. Solutions to Eq. (5.39) exist only when $\mathrm{Re}\,\Pi > 0$. This is the case in the upper triangle of the plot in Fig. 5.4 (a). As discussed before, a stable plasmon requires $\mathrm{Im}\,\Pi \approx 0$. In Fig. 5.4(b) we plot the imaginary part of the polarization function at the same value of parameters as in Fig. 5.4 (a). Although it is not zero, it is still negligibly small in the low-momentum limit. As a result, one may expect a long-wavelength underdamped plasmon mode with for all pratical purposes almost infinitely long lifetime. This implies that plasmons behave like quasi-particles for practical matters.

In the next section, we find an approximate description of the dispersion of the plasmon and its decay rate in the low-momentum limit. We furthermore determine the value of the momentum cutoff beyond which the plasmon are overdamped.

Analytical approximation

In this section, we will evaluate the energy spectrum and decay rate of the plasmon in the long-wavelength limit. To this end, we first decompose the polarization function into a sum of two terms accordingly to $\Pi^R(\vec{p},\omega) = \Pi^R_+(\vec{p},\omega) + \Pi^R_-(\vec{p},\omega)$. The first term, $\Pi_+(\vec{p},\omega)$, describes the contribution from intraband particle-hole pairs ($\lambda' = \lambda$), whereas $\Pi_-(\vec{p},\omega)$ comes from the interband transitions ($\lambda' = -\lambda$). The imaginary part of the polarization function accordingly reads

$$\mathrm{Im}\,\Pi^R(\vec{p},\omega) = \mathrm{Im}\,\Pi^R_+(\vec{r},t) + \mathrm{Im}\,\Pi_-(\vec{p},\omega) \tag{5.41}$$

and it amounts to a decay rate of the plasmon mode with

$$\begin{aligned}\mathrm{Im}\,\Pi^R_\pm(\vec{p},\omega) \quad &= \quad -2N\pi \sum_{\lambda=\pm1} \int \frac{d\vec{q}}{(2\pi)^2} \mathcal{F}_{\lambda\,\pm\lambda}(\vec{p}+\vec{q},\vec{q}) \\ &\qquad \Big[f_\lambda(\vec{q}) - f_{\pm\lambda}(\vec{p}+\vec{q})\Big]\delta(\omega + \epsilon_\lambda(\vec{q}) - \epsilon_{\pm\lambda}(\vec{p}+\vec{q})).\end{aligned} \tag{5.42}$$

The conservation of energy enters through the delta-function with the argument $\omega + \lambda v_F^R q - \lambda' v_F^R |\vec{p}+\vec{q}|$. This function forms either an

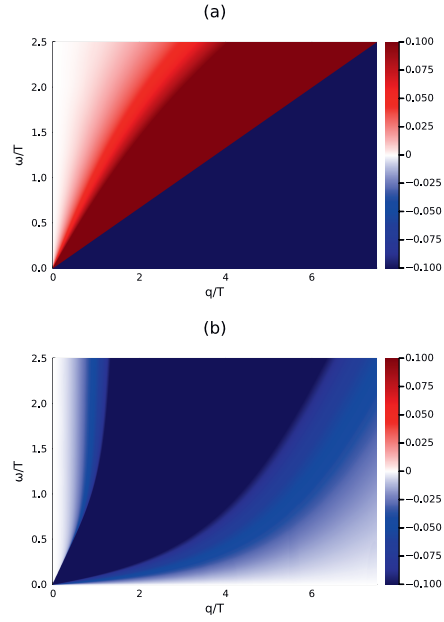

Figure 5.4: Polarization function, (a) real part and (b) imaginary part, at a nonzero temperature and chemical potential. We show the polarization function when the chemical potential $\mu/T = 1$.

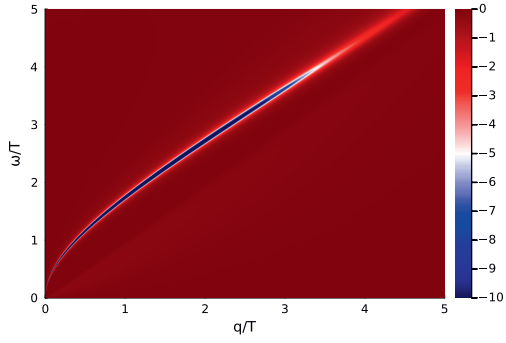

Figure 5.5: Spectral function of the plasmon at a non-zero temperature and chemical potential $\mu/T = 4$. The value of fine structure constant is chosen to mimic graphene device sandwiched in hBN ($\alpha = 0.3$).

.

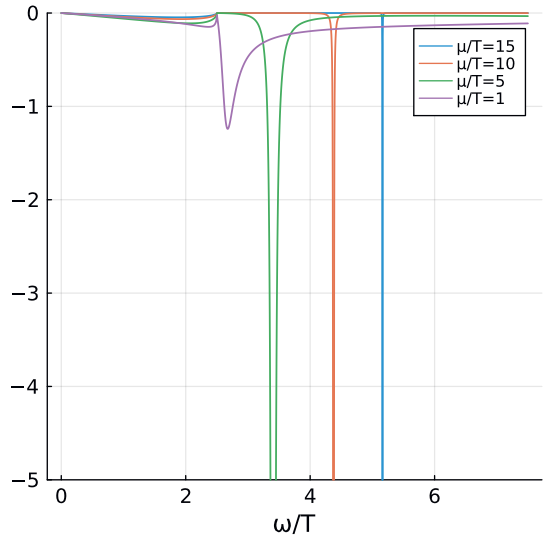

Figure 5.6: Spectral function of plasmon at various electron chemical potential at a small value of momentum $q/T = 2.5$. Here the fine structure constant $\alpha = 0.3$.

ellipse or a hyperbola in the $q_x q_y$-plane. It may be easy to see this by means of a transformation of the momentum variables into the elliptic coordinate system, (θ, μ), where $\theta \in [0, 2\pi)$ and $\mu \in [0, \infty)$. When $\lambda = -$ and $\lambda' = +$, this equation forms an ellipse with the value of μ determined by $\cosh\mu = \omega/p$. The size of the ellipse depends on the value of $\cosh\mu \leq 1$. We find that when ω is slightly bigger than p, the available phase is restricted since the size of the ellipse is small whereas when ω is much bigger than p, the available phase space in turn grow bigger and allows the decay process more likely to occur. However, when $\lambda' = \lambda$, this equation becomes an equation of a hyperbola centered at $(-p_x/2, -p_y/2)$. The width of the hyperbola is determined from the ratio of the frequency to the momentum given by $\cos\theta = \lambda\omega/p$. Therefore, the available phase space for the plasmon with the energy ω to decay into two fermions with the energies λp and $\lambda|\vec{p}+\vec{q}|$ is extended. This process is thus the

main mechanism for plasmon decay. We expand all the quantities appearing in the polarization function up to first order in $\vec{p}$. This gives

$$\begin{aligned}
\mathcal{F}_{\pm\pm}(\vec{p},\vec{q}) &= \frac{1}{2}\left(1+\cos\left(\theta_{\vec{p}+\vec{q}}-\theta_{\vec{q}}\right)\right)\approx 1,\\
\mathcal{F}_{\pm\mp}(\vec{p},\vec{q}) &= \frac{1}{2}\left(1-\cos\left(\theta_{\vec{p}+\vec{q}}-\theta_{\vec{q}}\right)\right)\approx \frac{1}{4}\left(\vec{p}\cdot\vec{\nabla}_{\vec{q}}\theta_{\mathbf{q}}\right)^2,\\
f_\lambda(\vec{p}+\vec{q}) &\approx f_\lambda(\vec{q})+\vec{p}\cdot\vec{\nabla}_{\vec{q}}f_\lambda(\vec{q}),\\
\epsilon_\lambda(\vec{p}+\vec{q}) &\approx \epsilon_\lambda(\vec{q})+\vec{p}\cdot\vec{\nabla}_{\vec{q}}\epsilon_\lambda(\vec{q}).
\end{aligned} \tag{5.43}$$

By substituting Eq.(5.43) into the imaginary part of the polarization followed by a straightforward calculation, we find

$$\mathrm{Im}\,\Pi^R(\vec{p},\omega)\approx -\frac{2N}{16}\frac{p^2}{\omega}\Big(f_+(|\omega/2|)-f_-(|\omega/2|)\Big), \tag{5.44}$$

which provides the main contribution to the decay rate whereas $\mathrm{Im}\,\Pi^R_+(\vec{p},\omega)$ gives an unimportant correction. In thermal equilibrium, the distribution function becomes the Fermi-Dirac distribution function at a temperature T and chemical potential μ , *i.e.*, $f_\lambda(\omega)=\frac{1}{\exp((\omega-\mu)/T)+1)}$.

At zero temperature, this becomes

$$\mathrm{Im}\,\Pi^R_-(\vec{p},\omega)\approx -\frac{2N}{16}\frac{p^2}{\omega}\Theta(|\omega|-2|\mu|). \tag{5.45}$$

It vanishes when $|\omega|<2|\mu|$, meaning in that region a long-lived plasmon mode exists. The real part of the polarization function is given by

$$\mathrm{Re}\,\Pi^R_\pm(\vec{p},\omega)=2N\sum_{\lambda=\pm1}\int\frac{d\vec{q}}{(2\pi)^2}\mathcal{F}_{\lambda\,\pm\lambda}(\vec{p},\vec{q})\frac{f_\lambda(\vec{q})-f_{\pm\lambda}(\vec{p}+\vec{q})}{\omega+\lambda v_F^R q\mp\lambda v_F^R|\vec{p}+\vec{q}|}. \tag{5.46}$$

We substitute these expressions into Eq. (5.43) followed by expanding its denominator to first order in p/ω. Based on numerics, we expect to find a stable plasmon mode in this limit. We can approximate the expression as

$$\mathrm{Re}\,\Pi^R_+(\vec{p},\omega)\approx 2N\sum_{\lambda=\pm1}\int\frac{d\vec{q}}{(2\pi)^2}\frac{-\vec{p}\cdot\vec{\nabla}_{\vec{q}}f_\lambda(\vec{q})}{\omega}\Big[1+\frac{\vec{p}\cdot\vec{\nabla}_{\vec{q}}\epsilon_\lambda(\vec{q})}{\omega}\Big],$$

which results in

$$\mathrm{Re}\,\Pi_{+}^{R}(\vec{p},\omega) \approx \frac{2Np^2}{4\pi\omega^2}\mathcal{N}, \tag{5.47}$$

where $\mathcal{N} = T\log\left(2+2\cosh\mu/T\right)$. When the Dirac system is exposed to external perturbations, the polarization function varies in position and time via the distribution function. In that case $\mathcal{N} = \int dq\Big[f_{+}(\vec{q}) - \left(f_{-}(\vec{q})-1\right)\Big]$. In contrast, the interband term gives a logarithmic correction which will be neglected from evaluating the plasmon energy.

$$\mathrm{Re}\,\Pi_{R}^{-}(\vec{p},\omega) \approx \frac{Np^2}{2\pi}\int dq\Big[f_{+}(\vec{q}) - f_{-}(\vec{q})\Big]\Big[\frac{1}{4\left(v_F^R\right)^2 q^2 - \omega^2}\Big]. \tag{5.48}$$

At nonzero doping and zero temperature, we find that $\mathrm{Re}\,\Pi_{-}^{R}(\vec{p},\omega) = \frac{Np^2}{16\pi\omega}\log\left(\left|\frac{\omega-2\mu}{\omega+2\mu}\right|\right)$. If we substitute Eqs. (5.47) and (5.17) into Eq. (5.39), we obtain the disperion relation of the plasmon at nonzero T,

$$\omega_p(\vec{p}) = \sqrt{\frac{N}{2}\alpha T p\log\left(2+2\cosh\mu/T\right)}\,, \tag{5.49}$$

with the decay rate

$$\gamma_p = \frac{\pi\omega_p(\vec{p})^2}{16\log(2+2\cosh\mu/T)}\Big(f_{+}(\omega_p(\vec{p})/2) - f_{-}(\omega_p(\vec{p})/2)\Big). \tag{5.50}$$

It is worthwhile pointing out that Eq. (5.49) agrees with the plasmon dispersion from the beyond hydrodynamic treatment in Eq. (4.76). In Fig. 5.7a and Fig. 5.7b, we show the dispersion relation and the decay rate of the plasmon for a relatively small fine structure constant ($\alpha = 0.3$) solved numerically from the Dyson equation in Eq. (5.37). The dispersion follows a square-root relation in the small momentum limit, as in the approximate solution. In that limit, the plasmon becomes one of the relevant quasi-particles for the interacting Dirac electron since its decay rate is parametrically small. Fig. 5.7b shows that the decay rate as obtained from Eq. (5.40) is much smaller than plasmon energy, see Fig. 5.7a. Additionally, we plot the spectral functions of the plasmons at two values of the chemical potentials in the $q\omega$-plane in Fig. 5.5. It shows that the spectral function is

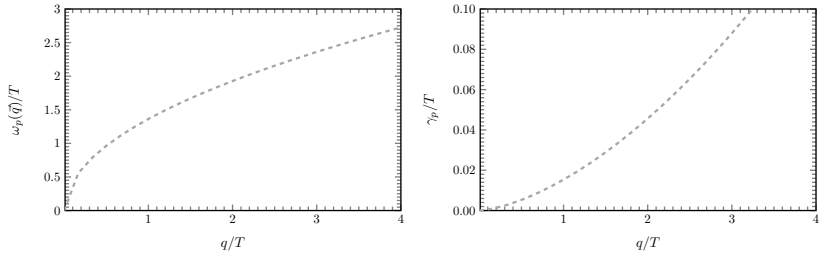

(a) Energy dispersion (b) decay rate

Figure 5.7: Numerical solution of the Dyson equation (5.37) at $\mu/T = 3$ Here we choose a relatively small value of the fine structure constant $\alpha = 0.3$.

pronounced in the small momentum region. Therefore, it is possible to treat the plasmon as a proper quasi-particles emerging from the interacting Dirac electron gas. This also allows to define a cutoff. It follows from the condition that at the momentum cutoff p_c, we have $\frac{p_c}{\omega_p(\vec{p})} = 1$ which invalidates the quasi-particle picture. As a result, we find $p_c = \frac{N}{2}\alpha T \log(2 + 2\cosh \mu/T)$. It is interesting to note that the combination of the linear dispersion relation for electrons and the plasmon dispersion kinematically allows a plasmon to decay into two electrons and hence contribute to its lifetime. Moreover, we observe that plasmon decay rate decreases significantly and therefore our quasi-particle assumption is more accurate as the electron density increases. This can be clearly seen in Fig.(5.6). We show the spectral function of plasmon at various electron chemical potential (μ/T). We find that the spectral function at a high doping away from the Dirac point manifests a narrow spike shape resemble the Dirac delta-function.

5.6 Kinetic equation of the plasmons

The starting point of our discussion is the gradient expanded version of the plasmon Keldysh equation, Eq. (5.13). We have estimated the real part of the polarization in the long-wavelength limit given by

Eq. (5.47). Using it here leads to

$$D_0^{-1} - \mathrm{Re}\,\Pi^R = \frac{p}{\pi\alpha} - \frac{2Np^2}{4\pi\omega^2}\mathcal{N} = \frac{p}{\pi\alpha\omega^2}\left(\omega^2 - \omega_p^2(\vec{p})\right). \qquad (5.51)$$

As a result, the derivatives appearing on the left-hand side of the above Keldysh equation are obtained.

$$\begin{aligned}
\partial_\omega\left(D_0^{-1} - \mathrm{Re}\,\Pi^R\right) &= \frac{Np^2}{\pi\omega^3}\mathcal{N}, \\
\partial_{\vec{p}}\left(D_0^{-1} - \mathrm{Re}\,\Pi^R\right) &= \frac{\hat{p}}{\pi\alpha} - \frac{Np\hat{p}}{\pi\omega^2}\mathcal{N}, \\
\partial_{\vec{x}}\left(D_0^{-1} - \mathrm{Re}\,\Pi^R\right) &= -\frac{Np^2}{2\pi\omega^2}\partial_{\vec{x}}\mathcal{N}. \qquad (5.52)
\end{aligned}$$

We substitute these expressions into Eq.(5.13). Next, we divide the resulting equation by the spectral weight that is $\partial_\omega(D_0^{-1} - \mathrm{Re}\,\Pi^R)$ and evaluate the resulting equation on-shell at the frequency $\omega = \omega_p(\vec{p})$. We assume that the excitations are long-lived and therefore the spectral function is sharply peaked at the energy dispersion $\omega_p(\vec{p})$. Finally, we obtain the Boltzmann equation for the plasmons according to

$$\begin{aligned}
&\partial_t b(\vec{x},\vec{p},t) + \frac{\omega_p(\vec{p})}{2p}\hat{p}\cdot\partial_{\vec{x}} b(\vec{x},\vec{p},t) - \frac{\omega_p(\vec{p})}{2\mathcal{N}}\partial_{\vec{x}}\mathcal{N}\cdot\partial_{\vec{p}} b(\vec{x},\vec{p},t) \\
&\quad = -\frac{2\alpha\pi^2 N\omega_p(\vec{p})}{p}\int\frac{d\vec{q}}{(2\pi)^2}\mathcal{F}_{\lambda\lambda'}(\vec{p}+\vec{q},\vec{q}) \\
&\qquad\qquad \delta(\omega_p(\vec{p}) + \epsilon_\lambda(\vec{q}) - \epsilon_{\lambda'}(\vec{p}+\vec{q})) \\
&\quad \Big[f_\lambda(\vec{q})\Big(1 - f_{\lambda'}(\vec{p}+\vec{q})\Big)b(\vec{p}) - \Big(1 - f_\lambda(\vec{q})\Big)f_{\lambda'}(\vec{p}+\vec{q})\Big(1 + b(\vec{p})\Big)\Big]. \qquad (5.53)
\end{aligned}$$

The left-hand side of the equation describes the changes of the distribution function by the streaming of the plasmon distribution with the group velocity $\vec{v}_p = \omega_p(\vec{p})\hat{p}/2p$. This is consistently identical to calculating the group velocity from taking a derivative of the plasmon energy with respect to its momentum, *i.e.*, $\vec{v}_p = \partial_{\vec{p}}\omega_p(\vec{p})$. The fluctuations of the underlying electron density have an effect on the plasmon dispersion and enter as a force given by $\vec{F} = -\frac{\omega_{\vec{p}}\partial_{\vec{x}}\mathcal{N}}{2\mathcal{N}}$.

Next, let us examine how the plasmon and the electrons coexist in the system. To this end, we consider the Keldysh equation of the fermions given by Eq.(5.33). We proceed in exactly the same steps as in the previous section to arrive at the kinetic equation for fermion in Eq.(3.91). We find that

$$\begin{aligned}
&\partial_t f_\lambda(\vec{x},t,\vec{p}) + \left(\lambda v_F \hat{p} + \lambda \partial_{\vec{p}} \operatorname{Re}\sigma^R(\vec{x},t,\vec{p})\right)\cdot \partial_{\vec{x}} f_\lambda(\vec{x},t,\vec{p}) \\
&- \partial_{\vec{x}}\left(V^H(\vec{x}) + \lambda \operatorname{Re}\sigma^R(\vec{x},t,\vec{p})\right)\cdot \partial_{\vec{p}} f_\lambda(\vec{x},t,\vec{p}) \\
&= -2\alpha\pi^2 \int \frac{d\vec{q}}{(2\pi)^2}\frac{\omega_p(\vec{q})}{q}\mathcal{F}_{\lambda\lambda'}(\vec{p}+\vec{q},\vec{q})\delta(\omega_p(\vec{q})+\epsilon_\lambda(\vec{p})-\epsilon_{\lambda'}(\vec{p}+\vec{q})) \\
&\Big[f_\lambda(\vec{p})\Big(1-f_{\lambda'}(\vec{p}+\vec{q})\Big)b(\vec{q}) - \Big(1-f_\lambda(\vec{p})\Big)f_{\lambda'}(\vec{p}+\vec{q})\Big(1+b(\vec{q})\Big)\Big] \\
&-2\alpha\pi^2 \int \frac{d\vec{q}}{(2\pi)^2}\frac{\omega_p(\vec{q})}{q}\mathcal{F}_{\lambda\lambda'}(\vec{p}-\vec{q},\vec{q})\delta(-\omega_p(\vec{q})+\epsilon_\lambda(\vec{p})-\epsilon_{\lambda'}(\vec{p}-\vec{q})) \\
&\Big[f_\lambda(\vec{p})\Big(1-f_{\lambda'}(\vec{p}-\vec{q})\Big)\Big(1+b(\vec{q})\Big) - \Big(1-f_\lambda(\vec{p})\Big)f_{\lambda'}(\vec{p}-\vec{q})b(\vec{q})\Big].
\end{aligned} \tag{5.54}$$

In this expression, $V^H(\vec{x})$ is the Hartree potential as defined in Eq.(4.25) and

$$\operatorname{Re}\sigma^R \approx \frac{\pi\alpha}{2p}\int \frac{d\vec{q}}{(2\pi)^2}\frac{q}{\omega_p(\vec{q})}\left(1+2b(\vec{q})\right)\sin^2\theta \tag{5.55}$$

is the correction to the fermion energy resulting from electron-plasmon interactions in the GW approximation. We define the angle θ between $\vec{p}$ and $\vec{q}$. We evaluate this self-energy using the long-wavelength approximation of the plasmon dispersion, Eq. (5.49).

The collision term comes from the Fock-like diagram shown in Fig. 5.3a. It is a sum of two terms. The first term describes a scattering process of an electron from the momentum state $\vec{p}$ into another momentum state $\vec{p}+\vec{q}$ by absorbing a plasmon of momentum $\vec{q}$. The second term describes an emission of a plasmon of momentum $\vec{q}$ from an electron of momentum $\vec{p}$ and as a result the electron scatters into the momentum state $\vec{p}-\vec{q}$. We need to write two terms of the collision integral separately because from the perspective of the electron in $\vec{k}$, the two events, the emission and absorption of a plasmon are essentially different. The coupled system of Boltzmann

equations in Eq.(5.53) and Eq.(5.54) constitutes one of the central results of this chapter.

5.7 Conservation laws

In this section we check whether the level of approximation indeed respects all the conservation laws. Compared to the weak-coupling consideration based on Eq. (4.29) we now have two coupled Boltzmann equations, Eq. (5.53) and Eq. (5.54). Let us denote the collision integrals, *i.e.*, the right-hand side of the Boltzmann equations of Eq. (5.53) and Eq. (5.54) by $C^b[f,b](\vec{p})$ and $C^f_\lambda[f,b](\vec{p})$, respectively. The collision integrals again have three collisional invariants that correspond to the conservation of electric charge, momentum, and energy. In that order, they read

$$\sum_{\lambda=\pm}\int \frac{d\vec{p}}{(2\pi)^2}\, C^f_\lambda[f,b](\vec{p}) = 0\,, \tag{5.56}$$

$$\sum_{\lambda=\pm}\int \frac{d\vec{p}}{(2\pi)^2}\, \vec{p}\, C^f_\lambda[f,b](\vec{p}) + \int \frac{d\vec{p}}{(2\pi)^2}\, \vec{p}\, C^b[f,b](\vec{p}) = 0\,, \tag{5.57}$$

and

$$\sum_{\lambda=\pm}\int \frac{d\vec{p}}{(2\pi)^2}\, \epsilon_\lambda(\vec{p}) C^f_\lambda[f,b](\vec{p}) + \int \frac{d\vec{p}}{(2\pi)^2}\, \omega_p(\vec{p}) C^b_\lambda[f,b](\vec{p}) = 0\,, \tag{5.58}$$

and these statements can be checked in a straightforward manner. By integrating Eq. (5.54) over all momenta $\vec{p}$ and then summing over the energy bands $\pm$ we obtain the continuity equation of charge

$$\partial_t n(\vec{x},t) + \partial_{\vec{x}}\cdot\vec{j}(\vec{x},t) = 0, \tag{5.59}$$

where the total charge density is given by

$$n(\vec{x},t) = N\int \frac{d\vec{p}}{(2\pi)^2}\, \left[f_+(\vec{x},t,\vec{p}) + (f_-(\vec{x},t,\vec{p})-1)\right]. \tag{5.60}$$

whereas the total charge current density reads

$$\vec{j}(\vec{x},t) = N\int \frac{d\vec{p}}{(2\pi)^2}\, (v_F\hat{p}+\partial_{\vec{p}}\,\mathrm{Re}\,\sigma^R_+)\,(f_+(\vec{x},t,\vec{p}) - (f_-(\vec{x},t,\vec{p})-1))\,. \tag{5.61}$$

In writing the above expression, we again subtract the infinite contribution from the Dirac sea and define the distribution function of holes as $f_-(\vec{x},t)-1$. This is allowed since subtracting this infinite constant does not affect the conservation law.

In addition, we multiply Eq.(5.53) and Eq.(5.54) by momentum $\vec{p}$ and then integrate the resulting equations over all momentum $\vec{p}$. We add them together and find the law of momentum conservation:

$$\begin{aligned}
&\partial_t \vec{n}^{\vec{p}}(\vec{x},t) + \partial_{\vec{x}} \cdot \vec{\vec{\Pi}}(\vec{x},t) = \\
&-\partial_{\vec{x}} V^H(\vec{x}) n(\vec{x},t) - \int \frac{d\vec{p}}{(2\pi)^2} \frac{\omega_p(\vec{p})}{2} \frac{\partial_{\vec{x}} \mathcal{N}}{\mathcal{N}} b(\vec{x},t,\vec{p}) \\
&-N \int \frac{d\vec{p}}{(2\pi)^2} \partial_{\vec{x}} \operatorname{Re}\sigma^R(\vec{x},t,\vec{p}) \left(f_+(\vec{x},t,\vec{p}) + (1-f_-(\vec{x},t,\vec{p}))\right).
\end{aligned} \tag{5.62}$$

The right-hand side of the equation has three terms. The first term is an internal force due to the Hartree potential from the other electrons. The second term describes a force on a plasmon due to electron inhomogeneity. It is proportional a gradient of the electron distribution function via $\partial_{\vec{x}}\mathcal{N}$ where $\mathcal{N} = \int dq \Big[f_+(\vec{x},t,\vec{q}) + (1 - f_-(\vec{x},t,\vec{q})) \Big]$. The third term is a reaction of the force in the second term. The total momentum density

$$\begin{aligned}
\vec{n}^{\vec{p}}(\vec{x},t) &= N \int \frac{d\vec{p}}{(2\pi)^2} \vec{p} \Big[f_+(\vec{x},t,\vec{p}) - (1-f_-(\vec{x},t,\vec{p})) \Big] \\
&\quad + \int \frac{d\vec{p}}{(2\pi)^2}\, \vec{p}\, b(\vec{x},t,\vec{p}),
\end{aligned} \tag{5.63}$$

the total momentum flux

$$\begin{aligned}
\vec{\vec{\Pi}}(\vec{x},t) &= N \int \frac{d\vec{p}}{(2\pi)^2}\, (v_F \hat{p} + \partial_{\vec{p}} \operatorname{Re}\sigma)\vec{p} \\
&\qquad (f_+(\vec{x},t,\vec{p}) + (1-f_-(\vec{x},t,\vec{p}))) \\
&\quad + \int \frac{d\vec{p}}{(2\pi)^2} \vec{v}_p\, \vec{p}\, b(\vec{x},t,\vec{p}).
\end{aligned} \tag{5.64}$$

Here $\vec{v}_p = \omega_p(\vec{p})\hat{p}/2p$ defines the group velocity of a plasmon. We find that the total momentum density is not locally conserved but

changed by the internal electric forces on the right-hand side of the equation. However, integrating over all space $\vec{x}$, the force terms vanish and the Hartree potential cancels by virtue of being a total derivative,

$$\int d\vec{x}\partial_{\vec{x}}V^H(\vec{x})n(\vec{x},t)=0. \tag{5.65}$$

In contrast, the other two forces do not vanish individually, but instead cancel each other:

$$\begin{aligned}-\int d\vec{x}\int\frac{d\vec{p}}{(2\pi)^2}\frac{\omega_p(\vec{p})}{2}\frac{\partial_{\vec{x}}\mathcal{N}}{\mathcal{N}}b(\vec{x},t,\vec{p})\\ -N\int d\vec{x}\int\frac{d\vec{p}}{(2\pi)^2}\partial_{\vec{x}}\,\mathrm{Re}\,\sigma^R(\vec{x},t,\vec{p})\Big(f_+(\vec{x},t,\vec{p})\\ +(1-f_-(\vec{x},t,\vec{p}))\Big)=0.\end{aligned} \tag{5.66}$$

On general grounds, this is a result of the Kadanoff-Baym conditions for approximate Green's function to maintain the macroscopic conservation laws [92]. As we discussed earlier, a self-energy included in the approximate Green's function must be generated from a diagram of a free energy functional and the contributions from those self-energies generated from the same free energy diagram will cancel out to ensure the conservation laws. We find the conservation of total momentum of the electrons

$$\partial_t\vec{P}=0 \tag{5.67}$$

where the total momemtum of the whole system

$$\vec{P}=\int d\vec{x}\;\vec{n}^{\vec{p}}(\vec{x},t). \tag{5.68}$$

Next, we multiply the electron Boltzmann equation of Eq.(5.53) by the energy $\epsilon_\lambda(\vec{x},t,\vec{p})=\lambda p+V^H(\vec{x})+\lambda\,\mathrm{Re}\,\sigma^R(\vec{x},t,\vec{p})$, integrate the resulting equation over all momentum $\vec{p}$ and then summing over the energy bands $\pm$. Similarly, we multiply the plasmon Boltzmann equation of Eq.(5.53) by its energy dispersion given by $\omega(\vec{x},\vec{p},t)=\sqrt{\frac{N}{2}\alpha p\mathcal{N}(\vec{x},t)}$ and integrate over the momentum. We add the resulting equations together, and find the conservation law of energy

for the total system.

$$\partial_t n^\epsilon(\vec{x},t) + \partial_{\vec{x}} \cdot \vec{j}^\epsilon(\vec{x},t) = 0, \tag{5.69}$$

where the total energy density

$$n^\epsilon(\vec{x},t) = N \int \frac{d\vec{p}}{(2\pi)^2} \Big[\epsilon_+(\vec{x},t,\vec{p}) f_+(\vec{x},t,\vec{p}) - \epsilon_-(\vec{x},t,\vec{p})(1-f_-(\vec{x},t,\vec{p}))\Big] + \int \frac{d\vec{p}}{(2\pi)^2} \omega(\vec{x},t,\vec{p}) b(\vec{x},t,\vec{p}), \tag{5.70}$$

and the total energy current density

$$\begin{aligned} \vec{j}^\epsilon(\vec{x},t) &= N \int \frac{d\vec{p}}{(2\pi)^2} \Big[\vec{v}_+ \epsilon_+(\vec{x},t,\vec{p}) f_+(\vec{x},t,\vec{p}) \\ &\quad - \vec{v}_-(\vec{x},t,\vec{p}) \epsilon_-(\vec{x},t,\vec{p})(1-f_-(\vec{x},t,\vec{p}))\Big] \\ &\quad + \int \frac{d\vec{p}}{(2\pi)^2} \vec{v}_p \omega_p b(\vec{x},t,\vec{p}). \end{aligned} \tag{5.71}$$

5.8 Conclusion

We use the random-phase approximation which naturally leads to the notion of a coupled field theory of electrons, holes, and plasmons. Contrary to in three dimensional metals, the emerging plasmons constitute proper low-energy degrees of freedom without an excitation gap. Furthermore, these plasmons are stable and do not decay easily. Based on this, we study a set of coupled Boltzmann equations. We explicitly establish in that framework, that the approach provides a consistent conserving approximation which respects the conservation of electrical charge, momentum, and energy. Our main findings are that, compared to weak-coupling theories, there are direct low-energy contributions of the plasmons to the heat current and the energy-momentum tensor that are on equal footing with electronic excitations. These implies that they should be measurable in transport experiments in encapsulated graphene devices that achieve the hydrodynamic regime. While we do not expect a similar effect in three-dimensional metals we also expect an enhancement close to the Dirac point of three dimensional Dirac and Weyl systems.

Chapter 6

The role of particle-hole pairs in thermo-electric response in two-dimensional Dirac systems: numerical results

Clean two-dimensional Dirac systems have received a lot of attention for being a prime candidate to observe hydrodynamical transport behavior in interacting electronic systems. This is mostly due to recent advances in the preparation of ultrapure samples with sufficiently strong interactions. In this chapter, we investigate the role of collective modes in the thermo-electric transport properties of those systems. By solving a coupled system of Boltzmann equations numerically, we find that dynamical particle-hole pairs, plasmons, make a sizeable contribution to the thermal conductivity. While the increase at the Dirac point is moderate, it becomes large towards larger doping. We suspect, that this is a generic feature of ultraclean two-dimensional electronic systems, also applicable to degenerate systems[1].

[1]This chapter is based on K. Pongsangangan, S. Grubinska, and L.Fritz, *Thermo-electric response in two-dimensional Dirac systems: the role of particle-hole pairs.* (accepted at PRResearch) (2022).

6.1 Introduction

The study of transport in metallic systems has a long and successful history, going back all the way to Drude transport theory [1]. Remarkably, a picture of non-interacting electrons scattering from disorder provides reasonably a description of transport properties of metals or more specifically Fermi liquids. In general, however, electrons are interacting and a question that has been discussed for 70 years is why the picture of independent electrons diffusing in a disordered background is so successful [4]. To rephrase the question: Why and how do the long-range correlations between electrons due to Coulomb interaction become ineffective? Bohm and Pines argued that there are two components associated with the Coulomb interaction, short- and long-range, and they play a very different role. The short-range part leads to a quasiparticle renormalization in the spirit of Landau's Fermi liquid theory, leading to 'new' almost free electrons. The primary manifestation of the long-range part are the plasma oscillations or plasmons [5, 6]. In the standard theory of metallic transport, interactions consequently play a minor role in the low temperature limit. There are two ways in which they enter: (i) as a source of inelastic scattering for the electronic quasiparticles [12] and (ii) as dynamical collective degrees of freedom like plasmons that make a direct contribution to transport properties. In conventional three dimensional Fermi liquids, neither of the two happens. (i) Inelastic scattering is subdominant compared to elastic impurity scattering. It is parametrically small in $(T/T_F)^2$ where $T_F \approx 10^3 - 10^5$ K is the Fermi temperature of the metallic system. (ii) In a three dimensional metal, stable plasmons are gapped, showing a gap that is even larger than the Fermi energy of the electronic system. This implies that they cannot be excited at energy scales relevant for transport [11]. As a consequence, only electrons are relevant in the low-energy limit, and they interact with each other through the residual short-range component of the interaction. The primary source of scattering is given by disorder (note that we do not consider the role of phonons throughout this work [77]). One of the consequences of this is the famous Wiedemann-Franz law which goes back to 1853 [79]. It states that at lowest temperatures in

metals the ratio

$$\lim_{T\to 0} \frac{\kappa}{T\sigma} = L_0 \tag{6.1}$$

is constant and independent of details of the system. In Eq. (6.1), T is the temperature, σ is the electrical conductivity, κ is the heat conductivity, and $L_0 = (\pi k_B)^2/(3e^2)$ is the Lorenz number (k_B is the Boltzmann constant and e the electron charge). One way to rationalize this finding is that at lowest energies only electrons carry charge and heat, and both transport channels undergo the same scattering mechanisms from disorder. This leads to the same scattering time for both charge and heat transport. The question whether inelastic scattering can be the dominant scattering mechanism in degenerate Fermi systems has been discussed in the 1960s [44, 9, 10] but recently gained more momentum [39, 93, 94, 63, 68, 69]. The general expectation is that one should then observe hydrodynamic transport phenomena.

Another variant of conducting and interacting electronic systems are Dirac- and/or Weyl-metals [14]. Their defining feature is a linear band crossing in isolated points in the Brillouin zone which strongly suppresses the density of states. These systems are semimetals or non-degenerate. The most famous example is graphene which has been at the forefront of research for almost two decades [16, 17].

Close to its Dirac point, pristine graphene has properties that are distinct from normal Fermi liquids. One major difference is that at the Dirac point the system is scale-free, resembling a quantum critical system [26]. Consequently, temperature T is the only energy scale, contrary to a degenerate fermionic system which possesses the Fermi temperature T_F. While this modifies thermodynamic properties, it also has consequences on the interaction properties: inelastic interaction scattering cannot be suppressed by the smallness of T/T_F (also in the vicinity of the Dirac point T/T_F remains large), it can even dominate elastic scattering from disorder. Therefore, in sufficiently clean samples, it is theoretically expected that one finds hydrodynamic transport behavior [95, 96, 32, 33, 34, 47, 97, 66, 98, 49]. Secondly, it is known that decreasing dimensionality increases the effect of long-range interactions in electronic systems. That not only increases inelastic scattering, it also makes the effect of col-

lective modes more prominent. It is known that plasmons in a one-dimensional conductor contribute significantly to thermal transport. This begs the question about two dimensions. In two dimensions, contrary to three dimensions, plasmons are massless [5, 6, 7] and follow a square root dispersion, *i.e.*, $\omega \propto \sqrt{q}$. Consequently, they are easily excited under non-equilibrium conditions and can therefore be relevant to the transport phenomena, especially thermal transport. It is important to note that the second point is not exclusive to Dirac systems but it is also true for two-dimensional degenerate systems.

In recent years, suspended samples or samples sandwiched in between boron-nitrid (BN) structures [58, 18, 85, 37, 36, 99, 38, 100, 65] allow to suppress disorder levels sufficiently to access the hydrodynamic regime. With the new ultrapure samples, it is thus possible to ask quantitative questions that could not be addressed before. In this chapter, we reinvestigate transport theory in ultraclean Dirac systems. Our special focus is on the role of Coulomb interactions and their unscreened long-range nature in thermo-electric transport.

As explained above, we expect Coulomb interaction to be responsible for mainly two effects in regards of transport phenomena: (i) charge carriers scatter from each other leading to an effective inelastic transport time or mean free path; (ii) collective excitations, such as plasmons, that possess their own dynamics. Consequently, they make a direct contribution to the heat current.

The thermo-electric response involves two types of currents: the electrical current J^e and the heat current $Q = J^E - \mu/eJ^e$, where J^E is the energy current. The Onsager relation states [56, 76]

$$\begin{pmatrix} \vec{J}^e \\ \vec{Q} \end{pmatrix} = \begin{pmatrix} \hat{\sigma} & \hat{\alpha} \\ T\hat{\alpha} & \hat{\bar{\kappa}} \end{pmatrix} \begin{pmatrix} \vec{E} \\ -\vec{\nabla}T \end{pmatrix} . \tag{6.2}$$

The thermal conductivity, $\hat{\kappa}$, is defined as the heat current response to a thermal gradient $-\vec{\nabla}T$ in the absence of an electrical current (electrically isolated boundaries), given by $\hat{\kappa} = \hat{\bar{\kappa}} - T\hat{\alpha}\hat{\sigma}^{-1}\hat{\alpha}$. In the following we drop 'hats' and only explicitly discuss the diagonal response σ and κ. The Wiedemann-Franz ratio $\kappa/(T\sigma)$ assumes the value $L_0 = \pi^2/3 \times (k_B/e)^2$ (L_0 is the Lorenz number) in a Fermi liquid [79], see Eq. (6.1). This is sometimes considered the hallmark of a Fermi liquid and it was argued before that it breaks down in

the vicinity of the Dirac point [75, 33, 85]. The main reason for this breakdown is that there are two completely independent hydrodynamic modes that are subject to different scattering mechanisms.

Instead of concentrating on two types of degrees of freedom, electrons and holes, we additionally consider plasmons. The situations are sketched in Fig. 1.4a for electrical transport and in Fig. 1.4b for heat transport. The potential drop in Fig. 1.4a acts on electrons and holes oppositely, but not on the plasmons: the plasmons experience no direct force, but they are subject to drag effects. Being neutral quasiparticles, they do not contribute to the charge current. In the case of a temperature gradient, see Fig. 1.4b, all particles experience a force in the same direction, and there is an additional direct contribution to the current through the plasmons. On a technical level, we derive and solve three coupled Boltzmann equations for electrons, holes, and plasmons, which includes relaxational processes and the respective streaming terms. We find that the plasmon contribution to the heat conductivity is seizable and cannot be neglected, neither at the Dirac point, nor in the degenerate limit.

6.2 The model

We study a model of Dirac fermions coupled through Coulomb interaction and subject to potential disorder:

$$\begin{aligned} H &= \int d^2\vec{r}\, \Psi_i^\dagger(\vec{r}) \left(-iv_F \vec{\partial}\cdot\vec{\sigma} + V_{\rm dis}(\vec{r}) \right) \Psi_i(\vec{r}) \\ &+ \frac{1}{2}\int d^2\vec{r} d^2\vec{r}' \Psi_i^\dagger(\vec{r}) \Psi_i(\vec{r}) V(\vec{r}-\vec{r}') \Psi_j^\dagger(\vec{r}') \Psi_j(\vec{r}') \ . \end{aligned} \tag{6.3}$$

$\Psi_i(\vec{r})$ is the two component wave function, i is the flavor index ranging from $i = 1, ..., N$ (for graphene $N = 4$ counting spin and valley), v_F the Fermi velocity, and $V(\vec{r}-\vec{r}') = \alpha \frac{v_F}{|\vec{r}-\vec{r}'|}$ the Coulomb interaction (note that double indices are summed over). The dimensionless fine structure constant sets the strength of interaction and is given by $\alpha = e^2/(4\pi\epsilon_0\epsilon_r v_F)$. The disorder potential $V_{\rm dis}(\vec{r})$ can be used to describe a variety of disorder types specified by the disorder correlation function. We only consider delta-correlated disorder, *i.e.*,

$\langle V_{\rm dis}(\vec{r})V_{\rm dis}(\vec{r}')\rangle = 4\pi\gamma^2\delta(\vec{r}-\vec{r}')$, but generalizations are straightforward. Consequently, the parameters of our theory are α and γ. Eq. (6.3) does not provide a convenient starting point for the study of the thermal conductivity due to the non-local Coulomb interaction.

A corresponding local field theory that easily lends itself to an interpretation in terms of plasmons can be derived using a Hubbard-Stratonovich transformation. It reads

$$\begin{aligned}\mathcal{L} = &- \frac{\epsilon_0\epsilon_r}{2}\phi(\vec{r},z,t)\left(\vec{\partial}^2+\partial_z^2\right)\phi(\vec{r},z,t)\\ &- e\Psi_\alpha^\dagger(\vec{r},t)\Psi_\alpha(\vec{r},t)\phi(\vec{r},z,t)\delta(z)\\ &+ \Psi_\alpha^\dagger(\vec{r},t)\left(i\partial_t - iv_F\vec{\partial}\cdot\vec{\sigma}+V_{\rm dis}(\vec{r})\right)\delta(z)\Psi_\alpha(\vec{r},t)\ ,\end{aligned} \tag{6.4}$$

where $\phi(\vec{r},z,t)$ is the real valued plasmon field. Importantly, the mapping between Eq. (6.3) and Eq. (6.4) is exact.
Current operators: The electrical charge current is only carried by electrons and holes and its density is given by

$$\mathbf{j}^e(\vec{r},t) = -ev_F\Psi_\alpha^\dagger(\vec{r},t)\,\vec{\sigma}\Psi_\alpha(\vec{r},t)\ . \tag{6.5}$$

The heat current density is given by $\mathbf{Q} = \mathbf{j}^E - \mu/e\mathbf{j}^e$ where the energy current density reads [101]

$$\mathbf{j}^E(\vec{r},z.t) = -iv_F\Psi_\alpha^\dagger(\vec{r},t)\vec{\sigma}\partial_t\Psi_\alpha(\vec{r},t)\epsilon_0\epsilon_r\vec{\partial}\phi(\vec{r},z,t)\partial_t\phi(\vec{r},z,t)\ . \tag{6.6}$$

This expression explicitly includes the plasmon contribution which is the main new aspect of this work.

6.3 Plasmon dynamics

Integrating out the photon modes outside the graphene sheet leads to an effective two-dimensional theory,

$$\mathcal{S}_\Phi = \frac{1}{2}\int dtdt'd^2\vec{r}d^2\vec{r}'\Phi(\vec{r},t)D_0^{-1}(\vec{r},\vec{r}',t,t')\Phi(\vec{r}',t') \tag{6.7}$$

with $\Phi(\vec{r},t) = \phi(\vec{r},z=0,t)$ and $D_0^{-1}(\vec{k},\omega) = \alpha(2\pi v_F)/(e^2k)$ with $k = |\vec{k}|$.

The dynamics is generated from within the fermionic system and corresponds to particle-hole pairs. We use the standard random phase approximation (RPA), formally justified in the limit of a large number N of flavors. The boson self energy is approximated through $e^2\Pi(\vec{r},\vec{r}',t,t')$, where $\Pi(\vec{r},\vec{r}',t,t')$ is the polarization function. The polarization function of two-dimensional Dirac systems has a closed analytical form at zero temperature [54]. The finite temperature properties at arbitrary chemical potential have been studied numerically in Ref. [55]. In the long wavelength limit, important for the plasmon dynamics, the retarded polarization function can be approximated as

$$\Pi^r(\vec{q},\omega,\mu,T) \approx \frac{Nq^2T}{4\pi\omega^2}\ln\left(2+2\cosh\left(\frac{\mu}{T}\right)\right) - i\frac{Nq^2}{32\omega}f(\mu,\omega,T)\ , \tag{6.8}$$

with $f(\mu,\omega,T) = \tanh\left(\frac{\mu}{2T}-\frac{\omega}{4T}\right) - \tanh\left(\frac{\mu}{2T}+\frac{\omega}{4T}\right)$. We obtain the plasmon dispersion from the poles of the retarded plasmon propagator

$$D^r(\vec{q},\omega) = \frac{D_0^r(\vec{q},\omega)}{1-e^2D_0^r(\vec{q},\omega)\Pi^r(\vec{q},\omega,\mu,T)}\ , \tag{6.9}$$

where $D_0^r(\vec{q},\omega) = 1/(2\epsilon_0\epsilon_r q)$, with ϵ_0 being the vacuum permittivity, while ϵ_r is the relative permittivity. Using the approximate polarization function, Eq. (6.8), we can approximate the plasmon propagator as

$$D^r(\vec{q},\omega) \approx \frac{1}{2\epsilon_0\epsilon_r}\frac{\omega^2}{q}\frac{1}{(\omega+i0^+)^2-\left(\omega_p(\vec{q})+i\gamma_p(\vec{q})\right)^2}\ , \tag{6.10}$$

with the plasmon dispersion $\omega_p(\vec{q})$ and damping $\gamma_p(\vec{q})$ given by

$$\begin{aligned}\omega_p(\vec{q}) &= \sqrt{\alpha\frac{N}{2}k_BTv_Fq\ln\left(2+2\cosh\left(\frac{\mu}{k_BT}\right)\right)}\ ,\\ \gamma_p(\vec{q}) &= -\frac{\pi\omega_p(\vec{q})^2}{16T}\frac{f(\mu,\omega_p(\vec{q}),T)}{\ln\left(2+2\cosh\left(\frac{\mu}{T}\right)\right)}\ .\end{aligned} \tag{6.11}$$

There are two possible momentum cutoffs for the plasmons of Eq.-(6.11). Either, when they cease to be well-defined quasiparticles, *i.e.*,

$\omega_p(\vec{q}_c) \approx \gamma_p(\vec{q}_c)$, or, when the square-root dispersion breaks down, *i.e.*, $q_c = \alpha N T/(2v_F) \ln(2 + 2\cosh(\mu/T))$. Numerically, we always choose the lower of the two. In practice, it turns out that it is always the latter. For all practical calculations in this chapter, we assume the plasmons to be well-defined quasiparticles since their decay rate is parametrically small in α. It turns out that below q_c plasmons are very stable against a single particle-hole decay channel. Therefore, the leading relaxation mechanisms might be from either the plasmon decay into two electron-hole pairs [90] or phonon-assisted Landau damping [89]. Both are neglected in this work for different reasons. The former channel is of higher order in perturbation theory, while the latter is forbidden in the electron hydrodynamic window. It is important to note that there is also a linear plasmon beyond the cutoff scale which is subleading and consequently negligible in our analysis.

6.4 The Boltzmann equation

We leave a systematic derivation of the Boltzmann equation starting from the Schwinger-Keldysh formalism (see for instance Ref. [81]) for an Appendix (see also the previous chapters). The key steps of the derivation are: (i) A conserving approximation of the fermion and boson self-energies to the lowest non-trivial order in α and γ. (ii) A lowest non-trivial order gradient expansion starting from the Wigner transform. (iii) an integration over the fermion and boson spectral functions, equivalent to an on-shell quasiparticle approximation; (iv) a projection into the quasiparticle basis. In the last step we only consider the diagonal parts and neglect Berry phase (these terms are second order in the gradient expansion) and Zitterbewegung terms (see Ref. [32, 33]). Eventually, we find three coupled Boltzmann equations for electrons, holes, and plasmons,

$$\begin{aligned} e\vec{E}\partial_{\vec{k}} f_\lambda(\vec{k}) - \lambda v_F \hat{\vec{k}}\sigma_z \vec{\nabla} T \partial_T f_\lambda(\vec{k}) &= I^\lambda_{\text{coll}}[f_\lambda, b] \,, \\ 2\frac{\vec{k}}{k^2}\vec{\nabla} T \omega_p(\vec{k}) \partial_T b_{\omega_p(\vec{k})}(\vec{k}) &= \tilde{I}_{\text{coll}}[f_\lambda, b] \,. \end{aligned} \tag{6.12}$$

Here, f_λ and b are the distribution functions of the electrons and holes ($\lambda = \pm$), and the plasmons, respectively.

Sources of current relaxation: The collision integral for the Dirac fermions consists of two independent parts,

$$\begin{aligned} I^{\lambda}_{\rm coll} &= \int \frac{d^2q}{(2\pi)^2} \sum_{\lambda'=\pm} \mathcal{C}^{\rm inel}_{\lambda\lambda'}(\vec{k},\vec{q}) \Big[f_{\lambda}(\vec{k}) \Big(1 - f_{\lambda'}(\vec{k}+\vec{q})\Big) \\ &- b_{\epsilon_\lambda(\vec{k})-\epsilon_{\lambda'}(\vec{k}+\vec{q})}(\vec{q}) \Big(f_{\lambda'}(\vec{k}+\vec{q}) - f_{\lambda}(\vec{k}) \Big) \Big] \\ &+ \int \frac{d^2q}{(2\pi)^2} \mathcal{C}^{\rm el}_{\lambda}(\vec{k},\vec{q}) \Big(f_{\lambda}(\vec{k}) - f_{\lambda}(\vec{k}+\vec{q}) \Big) \ . \end{aligned} \tag{6.13}$$

The first term accounts for inelastic scattering of electrons from plasmons, denoted $\mathcal{C}^{\rm inel}_{\lambda\lambda'}$. In this process, both energy and momentum are transferred between the fermions and the plasmons. Additionally, there is elastic scattering from disorder, encoded in $\mathcal{C}^{\rm el}_{\lambda}$. This term breaks momentum conservation and is important to relax the heat current. The collision integral for the plasmons reads

$$\begin{aligned} \tilde{I}_{\rm coll} &= \int \frac{d^2q}{(2\pi)^2} \sum_{\lambda,\lambda'=\pm} \tilde{\mathcal{C}}^{\rm inel}_{\lambda\lambda'} \Big[f_{\lambda'}(\vec{k}+\vec{q}) \left(f_{\lambda}(\vec{q}) - 1\right) \\ &- b_{\epsilon_{\lambda'}(\vec{k}+\vec{q})-\epsilon_{\lambda}(\vec{q})}(\vec{k}) \Big(f_{\lambda'}(\vec{k}+\vec{q}) - f_{\lambda}(\vec{q}) \Big) \Big] \ . \end{aligned} \tag{6.14}$$

It contains an inelastic part describing scattering from fermions, $\tilde{\mathcal{C}}^{\rm inel}_{\lambda\lambda'}$ (we defer the role of inelastic scattering from disorder to follow-up work). In the absence of disorder, the combined electron-plasmon system conserves momentum. The precise form of $\mathcal{C}^{\rm inel}_{\lambda\lambda'}$, $\mathcal{C}^{\rm el}_{\lambda}$, and $\tilde{\mathcal{C}}^{\rm inel}_{\lambda\lambda'}$ can be found in the supplemental materials. It is important to note, however, that momentum excited in the plasmon sector can be relaxed in the fermion sector from disorder.

Linearized Boltzmann equation: In equilibrium, the collision integrals are nullified by the thermal Fermi-Dirac and Bose-Einstein distributions, respectively, $f^0_{\lambda}(\vec{k}) = (e^{(\epsilon_\lambda(\vec{k})-\mu)/T}+1)^{-1}$ and $b^0_{\omega}(\vec{k}) = (e^{\omega_p(\vec{k})/T}-1)^{-1}$. In the presence of driving terms due to a potential gradient, a thermal gradient, or both, the distribution functions deviate from their equilibrium form. Importantly, even though an electric field does not couple directly to the plasmons, away from the Dirac point they are still driven out of equilibrium by a drag effect [2].

[2] At the Dirac point the underlying particle-hole symmetry forbids drag [35]

Since we are interested in linear response transport properties, we linearize the Boltzmann equations in $\vec{E}$ and $-\vec{\nabla}T$. This enforces the following parametrizations for the fermions and boson distribution functions:

$$f_\lambda(\vec{k}) = f^0_\lambda(\vec{k}) - \frac{1}{T}\frac{\partial f^0_\lambda(\vec{k})}{\partial \epsilon_\lambda(\vec{k})}\lambda v_F \hat{\vec{k}} \cdot \left(e\vec{E}\chi^E_\lambda(k) + \vec{\nabla}T\chi^T_\lambda(k)\right), \quad (6.15)$$

and

$$b_{\omega_p(\vec{k})}(\vec{k}) = b^0_{\omega_p(\vec{k})}(\vec{k}) - \frac{1}{T}\frac{\partial b^0_{\omega_p(\vec{k})}(\vec{k})}{\partial \omega_p(\vec{k})} v_F \hat{\vec{k}} \cdot \left(e\vec{E}\phi^E(k) + \vec{\nabla}T\phi^T(k)\right) . \quad (6.16)$$

As mentioned before, an electric field applied to the fermions 'drags' the plasmons out of equilibrium which is why we have to introduce ϕ^E. The functions $\chi^{T/E}_\lambda$ and $\phi^{T/E}$ have to be determined numerically and give access to the respective currents and related response functions. In terms of their parametrizations, we find the following set of equations

$$\begin{aligned} \mathcal{D}_\lambda[f] &= I^{\text{lin}}_{\text{inel}}[\chi_T, \chi_E, \phi_T, \phi_E] + I^{\text{lin}}_{\text{el}}[\chi_E, \chi_T], \\ \tilde{\mathcal{D}}[b] &= \tilde{I}^{\text{lin}}_{\text{inel}}[\chi_T, \chi_E, \phi_T, \phi_E] + \tilde{I}^{\text{el}}_{\text{inel}}[\phi_T, \phi_E]. \end{aligned} \quad (6.17)$$

where the driving terms are given by

$$\mathcal{D}_\lambda[f] = \lambda e v_F \hat{\vec{k}} \cdot \vec{E}\frac{\partial f^0_\lambda(\vec{k})}{\partial \epsilon_\lambda(\vec{k})} - \lambda v_F \hat{\vec{k}}\vec{\nabla}T\frac{\epsilon_\lambda(\vec{k}) - \mu}{T}\frac{\partial f^0_\lambda(\vec{k})}{\partial \epsilon_\lambda(\vec{k})} \quad (6.18)$$

$$\tilde{\mathcal{D}}[b] = -\frac{\vec{k}}{k^2}\vec{\nabla}T\frac{\omega^2_p(\vec{k})}{T}\frac{\partial b^0_{\omega_p(\vec{k})}(\vec{k})}{\partial \omega_p(\vec{k})} \quad (6.19)$$

with details to be found in the appendices. In the absence of disorder, the combined system of fermions and plasmons possesses a zero mode associated with momentum conservation, meaning the combination $C^{\text{inel}}_{\lambda\lambda'}$ and $\tilde{C}^{\text{inel}}_{\lambda\lambda'}$ together with the appropriate mode cannot relax momentum (we explicitly checked this point numerically). The intuition behind this is that momentum can always be transferred

between the fermion and plasmon sector without being dissipated. This implies that disorder scattering is vital as a source of momentum relaxation for the total system, and it plays an important role in the choice of modes, explained below (see Ref. [77] for a related discussion in the electron-phonon problem without Umklapp scattering).

6.5 Choice of modes

The above parametrization allows for a very transparent identification of the slow hydrodynamic modes of the problem. In the solution of the fermion only problem, Eq. (6.3), it was pointed out that in order to study thermoelectric transport in the vicinity of the Dirac point all the way to the Fermi liquid regime it suffices to study two types of modes for electrons and holes, respectively, $\chi_\lambda^{T/E}(k) = a_{0,\lambda}^{T/E} + \lambda a_{1,\lambda}^{T/E} k$ [33, 34]. The mode associated with $a_{0,\lambda}^{T/E}$ is called chiral mode, whereas the one associated with $a_{1,\lambda}^{T/E}$ corresponds to the momentum mode. For the plasmons, the equivalent ansatz reads $\phi^{T/E}(k) = b_0^{E/T} + b_1^{T/E} k$. We can convert the problem of solving the Boltzmann equation into a linear algebra problem by projecting the scattering integral onto the respective modes, see the discussion in the supplemental material.

6.6 Results

We have solved the coupled Boltzmann equations, Eq. (6.17), at and away from the Dirac point. This allows to access both the electrical and the heat conductivity, and consequently, the Wiedemann-Franz ratio. In the following we present two types of plots: (a) the conductivities as a function of the chemical potential (Fig. 6.1, Fig. 6.2,and Fig. 6.3) and (b), more experimentally relevant, as a function of the

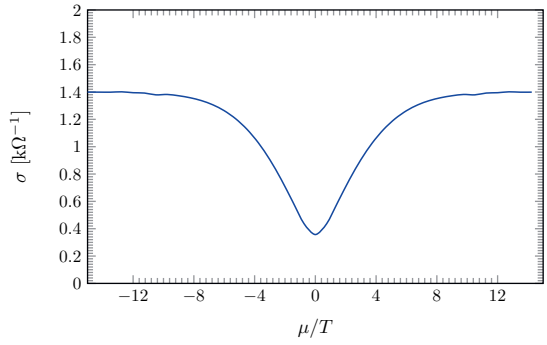

Figure 6.1: Electrical conductivity as a function of chemical potential. The curve was obtained as solution of the Boltzmann equation with $\alpha = 0.36$ and $4\pi\gamma^2 = 0.5$ at $T = 75K$.

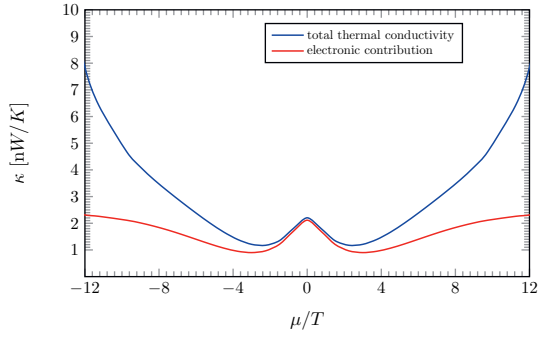

Figure 6.2: Thermal conductivity of graphene as a function of the chemical potential. The curves are calculated using the same set of parameters used in Fig. 6.1. The blue curve is the full response including the plasmons while the red curve only shows the electronic contribution. There is a slight plasmon enhancement close to the Dirac point and a massive one with increasing chemical potential.

electronic density (Fig. 6.4, Fig. 6.5,and Fig. 6.6). In all plots, we have fixed the temperature to be $T = 75$ K and the fine structure constant α to be $\alpha = 0.36$. For disorder, we made the assumption that it is short-ranged and $4\pi\gamma^2 = 0.5$ (our main point here is not to connect to a specific experiment). In all plots, we plot the

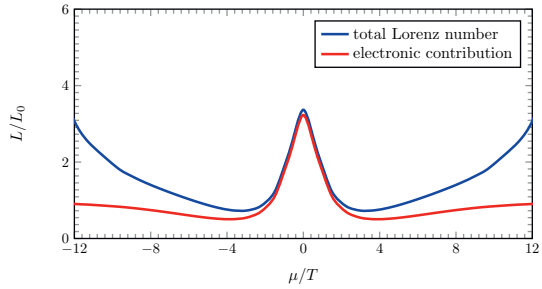

Figure 6.3: Wiedemann-Franz ratio as a function of the chemical potential. We observe two regions with enhancement: the well-known hydrodynamic regime in the vicinity of the Dirac point and at higher doping.

total conductivity including the plasmon contribution in blue and the electronic contribution only in red. Since the plasmons cannot make a direct contribution to the electrical conductivity, there is only a blue line in Fig. 6.1 and Fig. 6.4. We observe that there is an enhancement of the thermal conductivity close to the Dirac point. This enhancement increases the expected violation of the Wiedemann-Franz law at the Dirac point. A bit more surprisingly, however, there is a sizeable and increasing enhancement of the thermal conductivity towards the Fermi liquid regime, *i.e.*, $\mu \gg T$.

It is tempting to attribute the growth of the plasmon contribution to its dispersion relation, Eq. (6.11), which is $\sqrt{\mu}$ for $\mu/T \gg 1$. However, this is not the sole reason for the increase: Phenomenologically, one expects the thermal conductivity to follow a Drude type expression $\kappa \propto \int d^2q \omega_p(\vec{q}) \vec{v}_p^2(\vec{q}) \left(-\frac{\partial b}{\partial \omega_p(\vec{q})}\right) \tau_p(\vec{q},\mu)$, where $\tau_p(\vec{q},\mu)$ is a scattering time that comes from the solution of the Boltzmann equation. If we assume that $\tau_p(\vec{q},\mu)$ is constant as a function of $\vec{q}$ in the relevant momentum window, one ends up with $\kappa \propto \mu^0 \tau_p(0,\mu)$.

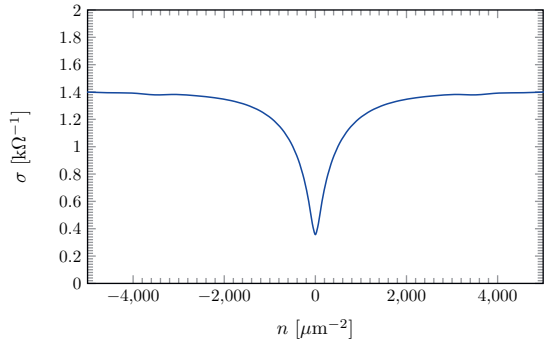

Figure 6.4: Electrical conductivity as a function of carrier density. The curve was obtained as solution of the Boltzmann equation with $\alpha = 0.36$ and $4\pi\gamma^2 = 0.5$ at $T = 75K$.

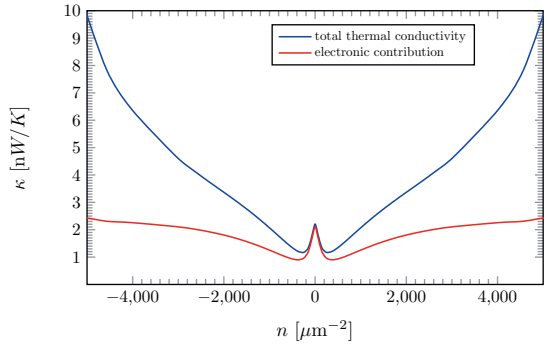

Figure 6.5: Thermal conductivity of graphene as a function of the charge carrier density. The curves are calculated using the same set of parameters used in Fig. 6.4. The blue curve is the full response including the plasmons while the red curve only shows the electronic contribution. There is a slight plasmon enhancement close to the Dirac point and a massive one with increasing chemical potential.

Consequently, the effect appears to strongly depend on the scattering time, which is born out by an analysis of the scattering integral. To summarize, the main observation is the growing enhancement of the thermal conductivity due to plasmons in the region of $\mu/T > 1$. It is important to note that the relaxation of the plasmons is due

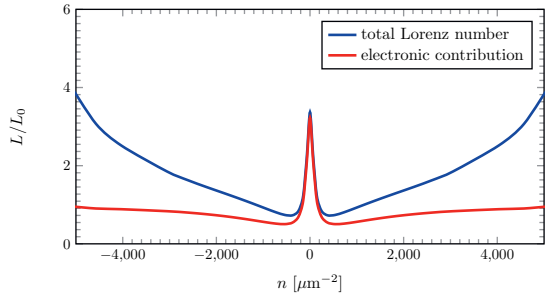

Figure 6.6: Wiedemann-Franz ratio as a function of the charge carrier density. We observe two regions with enhancement: the well-known hydrodynamic regime in the vicinity of the Dirac point and at higher doping.

to the disorder in the fermionic sector. Momentum that is excited in the plasmon sector through the thermal gradient is transferred to the fermionic subsystem via inelastic scattering. There it is relaxed from the momentum conservation breaking disorder. It is worthwhile noting that the around $\mu/T \approx 2$ there is a suppression of the Lorenz ratio below 1. This seems to be a feature that is also encountered in experiments [80].

6.7 Conclusion and Outlook

In this work we have analyzed the thermo-electric response of interacting two-dimensional Dirac systems at and away from the Dirac point. We have done so by deriving and solving coupled linearized Boltzmann equations for electrons, holes, and plasmons. At the Dirac point we find a moderate enhancement of the thermal conductivity due to plasmons, compared to the electronic contribution. However, away from the Dirac point, we find a strong enhancement of thermal transport due to plasmons. Compared to a conventional three dimensional metal, this is made possible by the undamped gapless nature of plasmons which have a square root dispersion, *i.e.*, $\omega \propto \sqrt{q}$. Consequently, this effect is special to two dimensions and is not expected to exist in three dimensions, in line with very early

works [5, 6]. The plasmon contribution to the heat conductivity and, connected to that, the violation of the Wiedemann-Franz law, increases as we tune into the Fermi liquid regime of a Dirac system. This suggests that the observed effect should also be observable in conventional degenerate two-dimensional metallic systems. While we do not expect a similar effect in three dimensional metals we also expect and enhancement close to the Dirac point of three dimensional Dirac-/Weyl-systems.

The results presented here immediately provoke a series of questions: (i) How can the results be connected to the known results for the disordered two-dimensional Fermi liquid [50]? (ii) How can we model relaxation processes, such as disorder, for plasmons? (iii) Can this effect be observed in experiments? (iv) Can we find a unified hydrodynamic description in which all degrees of freedom enter on equal footing? The answers to some of the above questions are left for future study.

6.8 Appendices

Keldysh equations

In the following we set up the Keldysh equations for describing transport phenomena in the coupled fermion-plasmon system. The procedure is akin a system of fermions coupled to phonons where drag effects have to be taken into account. Following standard procedure we parametrize the fermionic and bosonic Keldysh components as

$$\begin{aligned} G^K &= G^r \circ F - F \circ G^a \\ D^K &= D^r \circ B - B \circ D^a \end{aligned} \tag{6.20}$$

where F and B are hermitian matrices and $\circ$ denotes matrix multiplication in real space and time where $C = A \circ B$ corresponds to $C(\vec{x}_1, t_1, \vec{x}_2, t_2) = \int d\vec{x}' dt' A(\vec{x}_1, t_1, \vec{x}', t') B(\vec{x}', t', \vec{x}_2, t_2)$. Both F and B are, in thermal equilibrium, related to standard distribution function, where $F = 1 - 2f$ and $B = 1 + 2b$ with f being the Fermi-Dirac distribution and b the Bose-Einstein distribution. They obey

the kinetic equation according to

$$\begin{aligned}\left[F, G_0^{-1}\right]_-^\circ &= \Sigma^K - (\Sigma^r \circ F - F \circ \Sigma^a) \quad \text{and} \\ \left[B, D_0^{-1}\right]_-^\circ &= e^2 \left(\Pi^K - (\Pi^r \circ B - B \circ \Pi^a)\right) \ , \end{aligned} \tag{6.21}$$

where the left-hand sides is a commutator involving the bare Green's functions G_0 of the Dirac fermions and D_0 of the plasmons, whereas the right hand side is the so-called collision integral. We assume that $e^2\Pi$ is the self-energy of the bosons whereas Σ is the self-energy of the fermions which we leave unspecified for the moment. We are now going through a series of approximations which will eventually lead us to the Boltzmann equation. We start with a gradient expansion

$$\begin{aligned}\left[F, G_0^{-1}\right]_-^\star &= \left(\Sigma^K - (\Sigma^r \star F - F \star \Sigma^a)\right) \quad \text{and} \\ \left[B, D_0^{-1}\right]_-^\star &= e^2 \left(\Pi^K - (\Pi^r \star B - B \star \Pi^a)\right) \ , \end{aligned} \tag{6.22}$$

where we have introduced the Moyal product. It has to be interpreted in the following way: there are center of mass coordinates $X = (x_1 + x_2)/2$ and $\tilde{T} = (t_1 + t_2)/2$ as well as relative coordinates $x = x_1 - x_2$ and $t = t_1 - t_2$ (note that we introduce the notation $\tilde{T}$, here, to later distinguish it from the temperature T). Furthermore, we perform a Fourier transformation with respect to the relative coordinates, leading to $\vec{k}$ and ω. The Moyal product then reads

$$C\left(X, \tilde{T}, \vec{k}, \omega\right) = A\left(X, \tilde{T}, \vec{k}, \omega\right) \star B\left(X, \tilde{T}, \vec{k}, \omega\right) \tag{6.23}$$

with

$$\star = \exp\left[\frac{i}{2}\left(\overleftarrow{\partial}_{\vec{X}}\overrightarrow{\partial}_{\vec{k}} - \overleftarrow{\partial}_{\tilde{T}}\overrightarrow{\partial}_{\omega} - \overleftarrow{\partial}_{\vec{k}}\overrightarrow{\partial}_{\vec{X}} + \overleftarrow{\partial}_{\omega}\overrightarrow{\partial}_{\tilde{T}}\right)\right] \ . \tag{6.24}$$

We perform a leading order expansion of both the left- and right-hand sides of Eq. (6.22).

$$
\begin{aligned}
&i\left(\partial_{\vec{X}}F\partial_{\vec{k}}\bar{G}^{-1}-\partial_{\vec{k}}F\partial_{\vec{X}}\bar{G}^{-1}-\partial_{\tilde{T}}F\partial_{\omega}\bar{G}^{-1}+\partial_{\omega}F\partial_{\tilde{T}}\bar{G}^{-1}\right)\\
&\qquad\qquad=\Sigma^{K}-F\left(\Sigma^{r}-\Sigma^{a}\right),\\
&i\left(\partial_{\vec{X}}B\partial_{\vec{k}}\bar{D}^{-1}-\partial_{\vec{k}}B\partial_{\vec{X}}\bar{D}^{-1}-\partial_{\tilde{T}}B\partial_{\omega}\bar{D}^{-1}+\partial_{\omega}B\partial_{\tilde{T}}\bar{D}^{-1}\right)\\
&\qquad\qquad=e^{2}\Pi^{K}-e^{2}B\left(\Pi^{r}-\Pi^{a}\right).
\end{aligned}
\tag{6.25}
$$

where $\bar{G}^{-1}=G_0^{-1}-\mathrm{Re}\{\Sigma^r\}$ and $\bar{D}^{-1}=D_0^{-1}-e^2\,\mathrm{Re}\{\Pi^r\}$.

These two coupled equations constitute the basis of all further investigations. The next step towards the Boltzmann equation is to replace the function $F=1-2f$ and $B=1+2b$ with the respective distribution functions leading to

$$
\begin{aligned}
&i2\left(\partial_{\vec{k}}f\partial_{\vec{X}}G_0^{-1}-\partial_{\vec{X}}f\partial_{\vec{k}}G_0^{-1}+\partial_{\tilde{T}}f\partial_{\omega}G_0^{-1}-\partial_{\omega}f\partial_{\tilde{T}}G_0^{-1}\right)\\
&\qquad\qquad=\Sigma^{K}-(1-2f)\left(\Sigma^{r}-\Sigma^{a}\right)\ ,\\
&i2\left(\partial_{\vec{X}}b\partial_{\vec{k}}D_0^{-1}-\partial_{\vec{k}}b\partial_{\vec{X}}D_0^{-1}-\partial_{\tilde{T}}b\partial_{\omega}D_0^{-1}+\partial_{\omega}b\partial_{\tilde{T}}D_0^{-1}\right)\\
&\qquad\qquad=e^{2}\Pi^{K}-e^{2}(1+2b)\left(\Pi^{r}-\Pi^{a}\right)\ .
\end{aligned}
\tag{6.26}
$$

In this chapter we concentrate on heat and charge transport. For the left-hand sides of the kinetic equations this implies

$$
\begin{aligned}
&\partial_{\vec{k}}f\partial_{\vec{X}}G_0^{-1}-\partial_{\vec{X}}f\partial_{\vec{k}}G_0^{-1}+\partial_{\tilde{T}}f\partial_{\omega}G_0^{-1}-\partial_{\omega}f\partial_{\tilde{T}}G_0^{-1}\\
&\qquad=e\vec{E}\partial_{\vec{k}}f-v_F\vec{\sigma}\partial_{\vec{X}}f=e\vec{E}\partial_{\vec{k}}f-v_F\vec{\sigma}\cdot\partial_{\vec{X}}T\partial_T f\\
&\partial_{\vec{X}}b\partial_{\vec{k}}D_0^{-1}-\partial_{\vec{k}}b\partial_{\vec{X}}D_0^{-1}-\partial_{\tilde{T}}b\partial_{\omega}D_0^{-1}+\partial_{\omega}b\partial_{\tilde{T}}D_0^{-1}\\
&\qquad=2\epsilon_0\epsilon_r\frac{\vec{k}}{|\vec{k}|}\partial_{\vec{X}}b=2\epsilon_0\epsilon_r\frac{\vec{k}}{|\vec{k}|}\cdot\partial_{\vec{X}}T\partial_T b
\end{aligned}
\tag{6.27}
$$

where T is the temperature. The next step to convert this into a Boltzmann type equation is to perform the quasiparticle approximation. This is achieved by integrating over the spectral function. To that end we solve the Dyson equation to access the retarded Green's

functions G^r and D^r. For G^r suffices to state that the electrons of holes of graphene are well defined and we thus work with G_0^r thereby disregarding corrections to infinitely long lived quasiparticles. For the plasmons, we use

$$D^r(\vec{q},\omega) \approx \frac{1}{2\epsilon_0\epsilon_r}\frac{\omega^2}{q}\frac{1}{(\omega+i0^+)^2-\omega_p(\vec{q})^2} \tag{6.28}$$

with the plasmon dispersion

$$\omega_p(\vec{q}) \approx \sqrt{\alpha\frac{N}{2}k_BTv_Fq\ln\left(2+2\cosh\left(\frac{\mu}{k_BT}\right)\right)}\,, \tag{6.29}$$

as derived in the main text.

Sources of relaxation

The self-energy of the Dirac fermion consists of two parts: One due to interactions with the plasmons, another one due to scattering from impurities, to lowest order, is approximated as

$$\begin{aligned} 2i\,\mathrm{Im}\,\Sigma^r(\omega,\vec{k}) = -2e^2\int\frac{d\nu}{2\pi}\int\frac{d^2q}{(2\pi)^2}\Big[&\mathrm{Im}G^r(\omega+\nu,\vec{k}+\vec{q})\ \times \\ &D^K(-\nu,-\vec{q}) + \ G^K(\omega+\nu,\vec{k}+\vec{q})\ \mathrm{Im}D^r(-\nu,-\vec{q})\Big] \\ &+\frac{\gamma_0^2}{2}\int\frac{d^2q}{(2\pi)^2}\hat{f}(-\vec{q})\left(G^r(\omega,\vec{k}+\vec{q})-G^a(\omega,\vec{k}+\vec{q})\right), \end{aligned} \tag{6.30}$$

and

$$\begin{aligned} \Sigma^K(\omega,\vec{k}) \ &= \ ie^2\int\frac{d\nu}{2\pi}\int\frac{d^2q}{(2\pi)^2}\Big[G^K(\omega+\nu,\vec{k}+\vec{q})D^K(-\nu,-\vec{q}) \\ &\qquad -4\ \mathrm{Im}G^r(\omega+\nu,\vec{k}+\vec{q})\ \mathrm{Im}D^r(-\nu,-\vec{q})\Big] \\ &\quad +\frac{\gamma_0^2}{2}\int\frac{d^2q}{(2\pi)^2}\hat{f}(-\vec{q})G^K(\omega,\vec{k}+\vec{q}). \end{aligned} \tag{6.31}$$

where the first line in both cases accounts for scattering of plasmons whereas the second line accounts for disorder scattering.

For the plasmons we have

$$2i\,\mathrm{Im}\,\Pi^r(\omega,\vec{k}) = N\int\frac{d\nu}{2\pi}\int\frac{d^2q}{(2\pi)^2}\mathrm{tr}\Big(\mathrm{Im}G^r(\omega+\nu,\vec{k}+\vec{q})G^K(\nu,\vec{q}) - G^K(\omega+\nu,\vec{k}+\vec{q})\mathrm{Im}G^r(\nu,\vec{q})\Big) \tag{6.32}$$

$$\Pi^K(\omega,\vec{k}) = -\frac{i}{2}N\int\frac{d\nu}{2\pi}\int\frac{d^2q}{(2\pi)^2}\mathrm{tr}\Big(G^K(\omega+\nu,\vec{k}+\vec{q})G^K(\nu,\vec{q}) + 4\,\mathrm{Im}G^r(\omega+\nu,\vec{k}+\vec{q})\mathrm{Im}G^r(\nu,\vec{q})\Big). \tag{6.33}$$

Quasiparticle basis

In order to arrive at the final Boltzmann equation we have to project the kinetic equations into the quasiparticle basis. This is straightforward for the plasmons, for the fermions we need a momentum-dependent rotation. To that end we consider the retarded part of the noninteracting fermionic Green's function

$$\left(G^r\right)^{-1}(\omega,\vec{k}) = (\omega+\mu)\,\mathbb{1} - v_F k_x\sigma_x - v_F k_y\sigma_y \tag{6.34}$$

In order to project this onto the quasiparticle basis we need to diagonalize the Green function (or inverse Green function). The corresponding unitary transformation reads

$$\begin{aligned} U_{\vec{k}}^{-1} &= \frac{1}{\sqrt{2}k}\begin{pmatrix} k_x - ik_y & -k_x + ik_y \\ k & k \end{pmatrix} \\ U_{\vec{k}} &= \frac{1}{\sqrt{2}k}\begin{pmatrix} k_x + ik_y & k \\ -k_x - ik_y & k \end{pmatrix} \end{aligned} \tag{6.35}$$

with

$$\begin{aligned} \left(g^r\right)^{-1}(\omega,\vec{k}) &= U_{\vec{k}}\left(G^r\right)^{-1}(\omega,\vec{k})U_{\vec{k}}^{-1} \\ &= (\omega+\mu)\,\mathbb{1} + v_F k\sigma_z \end{aligned} \tag{6.36}$$

Coupled Boltzmann equations

After having derived the Keldysh equations and specified the collision integral the last missing pieces towards the Boltzmann equation are a projection into the quasiparticle basis followed by an integration over the spectral functions. To that end we need the retarded part of the Dyson equation. For the plasmons, as discussed before, this reads

$$\begin{aligned}(D^r)^{-1}(\omega,\vec{k}) &= (D_0^r)^{-1}(\omega,\vec{k}) - e^2\Pi^r(\omega,\vec{k}) \\ &\approx \frac{2\epsilon_0\epsilon_r k}{\omega^2}\left(\omega^2-\omega_p^2(\vec{k})\right) \end{aligned} \tag{6.37}$$

whereas for the fermions we resort to the unperturbed propagator. We furthermore define the form factors

$$\begin{aligned} M^{\lambda\lambda'}_{\vec{q},\vec{k}+\vec{q}} &= \left(U_{\vec{q}}\;\; U^{-1}_{\vec{k}+\vec{q}}\right)_{\lambda\lambda'} = \frac{1}{2}\left(1+\lambda\lambda'\frac{Q(K^\star+Q^\star)}{q|\vec{k}+\vec{q}|}\right) \\ T^{\lambda\lambda'}_{\vec{q},\vec{k}+\vec{q}} &= M^{\lambda\lambda'}_{\vec{q},\vec{k}+\vec{q}} M^{\lambda'\lambda}_{\vec{k}+\vec{q},\vec{q}} = \frac{1}{4}\left|\left(1+\lambda\lambda'\frac{Q(K^\star+Q^\star)}{q|\vec{k}+\vec{q}|}\right)\right|^2 . \end{aligned} \tag{6.38}$$

The poles of the Green function determine the dispersion $\epsilon_\lambda(\vec{k}) = \lambda v_F k$. This allows to write the coupled Boltzmann equations as

$$
\begin{aligned}
&e\vec{E}\partial_{\vec{k}} f_\lambda(\vec{k})\delta_{\lambda\bar{\lambda}} - v_F\left(\hat{\vec{k}}\sigma_z - \hat{\vec{k}}\times\hat{e}_z\sigma_y\right)_{\lambda\bar{\lambda}}\vec{\nabla}T\partial_T f_\lambda(\vec{k})\\
&= 4\pi v_F\alpha\int\frac{d^2q}{(2\pi)^2}\sum_{\lambda'=\pm}M^{\lambda\lambda'}_{\vec{k},\vec{k}+\vec{q}}M^{\lambda'\bar{\lambda}}_{\vec{k}+\vec{q},\vec{k}}\\
&\left(\delta\left(\epsilon_{\lambda'}(\vec{k}+\vec{q})-\epsilon_\lambda(\vec{k})+\omega_p(\vec{q})\right)+\delta\left(\epsilon_{\lambda'}(\vec{k}+\vec{q})-\epsilon_\lambda(\vec{k})-\omega_p(\vec{q})\right)\right)\times\\
&\times\frac{\epsilon_{\lambda'}(\vec{k}+\vec{q})-\epsilon_\lambda(\vec{k})}{q}\left[f_\lambda(\vec{k})\left(1-f_{\lambda'}(\vec{k}+\vec{q})\right)-b_{\epsilon_\lambda(\vec{k})-\epsilon_{\lambda'}(\vec{k}+\vec{q})}(\vec{q})\left(f_{\lambda'}(\vec{k}+\vec{q})-f_\lambda(\vec{k})\right)\right]\\
&+\frac{\gamma_0^2}{2\pi}\int\frac{d^2q}{(2\pi)^2}\hat{f}(-\vec{q})T^{\lambda\lambda}_{\vec{k},\vec{k}+\vec{q}}\delta_{\lambda\lambda'}\delta\left(\epsilon_\lambda(\vec{k})-\epsilon_\lambda(\vec{k}+\vec{q})\right)\left(f_\lambda(\vec{k})-f_\lambda(\vec{k}+\vec{q})\right),\\
&\text{and}\\
&\frac{\vec{k}}{k^2}\vec{\nabla}T\omega_p(\vec{k})\left(\partial_T b_{\omega_p(\vec{k})}(\vec{k})-\partial_T b_{-\omega_p(\vec{k})}(\vec{k})\right)\\
&= 4N\pi v_F\alpha\sum_{\lambda,\lambda'=\pm}\int\frac{d^2q}{(2\pi)^2}M^{\lambda\lambda'}_{\vec{q},\vec{k}+\vec{q}}M^{\lambda'\lambda}_{\vec{k}+\vec{q},\vec{q}}\\
&\left(\delta\left(\epsilon_{\lambda'}(\vec{k}+\vec{q})-\epsilon_\lambda(\vec{q})+\omega_p(\vec{k})\right)+\delta\left(\epsilon_{\lambda'}(\vec{k}+\vec{q})-\epsilon_\lambda(\vec{q})-\omega_p(\vec{k})\right)\right)\times\\
&\times\frac{\epsilon_{\lambda'}(\vec{k}+\vec{q})-\epsilon_\lambda(\vec{q})}{k}\left[f_{\lambda'}(\vec{k}+\vec{q})\left(f_\lambda(\vec{q})-1\right)-b_{\epsilon_{\lambda'}(\vec{k}+\vec{q})-\epsilon_\lambda(\vec{q})}(\vec{k})\left(f_{\lambda'}(\vec{k}+\vec{q})-f_\lambda(\vec{q})\right)\right]\ . \quad (6.39)
\end{aligned}
$$

In equilibrium we have

$$f^0_\lambda(\vec{k}) = \frac{1}{e^{(\epsilon_\lambda(\vec{k})-\mu)/T}+1} \quad \text{and} \quad b^0_\omega(\vec{k}) = \frac{1}{e^{\omega/T}-1}\,. \tag{6.40}$$

The second term in the l.h.s. of the first line corresponds to the Berry phase term which comes from the adiabatic projection into the quasiparticle basis. The fourth term is the thermal analogue of the Zitterbewegung. These terms makes no regular contribution in our calculation and are subsequently omitted.

Linearized Boltzmann equation

We then proceed to linearize the Boltzmann equations. To that end we introduce the parametrization

$$f_\lambda(\vec{k}) = f^0_\lambda(\vec{k}) - \frac{1}{T}\frac{\partial f^0_\lambda(\vec{k})}{\partial \epsilon_\lambda(\vec{k})}\lambda v_F \hat{\vec{k}} \cdot \left(e\vec{E}\chi^E_\lambda(k) + \vec{\nabla}T\chi^T_\lambda(k)\right), \tag{6.41}$$

and

$$b_{\omega_p(\vec{k})}(\vec{k}) = b^0_{\omega_p(\vec{k})}(\vec{k}) - \frac{1}{T}\frac{\partial b^0_{\omega_p(\vec{k})}(\vec{k})}{\partial \omega_p(\vec{k})} v_F \hat{\vec{k}} \cdot \left(e\vec{E}\phi^E(k) + \vec{\nabla}T\phi^T(k)\right)\,. \tag{6.42}$$

Using the linearization and neglecting the Berry phase as well as the off-diagonal contribution we obtain

$$
\begin{aligned}
&-\lambda e\frac{v_F}{T}\hat{\vec{k}}\cdot\vec{E}f^0_\lambda(\vec{k})\left(1-f^0_\lambda(\vec{k})\right)-\lambda\frac{v_F}{T}\hat{\vec{k}}\vec{\nabla}T\frac{\epsilon_\lambda(\vec{k})-\mu}{T}f^0_\lambda(\vec{k})\left(1-f^0_\lambda(\vec{k})\right)\\
&=\alpha\frac{4\pi v_F^2}{T^2}\int\frac{d^2q}{(2\pi)^2}\sum_{\lambda'=\pm}M^{\lambda\lambda'}_{\vec{k},\vec{k}+\vec{q}}M^{\lambda'\lambda}_{\vec{k}+\vec{q},\vec{k}}\\
&\left(\delta\left(\epsilon_{\lambda'}(\vec{k}+\vec{q})-\epsilon_\lambda(\vec{k})+\omega_p(\vec{q})\right)+\delta\left(\epsilon_{\lambda'}(\vec{k}+\vec{q})-\epsilon_\lambda(\vec{k})-\omega_p(\vec{q})\right)\right)\times\\
&\times\frac{\epsilon_{\lambda'}(\vec{k}+\vec{q})-\epsilon_\lambda(\vec{k})}{q}f^0_\lambda(\vec{k})\left(1-f^0_\lambda(\vec{k})\right)\left(1-f^0_{\lambda'}(\vec{k}+\vec{q})+b^0_{\epsilon_\lambda(\vec{k})-\epsilon_{\lambda'}(\vec{k}+\vec{q})}(\vec{q})\right)\times\\
&\times\Big[e\vec{E}\left(\lambda\frac{\vec{k}}{k}\chi^E_\lambda-\lambda'\frac{\vec{k}+\vec{q}}{|\vec{k}+\vec{q}|}\chi^E_{\lambda'}(|\vec{k}+\vec{q}|)+\frac{\vec{q}}{q}\phi^E(q)\right)\\
&+\vec{\nabla}T\left(\lambda\frac{\vec{k}}{k}\chi^T_\lambda-\lambda'\frac{\vec{k}+\vec{q}}{|\vec{k}+\vec{q}|}\chi^T_{\lambda'}(|\vec{k}+\vec{q}|)+\frac{\vec{q}}{q}\phi^T(q)\right)\Big]\\
&+\frac{\gamma_0^2v_F}{2\pi T^2}\int\frac{d^2q}{(2\pi)^2}\hat{f}(-\vec{q})T^{\lambda\lambda}_{\vec{k},\vec{k}+\vec{q}}\delta_{\lambda\lambda'}\delta\left(\epsilon_\lambda(\vec{k})-\epsilon_\lambda(\vec{k}+\vec{q})\right)f^0_\lambda(\vec{k})\left(1-f^0_\lambda(\vec{k})\right)\times\\
&\times\left[e\vec{E}\left(\lambda\frac{\vec{k}}{k}\chi^E_\lambda-\lambda'\frac{\vec{k}+\vec{q}}{|\vec{k}+\vec{q}|}\chi^E_{\lambda'}(|\vec{k}+\vec{q}|)\right)+\vec{\nabla}T\left(\lambda\frac{\vec{k}}{k}\chi^T_\lambda-\lambda'\frac{\vec{k}+\vec{q}}{|\vec{k}+\vec{q}|}\chi^T_{\lambda'}(|\vec{k}+\vec{q}|)\right)\right],
\end{aligned}
\tag{6.43}
$$

and

$$
\begin{aligned}
&\frac{\vec{k}}{k^2}\vec{\nabla}T\frac{\omega_p^2(\vec{k})}{T^2}b^0_{\omega_p(\vec{k})}(\vec{k})\left(1+b^0_{\omega_p(\vec{k})}(\vec{k})\right)\\
&=\alpha 4N\pi\frac{v_F^2}{T^2}\sum_{\lambda,\lambda'=\pm}\int\frac{d^2q}{(2\pi)^2}M^{\lambda\lambda'}_{\vec{q},\vec{k}+\vec{q}}M^{\lambda'\lambda}_{\vec{k}+\vec{q},\vec{q}}\\
&\left(\delta\left(\epsilon_{\lambda'}(\vec{k}+\vec{q})-\epsilon_\lambda(\vec{q})+\omega_p(\vec{k})\right)+\delta\left(\epsilon_{\lambda'}(\vec{k}+\vec{q})-\epsilon_\lambda(\vec{q})-\omega_p(\vec{k})\right)\right)\times\\
&\times\frac{\epsilon_{\lambda'}(\vec{k}+\vec{q})-\epsilon_\lambda(\vec{q})}{k}f^0_\lambda(\vec{q})\left(1-f^0_\lambda(\vec{q})\right)\left(f^0_{\lambda'}(\vec{k}+\vec{q})+b^0_{\epsilon_{\lambda'}(\vec{k}+\vec{q})-\epsilon_\lambda(\vec{q})}(\vec{k})\right)\times\\
&\times\Big[e\vec{E}\left(\lambda\frac{\vec{q}}{q}\chi^E_\lambda-\lambda'\frac{\vec{k}+\vec{q}}{|\vec{k}+\vec{q}|}\chi^E_{\lambda'}(|\vec{k}+\vec{q}|)+\frac{\vec{k}}{k}\phi^E(k)\right)\\
&+\vec{\nabla}T\left(\lambda\frac{\vec{q}}{q}\chi^T_\lambda-\lambda'\frac{\vec{k}+\vec{q}}{|\vec{k}+\vec{q}|}\chi^T_{\lambda'}(|\vec{k}+\vec{q}|)+\frac{\vec{k}}{k}\phi^T(k)\right)\Big].
\end{aligned}
\tag{6.44}
$$

Our ansatz for the deviation from equilibrium reads

$$\begin{aligned}
\chi^E_\lambda(k) &= a^E_{0,\lambda} + a^E_{1,\lambda} k = a^E_{0,\lambda}|E,0,\lambda\rangle + a^E_{1,\lambda}|E,1,\lambda\rangle \\
\chi^T_\lambda(k) &= a^T_{0,\lambda} + a^T_{1,\lambda} k = a^T_{0,\lambda}|T,0,\lambda\rangle + a^T_{1,\lambda}|T,1,\lambda\rangle \\
\phi^E(k) &= b^E_0 + b^E_1 k = b^E_0|E,0\rangle + b^E_1|E,1\rangle \\
\phi^T(k) &= b^T_0 + b^T_1 k = b^T_0|T,0\rangle + b^T_1|T,1\rangle \; . \qquad (6.45)
\end{aligned}$$

One can rewrite the Boltzmann equations in a more compact form as

$$\begin{aligned}
|Df,E,\lambda\rangle + |Df,T,\lambda\rangle &= |I_{\rm coll},E\rangle + |I_{\rm coll},T\rangle \\
|Db,T\rangle &= |\tilde{I}_{\rm coll},E\rangle + |\tilde{I}_{\rm coll},T\rangle \; . \qquad (6.46)
\end{aligned}$$

To determine the expansion coefficients in Eq. (6.46) we define a scalar product according to

$$\langle f|g\rangle = \int \frac{d^2k}{(2\pi)^2} f(k) \frac{\vec{k}}{k} g(\vec{k}) \; . \qquad (6.47)$$

This allows to convert the linearized Boltzmann equations into a linear algebra problem which we can solve for $a^{E/T}_{0/1,\lambda}$ and $b^{E/T}_{0/1}$.

Acknowledgements

Over the past four years, I have spent a lot of time working alone, but finishing this thesis would not be possible without the supports of many people and organizations in different ways.

First of all, I should like to thank the Institute for the Promotion of Teaching Science and Technology (IPST) of Thailand for a Ph.D. scholarship over the past four years. Without it, my PhD journey would not be possible.

The most important person I want to thank is my supervisor, Lars, who in all phases of this work has never hesitated to his unconditional supports . I was very lucky to have you as a supervisor. I appreciate your enthusiasm for physics and the advice you offered.

I am very grateful to the co-authors of the articles that form the basis for this thesis; In addition to Lars, there are Henk Stoof, Tim Ludwig, Simonas Grubinska. It is very enjoyable to discuss with you, thanks for numerous useful suggestions.

I would like to thank my colleagues and office mates: Jianshen, Tim, Pieter, Mikael, Chongchuo for the fruitful exchange of points of view, not only about physics but also their experiences outside academia.

I want to take this opportunity to thank my home institute, Institute for Theoretical Physics, Utrecht University.

Finally, I thank my family and Nitis for the many, many hours taken from their company in order to keep this thesis and my PhD going until the end. I thank their invaluable love, patiences, and supports. Without them, everything would have been impossible.

Bibliography

[1] P. Drude. Zur elektronentheorie der metalle. *Annalen der Physik*, 306(3):566–613, 1900.

[2] A. Sommerfeld. Zur elektronentheorie der metalle auf grund der fermischen statistik. *Zeitschrift für Physik*, 47(1):1–32, Jan 1928.

[3] Edwin H. Hall. Sommerfeld's electron-theory of metals. *Proceedings of the National Academy of Sciences of the United States of America*, 14(5):370–377, 1928.

[4] Neil W. Ashcroft and N. David Mermin. *Solid State Physics*. Saunders College Publishing, 1976.

[5] David Pines and David Bohm. A collective description of electron interactions: II. collective vs individual particle aspects of the interactions. *Phys. Rev.*, 85:338–353, Jan 1952.

[6] David Bohm and David Pines. A collective description of electron interactions: III. coulomb interactions in a degenerate electron gas. *Phys. Rev.*, 92:609–625, Nov 1953.

[7] L.D. Landau. The theory of a fermi liquid. In D. TER HAAR, editor, *Collected Papers of L.D. Landau*, pages 723–730. Pergamon, 1965.

[8] L.D. Landau. On the theory of the fermi liquid. In D. TER HAAR, editor, *Collected Papers of L.D. Landau*, pages 752–760. Pergamon, 1965.

[9] A A Abrikosov and I M Khalatnikov. The theory of a fermi liquid (the properties of liquid 3he at low temperatures). *Reports on Progress in Physics*, 22(1):329–367, jan 1959.

[10] D. Pines and P. Nozieres. *The Theory of Quantum Liquids: Normal Fermi Liquids*. CRC Press, 1966.

[11] David Pines. A collective description of electron interactions: IV. electron interaction in metals. *Phys. Rev.*, 92:626–636, Nov 1953.

[12] L.D Landau. Kinetic equation for the case of coulomb interaction. *Phys. Zs. Sov. Union*, 10:154–164, 1936.

[13] A A Vlasov. THE VIBRATIONAL PROPERTIES OF AN ELECTRON GAS. *Soviet Physics Uspekhi*, 10(6):721–733, jun 1968.

[14] N. P. Armitage, E. J. Mele, and Ashvin Vishwanath. Weyl and dirac semimetals in three-dimensional solids. *Rev. Mod. Phys.*, 90:015001, Jan 2018.

[15] K. S. Novoselov, A. K. Geim, S. V. Morozov, D. Jiang, Y. Zhang, S. V. Dubonos, I. V. Grigorieva, and A. A. Firsov. Electric field effect in atomically thin carbon films. *Science*, 306(5696):666–669, 2004.

[16] K. S. Novoselov, A. K. Geim, S. V. Morozov, D. Jiang, M. I. Katsnelson, I. V. Grigorieva, S. V. Dubonos, and A. A. Firsov. Two-dimensional gas of massless dirac fermions in graphene. *Nature*, 438(7065):197–200, Nov 2005.

[17] A. H. Castro Neto, F. Guinea, N. M. R. Peres, K. S. Novoselov, and A. K. Geim. The electronic properties of graphene. *Rev. Mod. Phys.*, 81:109–162, Jan 2009.

[18] Jesse Crossno, Jing K. Shi, Ke Wang, Xiaomeng Liu, Achim Harzheim, Andrew Lucas, Subir Sachdev, Philip Kim, Takashi Taniguchi, Kenji Watanabe, Thomas A. Ohki, and Kin Chung Fong. Observation of the dirac fluid and the breakdown of the wiedemann-franz law in graphene. *Science*, 351(6277):1058–1061, 2016.

[19] Fereshte Ghahari, Hong-Yi Xie, Takashi Taniguchi, Kenji Watanabe, Matthew S. Foster, and Philip Kim. Enhanced thermoelectric power in graphene: Violation of the mott relation by inelastic scattering. *Phys. Rev. Lett.*, 116:136802, Mar 2016.

[20] Dorri Halbertal, Moshe Ben Shalom, Aviram Uri, Kousik Bagani, Alexander Y. Meltzer, Ido Marcus, Yuri Myasoedov, John Birkbeck, Leonid S. Levitov, Andre K. Geim, and Eli Zeldov. Imaging resonant dissipation from individual atomic defects in graphene. *Science*, 358(6368):1303–1306, 2017.

[21] C. R. Dean, A. F. Young, I. Meric, C. Lee, L. Wang, S. Sorgenfrei, K. Watanabe, T. Taniguchi, P. Kim, K. L. Shepard, and J. Hone. Boron nitride substrates for high-quality graphene electronics. *Nature Nanotechnology*, 5(10):722–726, Oct 2010.

[22] L. Wang, I. Meric, P. Y. Huang, Q. Gao, Y. Gao, H. Tran, T. Taniguchi, K. Watanabe, L. M. Campos, D. A. Muller, J. Guo, P. Kim, J. Hone, K. L. Shepard, and C. R. Dean. One-dimensional electrical contact to a two-dimensional material. *Science*, 342(6158):614–617, 2013.

[23] S. J. Haigh, A. Gholinia, R. Jalil, S. Romani, L. Britnell, D. C. Elias, K. S. Novoselov, L. A. Ponomarenko, A. K. Geim, and R. Gorbachev. Cross-sectional imaging of individual layers and buried interfaces of graphene-based heterostructures and superlattices. *Nature Materials*, 11(9):764–767, Sep 2012.

[24] P. R. Wallace. The band theory of graphite. *Phys. Rev.*, 71:622–634, May 1947.

[25] Mikhail I. Katsnelson. *The Physics of Graphene*. Cambridge University Press, 2 edition, 2020.

[26] Daniel E. Sheehy and Jörg Schmalian. Quantum critical scaling in graphene. *Phys. Rev. Lett.*, 99:226803, Nov 2007.

[27] Valeri N. Kotov, Bruno Uchoa, Vitor M. Pereira, F. Guinea, and A. H. Castro Neto. Electron-electron interactions in

graphene: Current status and perspectives. *Rev. Mod. Phys.*, 84:1067–1125, Jul 2012.

[28] Pavan Hosur and Xiaoliang Qi. Recent developments in transport phenomena in weyl semimetals. *Comptes Rendus Physique*, 14(9):857–870, 2013. Topological insulators / Isolants topologiques.

[29] Andrew Lucas, Richard A. Davison, and Subir Sachdev. Hydrodynamic theory of thermoelectric transport and negative magnetoresistance in weyl semimetals. *Proceedings of the National Academy of Sciences*, 113(34):9463–9468, 2016.

[30] Vladyslav Kozii and Liang Fu. Thermal plasmon resonantly enhances electron scattering in dirac/weyl semimetals. *Phys. Rev. B*, 98:041109, Jul 2018.

[31] Pavan Hosur, S. A. Parameswaran, and Ashvin Vishwanath. Charge transport in weyl semimetals. *Phys. Rev. Lett.*, 108:046602, Jan 2012.

[32] Alexander B. Kashuba. Conductivity of defectless graphene. *Phys. Rev. B*, 78:085415, Aug 2008.

[33] Lars Fritz, Jörg Schmalian, Markus Müller, and Subir Sachdev. Quantum critical transport in clean graphene. *Phys. Rev. B*, 78:085416, Aug 2008.

[34] Markus Müller, Lars Fritz, and Subir Sachdev. Quantum-critical relativistic magnetotransport in graphene. *Phys. Rev. B*, 78:115406, Sep 2008.

[35] Lars Fritz. Quantum critical transport at a semimetal-to-insulator transition on the honeycomb lattice. *Phys. Rev. B*, 83:035125, Jan 2011.

[36] Denis A. Bandurin, Andrey V. Shytov, Leonid S. Levitov, Roshan Krishna Kumar, Alexey I. Berdyugin, Moshe Ben Shalom, Irina V. Grigorieva, Andre K. Geim, and Gregory Falkovich. Fluidity onset in graphene. *Nature Communications*, 9(1):4533, Oct 2018.

[37] D A Bandurin, I Torre, R Krishna Kumar, M Ben Shalom, A Tomadin, A Principi, G H Auton, E Khestanova, K S Novoselov, I V Grigorieva, L A Ponomarenko, A K Geim, and M Polini. Negative local resistance caused by viscous electron backflow in graphene. *Science*, 351(6277):1055–1058, February 2016.

[38] Joseph A Sulpizio, Lior Ella, Asaf Rozen, John Birkbeck, David J Perello, Debarghya Dutta, Moshe Ben-Shalom, Takashi Taniguchi, Kenji Watanabe, Tobias Holder, Raquel Queiroz, Alessandro Principi, Ady Stern, Thomas Scaffidi, Andre K Geim, and Shahal Ilani. Visualizing poiseuille flow of hydrodynamic electrons. *Nature*, 576(7785):75–79, December 2019.

[39] M. J. M. de Jong and L. W. Molenkamp. Hydrodynamic electron flow in high-mobility wires. *Phys. Rev. B*, 51:13389–13402, May 1995.

[40] Jonah Waissman, Laurel E. Anderson, Artem V. Talanov, Zhongying Yan, Young J. Shin, Danial H. Najafabadi, Mehdi Rezaee, Xiaowen Feng, Daniel G. Nocera, Takashi Taniguchi, Kenji Watanabe, Brian Skinner, Konstantin A. Matveev, and Philip Kim. Electronic thermal transport measurement in low-dimensional materials with graphene non-local noise thermometry. *Nature Nanotechnology*, 17(2):166–173, Feb 2022.

[41] Markus Müller, Jörg Schmalian, and Lars Fritz. Graphene: A nearly perfect fluid. *Phys. Rev. Lett.*, 103:025301, Jul 2009.

[42] Leonid Levitov and Gregory Falkovich. Electron viscosity, current vortices and negative nonlocal resistance in graphene. *Nature Physics*, 12(7):672–676, Jul 2016.

[43] Jan Zaanen. Electrons go with the flow in exotic material systems. *Science*, 351(6277):1026–1027, 2016.

[44] R.N. Gurzhi. Minimum of resistance in impurity-free conductors. *J.Exptl. Theoret.Phys.(U.S.S.R.)*, pages 771–772, February 1963.

[45] L.D. Landau and E.M. Lifshitz. *Fluid Mechanics: Course of Theoretical Physics*. Pergamon Press, 1987.

[46] Pavel Kovtun. Lectures on hydrodynamic fluctuations in relativistic theories. *Journal of Physics A: Mathematical and Theoretical*, 45(47):473001, nov 2012.

[47] Hong-Yi Xie and Matthew S. Foster. Transport coefficients of graphene: Interplay of impurity scattering, coulomb interaction, and optical phonons. *Phys. Rev. B*, 93:195103, May 2016.

[48] Andrew Lucas and Kin Chung Fong. Hydrodynamics of electrons in graphene. *Journal of Physics: Condensed Matter*, 30(5):053001, jan 2018.

[49] Boris N. Narozhny. Electronic hydrodynamics in graphene. *Annals of Physics*, 411:167979, 2019.

[50] G. Catelani and I.L. Aleiner. Interaction corrections to thermal transport coefficients in disordered metals: The quantum kinetic equation approach. *J. Exp. Theor. Phys*, 100:331–369, 2005.

[51] David Pines and J. Robert Schrieffer. Approach to equilibrium of electrons, plasmons, and phonons in quantum and classical plasmas. *Phys. Rev.*, 125:804–812, Feb 1962.

[52] M. Bard, I. V. Protopopov, and A. D. Mirlin. Plasmon localization, plasmon relaxation, and thermal transport in one-dimensional conductors. *Phys. Rev. B*, 100:115153, Sep 2019.

[53] Frank Stern. Polarizability of a two-dimensional electron gas. *Phys. Rev. Lett.*, 18:546–548, Apr 1967.

[54] B Wunsch, T Stauber, F Sols, and F Guinea. Dynamical polarization of graphene at finite doping. *New Journal of Physics*, 8(12):318–318, dec 2006.

[55] S. Das Sarma and Qiuzi Li. Intrinsic plasmons in two-dimensional dirac materials. *Phys. Rev. B*, 87:235418, Jun 2013.

[56] G.D. Mahan. *Many-Particle Physics*. Springer New York, NY, 3 edition, 2000.

[57] J. González, F. Guinea, and M.A.H. Vozmediano. Non-fermi liquid behavior of electrons in the half-filled honeycomb lattice (a renormalization group approach). *Nuclear Physics B*, 424(3):595–618, 1994.

[58] D. C. Elias, R. V. Gorbachev, A. S. Mayorov, S. V. Morozov, A. A. Zhukov, P. Blake, L. A. Ponomarenko, I. V. Grigorieva, K. S. Novoselov, F. Guinea, and A. K. Geim. Dirac cones reshaped by interaction effects in suspended graphene. *Nature Physics*, 7(9):701–704, Sep 2011.

[59] L.P. Kadanoff and G. Baym. *Quantum Statistical Mechanics: Green's Function Methods in Equilibrium and Nonequilibrium Problems*. CRC Press, 1962.

[60] H. Kleinert. Collective quantum fields. *Fortschritte der Physik*, 26(11-12):565–671, 1978.

[61] J. Hubbard. Calculation of partition functions. *Phys. Rev. Lett.*, 3:77–78, Jul 1959.

[62] J. Gooth, F. Menges, N. Kumar, V. Süß, C. Shekhar, Y. Sun, U. Drechsler, R. Zierold, C. Felser, and B. Gotsmann. Thermal and electrical signatures of a hydrodynamic electron fluid in tungsten diphosphide. *Nature Communications*, 9(1):4093, 2018.

[63] Alexandre Jaoui, Benoît Fauqué, and Kamran Behnia. Thermal resistivity and hydrodynamics of the degenerate electron fluid in antimony. *Nature Communications*, 12(1):195, Jan 2021.

[64] Youngwoo Nam, Dong-Keun Ki, David Soler-Delgado, and Alberto F. Morpurgo. Electron–hole collision limited transport in charge-neutral bilayer graphene. *Nature Physics*, 13(12):1207–1214, Dec 2017.

[65] Patrick Gallagher, Chan-Shan Yang, Tairu Lyu, Fanglin Tian, Rai Kou, Hai Zhang, Kenji Watanabe, Takashi Taniguchi, and Feng Wang. Quantum-critical conductivity of the dirac fluid in graphene. *Science*, 364(6436):158–162, 2019.

[66] B. N. Narozhny, I. V. Gornyi, M. Titov, M. Schütt, and A. D. Mirlin. Hydrodynamics in graphene: Linear-response transport. *Phys. Rev. B*, 91:035414, Jan 2015.

[67] Yu.G. Gurevich and O.L. Mashkevich. The electron-phonon drag and transport phenomena in semiconductors. *Physics Reports*, 181(6):327–394, 1989.

[68] Alex Levchenko and Jörg Schmalian. Transport properties of strongly coupled electron–phonon liquids. *Annals of Physics*, 419:168218, 2020.

[69] Xiaoyang Huang and Andrew Lucas. Electron-phonon hydrodynamics. *Phys. Rev. B*, 103:155128, Apr 2021.

[70] D. Pines. *Elementary Excitations in Solids Lectures on Protons, Electrons, and Plasmons*. CRC Press, 1999.

[71] M. Beens, R. A. Duine, and B. Koopmans. Modeling ultrafast demagnetization and spin transport: The interplay of spin-polarized electrons and thermal magnons. *Phys. Rev. B*, 105:144420, Apr 2022.

[72] H. W. Wyld and D. Pines. Kinetic equation for plasma. *Phys. Rev.*, 127:1851–1855, Sep 1962.

[73] Kitinan Pongsangangan, Simonas Grubinskas, and Lars Fritz. Thermo-electric response in two-dimensional dirac systems: the role of particle-hole pairs, 2020.

[74] Egor I. Kiselev and Jörg Schmalian. Nonlocal hydrodynamic transport and collective excitations in dirac fluids. *Phys. Rev. B*, 102:245434, Dec 2020.

[75] Markus Müller and Subir Sachdev. Collective cyclotron motion of the relativistic plasma in graphene. *Phys. Rev. B*, 78:115419, Sep 2008.

[76] Lars Onsager. Reciprocal relations in irreversible processes. i. *Phys. Rev.*, 37:405–426, Feb 1931.

[77] John Ziman. *Electrons and phonons*. Oxford University Press, 2000.

[78] L.P. Pitaevskii and E.M. Lifshitz. *Physical Kinetics: Course of Theoretical Physics*. Butterworth-Heinemann, 1981.

[79] R. Franz and G. Wiedemann. Ueber die wärmeleitungsfähigkeit der metalle. *Annalen der Physik*, 165(8):497–531, 1853.

[80] J. Waissman. (private communication).

[81] Alex Kamenev. *Field Theory of Non-Equilibrium Systems*. Cambridge University Press, 2011.

[82] H.T.C Stoof, K.B. Gubbels, and D.B.M Dickerscheid. *Ultracold Quantum Fields*. Springer Science+Business Media B.V, 2009.

[83] Petr Král. Generalized gradient expansions in quantum transport equations. *Journal of Statistical Physics*, 86(5):1337–1358, Mar 1997.

[84] J. Knoll, Yu.B. Ivanov, and D.N. Voskresensky. Exact conservation laws of the gradient expanded kadanoff–baym equations. *Annals of Physics*, 293(2):126–146, 2001.

[85] Andrew Lucas, Jesse , Kin Chung Fong, Philip Kim, and Subir Sachdev. Transport in inhomogeneous quantum critical fluids and in the dirac fluid in graphene. *Phys. Rev. B*, 93:075426, Feb 2016.

[86] E. H. Hwang, Ben Yu-Kuang Hu, and S. Das Sarma. Density dependent exchange contribution to $\partial\mu/\partial n$ and compressibility in graphene. *Phys. Rev. Lett.*, 99:226801, Nov 2007.

[87] E. G. Mishchenko. Effect of electron-electron interactions on the conductivity of clean graphene. *Phys. Rev. Lett.*, 98:216801, May 2007.

[88] D. A. Pesin. Two-particle collisional coordinate shifts and hydrodynamic anomalous hall effect in systems without lorentz invariance. *Phys. Rev. Lett.*, 121:226601, Nov 2018.

[89] E. G. Mishchenko, M. Yu. Reizer, and L. I. Glazman. Plasmon attenuation and optical conductivity of a two-dimensional electron gas. *Phys. Rev. B*, 69:195302, May 2004.

[90] D. F. DuBois and M. G. Kivelson. Electron correlational effects on plasmon damping and ultraviolet absorption in metals. *Phys. Rev.*, 186:409–419, Oct 1969.

[91] David Pines and J. Robert Schrieffer. Approach to equilibrium of electrons, plasmons, and phonons in quantum and classical plasmas. *Phys. Rev.*, 125:804–812, Feb 1962.

[92] Gordon Baym and Leo P. Kadanoff. Conservation laws and correlation functions. *Phys. Rev.*, 124:287–299, Oct 1961.

[93] Andrew Lucas and Sankar Das Sarma. Electronic sound modes and plasmons in hydrodynamic two-dimensional metals. *Phys. Rev. B*, 97:115449, Mar 2018.

[94] Gabriele Giuliani and Giovanni Vignale. *Quantum Theory of the Electron Liquid*. Cambridge University Press, 2005.

[95] Sean A. Hartnoll and Pavel K. Kovtun. Hall conductivity from dyonic black holes. *Phys. Rev. D*, 76:066001, Sep 2007.

[96] Sean A. Hartnoll, Pavel K. Kovtun, Markus Müller, and Subir Sachdev. Theory of the nernst effect near quantum phase transitions in condensed matter and in dyonic black holes. *Phys. Rev. B*, 76:144502, Oct 2007.

[97] M. Schütt, P. M. Ostrovsky, I. V. Gornyi, and A. D. Mirlin. Coulomb interaction in graphene: Relaxation rates and transport. *Phys. Rev. B*, 83:155441, Apr 2011.

[98] Boris N. Narozhny, Igor V. Gornyi, Alexander D. Mirlin, and Jörg Schmalian. Hydrodynamic approach to electronic transport in graphene. *Annalen der Physik*, 529(11):1700043, 2017.

[99] B. A. Braem, F. M. D. Pellegrino, A. Principi, M. Röösli, C. Gold, S. Hennel, J. V. Koski, M. Berl, W. Dietsche, W. Wegscheider, M. Polini, T. Ihn, and K. Ensslin. Scanning gate microscopy in a viscous electron fluid. *Phys. Rev. B*, 98:241304, Dec 2018.

[100] A. I. Berdyugin, S. G. Xu, F. M. D. Pellegrino, R. Krishna Kumar, A. Principi, I. Torre, M. Ben Shalom, T. Taniguchi, K. Watanabe, I. V. Grigorieva, M. Polini, A. K. Geim, and D. A. Bandurin. Measuring hall viscosity of graphene electron fluid. *Science*, 364(6436):162–165, 2019.

[101] Michael Edward Peskin and Daniel V. Schroeder. *An Introduction to Quantum Field Theory*. CRC Press, 2018.